

https://dspace.org/

Assessing groundwater access by trees growing above contaminated groundwater plumes originating from gold tailings storage facilities

Govender, Marilyn

2012-02-01
http://hdl.handle.net/10539/11221

Downloaded from a DSpace repository. https://dspace.org/

Assessing Groundwater Access by Trees Growing above Contaminated Groundwater Plumes Originating from Gold Tailings Storage Facilities

by

M Govender

MSc (Hydrology)

Submitted in partial fulfilment of the requirements for
the degree of
Doctor of Philosophy

Restoration and Conservation Biology Research Group
School of Animal, Plant and Environmental Sciences
University of the Witwatersrand
Johannesburg

***Supervisor**:* *Dr P.J. Dye*
***Co Supervisor**:* *Prof. E.T.F. Witkowski*

***Submitted**:* *September2011*

ABSTRACT

Deep-level gold mining in the Witwatersrand Basin Goldfields (WBG) of central South Africa is characterised by the production of extensive unlined tailings storage facilities (TSFs) comprising large quantities of pulverised rock and water contaminated with salts and a wide range of other inorganic pollutants (Weiersbye *et al*., 2006). There are more than 200 such TSFs covering a total area of more than 400 km^2 (Rosner *et al*., 2001), and significant contaminated "footprint" areas occur after removal and reprocessing of the original TSFs (Chevrel *et al*., 2003). It is estimated that the Witwatersrand Basin contains six billion tons of gold and uranium tailings (Chevrel *et al*., 2003), 430 000 tons of uranium (Council of Geoscience, 1998; Winde, 2004a; b; c) and approximately 30 million tons of sulphur (Witkowski and Weiersbye, 1998a). An estimated 105 million tons of waste per annum is generated by the gold mining industry within the WBG (Department of Tourism, Economic and Environmental Affairs, 2002; Chamber of Mines of South Africa, 2004).

A major environmental problem resulting from deep level mining in the WBG is the contaminated water that seeps from TSFs into adjacent lands and groundwater. Van As (1992) reported on the significant environmental hazards resulting from the storage of highly pulverised pyrite rock waste in TSFs (Straker *et al*., 2007). Adjacent lands become polluted through near-surface seepage, and this is enhanced by the movement of polluted groundwater in shallow aquifers that are commonly 1-30 m below ground (Funke, 1990; Hodgson *et al*., 2001; Rosner *et al*., 2001; Naicker *et al*., 2003). The impact of the mines and the TSFs extends far beyond their localities (Cogho *et al*., 1990). The Vaal River catchment receives a large proportion of the pollutants from WBG mining activities, with consequent acidification and salinisation of surface and ground waters. Salt discharges to the Vaal River were estimated to be 170 000 t/annum (Best, 1985), whereas discharges from the Free State gold mines south of the Vaal catchment were estimated at 350 000 t/annum of salts (Cogho *et al*., 1990). Concern also exists over the spread of dangerous contaminants such as uranium, chromium and mercury (Coetzee *et al*., 2006; Winde, 2009).

Engineering solutions to these problems are hindered by the large sizes and great extent of TSFs, the high and indefinite costs involved, and the typically low hydraulic conductivity in affected aquifers, which makes the "pump and treat" option impractical. An alternative phytoremediation strategy is to establish belts or blocks of trees in strategic areas surrounding the TSFs in order to reduce the seepage of contaminated water into adjacent lands and groundwater bodies. The major reasons why trees are likely to have a greater impact on seepage water than the existing grasslands that characterise the area around most TSFs in the WBG, are that some tree species have the potential to develop very deep root systems and to continue transpiring water throughout the year. This is in contrast to seasonally dormant grasslands. In addition, some tree species are known to be tolerant to salts and other pollutants. Trees are thus potentially able to reach deep water tables, take up large quantities of water, and remove some of the pollutants in this water. It is crucial for a successful implementation of this strategy to know on what sites trees are able to access mine seepage water, and consequently maintain a high year-round rate of water use. If this access is limited, then growth and water use will be curtailed during the long winter dry season, and control of seepage will be considerably below potential.

A primary aim of this study was to develop methodologies to discriminate between water-stressed and non-water-stressed trees currently growing in three gold mining districts (Welkom, Vaal River, West Wits) within the WBG. This information was required to assess what site types are likely to support adequate tree growth and permit high rates of water use and seepage control. The tree species selected were those most widely occurring in these areas, and include the non-native species *Eucalyptus sideroxylon* A. Cunningham ex Woolls and *Eucalyptus camaldulensis* Dehnhardt, as well as the indigenous species *Searsia lancea* L.f. Various remote sensing technologies including leaf-level spectroscopy, satellite and airborne remote sensing images were evaluated for their usefulness in detecting levels of winter-time water stress. Four commonly used ground-truthing techniques (predawn leaf water potential, leaf chlorophyll fluorescence, leaf chlorophyll and carotenoid pigment content, and leaf water content) were used for localised measurements of plant water stress and for ground-truthing of remotely sensed data on 75 sample sites and 15 sample sites. This study provided a unique opportunity to test and compare the use of stress reflectance models

derived from different remote sensing data acquired at different spatial and spectral resolutions (i.e. multispectral and hyperspectral) for the same geographical location.

The use of remote sensing to examine the spectral responses of vegetation to plant stress has been widely described in the scientific literature. A collation of published spectral reflectance indices provided the basis for investigating the use of hand-held remote sensing technology to detect plant water stress, and was used as a stepping stone to further develop spectral plant water stress relationships for specific tree species in this study. Seventy seven spectral reflectance indices and specific individual spectral wavelengths useful for detecting plant water stress, plant pigment content, the presence of stress related pigments in vegetation, and changes in leaf cellular structure, were investigated using hand-held spectroscopy. Ground-based measurements of plant water stress were taken on 75 sample trees. In this study, the measurement of predawn leaf water potential has been identified as a key methodology for linking remotely sensed assessments of plant water stress to actual plant water stress; a reading of -0.8 MPa was used to separate stressed trees from unstressed trees in the landscape (Cleary and Zaerr, 1984). The results of the predawn leaf water potential measurements ranged from -0.56 to -0.68 MPa at unstressed sites, and from -0.93 to -1.78 MPa at stressed sites. A novel approach of using spectral reflectance indices derived from previous studies was used to identify specific indices which are applicable to South Africa and to the three species investigated in the WGB. Maximal multiple linear regression models were derived for all possible combinations of plant water stress measurements and the 77 spectral reflectance indices extracted from leaf-level spectral reflectance data, and included the interactions of district and species. The results of the multiple linear regression models indicated that the (695/690) index, DATT index (850-710)/(850-680), near infra-red index (710/760) and the water band (900/970) index performed well and accounted for more than 50% of the variance in the data. The stepwise regression model derived between chlorophyll b content and the DATT index was selected as the "best" model, having the highest adjusted R^2 of 69.3%. This was shown to be the most robust model in this application, which could be used at different locations for different species to predict chlorophyll content at the leaf-level.

Satellite earth observation data were acquired from two data sources for this investigation; the Hyperion hyperspectral sensor (United States Geological Survey Earth Resources Observation Systems) and the Proba Chris pseudo-hyperspectral sensor (European Space Agency). The Hyperion sensor was selected to obtain high spatial and spectral resolution data, whereas the Proba Chris sensor provided high spatial and medium spectral resolution earth observation data. Twelve vegetation indices designed to capture changes in canopy water status, plant pigment content and changes in plant cellular structure, were selected and derived from the satellite remote sensing imagery. Ground-based measurements of plant water stress undertaken during late July 2004 were used for ground-truthing the Hyperion image, while measurements undertaken during July 2005 and August 2005 were used for ground-truthing the Proba Chris images. Predawn leaf water potential measurements undertaken for the three species, ranged from -0.42 to -0.78 MPa at unstressed sites, and -0.95 to -4.66 MPa at stressed sites. Predawn leaf water potentials measured for *E. camaldulensis* trees sampled in species trials in Vaal River were significantly different between stressed and non stressed trees ($t = 3.39$, 8df, $P = 0.009$). In contrast, *E. camaldulensis* trees sampled near a pan within the Welkom mining district, which had greater access to water but were exposed to higher concentrations of salts and inorganic contaminants, displayed differences in total chlorophyll content ($t = -2.20$, 8df, $P = 0.059$), carotenoid content ($t = -5.68$, 8df, $P < 0.001$) and predawn leaf water potential ($t = 4.25$, 8df, $P = 0.011$) when compared to trees sampled on farmland. *E. sideroxylon* trees sampled close to a farm dam in the West Wits mining district displayed differences in predawn leaf water potential ($t = 69.32$, 8df, $P < 0.001$) and carotenoid content ($t = -2.13$, 8df, $P = 0.066$) when compared to stressed trees further upslope away from the water source. Multiple linear regressions revealed that the predawn leaf water potential greenness normalised difference vegetation index model, and the predawn leaf water potential water band index model were the "best" surrogate measures of plant water stress when using broad band multispectral satellite and narrow-band hyperspectral satellite data respectively. It was concluded from these investigations that vegetation indices designed to capture changes in plant water content/plant water status and spectral changes in the red edge region of the spectrum, performed well when applied to high spectral resolution remote sensing data. The greenness normalised difference vegetation index was considered to be a fairly robust index, which was

highly correlated to chlorophyll fluorescence and predawn leaf water potential. It is recommended that this index has the potential to be used to map spatial patterns of winter-time plant stress for different genera/species and in different geographical locations.

Airborne remote sensing surveys were conducted to investigate the application of high spatial resolution remote sensing data to detect plant water stress. Multispectral airborne imagery was acquired by Land Resource International (PTY) Ltd, South Africa. Ground-based measurements of plant water stress were carried out during July and August 2005.Four individual spectral bands and two vegetation spectral reflectance indices, which are sensitive to changes in plant pigment content, were derived from the processed multispectral images *viz*. red, green, blue and near-infrared spectral bands and the normalised difference vegetation index (NDVI) and greenness normalised difference vegetation index (GNDVI).The results of the multispectral airborne study revealed that carotenoid content together with the green spectral waveband resulted in the "best" surrogate measure of plant water stress when using broad-band multispectral airborne data.

Airborne remote sensing surveys were conducted by Bar-Kal Systems Engineering Ltd, Israel, to investigate the application of hyperspectral airborne imagery to detect plant water stress. Six vegetation spectral reflectance indices designed to capture changes in plant pigment and plant water status/content, were derived from the processed hyperspectral images. When using airborne hyperspectral data, predawn leaf water potential with the normalized difference water index was selected as the most appropriate model. It was concluded, upon evaluation of the multiple linear regression models, that the airborne hyperspectral data produced several more regression models with higher adjusted R^2 values (R_a^2 range 6.2 - 76.2%) when compared to the airborne multispectral data (R_a^2 range 6 - 50.1).

Exploration of relationships between vegetation indices derived from leaf-level, satellite and airborne spectral reflectance data and ground-based measurements used as "surrogate" measures of plant water stress, revealed that several prominent and recurring spectral reflectance indices could be applied to identify species-specific plant water stress within the

Welkom, Vaal River and West Wits mining districts. The models recommended for mapping and detecting spatial patterns of plant water stress when using different sources of remote sensing data are as follows:

- the chlorophyll b DATT spectral reflectance model when derived from leaf-level spectral reflectance data, can be applied across all three mining districts
- the predawn leaf water potential GNDVI spectral reflectance model and predawn leaf water potential water band index spectral reflectance model when utilising satellite multispectral and hyperspectral remote sensing data
- carotenoid content green band spectral reflectance model can be used for airborne multispectral resolution data
- predawn leaf water potential NDVI spectral reflectance model is best suited for airborne high spatial and hyperspectral resolution data.

These results indicate that measurements of predawn leaf water potential and plant pigment content have been identified as key methodologies for ground-truthing of remotely sensed data and can be used as surrogate measures of plant water stress.

Some preliminary research was undertaken to evaluate if wood anatomy characteristics could be used as a non-destructive and rapid low-cost survey approach for identifying trees which are experiencing long-term plant stress. Seventy two wood core samples were extracted and analysed. Predawn leaf water potential measurements were used to classify stressed and unstressed trees. Relative differences in radial vessel diameter, vessel frequency and wood density were examined. Comparison of the radial vessel diameter and vessel frequency measurements revealed significant differences in three of the five comparative sampling sites ($p < 0.05$). The results of the density analyses were significantly different for all five comparative sampling sites ($p < 0.01$). In general, trees experiencing higher plant water stress displayed smaller vessel diameters, compared to less stressed or healthy trees. Sites which were influenced by high levels of contaminated water also displayed smaller vessel diameters, indicating that the uptake of contaminants could affect the wood anatomy of plants. Trees considered to be experiencing higher plant water stress displayed higher vessel frequency. This preliminary study showed that plant stress does influence the wood

anatomical characteristics (radial vessel diameter, vessel frequency and wood density) in *E. camaldulensis*, *E. sideroxylon* and *S. lancea* in the three mining districts.

Spatial patterns of trees, mapped in the three gold mining districts, Welkom (27º57´S, 26º34´E) in the Free State Province, Vaal River (26º55´S, 26º40´E) located in the North West Province, and West Wits (26º25´S, 27º21´E) located in Gauteng, which were not experiencing winter-time water stress were correlated to site characteristics such as average soil depth, percent clay in the topsoil, groundwater chloride and sulphate concentrations, total dissolved solids, electrical conductivity and groundwater water level. The spectral reflectance model derived between predawn leaf water potential and the green normalised difference vegetation index using broad-band multispectral Proba Chris satellite data was used to map spatial patterns of unstressed trees across the three mining districts. Very high resolution (75 cm) multispectral airborne images acquired by LRI in 2005 were used to demarcate and classify vegetation using the maximum likelihood supervised classification technique. Interpolated surfaces of groundwater chloride and sulphate concentrations, total dissolved solids, electrical conductivity, pH and groundwater table levels were created using the kriging geostatistical interpolation technique for each mining district. Random sample analyses between stressed and unstressed trees were extracted in order to determine whether site characteristics were significantly different (using t-tests). Site characteristic surfaces which were significantly different from stressed areas were spatially linked to trees which were not experiencing winter-time plant water stress for each tree species investigated in each mining district. This spatial correlation was used to make recommendations and prioritise sites for the establishment of future block plantings. Analysis of the site characteristic data and the geophysical surveys undertaken in the three mining districts which provided detailed information on groundwater saturation and an indication of the salinity conditions, confirmed the presence of relatively shallow and saline groundwater sources. This would imply that tree roots could access the relatively shallow groundwater even during the dry winter season and assist in containing contaminated groundwater seeping into surrounding lands.

Keywords : airborne imagery, ground-based measurements of plant water stress, hyperspectral, leaf-level spectroscopy, multispectral, satellite imagery, spatial patterns of unstressed trees, spectral reflectance indices

DECLARATION

The work described in this thesis was carried out for post-graduate degree purposes within the School of Animal, Plant and Environmental Sciences, University of the Witwatersrand, Johannesburg under the supervision of Dr P.J. Dye, Prof E.T.F. Witkowski and Prof. F. Ahmed. It has also contributed towards an externally funded contract research project which was undertaken by a larger project team.

I wish to certify that the work reported in this thesis is my own original and unaided work, except where specific acknowledgment is made.



7 September 2011

Signed by Marilyn Govender *Date*

ACKNOWLEDGEMENTS

I would like to thank the Mine Woodlands Project (School of Animal, Plant and Environmental Sciences, University of the Witwatersrand, Johannesburg, South Africa), the South African Department of Trade and Industry (THRIP funding), AngloGold Ashanti Ltd and the CSIR for support and funding of this study.

I would like to acknowledge and thank the following organisations, institutions, and individuals for the technical assistance and support during field campaigns:

- The University of Witwatersrand for the use of the chlorophyll fluorescence meter.
- AngloGold Ashanti for assistance during predawn field measurements.
- The Agricultural Research Council for the use of the ASD spectrometer and for use of national land-type soils data.
- The CSIR for the use of the wood corer, the Forestry and Forest Products Group for undertaking the wood anatomy and density measurements and the geophysical specialists from the Stellenbosch office for undertaking the resistivity measurements.
- Access to the Horticulture Laboratory from the University of Kwa-Zulu Natal, Pietermaritzburg, for the analysis of chlorophyll and carotenoid pigment contents from leaf samples.
- Land Resource International (PTY) Ltd and Bar-Kal Systems Engineering Ltd for their services when conducting the respective multispectral and hyperspectral airborne remote sensing surveys.
- Africa Geo-Environmental Services (AGES), School of Animal Plant and Environmental Sciences at Witwatersrand University (APES) and Anglogold Ashanti for the use of relevant hydrochemistry and soils data.
- Ms Isabel Weiersbye and Dr Peter Dye for their advice, guidance and support during field campaigns.
- Mr Joshua Xaba and Mr Alistair Clulow for their technical assistance during field measurements.

I would like to express my sincere appreciation to:

Prof F. Ahmed and Dr P.J. Dye for their supervision and guidance throughout this research. Prof. E.T.F. Witkowski and Dr I. Weiersbye for their comments, support and guidance in this study.

Prof. A. Fossey for her most valuable supervision, mentorship and advice; specifically in the principles of scientific writing.

Mr H. Dicks for his statistical guidance and supervision.

My colleagues from the CSIR for their valuable advice and support.

The European Space Agency (ESA ®) for their support with remote sensing data through the Tiger Initiative.

My family for their unending support, love and encouragement, and finally to:

My husband Mevelin, and my two very special girls, Jadean and Ceann, for their love, support and understanding which helped make the completion of this thesis possible.

The fear of the Lord is the beginning of wisdom, and knowledge of the Holy One is understanding (Proverbs 9:10). I can do all things through him who gives me strength (Philippians 4:13).

CONTENTS

ABSTRACT _____ *i*

DECLARATION _____ ix

ACKNOWLEDGEMENTS _____ x

TABLES _____ 4

FIGURES _____ 6

CHAPTER 1. GENERAL INTRODUCTION 9

1.1 Research problem 9
1.2 Research strategy 13
1.3 Aimsand objectives 14
1.4 Hypotheses 17
1.5 Reporting structure 17

CHAPTER 2. TREE SPECIES SELECTION AND STUDY AREAS 19

2.1 Introduction 19
2.2 Selection of tree species 19
2.3 Mining districts 21
2.4 Sampling sites 25

CHAPTER 3. REVIEW OF COMMONLY USED REMOTE SENSING AND GROUND-BASED TECHNOLOGIES TO MEASURE PLANT WATER STRESS 30

3.1 Introduction 31
3.2 Brief overview of plant water stress interactions 33
3.3 Detection of plant water stress using remote sensing 37
3.3.1 Spectral indicators of plant chlorophyll content 43
3.3.2 Spectral indicators of plant water content 44
3.3.3 Factors affecting spectral reflectance from leaf to canopy scales 46
3.4 Detection of plant water stress using ground-based measurements 49
3.4.1 Predawn leaf water potential 50
3.4.2 Leaf chlorophyll fluorescence 52
3.4.3 Chlorophyll and carotenoid pigment concentration 55
3.4.4 Leaf water content 56
3.4.5 Comparison of ground-based measurement techniques of plant water stress 58

3.5 Concluding remarks 60

CHAPTER 4. SPECTROSCOPY AS A TOOL FOR IDENTIFYING PLANT WATER STRESS AT THE LEAF-LEVEL 61

4.1 Introduction 62
4.2 Materials and methods 63
4.2.1 Sampling design 64
4.2.2 Ground measurements of plant water stress 64
4.2.2.1. Predawn leaf water potential 65
4.2.2.2. Leaf chlorophyll fluorescence 65
4.2.2.3. Leaf chlorophyll and carotenoid pigment content 66
4.2.2.4. Leaf water content 66
4.2.3 Leaf spectral reflectance measurements 67
4.2.3.1. ASD hand-held spectral measurements at leaf-level 67
4.2.3.2. Vegetation spectral reflectance indices derived from leaf-level spectral measurements 67
4.2.4 Analysis of data 69
4.3 Results 72
4.3.1 Ground-based measurements of plant water stress and leaf spectral reflectance 72
4.3.2 Relationships identified at the leaf-level 82
4.3.2.1. Maximal models identified at leaf-level 82
4.3.2.2. Model refinements using stepwise regression 87
4.3.2.3. Selection of the best model 88
4.3.2.4. Validation of the selected model 89
4.4 Discussion 91
4.5 Conclusions 93

CHAPTER 5. EVALUATION OF MEDIUM TO HIGH RESOLUTION SATELLITE EARTH OBSERVATION DATA TO DETECT SPATIAL PATTERNS OF PLANT WATER STRESS 94

5.1 Introduction 96
5.2 Materials and Methods 100
5.2.1 Selection and requisition of satellite earth observation data 100
5.2.2 Selection and derivation of vegetation spectral reflectance indices 102
5.2.3 Analysis of data 103
5.3 Results 104
5.3.1 Ground-based measurements of plant water stress 104
5.3.2 Relationships identified using multispectral satellite data 113
5.3.2.1. Maximal models identified using multispectral satellite data 113
5.3.2.2. Model refinements using stepwise regression 114
5.3.2.3. Selection of the best multispectral satellite model 114
5.3.2.4. Validation of the best model using multispectral satellite data 117
5.3.3 Relationships identified using hyperspectral satellite data 118
5.3.3.1. Maximal models identified using hyperspectral satellite data 118
5.3.3.2. Model refinements using stepwise regression 119
5.3.3.3. Selection of the “best” model derived from hyperspectral satellite data 120

5.3.3.4. Validation of the "best" model derived from hyperspectral satellite data 121
5.4 Discussion 123
5.5 Conclusions 125

CHAPTER 6. EVALUATION OF AIRBORNE MULTISPECTRAL AND HYPERSPECTRAL REMOTE SENSING DATA TO DETECT SPATIAL PATTERNS OF PLANT WATER STRESS 126

6.1 Introduction 127
6.2 Materials and methods 129
6.2.1 Airborne remote sensing surveys 129
6.2.2 Spectrometer measurements 132
6.2.3 Selection and derivation of the vegetation spectral reflectance indices 132
6.2.4 Analysis of data 134
6.3 Results 135
6.3.1 Relationships identified using airborne multispectral data 135
6.3.1.1. Maximal models identified using airborne multispectral data 135
6.3.1.2. Model refinements using stepwise regression 138
6.3.1.3. Selection of the best model derived from airborne multispectral data 138
6.3.1.4. Validation of the best airborne multispectral data 140
6.3.2 Relationships identified using airborne hyperspectral data 142
6.3.2.1. Maximal models identified using airborne hyperspectral data 142
6.3.2.2. Model refinements using stepwise regression 143
6.3.2.3. Selection of the best model derived from airborne hyperspectral data 143
6.3.2.4. Validation of the best model derived from airborne hyperspectral data 145
6.4 Discussion 147
6.5 Conclusions 148

CHAPTER 7. CORRELATION OF PLANT STRESS PATTERNS TO SITE CHARACTERISTICS IN THREE GOLD MINING DISTRICTS IN CENTRAL SOUTH AFRICA 150

7.1 Introduction 152
7.2 Materials and methods 153
7.2.1 Vegetation classification 153
7.2.2 Mapping spatial patterns of unstressed trees 158
7.2.3 Creation of spatial layers of site characteristic data 167
7.3 Results 168
7.3.1 Differences between the site characteristic data of stressed and unstressed sites 168
7.4 Discussions and recommendations for future plantings 174
7.5 Conclusions 190

CHAPTER 8. GENERAL SYNTHESIS, CONCLUSIONS AND RECOMMENDATIONS 193

8.1 Literature review concluding statements 193

8.2 General synthesis on vegetation spectral reflectance indices 194
8.3 Concluding remarks 196
8.4 Recommendations 197

REFERENCES **200**

APPENDICES

Appendix 1	Review paper
Appendix 2	Protocols for ground-based measurements of plant water stress
Appendix 3	Results of the complete regression analysis
Appendix 4	Observation points used to create interpolated hydrochemistry surfaces
Appendix 5	Interpolated surfaces used to characterise unstressed sites in each mining district
Appendix 6	Differences in xylem vessel characteristics and wood density resulting from plant stress

TABLES

Table 2.1 Characteristics of the tree species sampled in this study. (Compiled from Poynton, 1979; Venter and Venter, 1996). 21

Table 2.2 Description of the Welkom, Vaal River and West Wits mining districts. 23

Table 2.3 Description of sample sites in the Welkom (W), Vaal River (VR) and West Wits (WW) mining districts. (Data obtained through field surveys and from AngloGold Ashanti, 2004). 29

Table 3.1 Some milestones in the historical development of the relationships of vegetation spectral reflectance characteristics in specific regions of the electromagnetic spectrum. 40

Table 3.2 Advantages and disadvantages of four ground-based methods for measuring plant water stress. 58

Table 4.1 Spectral wavelengths and reflectance indices used in the leaf-level analysis. 68

Table 4.2 Measurements of plant stress undertaken in the Welkom, Vaal River and West Wits mining districts during July 2004. 75

Table 4.3 Adjusted R^2 values ranked in descending order for each maximal model derived between plant water stress measurement (Y) and spectral reflectance index (X) resulting from leaf-level data. 83

Table 4.4 Comparison of the maximal and stepwise regression models obtained in the leaf-level analysis, for the three models with the highest adjusted R^2 values exceeding 50%. 87

Table 4.5 Validation models used in the leaf-level analysis to predict chlorophyll b. 90

Table 5.1 Spectral wavelengths and reflectance indices derived from the satellite earth observation data. 103

Table 5.2 Ground measurements of plant stress undertaken during July 2005 in the Welkom, Vaal River and West Wits mining districts. 106

Table 5.3 Ground measurements of plant stress undertaken during August 2005 in the Welkom, Vaal River and West Wits mining districts. 108

Table 5.4 Adjusted R^2 values, ranked in descending order, for each maximal model determined between plant water stress methods (Y) and spectral reflectance index (X) derived from Proba Chris satellite data. 113

Table 5.5 Comparison of the maximal and stepwise regression models derived using Proba Chris satellite data. 114

Table 5.6 Validation models derived from multispectral satellite data used to predict predawn leaf water potential. 117

Table 5.7 Adjusted R^2 values, ranked in descending order, for each maximal model derived between plant water stress measurement (Y) and spectral reflectance index (X) derived from Hyperion satellite data. 119

Table 5.8 Comparison of the maximal and stepwise regression models, obtained in the Hyperion satellite data analysis for the three models with the highest adjusted R^2 values exceeding 50%. 120

Table 5.9 Validation models, derived from hyperspectral satellite data, used to predict predawn leaf water potential in the West Wits mining district. 122

Table 6.1 Spectral wavelengths and reflectance indices derived from the airborne multispectral and hyperspectral remote sensing data. 133

Table 6.2 Adjusted R^2 values, ranked in descending order, for each maximal model derived between plant water stress measurement (Y) and spectral reflectance indices (X) derived from airborne multispectral data. 137

Table 6.3 Validation models used to predict carotenoid content using airborne multispectral data. 141

Table 6.4 Adjusted R^2 values, ranked in descending order, for each maximal model determined between plant water stress measurement (Y) and the spectral reflectance indices (X) derived from airborne hyperspectral data. 142

Table 6.5 Comparison of the maximal and the step-wise regression models, derived from the airborne hyperspectral data, with the highest adjusted R^2 values exceeding 50%. 143

Table 6.6 Validation models used to predict predawn leaf water potential, using airborne hyperspectral data. 146

Table 7.1 Accuracy assessments of the supervised classifications for the Vaal River mining district. 155

Table 7.2 Accuracy assessments of the supervised classifications for the Welkom mining district. 156

Table 7.3 Accuracy assessments of the supervised classifications for the West Wits mining district. ____156

Table 7.4 Best performing spectral reflectance models derived from leaf, satellite and airborne remote sensing data._____158

Table 7.5 Comparisons (mean+standard deviation) of the site characteristics geology, soils, salinity and groundwater table level between stressed and unstressed trees of Eucalyptus camaldulensis and Searsia lancea in the Welkom mining district. Differences between stressed and unstressed trees per species were tested using t-tests (P<0.05. _____169

Table 7.6 Comparisons (mean+standard deviation) of the site characteristics geology, soils, salinity and groundwater table level between stressed and unstressed trees of Eucalyptus camaldulensis and Searsia lancea in the Vaal River mining district. Differences between stressed and unstressed trees per species were tested using t-tests (P<0.05).____171

Table 7.7 Comparisons (mean+standard deviation) of the site characteristics such as geology, soils, salinity and groundwater table level between stressed and unstressed trees of Eucalyptus camaldulensis and Eucalyptus sideroxylon in the West Wits mining district. Differences between stressed and unstressed trees per species were tested using t-tests (P<0.05).____172

Table 7.8 Descriptive statistics (minimum, maximum, mean, standard deviation) of the site variables geology, soils, salinity and groundwater table level used to characterise unstressed trees per species in each mining district._____174

FIGURES

Figure 2.1 Geographical location of the mining districts selected for the study demarcated in red, in relation to South Africa._____22

Figure 2.2 Geological formations within (a) Vaal River and (b) West Wits study areas. (Data obtained from AngloGold Ashanti, 2004).____ _____25

Figure 2.3 Sampling sites selected in each mining district. Shaded circles represent the location of each sampling site (Google Earth, 2008).____ _____27

Figure 2.4 Sampling sites in Welkom (a and b), West Wits (c and d) and Vaal River (e to i) mining district. Arrows represent the location of trees at each sampling site in each mining district. Samplings sites are illustrated as stands of trees (a, b, c, f), small-plot species trials (d), clumps (e, g) and rows of trees (h, i). (Images obtained from Land Resources International, 2005).____ _____28

Figure 3.1 Typical reflectance sensitivities as controlled by leaf pigments, cell structure and water content. (Adapted from Gaussman, 1977).____39

Figure 4.1 Box plots of plant water stress measurements a) predawn leaf water potential, b) photochemical efficiency, c) chlorophyll a content, d) chlorophyll b content e) total chlorophyll (a+b) content and f) carotenoid content for Vaal River, Welkom and West Wits._____78

Figure 4.2 Box plots of plant water stress measurements a) predawn leaf water potential, b) photochemical efficiency, c) chlorophyll a content, d) chlorophyll b content e) total chlorophyll (a+b) content and

f) carotenoid content for the three tree species E. camaldulensis, E. sideroxylon and S. lancea. 80

Figure 4.3 Typical average leaf reflectance spectra with standard deviation error bars (a) E. camaldulensis measured in Vaal River near the Western Complex tailing storage facility, (b) E. sideroxylon measured in West Wits and, (c) S. lancea measured in Welkom. 81

Figure 4.4 Standardised residual plot of fitted values of chlorophyll b content using the DATT spectral reflectance model. 89

Figure 5.1 Box plots of plant water stress measurements a) predawn leaf water potential, b) photochemical efficiency, c) total chlorophyll (a+b) content, d) carotenoid content and e) relative leaf water content undertaken for Vaal River, Welkom and West Wits in July 2005. 110

Figure 5.2 Box plots of plant water stress measurements a) predawn leaf water potential, b) photochemical efficiency, c) total chlorophyll (a+b) content, d) carotenoid content and e) relative leaf water content measured for E. camaldulensis, E. sideroxylon and S. lancea in July 2005. 112

Figure 5.3 Standardised residual plot of fitted values of predawn leaf water potential using the green normalised difference vegetation spectral reflectance model. 116

Figure 5.4 Standardised residual plot of fitted values of predawn leaf water potential using water band spectral reflectance model 121

Figure 6.1 Location of multispectral and hyperspectral surveys in the Welkom, Vaal River and West Wits mining districts. Multispectral survey areas are patterned, while hyperspectral survey areas are unshaded. 130

Figure 6.2 Standardised residual plot of fitted values of carotenoid content using the green waveband spectral reflectance model. 140

Figure 6.3 Standardised residual plot of fitted values of predawn leaf water potential spectral reflectance model. 145

Figure 7.1 Spatial patterns of unstressed Eucalyptus camaldulensis sites mapped in the Welkom mining district using the Predawn leaf water potential and the Green normalized difference vegetation index derived from Proba Chris satellite imagery. 160

Figure 7.2 Spatial patterns of unstressed Searsia lancea sites mapped in the Welkom mining district using the Predawn leaf water potential and the Green normalized difference vegetation index derived from Proba Chris satellite imagery. 161

Figure 7.3 Spatial patterns of unstressed Eucalyptus camaldulensis sites mapped in the Vaal River mining district using the Predawn leaf water potential and the Green normalized difference vegetation index derived from Proba Chris satellite imagery. 163

Figure 7.4 Spatial patterns of unstressed Searsia lancea sites mapped in the Vaal River mining district using the Predawn leaf water potential and the Green normalized difference vegetation index derived from Proba Chris satellite imagery. 164

Figure 7.5 Spatial patterns of unstressed Eucalyptus camaldulensis sites mapped in the West Wits mining district using the Predawn leaf water potential and the Green normalized difference vegetation index derived from Proba Chris satellite imagery. 165

Figure 7.6 Spatial patterns of unstressed Eucalyptus sideroxylon sites mapped in the West Wits mining district using the Predawn leaf water potential and the Green normalized difference vegetation index derived from Proba Chris satellite imagery. 166

Figure 7.7 A shaded selection of unstressed areas in the Welkom mining district recommended for planting Eucalyptus camaldulensis and Searsia lancea tree species. The graded scale represents the maximum (light grey) and minimum (black) values of site characteristic data representative of these unstressed areas. 177

Figure 7.8a Dankbaar Pan resistivity sampling site in the Welkom mining district, (clockwise) arrows in the picture represent the location of trees at each sampling site; the block demarcated in red represents the resistivity sampling area; unstressed areas mapped in green and the resistivity profile observed at the sampling site. 178

Figure 7.8b Boet Van Der Berg Farm resistivity sampling site in the Welkom mining district, (clockwise) arrows in the picture represent the location of trees at each sampling site; block demarcated in red represents the resistivity sampling area; unstressed areas mapped in green and the resistivity profiles observed on the farm at the S. lancea and E. camaldulensis sampling areas. 179

Figure 7.9 A shaded selection of unstressed areas in the Vaal River mining district recommended for planting Eucalyptus camaldulensis and Searsia lancea tree species. The graded scale represents the maximum (light grey) and minimum (black) values of site characteristic data representative of these unstressed areas. 182

Figure 7.10 Western Complex resistivity sampling site in the Vaal River mining district, (clockwise) arrows in the picture represent the location of trees at each sampling site; block demarcated in red represents the resistivity sampling area; unstressed areas mapped in green and the resistivity profile observed near the tailing storage facility. 183

Figure 7.11 A shaded selection of unstressed areas in the West Wits mining district recommended for planting Eucalyptus camaldulensis and Eucalyptus siderxylon tree species. The graded scale represents the maximum (light grey) and minimum (black) values of site characteristic data representative of these unstressed areas. 185

Figure 7.12aDeelkraal farm resistivity sampling site in the West Wits mining district, (clockwise) arrows in the picture represent the location of trees at each sampling site; block demarcated in red represents the resistivity sampling area; unstressed areas mapped in green and the resistivity profile observed at the site. 186

Figure 7.12bElandsridge resistivity sampling site in the West Wits mining district, (clockwise) arrows in the picture represent the location of trees at each sampling site; block demarcated in red represents the resistivity sampling area; unstressed areas mapped in green and the resistivity profile observed downslope from the tailing storage facility. 188

CHAPTER 1. GENERAL INTRODUCTION

1.1 RESEARCH PROBLEM

In South Africa deep-level gold mining is characterised by the production of extensive tailing storage facilities (TSFs), which contain large quantities of slimes consisting of pulverised rock and water contaminated with salts and a wide range of other inorganic pollutants (Weiersbye *et al*., 2006). Approximately 400 km^2 of the Witwatersrand Basin gold fields are covered with more than 200 gold TSFs (Rosner *et al*., 2001) and contaminated areas left behind after removal and reprocessing of the original TSFs (Chevrel *et al*., 2003). It is estimated that the Witwatersrand Basin contains six billion tons of gold and uranium tailings (Chevrel *et al*., 2003), 430 000 tons of uranium (Council of Geoscience, 1998; Winde, 2004a; b; c) and approximately 30 million tons of sulphur (Witkowski and Weiersbye, 1998a). In South Africa approximately 488 million tons of waste is generated by the mining industry per year (Gaia, 2003). Of this waste, 105 million tons per annum is generated by the gold mining industry in the Witwatersrand Basin at an average rate of 200 tons of waste per ton of gold (Department of Tourism, Economic and Environmental Affairs, 2002; Chamber of Mines of South Africa, 2004).

Van As (1992) reported on the significant environmental hazards resulting from the storage of highly pulverised pyrite rock waste in TSFs within the gold and uranium mining regions of South Africa (Straker *et al*., 2007). Lands adjacent to such TSFs become polluted through near-surface seepage, and this is enhanced by the movement of polluted groundwater in shallow aquifers that are commonly 1-30 m below ground (Funke, 1990; Hodgson *et al*., 2001; Rosner *et al*., 2001; Naicker *et al*., 2003). Environmental degradation spreads far beyond the TSFs in the form of dust pollution (Van As *et al*., 1992) as well as seepage from TSFs, and impacts severely on nutrient cycling in polluted soils (Witkowski and Weiersbye,1998b; Weiersbye *et al*., 2006). Furthermore, TSFs are highly susceptible to erosion as they are elevated above the ground with steep slope angles (Mizelle *et al*., 1996).

Erosion losses are as much as 30 times more from the slopes of gold TSFs than from agricultural fields, and may exceed 500 tons per hectare per year (Blight, 1991).

The impact of the mines and the TSFs extends far beyond their localities as a result of dust pollution and the extent of groundwater plumes (Cogho *et al*., 1990). It has been estimated that 400 Ml/day of water passes through all the major gold mines, with 260 Ml/day passing into groundwater and 130 Ml/day into surface waters (Pulles, 1992). The Vaal River catchment receives a large proportion of the pollutants from gold mining activities, with consequent acidification and salinisation of surface and ground waters. Total pollution discharges to the Vaal River catchment were estimated to be at a rate of 170 000 t/annum of salts (Best, 1985), whereas discharges from the Free State gold mines beyond the Vaal catchment were estimated at 350 000 t/annum of salts (Cogho *et al*., 1990).

The total dissolved solid (TDS) concentrations of three plumes were reported for Welkom in the Free State Province, at Vaal River located in the North West Province, and at West Wits located in Gauteng, in South Africa (Vivier *et al*., 2001). The TDS of the Mahemspruit plume in Welkom averaged 18 000 mg/l and extends over 30 000 ha (Van Rensburg, 2001). The Bokkamp-West Complex groundwater plume in Vaal River near Orkney was reported to have a mean TDS concentration of 3 500 mg/l (Vivier *et al*., 2001) which underlies an area of 1800 ha, and the West Wits groundwater plume near Carletonville underlies a larger area compared to Bokkamp-West Complex groundwater plume with TDS concentrations of 1000 to 3000 mg/l (Vivier *et al*., 2001). These TDS concentrations indicate that this water should not be utilised for farming or for drinking purposes.

The application of engineering solutions to the problem of the spread of contaminants is generally impractical. Lining of TSFs to prevent rainfall infiltration and reduce seepage is not always feasible due to the high cost of materials, probability of failure of the lining and inability to repair lined TSFs (United States Environmental Protection Agency, 1997). TSFs could continue to leak water from their cores for decades to come, even if their surfaces are covered. Furthermore, due to the vast areas covered by TSFs, the method of pumping and treating contaminated groundwater is an impractical solution, as costs would necessarily

continue to be incurred long after mine closure (United States Environmental Protection Agency, 1997).

The Mine Woodlands Project is aimed at assessing the feasibility of establishing trees in belts and blocks close to the TSFs and across major seepage routes in order to contain groundwater seepage and reduce movement of pollutants to streams and rivers. The purpose of these tree belts is to absorb and transpire greater quantities of water than the grasslands and wetlands presently in close proximity to the TSFs, thereby reducing water table depths and slowing lateral flow into the surrounding lands. The trees will also be used for pollutant sequestration around the TSFs.

Many tree species continue transpiring water throughout the year. This is in contrast to seasonally dormant grasslands and wetlands (Dye *et al*., 2005; Bell, 2006). Many tree species also have the ability to develop deep root systems that are able to penetrate fissured subsoil strata to reach groundwater (Bell, 2006). Therefore, such species would annually absorb and transpire greater quantities of water than seasonally dormant shallow rooted grasslands and wetland plants.

Some tree species also have physiological characteristics that allow them to grow in polluted soils and water (Dickinson *et al*., 2000; Meagher *et al*., 2000). Such species of trees can take up and sequester a significant proportion of contaminants in the tree biomass (Pepper and Craig, 1986). In addition, certain species are tolerant of saline conditions which may develop in the rooting zone as large quantities of groundwater are absorbed by the tree roots over time (George *et al*., 1999). Therefore the use of tree belts to contain groundwater seepage and reduce the movement of pollutants to streams and rivers has been promoted (Pepper and Craig, 1986; George *et al*., 1999; Dickinson *et al*., 2000; Meagher *et al*., 2000).

Various species trials and block plantings have been established at different locations in the Welkom, Vaal River and West Wits mining districts. In 2002, approximately 20 species of indigenous and 20 species of non-native trees were planted (Weiersbye *et al*., 2002). There are several existing laws which ensure that landowners and users have a legal obligation to

control invader plants and weeds on their lands; this includes regulation in terms of the Conservation of Agricultural Resources Act, 1983 (ACT No. 43 of 1983). The Conservation of Agricultural Resources Act (CARA) regulates various activities that may have an impact on agricultural resources, including water sources, and deals directly with the combating of invader plants and weeds. Regulations 15 and 16 under this Act, which concern problem plants, were amended during March 2001. CARA is currently in the process of being revised by the Department of Agriculture Forestry and Fisheries. The amended regulations make provision for four groups: declared weeds (Category 1 plants), plant invaders (Category 2 and Category 3 plants) and indicators of bush encroachment. The first three groups consist of undesirable alien plants and are covered by Regulation 15. Bush encroachers, which are indigenous plants that require sound management practices to prevent them from becoming problematic, are covered separately by Regulation 16.

Category 1 may not occur on any land or on any inland water surface in South Africa except with written permission or in an approved bio control reserve. Category 2 are plants with the proven potential of becoming invasive, but which nevertheless have certain beneficial properties that warrant their continued presence in certain circumstances which includes several species of pines, wattles, eucalyptus, that are more commonly grown for commercial purposes or viable woodlots, fire belts, building material, animal fodder or soil stabilisation. Category 3 are generally ornamental plants which may be retained but no new planting, trade or propagating of these plants are permitted. Therefore, non-native tree species selected for planting comprised mainly CARA-listed (Category 2) acacias, poplars, pines and eucalypts (Weiersbye *et al.*, 2002). These species were selected because of their potential for fast growth and survival in the harsh highveld environment. The success of these plantings, and future block plantings, depends on the trees quickly establishing contact with the groundwater. Should they fail, rates of growth and water use will be severely limited by low rainfall and low soil water availability, and the trees will be ineffective in reducing the rate of spread of the polluted water.

There is limited information to indicate where tree roots will be able to penetrate down to groundwater, and which sites will prove unsuitable due to impenetrable subsoils, deep or no

water tables, or poor groundwater quality. Due to the low mean annual rainfall characteristic of these regions, ranging from 497 to 651 mm, attempts to establish trees on unsuitable sites which may be characterised by deep or no water tables, impenetrable soils or poor groundwater quality could lead to considerable planting losses. Therefore, knowledge of the relation between site types, and the ability of stands of trees to access groundwater and survive is crucial. Important site characteristics are likely to include depth to water table, subsoil permeability, the extent of fissuring in the rock strata, groundwater electrical conductivity levels, the presence of impervious soil and subsoil layers, and the degree to which the site is influenced by surface water drainage patterns (Weiersbye *et al*., 2002).

The purpose of this study is to develop an understanding of remote sensing technologies which will contribute to detecting trees which are not experiencing winter-time water stress, and which could lead to identifying potential sites which could assist in the sustainable containment or reduction of contaminated seepage water from TSFs.

1.2 RESEARCH STRATEGY

The Mine Woodlands Project was initiated in 2001 to investigate hydrological control and pollutant sequestration on and beyond the TSFs using trees in belts and blocks planted close to the TSFs to contain contaminated mine water (Weiesbye *et al*., 2002). It is hoped that such information will be used to develop plans for mine closure, which are based on appropriate geochemical and geohydrological backgrounds. As new mining operations are commissioned and developed, in some older mines the ore-extracting activities of the mines cease and are closed. However, from an environmental perspective, true closure may often only be achieved long after the mine operations have ceased and involves extensive planning which includes rehabilitation plans and close collaboration with regulatory authorities inorder to obviate any negative environmental consequences and satisfy regulatory requirements (AngloGold Ashanti, 2004a). A component of the Mine Woodlands Project, covered by this research, involved the measurement and detection of plant water stress using remote sensing technologies, and the recommendation of suitable sites for future block

plantings, where trees would most likely not experience stress during the dry season, thereby resulting in higher annual evapotranspiration and a greater impact on seepage containment.

The research strategy was based on the principle that differences in tree water status during the dry season are likely to be the best indicators of groundwater access by trees (Bordiert, 1994; O'Grady *et al*., 1999; Timmermans and Meijerink, 1999). Several different techniques are available for measuring the degree of water stress experienced by trees. This strategy was based on the assumption that one of the most practical and convenient techniques for this purpose was to utilise remote sensing to detect differences in the spectral reflectance properties of leaves and canopies. The literature shows that such changes are readily detected in a wide range of plant species, and that they are generally linked to the degradation of leaf chlorophyll (Curran *et al*., 1990; Gitelson and Merzylak, 1996; Lichtenthaler *et al*., 1996; Blackburn, 1998a; Blackburn, 1998b; Blackburn, 1999; Datt, 1999; Stone *et al*., 2001) and often the results being specific to the tree species investigated.

Although the main focus of the research was to measure and detect plant water stress using remote sensing technologies with ground-truthing techniques, the influence of specific elements, namely chloride and sulphate concentrations in the groundwater, was recognised as important, as several studies on the surrounding lands and water systems of the Welkom, Vaal River and West Wits mining district have illustrated increasing salinity levels over the years (Roos and Pieterse, 1995; Viver *et al*., 2001; Naicker *et al*., 2003; Winde *et al*., 2004a,b,c).

1.3 AIMS AND OBJECTIVES

The principal aim of this thesis was to develop an understanding and evaluate various remote sensing technologies which could contribute to detecting trees which are not experiencing winter-time plant water stress, potentially resulting in higher annual evapotranspiration and a greater impact on contaminated seepage water. This could lead to identifying and prioritising sites for the establishment of future plantings to assist in containing and reducing contaminated seepage water from the TSFs.

This was broken down into a series of more specific aims:

1. Identify trees which were stressed and unstressed during the dry winter season using four commonly used ground-based measurements of plant water stress and various remote sensing technologies.
2. Evaluate different remote sensing technologies operating at different spatial and spectral scales for predicting spatial patterns of trees not experiencing winter-time plant water stress (unstressed trees).
3. Link the spatial distribution of unstressed trees to particular site characteristics that may be recognised and used to prioritise sites for the establishment of future block plantings.

In order to achieve these aims, the following research objectives were identified:

1. To characterise the most common non-native (alien) and indigenous tree species growing in close proximity to TSFs as stressed or unstressed, using four commonly used ground-based measurements of plants water stress, *viz.* predawn leaf water potential, relative leaf water content, chlorophyll and carotenoid pigment, and chlorophyll fluorescence.
2. To acquire spectral reflectance data using hand-held spectroscopy, satellite and airborne remote sensing data sources from both stressed and unstressed sample trees occurring on a range of WBC gold mining sites.
3. To extract and derive from each remote sensing data source, the individual spectral reflectance wavelengths and vegetation spectral reflectance indices, which have been shown in the literature to be useful for detecting plant water stress, plant pigment content, the presence of stress related pigments in vegetation, and changes in leaf cellular structure.
4. To use multiple linear regressions to investigate spectral models for predicting plant water stress when using indices derived from the hand-held, satellite and airborne

remote sensing data and the four commonly used ground-based measurements of plant water stress.

5. To evaluate and select appropriate spectral models when using earth observation data (airborne and satellite) to map the spatial distribution of trees that were not stressed during the dry season.
6. To link and analyse the spatial distribution of unstressed trees (groundwater linked trees) in relation to particular site characteristics such as average soil depth, percent clay in the topsoil, groundwater chloride and sulphate concentrations, total dissolved solids, groundwater electrical conductivity and groundwater water level.
7. Use remote sensing and geographical information system analyses to make spatial recommendations on a selection of sites/locations within the three mining districts where tree plantations are likely to avoid dry season stress, potentially have higher annual evapotranspiration and could then assist in the sustainable containment or reduction of contaminated seepage water from TSFs.

In this study, it is assumed that trees currently growing in close proximity to TSFs that have free access to groundwater will not experience plant water stress during the dry winter season (Bordiert, 1994; O'Grady *et al*., 1999; Timmermans and Meijerink, 1999).

Trees growing in stands or blocks (such as those saplings planted in recent years and more envisaged in future tree belts) are expected to experience a relatively higher degree of competition from neighbouring trees, and without access to groundwater, would experience dry season water stress more readily than trees growing singly or in isolated rows (Shackleton, 2002; Lawes *et al*., 2008; Meyer *et al*., 2008; Giovanni, 2009). Although patterns of stress development in closed-canopy plantations are expected to be very informative about the accessibility of groundwater to tree roots (Hatton *et al*., 1998; Dye *et al*., 2001), unfortunately stands or blocks of mature trees are scarce at present in the WBG mining areas. Thus, this research was heavily dependent on trees growing singly, in rows or in small groups, which experienced lower levels of competition from neighbouring plants. Furthermore, these trees would have had a greater opportunity for extending root systems

laterally, and the link between dry season tree water stress and groundwater accessibility might have been influenced, and was considered when interpreting the results.

1.4 HYPOTHESES

The two hypotheses proposed for this research study were:

- Trees with access to contaminated groundwater plumes will exhibit certain physiological and structural differences to trees with no access to such groundwater. It was hypothesised that trees with no access to groundwater, those which are considered to be experiencing dry season water stress, will exhibit different spectral reflectance characteristics with lower predawn leaf water potentials (more negative), lower relative leaf water content, lower leaf chlorophyll content, lower leaf chlorophyll fluorescence and reduced xylem vessel diameters.
- It was also hypothesised that the characteristics of sites on which trees have access to groundwater can be used as the criteria for site suitability for the establishment of future tree belts.

1.5 REPORTING STRUCTURE

The information contained in this thesis has been partitioned into reviews and research chapters, which will be submitted to accredited journals for publication.

In *Chapter 1* the research background and problem, research strategy, aims and objectives and hypotheses are presented.

Chapter 2 describes the tree species and study areas selected for this study.

Chapters 3 to 6 present the content of individual research papers. These chapters, together with chapter 7, comprise the core of this study.

Chapter 3 is a review of ground-based and remote sensing-based methods to detect plant water stress in plants.

Chapter 4 reports on the potential of hand-held spectroscopy as a tool for identifying plant water stress at the leaf-level. The results of the hand-held spectrometry measurements and ground-truthing used to interpret leaf spectral reflectance characteristics are presented and discussed in this chapter.

Chapters 5 provides a broader evaluation of satellite remote sensing technologies to detect patterns of winter-time plant water stress, together with the results of concurrent ground-truthing measurements.

Chapters 6 reports on the multispectral and hyperspectral airborne investigations which were undertaken to detect and map spatial patterns of winter-time plant water stress.

Chapter 7 presents the analysis of spatial patterns of trees not experiencing winter-time plant stress inferred from remote sensing investigations to site characteristics in the WBG mining environments. This chapter includes recommendations on which sites are most suitable for tree establishment around TSFs to reduce contaminated groundwater table levels and seepage.

Chapter 8 is a consolidation of the entire research study providing a general synthesis, concluding remarks, and recommendations relating to the research.

References associated with each chapter are listed after chapter 8.

Given that most of these chapters are structured in order to be published as journal papers, there is some degree of repetition in terms of the study sites and methods, although this has been kept to a minimum. Differences in xylem vessel and wood density characteristics resulting from plant stress are presented and discussed in Appendix 6.

CHAPTER 2. TREE SPECIES SELECTION AND STUDYAREAS

2.1 INTRODUCTION

In this research, tree species were selected for sampling in the AngloGold Ashanti mining districts in the Gauteng, North-West and Free State Provinces. Within each mining district, sampling sites were selected for ground-based measurements of plant water stress and remote sensing surveys.

2.2 SELECTION OF TREE SPECIES

Only a few tree species are able to grow and survive in the harsh conditions experienced in the mining environments. Tree plantations or large stands of mature trees are scarce in the WBG mining areas. Therefore, stands or blocks of trees within the study areas districts are limited, with some clumps or rows of indigenous and non-native tree species growing in close proximity to TSFs.

Research studies on the indigenous and non-native tree species appropriate for the mining environment was undertaken in the Sustainable Vegetation of Gold Slimes Dam Project (Weiersbye, 2002). These studies provided scientific information for the selection and production of plant species for the silvicultural and geohydrological trials in the Mine Woodlands Project. Indigenous species were preferred compared to non-native and invasive plant species. However, research suggests that certain non-native species, particularly *Eucalyptus* and *Pinus* species, transpire larger quantities of water than indigenous species (Dye, 2002; Whitehead and Beadle, 2004).

Several criteria were considered when selecting trees species for the Mine Woodlands project, which included: plant availability, easy establishment and ability to stabilise the

landscape, fast growth to promote early contact with groundwater, deep rooted systems, high transpiration rates, high tolerance to high electrical conductivity levels, heavy metals, low nutrient levels and frost, low invasive potential, reasonable wood quality, indications of good survivorship under current TSF conditions, ability to reduce infiltration and recharge of groundwater sources, reduce wind erosion, and capable of pollutant sequestration (Weiersbye and Witkowski, 1998a; Weiersbye *et al.*, 2006). The non-native tree species *Eucalyptus sideroxylon* A. Cunningham ex Woolls, *Eucalyptus camaldulensis* Dehnhardt, and the indigenous species *Searsia lancea* L.f., which are relatively common throughout these mining areas, and which have displayed good survivorship to many of the factors listed above, were selected for this study.

E. camaldulensis and *E. sideroxylon* are native to Australia, but have been distributed throughout the world, including countries in southern Africa such as Angola, Botswana, Lesotho, Malawi, Mozambique, Zimbabwe and South Africa (Poynton, 1979). Eucalypts, in general, are adapted to a wide range of climates occurring naturally from latitude 7º 00´N to 43º 39´S and from sea level to about 1 800 m (Poynton, 1979). They grow in regions where rain falls only during the warmer months, to regions in which rainfall is uniformly distributed or confined to the cooler seasons of the year (Poynton, 1979). Furthermore, they also grow in humid forested areas, where rainfall averages 3 000 mm or more per year, as well as in semi-desert regions in which less than one tenth of such mean annual rainfall is expected (Poynton, 1979).

S. lancea is indigenous to Zambia, Zimbabwe, Swaziland and parts of South Africa. This species has adapted to the lower rainfall regions of southern Africa (Venter and Venter, 1996). It grows in the Western Cape Province, with a mean annual rainfall of 348 mm, as well in the Free State Province, with a mean annual rainfall of 532 mm (Schulze *et al.*, 1997). *S. lancea* is particularly common in the Vaal River (VR) and Welkom (W) area, but less common in West Wits (WW) area. This species has been planted in rows along the perimeter of numerous TSFs to provide partial screening. It also occurs in the drier regions of the Kalahari and Karoo and is often found in suburbs or gardens of southern Africa (Venter and Venter, 1996).The three species *E. camaldulensis*, *E. sideroxylon* and *S. lancea* chosen for this study are known to generally grow well on sites that are in close proximity to

the TSFs and thus clearly have the necessary physiological characteristics to ensure their survival. They are all evergreen with dense canopies, which potentially promote continuous and high evaporation rates throughout the year. The eucalyptus species are fast growing, and are highly tolerant of arid or infertile sites, and acidic or saline soils (Poynton, 1979). *S. lancea* is also characterised as being hardy, frost resistant and is also highly adaptable to poorly drained soil conditions. Table 2.1 provides a list of the characteristics of the three species as reported by Poynton (1979) and by Venter and Venter (1996).

Table 2.1 Characteristics of the tree species sampled in this study. (Compiled from Poynton, 1979; Venter and Venter, 1996).

Characteristic	**Tree Species**		
	Eucalyptus camaldulensis	***Eucalyptus sideroxylon***	***Searsia lancea***
Common name	River red gum	Red ironbark	African sumac or Karee
Family	Myrtaceae	Myrtaceae	Anacardiaceae
Deciduous/ Evergreen	Evergreen	Evergreen	Evergreen
Form	Tall, single stemmed	Tall, single stemmed	Round, single or multi-stemmed, dense canopy when young
Leaf shape and colour	Lance shaped, simple 250 mm long, blue grey colour	Lance shaped, simple, dull greyish colour	Trifoliate (compound with 3 leaflets), lance shaped leaflets, dark green above and pale green below
Leaf texture	Membranous, thick and leathery	Membranous, thick and leathery	Leathery
Mature tree height (m)	30 – 40	10 – 30	7
Non-native/Indigenous	Non-native	Non-native	Indigenous
Wood type	Hard	Very hard	Hard
Bark type	Smooth bark, white or greyish in colour, except at the trunk base where often the bark is rough	Hard furrowed bark, dark brown to black colour	Coarse textured bark, dark grey or brown colour

2.3 MINING DISTRICTS

The three gold mining districts located in central and north-western South Africa investigated in this study include Welkom (27º57´S, 26º34´E) in the Free State Province,

Vaal River (26º55´S, 26º40´E) located in the North West Province, and West Wits (26º25´S, 27º21´E) located in Gauteng (Figure 2.1).

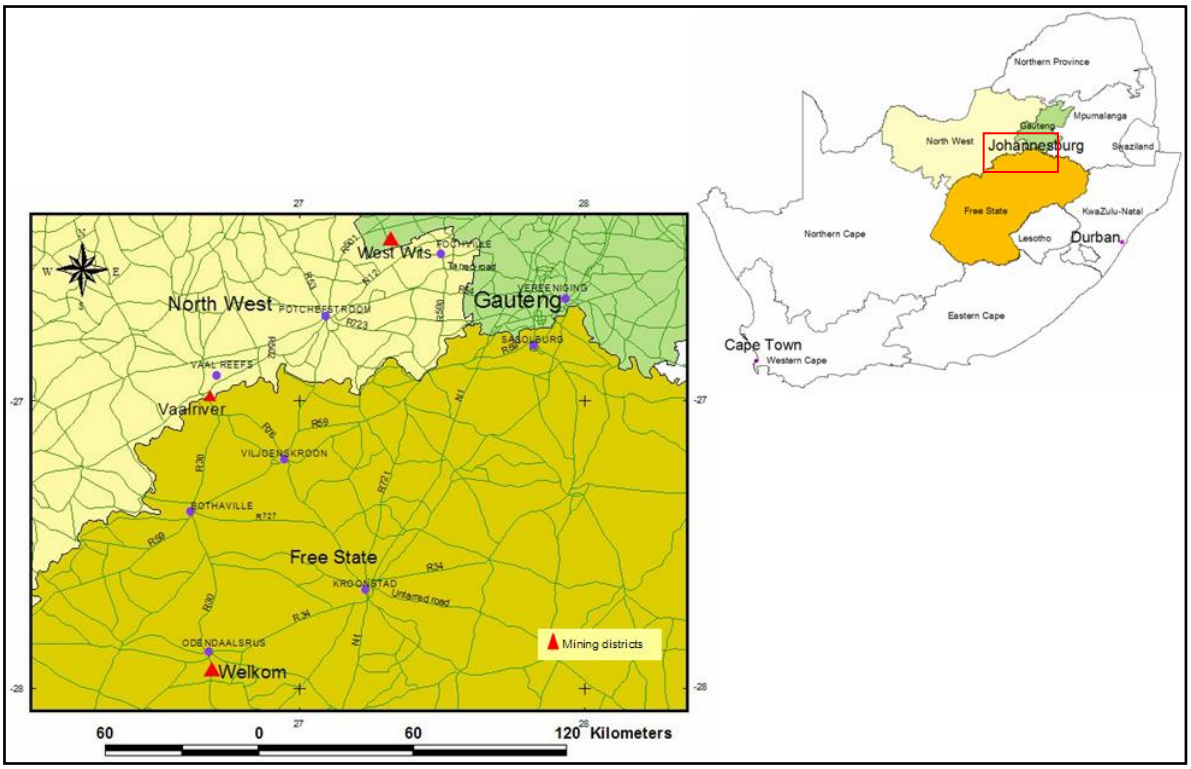


Figure 2.1 Geographical location of the mining districts selected for the study demarcated in red, in relation to South Africa.

A general description of each mining district, which includes the geographical location, altitudinal range, rainfall and climate, dominant vegetation, geology and soils characteristics of these districts, is listed in Table 2.2.

Table 2.2 Description of the Welkom, Vaal River and West Wits mining districts.

Mining District	Geographical Coordinates (dm)	Mean Altitude Range (m)	Mean Annual Rainfall (mm)	Mean Annual Temperature (ºC)	Mean Maximum Temperature (ºC)	Mean Minimum Temperature (ºC)	Dominant Vegetation Type	Dominant Biomes	Dominant Bioregions	Geology	Soils
Welkom	27º57´S, 26º34´E	1258 - 1293	497	16	38.7	-10	Vaal-Vet Sandy Grassland; Western Free State Clay Grassland; Highveld Salt Pans	Grassland Biome; Azonal Vegetation	Dry Highveld Grassland Bioregion; Inland Saline Vegetation	Ecca shales	eutrophic soils with a high base status and, non calcareous structured soils with a high clay concentration
Vaal River	26º55´S, 26º40´E	1481 - 1522	573	17	35.9	-8.4	Vaal-Vet Sandy Grassland; Vaal Reefs Dolomite Sinkhole Wetland	Grassland Biome	Dry Highveld Grassland Bioregion	Chert rich dolomite and dolomite and sand	eutrophic and mesotrophic shallow and often occur over hard weathering rock, traces of lime
West Wits	26º25´S, 27º21´E	1540 - 1599	651	18	34.7	-8	Carletonville Dolomite Grassland; Gauteng Shale Mountain Bushveld	Grassland Biome; Savanna Biome	Dry Highveld Grassland Bioregion; Central Bushveld Bioregion	Chert rich dolomite and shale	eutrophic and mesotrophic occurrence of lime is common

The topography of all three districts is relatively flat. A distinct rainfall gradient is apparent across the three districts (Mucina and Rutherford, 2006). Mean annual rainfall, estimated over a 30-year period for Welkom, Vaal River and West Wits, ranges from 497 to 651 mm (South African Weather Service, 2006), with high inter-annual variability (25-30%) and high evapotranspiration potentials, between 2-2.5 times higher than the rainfall (Lynch and Schulze, 2006).

The mining districts are classified according to three dominant biomes *viz.* grassland, savanna and azonal vegetation (Mucina and Rutherford, 2006). Present regional land uses include cattle ranching, game farming, agricultural crop farming such as maize and sunflower, but does not include commercial forestry plantations. Commercial forestry is unsuited to these areas, given the low annual rainfall and cold winter temperatures. However, some small stands, rows and isolated trees do exist along some water courses, farm boundaries and in areas adjacent to TSFs through planting and natural establishment.

The underlying geology in Welkom is predominantly Ecca shales (Vegter, 1995). Predominant geological formations in Vaal River and West Wits study areas include dolomite and sand, chert-rich dolomite and shale, as shown in Figure 2.2 (AngloGold Ashanti, 2004).

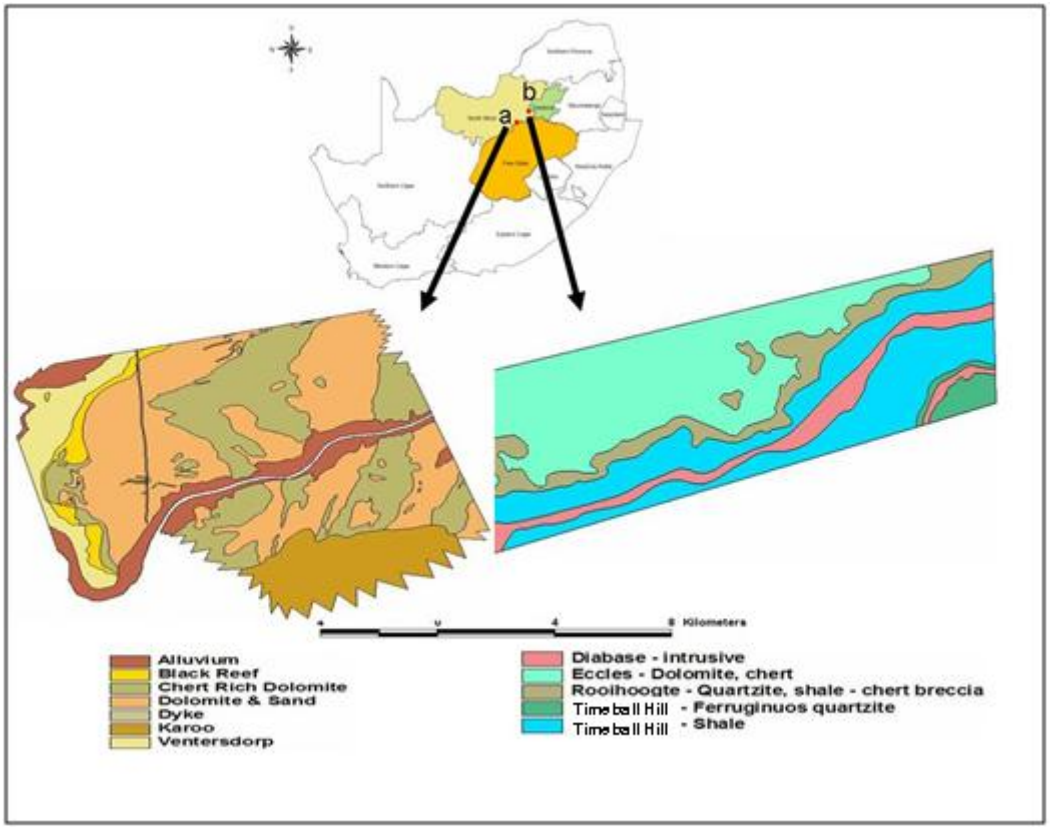


Figure 2.2 Geological formations within (a) Vaal River and (b) West Wits study areas. (Data obtained from AngloGold Ashanti, 2004).

The soils in Welkom can be described as eutrophic, with a high base status, and non calcareous structured soils with a high clay concentration (ISCW, 1993). In Vaal River and West Wits the soils are predominantly eutrophic and mesotrophic, are shallow and often occur over hard weathering rock (ISCW, 1993). The occurrence of lime is common in the West Wits region; however, soils with a high base status with traces of lime are characteristic of the Vaal River study area (ISCW, 1993).

2.4 SAMPLING SITES

Although tree plantations are rare in these mining districts, sample sites were selected from stands, single trees or rows of trees and small-plot species trials in each mining district (Dye, 2004; I. Weiersbye, 2005 pers comm.). Fifteen sample sites were selected across the three mining districts; four each in the Welkom and West Wits districts and seven in the Vaal

River district (Figure 2.3). Five sample trees were selected at each sampling site, making a total of 75 sample trees across the three mining districts.

The following criteria were used in the selection of the sampling sites (Figure 2.3):

- Stands, single trees or rows of trees and small-plot species trials were used that covered a range of conditions, which included different levels of groundwater contaminants and concentrations of total dissolved solids (I. Weiersbye, 2004; 2005 pers comm.).
- Sites were selected to maximise the chance of incorporating extremes of high and low water availability to the trees (P. Dye, 2004 pers comm.). The validity of this sampling strategy is supported by similar studies, in which an assumption of linearity between ground-truth measurements and reflectance indices between the extremes of high and low tree water availability is made (Young and Wallis, 1985; Allen and Nakayama, 1988; Stimson *et al*., 2005; Eitel *et al*., 2006).
- Trees experiencing high water stress during the dry season were initially identified from leaf colour and canopy density. Predawn leaf water potential measurements were then used to confirm the degree of plant water stress in the tree species investigated in this study. A reading of -0.8 MPa was used to separate stressed trees from unstressed trees (Cleary and Zaerr, 1984).

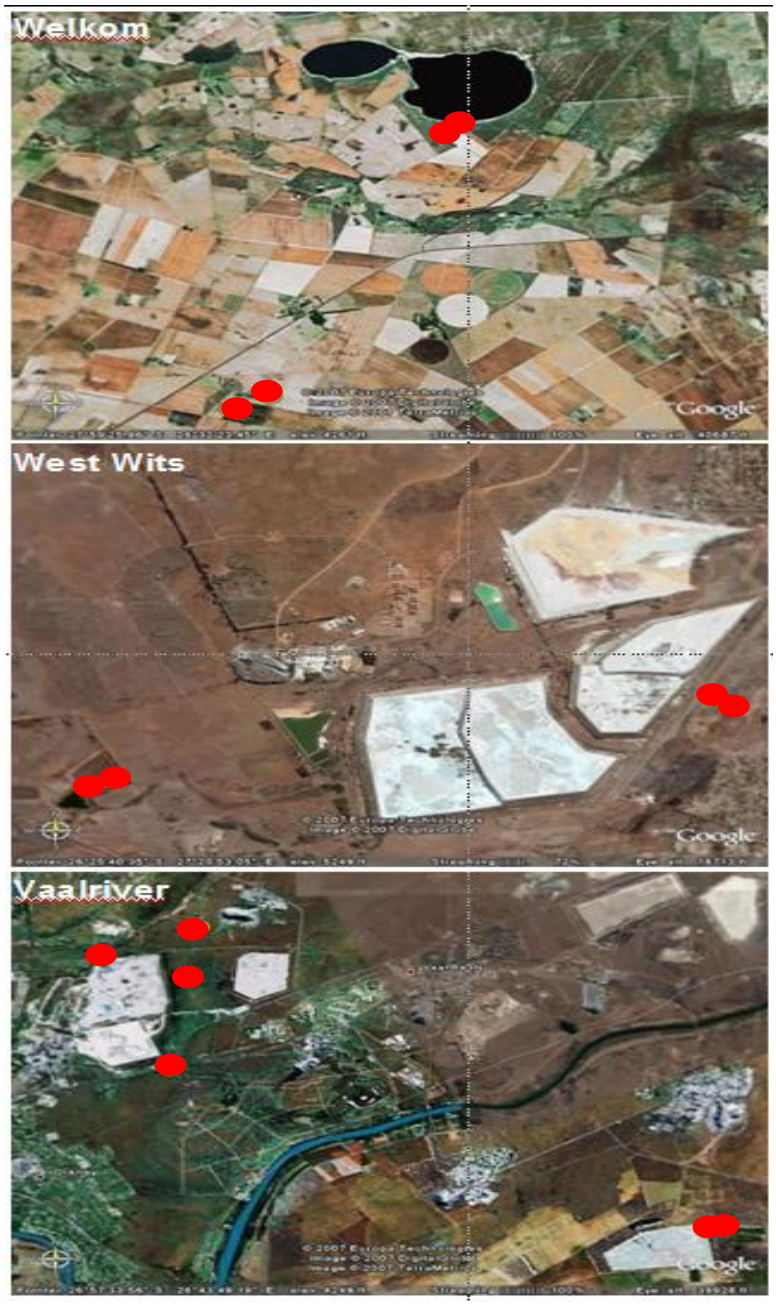


Figure 2.3 Sampling sites selected in each mining district. Shaded circles represent the location of each sampling site (Google Earth, 2008).

The density and spatial arrangement of trees were variable across each mining district. Examples of the spatial arrangement of trees are shown in Figure 2.4. Stands comprised of established trees in rows arranged in a block design (Figures 2.4a, b, c, f), small-plot species trials consisted of young planted trees (Figures 2.4d), clumps representing a group of self-established trees with no fixed spatial arrangement (Figures 2.4e, g) and a row representing a single arrangement of established trees (Figures 2.4h, i).

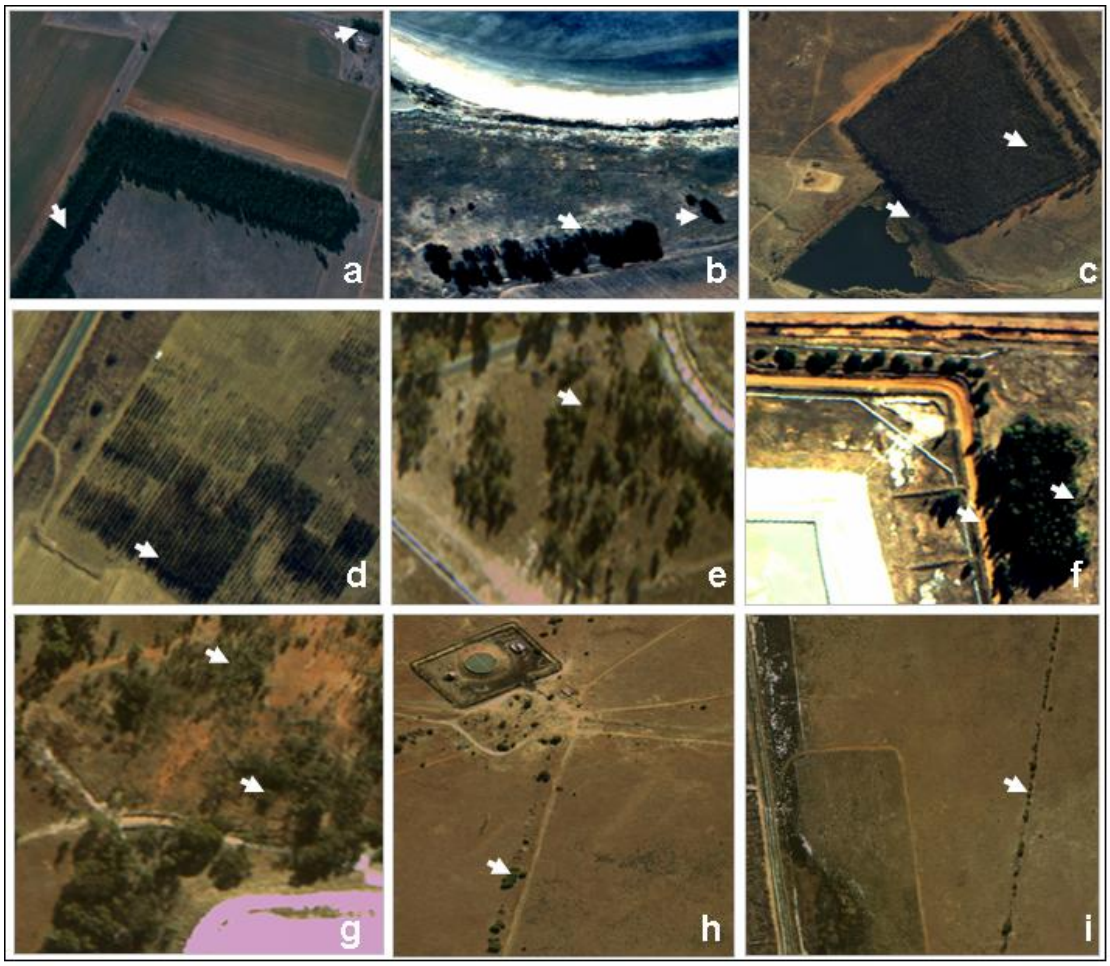


Figure 2.4 Sampling sites in Welkom (a and b), West Wits (c and d) and Vaal River (e to i) mining district. Arrows represent the location of trees at each sampling site in each mining district. Samplings sites are illustrated as stands of trees (a, b, c, f), small-plot species trials (d), clumps (e, g) and rows of trees (h, i). (Images obtained from Land Resources International, 2005).

A general description of each sampling site, its geographic location, spatial arrangement, average tree heights and diameter at breast height, measured in July 2004 is listed in Table 2.3.

Table 2.3 Description of sample sites in the Welkom (W), Vaal River (VR) and West Wits (WW) mining districts. (Data obtained through field surveys and from AngloGold Ashanti, 2004).

Mining District	Tree Species	Geographic Coordinates (dd)	Spatial Arrangement	Average Tree Height ± SD (m)	Average DBH ± SD (cm)	General Site Description
W	EC	-28.03052; 26.51879	Stand	6.9 ± 3.1	37.5 ± 19.9	Shale, eutrophic soils, farmland
W	EC	-27.96743; 26.55001	Stand	9.1 ± 2.8	39.7 ± 7.6	Shale, eutrophic and non calcareous soils, high water availability, near pan
W	SL	-28.03361; 26.51199	Row	7.3 ± 0.6	53.3 ± 13.7	Shale, eutrophic soils, farmland
W	SL	-27.96695; 26.55075	Single	5.9 ± 1.6	51.1 ± 24.4	Shale, non calcareous soils, high water availability, near pan
WW	ES	-26.43969; 27.32871	Stand	8.3 ± 3.1	29.6 ± 13.6	Shale, non calcareous soils, high water availability, farm dam, shallow groundwater table < ~ 5 m
WW	ES	-26.43899; 27.33024	Stand	6.6 ± 1.9	16.5 ± 7.8	Shale, non calcareous soils, lower water availability
WW	EC	-26.43207; 27.36888	Small-plot species trial	4.0 ± 0.5	11.3 ± 2.9	Shale, non calcareous soils, higher water availability, riparian zone
WW	EC	-26.43158; 27.36155	Small-plot species trial	3.9 ± 0.3	10.4 ± 1.3	Shale, non calcareous soils, low water availability
VR	EC	-26.95590; 26.69330	Clump	9.2 ± 1.9	13.6 ± 3.5	Dolomite, meso-eutrophic soils, high total dissolved solids
VR	EC	-26.99288; 26.78289	Stand	7.4 ± 2.2	31.4 ± 13.2	Dolomite, eutrophic soils, deep groundwater table ~ 20 m
VR	EC	-26.92922; 26.68182	Clump	2.7 ± 1.3	6.9 ± 4.1	Andesite, eutrophic soils, close to tailing storage facility
VR	EC	-26.92970; 26.62100	Clump	6.2 ± 0.5	19.8 ± 4.3	Andesite, eutrophic soils, close to tailing storage facility
VR	EC	-26.99332; 26.78250	Row	9.0 ± 1.7	46.6 ± 13.4	Dolomite, eutrophic soils, high water availability, water channel
VR	SL	-26.92301; 26.69820	Row	6.1 ± 0.8	46.0 ± 28.4	Quartzite, meso-eutrophic soils, low total dissolved solids
VR	SL	-26.93418; 26.69592	Row	5.6 ± 1.2	30.2 ± 13.9	Dolomite, meso-eutrophic soils, high total dissolved solids, higher water availability

SD = Standard Deviation; DBH = Diameter at breast height; EC = E. camaldulensis; ES = E. sideroxylon; SL = S. lancea

W = Welkom; VR = Vaal River; WW = West Wits

CHAPTER 3.
REVIEW OF COMMONLY USED REMOTE SENSING AND GROUND-BASED TECHNOLOGIES TO MEASURE PLANT WATER STRESS

Sections of this review has been published by GOVENDER, M., DYE, P.J., WEIERSBYE, I.M., WITKOWSKI, E.T.F. and AHMED, F., 2009, Review of commonly used remote sensing and ground-based technologies to measure plant water stress. *Water SA*, **35**, 739-750. A reprint of the review paper is provided in Appendix 1.

ABSTRACT

This review provides an overview of the use of remote sensing data, the development of spectral reflectance indices for detecting plant water stress, and the usefulness of field measurements for ground-truthing purposes. Reliable measurements of plant water stress over large areas are often required for management applications in the fields of agriculture, forestry, conservation and land rehabilitation. The use of remote sensing technologies and spectral reflectance data for determining spatial patterns of plant water stress is widely described in the scientific literature. Airborne, space-borne and hand-held remote sensing technologies are commonly used to investigate the spectral responses of vegetation to plant stress. Earlier studies utilised multispectral sensors which commonly collect four to seven spectral bands in the visible and near-infrared region of the electromagnetic spectrum. Advances in sensor and image processor technology over the past 3 decades now allow for the simultaneous collection of several hundred narrow spectral bands resulting in more detailed hyperspectral data. The availability of hyperspectral data has led to the identification of several spectral indices that have been shown to be useful in identifying plant stress. Such studies have revealed strong linear relationships between plant pigment concentration and the visible (VIS) and near-infrared (NIR) reflectance, while plant water content has been linked to specific bands in the short-wave infrared (SWIR) region of the spectrum.

Ground-truthing is essential to identifying useful reflectance information for detecting plant water stress, and four commonly used ground-based methods *viz*. predawn leaf water potential, leaf chlorophyll fluorescence, leaf pigment concentrations and leaf water content are reviewed for their usefulness and practical application.

***Key words*:** leaf chlorophyll fluorescence, leaf-water content, plant pigment concentrations, plant water stress, predawn leaf water potential, remote sensing

3.1 INTRODUCTION

All living organisms, including plants need an adequate supply of water to ensure both their growth and survival. Water in plants is required for vital processes such as photosynthesis, respiration and nutrient uptake. Plants absorb water from the soil through their roots, which is then transported to their stems, leaves and flowers for the maintenance of the different vital processes. When water supply is insufficient, plants may suffer water stress, which could then compromise their growth and survival.

Water stress in plants is a complex physiological response to the limited availability of water to a plant. When plants suffer from water stress, a series of harmful plant water interactions occur, which may disrupt a plant's physiology. These include a decrease in cell water potential, cell turgor and relative water content (Hsiao, 1973).

The available water to plants is usually expressed in terms of water potential. Water potential is commonly assessed by measuring predawn leaf water potential, a direct measure of plant water stress. Measurements at predawn directly evaluate the water status of the plant, because during night time conditions of zero transpiration, plant water potential equilibrates to the available soil water (Cleary and Zaerr, 1984). Cleary and Zaerr (1984) suggested that a predawn leaf water potential of less than -0.8 MPa is an indication of stressed vegetation. Indirect measurements may also be used to detect plant water stress.

The more commonly used techniques include measurements of relative leaf water content, plant chlorophyll pigment content and chlorophyll fluorescence. Other, less frequently applied field measurements include variations in trunk or stem diameters or even xylem vessel characteristics. Although characterising cavitation in xylem vessels is potentially a useful technique for understanding the response to water stress in a plant, this method is time-consuming, costly and not suitable for use over large spatial scales. It has been shown in many plant species that roots are more vulnerable to cavitation than stems, and thus root cavitation is more suited to characterise plant water stress between species (Sperry and Saliendra, 1994; Alder *et al*., 1996; Hacke and Sauter, 1996; Linton *et al*., 1998).

Reliable detection and prediction of plant water stress is desirable for numerous agricultural, forestry, conservation and land rehabilitation applications. Various remote and ground-based technologies are available for the measurement of plant water stress.

Remote sensing technologies using spectral reflectance data have increasingly been used for determining spatial patterns of plant water stress (Yamasaki and Dillenburg, 1999; Ceccato *et al.*, 2001; Sims and Gamon, 2002; Pu *et al*., 2003; Jackson *et al*., 2004; Stimson *et al*., 2005; Chun-Jiang *et al*., 2006; Clay *et al*., 2006; De Tar *et al*., 2006; Eitel *et al*., 2006; Fitzgerald *et al*., 2006; Harris *et al*., 2006; Sepulcre-Cantó *et al.*, 2006; Campbell *et al*., 2007). Important advantages of remote sensing technologies include cost-effectiveness, efficiency in displaying spatial patterns on a variety of scales, and versatility in revealing a variety of structural and physiological characteristics of water stressed plants. Despite numerous successful case studies, the selection of suitable remote sensing methodologies and reflectance algorithms remain difficult, due to the influence of vegetation diversity and site conditions on vegetation spectral reflectance.

This paper reviews the detection of plant water stress using remote sensing technologies and ground-based techniques commonly used to identify water stress in plants, and which are suitable for ground-truthing remotely-sensed imagery.

No distinction is made between the technologies used for acquiring the remote sensing data, but rather the focus is on highlighting vegetative spectral difference which has been used to detect plant water stress. The ground-based techniques reviewed include measurements of predawn leaf water potential (Dixon, 1914), leaf chlorophyll fluorescence (Müller, 1874), leaf water content (Weatherley, 1950) and leaf pigment concentrations (Lichtenthaler, 1987).

3.2 BRIEF OVERVIEW OF PLANT WATER STRESS INTERACTIONS

Understanding how plants respond to water stress, salt and co-occurring stresses is complex but important in evaluating their performance during conditions of reduced water availability and in the protection of natural vegetation. Water stress is known to alter several physiological, morphological and anatomical processes, as well as triggering defense mechanisms in many plant species (Silva *et al*., 2009). Responses to water stress conditions have been first observed through changes in leaf and stem water potential, water content, turgor pressure and stomatal conductivity, with subsequent changes reported in transpiration, photosynthesis and photochemistry rates (Angelopoulos *et al*., 1996). Defense mechanisms have also be observed which can include a reduction in transpiration rates to control water loss, root generated chemical signals through the synthesis of organic solutes and other gene relations (Chaves *et al*., 2009). Wilting a visual symptom of water stress however only occurs when a plant loses water, its vessels contract and turgor pressure on the cell walls is reduced resulting in the cells becoming flaccid and wilting.

Investigations of plants under water stress have reported considerable decreases in leaf water potential (more negative values) and turgor pressure, followed by progressive stomatal closure, reduced carbon dioxide assimilation and transpiration, with subsequent decline in photosynthetic and photochemistry rates (De Menezes *et al*., 2004). The latter responses are largely ascribed to stomatal restrictions on the supply of carbon dioxide to the leaf, inactivation of photosynthetic processes hence lower pigment concentrations, inhibition of primary photochemistry and declining chlorophyll fluorescence activity (Boyer *et al.*,1987; Angelopoulos *et al*., 1996; Chaves *et al*., 2009).

The reduction in photosynthetic rates commonly observed in plants under water deficit conditions range from the restriction on carbon dioxide diffusion into the chloroplast, through limitations on stomata opening which is mediated by shoot- and root-generated hormones, and on the mesophyll transport of carbon dioxide, to alterations in leaf photochemistry and carbon metabolism. These effects vary according to the intensity and duration of the stress as well as with the leaf age; older leaves being more affected by drought and accumulating higher amounts of salt and the plant species (Chaves *et al*., 2009). Under conditions of water stress, photosynthetic pigment composition such as chlorophyll and carotenoid pigment contents decrease, with chlorophylls shown to decline more rapidly than carotenoids (Sikuku *et al*., 2010). Hence due to the importance of photosynthetic pigments in correct plant functioning, variations in chlorophyll a, chlorophyll b, total chlorophyll and carotenoids are commonly used to provide information concerning the physiological status of plants (Netondo, *et al*., 2004). Pirzad *et al*. (2011) showed that water stress resulted in significant decreases in chlorophyll content (chlorophyll a, b and total chlorophyll concentrations), light harvesting chlorophyll a/b protein and relative leaf water content, with total chlorophyll content being reduced by as much as 55%.

Similar trends have been observed with photochemistry rates illustrating a reduction in primary photochemistry and chlorophyll fluorescence under conditions of water stress. Significant decreases in Fv/Fm ratio ($P < 0.05$) and significant increases in the Fo values ($P < 0.05$) were shown (Pirzad *et al*., 2011). Alterations to these chlorophyll fluorescence expressions under water stress represent damage to the photosystem II reaction centers, triggering reduced photosynthetic capacity and photochemical efficiency (Pirzad *et al*., 2011).

A chemical communication between the roots and shoots including stomata movement, which triggers a growth substance produced in the roots called ABA, has also been reported linked to the reduced transpiration rates and stomatal conductance after periods of water stress. ABA increases in the roots and is transported to the shoot through the xylem, causing stomatal closure (Gomes *et al*., 2004; Silva *et al*., 2009). Thomas and Emus (1999) found that ABA accumulation in the leaves of *Eucalytpus tetrodonta* contributed towards a decrease in stomatal conductance.

Transgenic and molecular biology studies on plant responses to water stress and phospholipid-based signalling has emerged as a component of drought-responsive signal pathways (Mane *et al*., 2011). During periods of water stress, stomata close, there is a reduction in water loss as well as gas exchange, leading to reduced carbon assimilation and to a near optimization of carbon assimilation in relation to water supply (Mane *et al*., 2011). Using transcriptome analysis, several new genes regulated by progressive drought were identified and genes whose expression may be part of the phospholipid-based signalling pathway were also found, suggesting that further exploration of process regulated by transgenic genes is required.

During periods of water stress plants also have the ability to maintain functioning but at a reduced capacity. Several studies indicate that woody species display different tolerances to water stress, with some trees still functioning even during severe droughts, at a very low level of physiological activity and much lower plant water potentials (Tyree *et al*., 2003; Greven *et al*., 2009; Wagner *et al*., 2011). As water availability in the soil decreases, the transpiration rate also decreases, as a result of stomatal closure. The instantaneous control of transpiration is an important defense mechanism used by many species in arid environments to avoid excessive water loss and possible death by dehydration (Silva *et al*., 2009). Osmotic adjustment is considered an important mechanism to allow for the maintenance of water uptake and cell turgor under stress conditions. Olive trees typically use osmotic adjustment as a stress avoidance mechanism to maintain turgor potential between the tissues (Dichio *et al*., 2006), with leaf water potential below 4 MPa. Olive trees can lose almost 40% of their tissue water content and still maintain their re-hydration capacity, due to the establishment of a high gradient of water potentials between the tissues, roots, and soils, which allows the trees to take up water even at soil potentials below permanent wilting point (Greven *et al*., 2009). Few species would be able to continue water uptake at a stem water potential of less than 4.0 MPa.

Other defense mechanisms triggered in plants under water stress include alterations in the diffusion of carbon dioxide from the sub-stomatal cavities to carboxylation sites which thus contribute towards the maintenance of photosynthetic rates despite the low stomatal

conductance. Also observed under water deficit conditions are increases in stomata density and the number of smaller sized mesophyll cells of the leaf resulting in improved control of water loss (Silva *et al*., 2009).

Although Eucalyptus species have evolved in a dry environment, changes in plant water status strongly influence their growth and physiology (Batchelard, 1986; Metcalfe *et al*., 1990). Predawn leaf water potential has been used to estimate changes in minimum levels of water stress, with measurements from Eucalyptus illustrating values less than 4 MPa (White *et al*., 2000). This measure of plant water status often assumes equilibrium in water potential at the soil–root interface though this may not always be the case (Whitehead and Beadle, 2004).

In *E. camaldulensis* and *E. nitens*, the high stomatal sensitivity is associated with in-elastic tissues and in *E. camaldulensis*, its capacity to access groundwater. As leaf water potential becomes more negative with soil drying, manipulation of both osmotic and elastic properties occurs to sustain a positive turgor pressure over a wider range of water stress conditions. In-elastic tissues that promote rapid loss of turgor are associated with a high stomatal sensitivity and drought avoidance. Such characteristics are an essential pre-requisite for matching species to sites where the major limitation to growth is available water and in combining species for managing the use of water throughout the soil profile, including groundwater recharge (White *et al*., 2000).

Several studies have reported on the ability of tree root systems to access water. Whitehead and Beadle (2004), showed that the roots of Eucalyptus trees comprise of a widely spreading lateral system just below the soil surface and a deep tap root system in young trees that develops deep sinker roots as the trees mature. Roots are described as being opportunistic and grow along gradients of increasing water availability for considerable distances. Measurements from *Eucalyptus grandis* trees exposed to progressive water stress showed that trees abstracted water to 8 m depth, while 9 year old trees obtained most of their water from depths below 8 m and deep drilling revealed that live roots reached 28 m below the surface (Dye, 1996). Dye (1996) concluded that water is recharged possibly by infiltration along old root channels. In a comparative study of four Eucalyptus species in close

proximity, at different leaf water potentials during the dry season, results indicated that varying strategies were adopted by the species in accessing water from the soil profile, were two were reliant on parts subjected to large changes in soil water content and two used water from the capillary fringe (White *et al*., 2000). Whitehead and Beadle (2004) showed that transpiration and evaporation for four Eucalyptus species planted in contour belts were effective at reducing groundwater recharge with minimal competition for water with adjacent crops. Dawson and Pate (1996) reported on the adaptation of deep rooted trees to access different sources of water from within the soil profile in relation to seasonal water availability, were *Eucalyptus globulus* and *Eucalyptus camaldulensis* accessed groundwater using sinker roots in the summer, but the proportion of groundwater in stems were found to be greater in *Eucalyptus camaldulensis* (26-47%) compared to *Eucalyptus globulus* (9-15%). When roots of *Eucalyptus camaldulensis* and *Eucalyptus platypus* grow through layers of soil with different water contents, they are able to redistribute water between the layers by transferring significant quantities along gradients of water potential (Burgess *et al*., 2001). According to Burgess *et al*. (2001), the direction of the movement of water termed hydraulic lift may be upwards or downwards depending on the timing of rainfall and availability of water stored in different layers and has many ecological benefits including reduced water-logging of surface soils during wet periods, increased water content in deeper soil layers during dry periods and improved nutrient availability.

3.3 DETECTION OF PLANT WATER STRESS USING REMOTE SENSING

Remote sensing data are often described by their spatial and spectral properties or resolutions. Spatial resolution is the size of a pixel recorded in the remote sensing image, and could range from 1 m (higher spatial resolution) to 1000 m (lower spatial resolution). Spectral resolution is related to the width and number of wavelength bands recorded by the remote sensing system, with lower spectral resolutions often representing a fewer broad spectral bands such as multispectral data, and higher spectral resolutions representing sometimes more than a hundred narrow spectral bands such as hyperspectral data. These terms are often referred to in following sections and chapters.

During the 1980s, the application of remote sensing technologies for plant and environmental studies became widespread. These studies made use of low spatial and spectral resolution multispectral data. Multispectral remote sensing data commonly consist of four to seven broad spectral bands in the visible (VIS) and near infrared (NIR) regions of the electromagnetic spectrum. These datasets were acquired using airborne, satellite and ground-based spectrometers. Early airborne systems consisted of a multispectral camera mounted on board a small aircraft or helicopter which collected three to four spectral bands. Spectrometers at this time were bulky, heavy instruments which were not easily transportable in the field. Therefore most spectral measurements were taken in laboratories.

Remote sensing technologies have advanced significantly over the past 10 to 15 years. With the development of hyperspectral remote sensing technologies, researchers have benefited from significant improvements in the spectral and spatial properties of the data, thus allowing for more detailed plant and environmental studies. These technologies acquire many hundreds of spectral bands across the spectrum from 400 to 2500 nm. Such hyperspectral technologies also use airborne, satellite and hand-held spectrometers.

Airborne hyperspectral imagers, such as the commonly used Casi or Hymap imagers, acquire high spectral and spatial resolution images. A distinct advantage of most airborne imagers is their capability to acquire at least two hundred or more spectral bands at less than 5 m spatial resolution. However, airborne imagery is generally more costly than satellite imagery, due to the logistical costs associated with flight surveys and the costs of hiring airborne hyperspectral or multispectral imagers. Advances in spectrometry have resulted in state-of-the-art portable field instruments which allow for the collection of hand-held hyperspectral signatures from 400 to 2500 nm. The Hyperion sensor is currently the only hyperspectral satellite system available for research.

In recent years, there has been an expanding body of literature concerning the relationship between the spectral reflectance properties of vegetation and the structural characteristics of vegetation and pigment concentration in leaves. The spectral characteristics of vegetation are governed primarily by scattering and absorption characteristics of the leaf internal structure and biochemical constituents, such as pigments, water, nitrogen, cellulose and lignin (Asner,

1998; Coops *et al*., 2002). Pigments are the main determinants controlling the spectral responses of leaves in the visible wavelengths (Gaussman, 1977). Chlorophyll pigment content, in particular, is directly associated with photosynthetic capacity and productivity. Reduced concentrations of chlorophyll are indicative of plant stress (Curran *et al*., 1992). On the other hand, cellular structure and water content of leaves are the main determinants in the near- and shortwave-infrared wavelengths as shown in Figure 3.1.

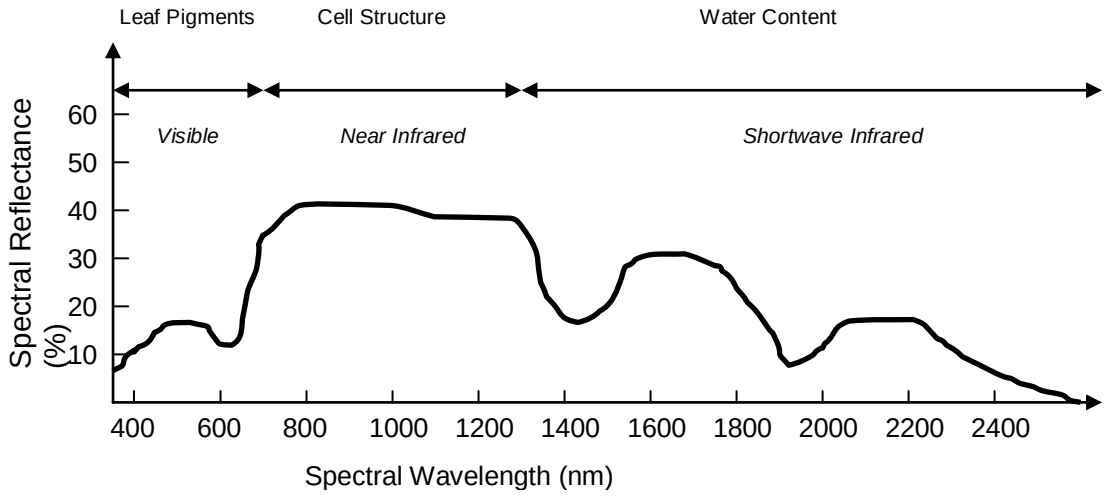


Figure 3.1 Typical reflectance sensitivities as controlled by leaf pigments, cell structure and water content. (Adapted from Gaussman, 1977).

Over the years research findings have advanced our understanding of vegetation in relation to plant stress. Table 3.1 summarises findings since the early 1980s, highlighting specific regions of the electromagnetic spectrum and their relations to vegetation spectral reflectance properties. Many of the earlier studies highlighted specific regions of the spectrum such as the VIS and NIR regions, which could be used in vegetation studies. More recent work has highlighted the importance of specific regions such as the red edge (maximum slope of vegetation reflectance from 690 to 740 nm) for predicting plant stress (Clay *et al*., 2006; Fitzgerald *et al*., 2006; Blackburn, 2007; Campbell *et al*., 2007). The extent of the literature is indicative of the importance of relationships between plant stress and both plant chlorophyll and water content. Plant chlorophyll and water content have thus been used as 'surrogates' of plant stress, under the assumption that decreases in chlorophyll and water content are indicative of plant stress. Therefore, in remote sensing studies numerous individual spectral bands and vegetation spectral reflectance indices have been used to predict plant chlorophyll content and water content.

Table 3.1 Some milestones in the historical development of the relationships of vegetation spectral reflectance characteristics in specific regions of the electromagnetic spectrum.

Region of the Spectrum	**Vegetation Spectral Reflectance Characteristics**	**Author(s)**
VIS, NIR and MIR	Pigments, cellular structure and water content of leaves.	Gaussman (1977)
1550 to 1750 nm	Correlation of MIR reflectance to leaf water contents.	Tucker (1980)
SWIR (1400 to 2500 nm)	Reflectance is influenced by liquid water in plant tissue.	Tucker (1980), Ceccato *et al*. (2001)
VIS	Changes in red, green and blue reflectance due to chloroplast deterioration.	Murtha (1982)
Red Edge	Movement of red edge towards shorter wavelengths during senescence or stress induced chlorosis.	Collins *et al*. (1983), Rock *et al*. (1988), Milton *et al*. (1989)
Red Edge	Red edge defined from 690 to 740 nm is also sensitive chlorophyll content.	Horler *et al*. (1983), Curran *et al*. (1990), Blackburn (1999)
Red Wavelengths	Displacement in the slope of the red wavelengths towards longer wavelengths as chlorophyll content increases.	Horler *et al*. (1983)
Thematic Band 5 to 7 (1550 – 1750 nm and 2080 – 2350 nm)	Ratio of Band 5 to 7 highly correlated with water content of soils and vegetation.	Musick and Pelletier (1986; 1988)
VIS and NIR	Estimated chlorophyll a, b and total carotenoid content using equations and specific extinction coefficients.	Lichtenthaler (1987)
Red Edge	Increase in the relative proportion of chlorophyll a will result in movement of red edge towards longer wavelengths, independent of total chlorophyll content and vice versa.	Guyot and Baret (1988)
NIR (700 – 1300 nm) and MIR (1300 – 2500 nm)	Detection of plant water stress in oak, sweet gum and conifers.	Hunt and Rock (1989)
820 and 1600 nm	Significant relationship between the equivalent water thickness and a moisture stress index between reflectance value measured at 1600 nm and reflectance value measured at 820 nm.	Hunt and Rock (1989)
550 and 700 nm	Maximum sensitivity to a wide range of chlorophyll contents.	Curran *et al*. (1990), Gitelson and Merzlyak (1996), Lichtenthaler *et al*. (1996), Datt (1999)
Red Edge	Chlorophyll content of branches of Slash Pine (*Pinus elliottii engelm*) predicted using red edge.	Curran *et al*. (1990)
VIS (491-575 nm); Red (647-760 nm)	Increased reflectance in response to plant stress regardless of the stress agent.	Carter (1993)
NIR plateau	Weak water absorption features at 1000 and 1200 nm. Deepening of the two water absorption features as leaf area index increased.	Gao (1995), Asner (1998)
860 nm and 1240 nm	Normalised difference water index as an estimate of vegetation water content.	Gao (1995)

Region of the Spectrum	**Vegetation Spectral Reflectance Characteristics**	**Author(s)**
550, 700 and longer than 750 nm	Specific wavelengths sensitive to pigment variations and chlorophyll assessment at leaf level for maple and chestnut leaves.	Gitelson and Merzlyak (1996)
Reflectance at 550 and 700 nm, and 500 and 670 nm	Highly correlated in yellow-green to dark green leaves.	Gitelson and Merzlyak (1996)
Maximum reflectance at 750 nm, lowest reflectance between 400 to 500 nm.	Highly correlated in chestnut leaves.	Gitelson and Merzlyak (1996)
670-680 nm	Reflectance at 670-680 nm was insensitive to chlorophyll a above 70 mg m-2 in tobacco leaves (*Nicotiana tabacum L.*) due to saturation of the relationship between light absorption and pigment concentration.	Lichtenthaler *et al.* (1996)
VIS, NIR	Reflectance at wavelengths with high absorption coefficients should be more sensitive to low concentrations of chlorophyll a, while spectral regions with low absorption should be more sensitive to higher chlorophyll a concentrations.	Lichtenthaler *et al.* (1996), Blackburn (1999)
550, 700 and 750 nm	The reflectance indices (R750/ R700 and R750/ R550) were identified as having strong linear relationships with total chlorophyll concentration at the leaf scale in horse chestnut (*Aesculus hippocastanum L.*) and Norway maple (*Acer platanoides L.*) leaves.	Lichtenthaler *et al.* (1996), Gitelson and Merzlyak (1996), Gitelson *et al.* (2002), Blackburn (1999)
SWIR (1530 and 1720 nm)	Reflectance is influenced by liquid water in plant tissue and can be used as an estimate for vegetation water content.	Foutry and Baret (1997)
VIS, NIR, SWIR	Variability in tissue optical properties is wavelength dependent. Green foliage lowest variation in VIS, highest NIR. Standing litter minimum variation in VIS and NIR, highest in SWIR Woody stems lowest variation in SWIR, highest in NIR.	Asner (1998)
1700 nm, 2000 nm, 2200 nm	Features associated with lignin and other organic compounds.	Asner (1998)
650, 635, and 470 nm	Concentrations of chlorophyll a, chlorophyll b, and carotenoids were best correlated with reflectance indices (R_{650}, R_{635}, and R_{470}), respectively in the leaves of four deciduous tree species at different stages of senescence.	Blackburn (1998a)
676 and 810 nm	Chlorophyll a and chlorophyll b concentrations were strongly correlated with reflectance index (R676) in the visible wavelengths and reflectance index (R810) in the near-infrared on bracken (*Pteridium aquilinum*) canopies. Possible correlation to canopy structural development which has a direct influence on near-infrared reflectance.	Blackburn (1998b)
740 to 820 nm; 680 and 760 nm	Higher reflectance values between 740 to 820 nm; and more pronounced maximum slope between 680 and 760 nm (red edge) is related to vegetation with healthier green leaf development i.e. higher biomass and leaf area index.	Lelong *et al*. (1998), Jacquemoud (1993), Baret and Jacquemoud (1994), Baret *et al.* (1994), Filella and Penuelas (1994)
Red and NIR	Relation between water deficiency (stress) to spectral features in the 740 to 820 nm and red edge range in wheat.	Lelong, *et al*. (1998)

Region of the Spectrum	Vegetation Spectral Reflectance Characteristics	Author(s)
Red Edge	The first derivative of pseudo absorbance, δ(Log 1/Reflectance), was highly correlated with canopy pigment concentration per unit area in the red edge region. Canopy and leaf scale concentrations per unit mass of chlorophyll a, chlorophyll b, and carotenoids were strongly related to δ(Log 1/Reflectance) and the second derivative of pseudo absorbance (δδ(Log 1/Reflectance), but different wavelengths were optimal at each scale.	Blackburn (1999)
VIS	Moderately correlated to chlorophyll concentration.	Blackburn (1999)
VIS (Green) and NIR	Ratio indices highly correlated to chlorophyll concentration.	Blackburn (1999)
Red Edge	Wavelength position of red edge related to chlorophyll concentration, and characteristics of the amplitude of the first and second derivatives of reflectance and pseudo absorbance were more strongly correlated with chlorophyll.	Blackburn (1999)
Red, NIR (850 nm, 710 nm, 680 nm)	Vegetation indices used to predict chlorophyll content of eucalypt vegetation at the leaf and crown scale.	Datt (1999)
850, 710 and 680 nm	850, 710 and 680 nm wavelengths produced the highest correlations with leaf chlorophyll content.	Datt (1999)
Red Edge	With decreasing chlorophyll content, senescence or stressed induced chlorosis the red edge moves to shorter wavelengths, and is due to a reduction in the depth and breadth of the chlorophyll absorption feature.	Stone *et al*. (2001), Rock *et al*. (1988), Datt (1999)
VIS, NIR	Relationships between spectral reflectance properties of Eucalypt vegetation and a range of physiological and morphological parameters. Results indicate a shift of red edge towards shorter wavelengths with decreasing chlorophyll content.	Stone *et al*. (2001)
900 and 970 nm	Water index is derived from the ratio between reflectance measured at 900 nm and 970 nm and used as a measure of plant water content.	Champagne *et al*. (2003)
VIS, NIR and Red Edge	Universal broad leaf chlorophyll indices using the PROSPECT model	le Maire *et al*. (2004)
NIR, Red Edge	Canopy level spectral and thermal estimation of water status and nitrogen content using spectral and thermal indices.	Fitzgerald *et al*. (2006)
NIR and VIS	Degree of water stress strongly correlated to spectral bands from VIS and NIR regions viz. 686, 811, 860, 850 bands using hyperspectral and multispectral data.	De Tar *et al*. (2006)
Thermal bands	Detection of water stress using thermal remote sensing imagery.	Sepulcre-Cantó *et al*. (2006)
NIR and SWIR	Indices formulated from the weaker NIR liquid water absorption bands (980 and 1200) are linear in response to moisture fluctuations, and are strongly correlated to hydrological measures. Could be used to estimates near-surface and surface wetness at the landscape scale.	Harris *et al*. (2006)
Red Edge	Detection of plant water stress using wavelengths associated with red edge.	Clay *et al*. (2006), Blackburn (2007), Campbell *et al*. (2007)

VIS = Visible; NIR = Near Infrared; MIR = Middle Infrared; SWIR = Shortwave Infrared

3.3.1 Spectral indicators of plant chlorophyll content

In stressed vegetation, leaf chlorophyll content decreases, thereby changing the proportion of light-absorbing pigments, leading to less overall absorption of light, which affects the spectral reflectance signatures of plants (Murtha, 1982; Zarco-Tejada *et al*., 2000). This leads to a reduction in green reflection and an increase in red and blue reflections, resulting in changes in the normal spectral reflectance patterns. Thus, detecting changes from the normal spectral reflectance patterns is the key to interpreting plant water stress.

Specific reflectance wavelengths in the red and near infrared region of the spectrum, which are sensitive to plant chlorophyll pigment variation, have been identified. Reflectance from 550 and 700 nm show maximum sensitivity to a wide range of chlorophyll contents (Curran *et al*., 1990; Carter, 1993; Gitelson and Merzlyak, 1996; Lichtenthaler *et al*., 1996, Datt, 1999). However, there is little agreement on the optimum wavelengths to be used in the remote assessment of plant chlorophyll content.

Indices have been derived using a combination of specific reflectance wavelengths for the remote assessment of chlorophyll content (Curran *et al*., 1990; Jacquemoud, 1993; Baret and Jacquemoud, 1994; Baret *et al*., 1994; Filella and Penuelas, 1994; Gitelson and Merzylak, 1996; Lichtenthaler *et al*., 1996; Blackburn, 1998a; Blackburn, 1998b; Lelong *et al*., 1998; Blackburn, 1999; Datt, 1999; Stone *et al*., 2001; Coops *et al*., 2003). These indices have been typically derived through correlations between leaf reflectance and leaf chlorophyll content, and are often developed for a single species with constant leaf size and shape, leaf surface and internal structure (Datt, 1999). However, the relationship between chlorophyll content and leaf or canopy reflectance is not necessarily generic, and caution needs to be taken when applying these indices over different vegetation types or biomes for the prediction of plant water stress (Coops *et al*., 2003).

In the remote assessment of plant water stress, total chlorophyll and chlorophyll *a* content have been identified as key spectral indicators. Chlorophyll *a* absorbs strongly in the red wavelengths because of electron transitions of the chlorophyll molecules. As the chlorophyll concentration increases, there is an apparent displacement in the slope of the red

wavelengths towards longer wavelengths (Horler *et al*., 1983). However, in a stressed plant there is a shift towards shorter wavelengths, often reported as the "blue shift" (Carter, 1993).The interdependence of chlorophyll *a* and total chlorophyll provide an appropriate measure of changes in spectral reflectance due to plant water stress. If the relative proportion of chlorophyll *a* were to increase, there would be a movement of the red edge to longer wavelengths, independent of total chlorophyll content. Likewise, a decrease in the relative proportion of chlorophyll *a* would result in a movement of the red edge to shorter wavelengths, also independent of total chlorophyll content. However, the effect of a changing $^{\text{chlorophyll a}}/_{\text{chlorophyll b}}$ ratio on the red edge is likely to be minor, and has proved difficult to observe compared to the effect of the total chlorophyll content (Guyot and Baret, 1988). Therefore, red reflectance is considered a reliable metric for total chlorophyll content and changes in leaf pigments (Horler *et al*., 1983).

When chlorophyll content is used as a measure of plant water stress, the placement and shape of the spectral red-edge are important indicators of plant water stress (Horler *et al*., 1983, Curran *et al*., 1990, Blackburn, 1999; Blackburn, 2007). This relationship is used to explain the movement of the red edge to shorter wavelengths during different expressions of plant water stress, such as senescence or stress-induced chlorosis (Collins *et al*., 1983; Rock *et al*., 1988; Milton *et al*., 1989; Clay *et al*., 2006; Campbell *et al*., 2007).

3.3.2 Spectral indicators of plant water content

Plant water content at the leaf and canopy scales are often estimated using reflectance data from the near infrared (NIR), middle infrared (MIR) and short wave infrared (SWIR) regions of the electromagnetic spectrum (Tucker, 1980; Hunt and Rock, 1989; Gao, 1995; Zarco-Tejada *et al*., 2003; Jackson *et al*., 2004; Shen *et al*., 2005; Chun-Jiang *et al*., 2006). Specific spectral bands and spectral indices designed to capture changes in plant water content have been derived using a combination of spectral bands from the NIR, MIR and SWIR regions.

NIR and MIR spectral bands are highly correlated to water content of vegetation and soils (Tucker, 1980; Hunt and Rock, 1989; Musick and Pelletier, 1986; 1988). Spectral bands from these regions have been used to differentiate stressed trees from non-stressed trees (Tucker, 1980; Hunt and Rock, 1989; Musick and Pelletier, 1986; 1988). In these regions of

the electromagnetic spectrum, leaf water content has been assessed remotely using bands 1550 to 1750 nm (Tucker, 1980), as well as the ratio of spectral bands 1550 – 1750 nm and 2080 – 2350 nm (Musick and Pelletier, 1986; 1988). However, in laboratory experiments a good relationship was identified between water content, leaf area, and the spectral index derived using 820 and 1600 nm spectral reflectance bands (Hunt and Rock, 1989). In these experiments MIR reflectance increased with decreasing leaf water content (Hunt and Rock, 1989).

In the SWIR region (1400 to 2500 nm), field measurements have shown significant changes to this region of the spectrum resulting from changes in the water content of plants (Tucker, 1980; Ceccato *et al*., 2001). Several relationships have been identified between specific spectral bands in the SWIR region, and different ground-based measurements of plant water stress such as relative water content, leaf water potential, stomatal conductance, and cell wall elasticity (Foutry and Baret, 1997; Pu *et al*., 2003). In particular, Foutry and Baret (1997) reported that the spectral wavelengths at 1530 and 1720 nm are most appropriate for assessing plant water content.

Several spectral indices have been derived to detect changes in plant water content for the remote assessment of plant water stress. The sensitivity of such spectral indices to changes in plant water content is influenced by the leaf internal structure. Therefore, some spectral indices may not be suitable for the detection of low or moderate levels of plant water stress (Eitel *et al*., 2006). Two spectral indices that have been successfully used are the normalised difference water index (Gao, 1995) and the water band index (Penuelas *et al*., 1995).

The normalised difference water index (Gao, 1995) is commonly used and accepted as an accurate estimate of plant water content. This index consists of the ratio of the difference between reflectance measured at 860 and 1240 nm, and the sum of reflectance measured at 860 and 1240 nm respectively (Gao, 1995). At these narrowband wavelengths, vegetation canopies have similar radiation scattering properties, but slightly different liquid water absorption properties. Therefore, this index has been successfully applied to detect plant water content remotely for various tree species (Gao, 1995; Jackson *et al*., 2004; Stimson *et al*., 2005; Eitel *et al*., 2006). On the other hand, the water band index is derived from the

ratio of reflectance measured at 900 nm and 970 nm (Penuelas *et al*., 1995). This spectral index has been correlated with ground-based measurements of plant water content at both the leaf and canopy scales. It is, however, more sensitive to leaf water content than the water content of the whole plant. This is advantageous in agricultural applications, where leaf water content changes more noticeably in response to drought conditions than the water content of the entire plant biomass (Champagne *et al*., 2003).

3.3.3 Factors affecting spectral reflectance from leaf to canopy scales

The levels of spectral reflectance from a plant leaf or canopy are determined by a variety of factors. The factors that play a role in the spectral reflectance from a plant leaf or canopy include:-

- type of species,
- site,
- age of plant or foliage,
- nutrient status,
- leaf orientation,
- effects of variable irradiance,
- geometrical arrangement of the object/scene,
- orientation of the ground surface in relation to the location of the sun,
- remote sensing device or sensor, and
- meteorological conditions (Asner, 1998; Coops *et al*., 2003).

Their individual or combined effects are relevant to ground-based field spectrometers, airborne and satellite remote sensing technologies.

Remote sensors differ extensively in their ability to discriminate targets. Spatial resolution varies from less than a metre to several kilometres, with some models requiring input parameters from various data sources with different spatial resolutions (Chen, 1999). Furthermore, vegetation cover can be highly heterogeneous spatially, with the variability within a pixel likely to introduce uncertainties when processing and applying remote sensing imagery at different spatial resolutions (Jiang *et al*., 2006).

Spectral data collected at the leaf scale usually contain the least amount of variability and are most easily correlated to ground-truthing measurements at the same spatial scale. Ground-truthing of remote sensing surveys is often undertaken at the leaf scale, due to the complexity of ground-truthing at higher spatial scales, and the difficulty in mimicking the significant variability in canopy reflectance. Therefore, spectral features and relationships which have been identified at the leaf scale, in conjunction with ground-truthing experiments have often also been applied generically at canopy and landscape scales (Mohammed *et al*., 1997; Datt, 1999; Zarco-Tejada *et al*., 2000; Coops *et al*., 2003).

Despite the difficulty in mimicking whole-canopy reflectance, attempts have been made by stacking leaves on top of each other for below-canopy spectral measurements (Blackburn, 1999; Datt, 1999; Coops *et al*., 2003). The disadvantage of the leaf stacking method is that it is unable to represent the absolute radiation interactions which occur at the canopy scale. It also fails to replicate, for example, canopy architecture, leaf angle distribution, the reflectance of trunks and branches, and the contribution of the wider canopy outside of the instrument field of view. Thus its use is limited. It does, however, assist in controlling the impact of variables such as background reflectance, irradiation levels and sun-target sensor geometry, which do affect spectral reflectance measurements at the canopy scale.

Remote sensing applications at landscape and ecosystem scales require the evaluation and monitoring of multiple species at multiple spatial and temporal scales in order to better understand species interactions and community dynamics, both of which have important implications under changing environmental conditions (Marignani *et al*., 2007). Validation of different types of remote sensing data is usually dictated by their spatial resolution (Zwart and Bastiaassen, 2007), with fine resolution products (<100 m) such as Landsat being adequately validated with ground-based measurements. However, as the spatial resolution of the remote sensing data decreases, resulting in coarser resolution products such as MODIS (1000 m in thermal band), using ground-based measurements is very difficult because of the scale disparity between ground or point measurements and the coarse spatial resolution imagery. Therefore remote sensing research has developed over the years to utilize ground-based measurements to validate high resolution remote sensing imagery and thereafter using

the high resolution remote sensing imagery to validate and up-scale or aggregate coarse or low resolution remote sensing data (Zwart and Bastiaassen, 2007; Choi *et al.*, 2009).

Many studies regarding the effect of up-scaling remote sensing datasets have been reported (Zarco-Tejada *et al.*, 2003; Marignani *et al.*, 2007; Zwart and Bastiaassen, 2007; Choi *et al.*, 2009; Hong *et al.*, 2009; He and Mui, 2010). During an aggregation or up-scaling process, the raster spatial data are reduced to a smaller number of data pixels covering the same spatial extent. It is generally recognized that data aggregation modifies the statistical and spatial characteristics of the data (Bian *et al.*, 1999). Since the total number of pixels is reduced, the variance and frequency distribution of the sampled data at a reduced spatial resolution may deviate from the original data set (Bian *et al.*, 1999).

Several methods exist for scaling land surface and vegetation parameters from leaf to canopy levels including direct extrapolation, canopy integrated methods and modelling approaches. The extrapolation method is the simplest way to scale remote sensing data from the leaf to the canopy level. Empirical estimation or extrapolation methods use uni-variate or multi-variate models to scale the target properties of plants such as biochemical content from leaf to a canopy level (He and Mui, 2010). Empirically based methods apply leaf level relationships between reflectance or reflectance indices and land surface or vegetation parameters directly to the canopy level spectral reflectance data measured by airborne or satellite sensors.

The canopy integrated methods are applied by multiplying vegetation parameters at the leaf level with the corresponding canopy biophysical parameters such as leaf biochemical content, leaf area index or biomass. Similar applications have derived parameters such as canopy chlorophyll content by multiplying leaf chlorophyll content with biomass within an area covered by a pixel. The major assumption of the canopy integrated method is that all leaves in the plant have the same biochemical content (He and Mui, 2010).

Physically based methods or models have also been developed which involve the use of radiative transfer models such as SAILH, PROSPECT or LEAFMOD to estimate the biometric properties and biochemical content from leaf to canopy and over larger spatial

scales (Glenn *et al*., 2008). Such models include assumptions and commonly use inputs on the leaf characteristics, geometry of vegetation in the field of view, and the nature of the surrounding environment including weather conditions. Airborne and satellite data sets have contributed significantly to scaling various land surface and vegetative parameters from leaf to canopy and stand levels, as vegetation parameters are clearly not uniform at increasing spatial scales, varying in vegetation type, its state, spatial distribution and canopy composition (He and Mui, 2010). Physically based models require the application of inversion models in order to retrieve vegetation characteristics from reflectance data. Commonly used inversion algorithms include numerical optimization methods, look-up table approaches, artificial neural network methods, and support vector machine regression (Glenn *et al*., 2008). Vegetation indices have also been used in temporal vegetation or land surface studies or as inputs into models such as soil-vegetation-atmosphere transfer, surface energy balance or global climate models, to estimate a wide variety of canopy attributes such as net primary production and evapotranspiration. Such applications simplify the task of modelling complex landscapes (Glenn *et al*., 2008).

Removal of atmospheric and background interferences is necessary when processing remote sensing data. Various types of calibration models can be applied depending upon the quantity and quality of calibration data recorded during the remote sensing acquisition surveys. Alternatively, the removal of atmospheric and background interferences could be omitted when vegetation spectral reflectance indices, which account for differences in atmospheric and background effects, were applied in sparsely vegetated environments (Giannico, 2004). Furthermore, the magnitude of atmospheric and background interferences is greater as spatial resolution decreases from ground to stand and canopy levels; and spectral resolution increases from multispectral to hyperspectral data.

3.4 DETECTION OF PLANT WATER STRESS USING GROUND-BASED MEASUREMENTS

Simple, quick and portable ground-truthing methods are needed for the measurement of plant water stress. Commonly-used techniques address aspects of the plant water status and plant pigment condition.

3.4.1 Predawn leaf water potential

Predawn leaf water potential measurements, often undertaken with a pressure chamber, are of significant value when determining plant water stress. At predawn, xylem water potential has equilibrated with soil water potential after a night of negligible transpiration. At this time, plant water potential is usually at its minimum for the day (Cleary and Zaerr, 1984).

The pressure chamber is most commonly used for estimating leaf water potential, having the advantage of simplicity, reliability, instantaneous measurements, low capital cost and portability (Scholander *et al*., 1965; Boyer, 1968; Ritchie and Hinckley, 1975). The equipment design has not changed significantly over the past four decades since Scholander *et al*. (1965) used this technique to measure the water relations of trees and shrubs. However, this technique is considered slow and time-consuming for any commercial or operational applications (Jones, 2004).

Measurement of predawn leaf water potential has gained wide acceptance among researchers. It is commonly used as a plant water stress indicator (Aranda *et al*., 2005; Nortes *et al*., 2005; Intrigliolo and Castel, 2006; Pellegrino *et al*., 2006) and has also been used to describe the water status of different species within a habitat (Scholander *et al*., 1965; Lamont and Witkowski, 1995). It has been shown that species within the same habitats differ in predawn leaf water potentials (Witkowski *et al*., 1992; Lamont and Witkowski, 1995), while predawn leaf water potentials often differ within a single species between different habitats, and with leaf age (Witkowski *et al*., 1992) and plant size (Lamont *et al*., 1994). Typical plant water potential measurements of unstressed plants range from -0.15 MPa for plants under saturated soil conditions and low atmospheric demand (Cleary and Zaerr, 1984) to -2.0 MPa for ‘tank’ plants such as cactus, which can store water (Scholander et al., 1965). Conversely, stressed plants such as creosote bush and juniper growing in more arid regions could achieve plant water potentials of -8.0 MPa (Scholander et al., 1965), while for desert plants it can be much higher. Predawn leaf water potential measurements have also been successfully used in agricultural applications to evaluate plant water stress. Such applications have included estimates of total transpirable soil water and assessments of crop water stress resulting from irrigation scheduling of grapevine field sites and fruit orchards (Intrigliolo *et al*., 2006; Pellegrino *et al*., 2006). Predawn leaf water potentials have also

been coupled with stem water potential measurements and fluctuations in trunk diameters to quantify water stress of young almond trees for irrigation management (Nortes *et al*., 2005).

Despite the wide application of predawn pressure chamber measurements, numerous sources of error and measurement problems have been identified (Ritchie and Hinckley, 1975). These sources of error need to be minimised in order to ensure accurate readings, and can be grouped into four categories *viz*. speed of measurement in the field, accurate selection and processing of samples, reduction in pressurisation problems with the chamber, and correct identification of the end point.

In the field, speed of measurement is of major importance. Moisture loss between time of sampling and measurement must be minimised (Ritchie and Hinckley, 1975; Turner, 1988; Campbell, 1990; Hsiao, 1990; Smith and Prichard, 2003). Measurements should take place directly after excision of the plant sample. If this is not possible, samples should be enclosed in plastic bags immediately after cutting, and stored in a cool dark place until required. However, if time delays occurred between predawn sampling and actual measurements, this could result in inaccurate estimates of predawn water potential (Clear and Zaerr, 1964; Turner, 1988).

Great care should be taken in selecting and processing samples. It is important to standardise the sampling process with respect to leaf age and development stages when comparing between plant species (Witkowski *et al*., 1992). Damaged samples (crushed leaf petiole or torn leaf blades) and re-cutting of sample stems (Scholander *et al*., 1965) lead to a break in the tension in the xylem water, and should thus be avoided (Clear and Zaerr, 1964; Turner, 1988). Furthermore, the portion of the leaf or stem external to the seal in the pressure chamber unit must be minimised to reduce exclusion errors (Miller and Hansen, 1975; Hsiao, 1990).

Several technical guidelines must be adhered to in order to reduce pressurisation problems with the chamber. Failure to achieve pressure equilibrium should be addressed by ensuring that the seal used in the pressure chamber is made of rubber that is sufficiently elastic to fill the indentations of irregularly shaped petioles, but not so soft that it disintegrates under

pressure. For very irregular petioles, a quick-setting silicon compound can be used. However, this slows down the number of leaves that can be measured (Turner, 1988). High pressure grease or a silicon adhesive compound should be used on the stopper to prevent or reduce leakage and to prevent leaf damage. Studies on the optimal rates of pressurisation of the chamber and the effects of rapid pressure and heat accumulation within the chamber have shown that fast rates of pressurisation can lead to both underestimates or overestimates of water potential, depending on the gradients of water potential in the sample (Waring and Cleary, 1967; Blum *et al*., 1973; Tyree and Dainty, 1973; Turner, 1981). Therefore Turner (1981) suggested an average pressurisation rate of 0.025 $MPas^{-1}$. Furthermore, caution must be taken in the use of the compressed gas with the pressure chamber. Pressure release valves protect the pressure gauges, and also help prevent over-pressurisation of the chamber (Turner, 1988). A binocular microscope or safety glasses should be used to protect the operator's eyes if any material is forced out through the seal during pressurisation (Turner, 1988).

Correct identification of the endpoint, when the xylem sap just returns to the cut surface of the xylem, is critical for accurate estimation of the water potential (Ritchie and Hinckley, 1975; Turner, 1988; Campbell, 1990; Hsiao, 1990; Smith and Prichard, 2003). Use of binocular microscope or magnifying glass is necessary to minimise poor recognition of the endpoint.

Field equipment required for leaf water potential measurements is relatively easy to setup within a specific location, but can be cumbersome when there are many sample sites which are not in close proximity to each other. When accounting for the time required for setting up the instrument, gathering of samples and the actual measurement at predawn, only a limited number of measurements are possible within this timeframe. Therefore, from a practical view point, this method is more appropriate for localised measurements, as compared to large scale measurements.

3.4.2 Leaf chlorophyll fluorescence

Over the past decade, chlorophyll fluorescence kinetics has been used more extensively to provide considerable information on the organisation and function of the photosynthetic

apparatus (Govindjee *et al*., 1981). Information is gathered more readily and can be sampled more often outside the laboratory using portable optical systems and compact chlorophyll fluorescence meters.

The functioning of the photosynthetic apparatus is dependent on the process of photosynthesis, whereby light energy is absorbed and converted into organic compounds. Several environmental factors, including water, light and nutrients, affect this process and may lead to plant stress. Therefore, the photosynthetic apparatus has been recognised as being a good indicator of stress and stress adaptation of a plant (Salisbury and Ross, 1992; Strasser and Tsmilli-Michael, 2001), which is associated with the measurement of chlorophyll fluorescence (Strasser *et al*., 2001). Also, because changes in chlorophyll fluorescence may occur before any physical signs of tissue or chlorophyll deterioration are manifested in the plant, stress can be detected before the onset of physical damage (Lichtenthaler *et al*., 2007).

Chlorophyll fluorescence measurements can be described using the typical phases of a fluorescence transient. During a typical fluorescence transient, the fluorescence rises rapidly from a ground state, O (or F_o), when all electron acceptors are fully oxidised, or open, to a maximum level, P (or F_m), when all electron acceptors are highly reduced, or closed and are unable to accept and transfer electrons (Rolando and Little, 2003). Various parameters representing subsequent phases in a typical fluorescence transient can yield information on how stress affects the functioning of the photosynthetic system (Strasser *et al*., 2001; Rolando and Little, 2003). Photochemical efficiency is a common parameter used to assess the effect of environmental stresses on the photosynthetic mechanism (Strasser and Tsmilli-Michael, 2001). The photochemical efficiency of photosystem II (PSII) is estimated by F_v/F_m, which is the ratio of variable fluorescence (F_v) to maximum fluorescence (F_m). Most healthy plants exhibit F_v/F_m values around 0.8 (Peterson *et al*., 2001).

Most studies on the applications of chlorophyll fluorescence have utilised the F_v/F_m ratio as an indicator of water stress (Govindjee *et al*., 1981; Havaux and Lannoye, 1983; Ögren, 1990; Van Rensburg *et al*., 1996; Van der Mescht *et al*., 1997; Lu and Zhang, 1999; Peterson *et al*., 2001; Rolando and Little, 2003; Cifre *et al*., 2005). In these studies, it has been well

documented that at the chloroplast level, the function of the thylakoid membrane is sensitive to environmental stress (Öquist, 1987). Studies which have focused on deep rooted non-native tree species have suggested that the decrease in F_v/F_m was due to drought induced injury to the thylakoid structures affecting photosynthetic electron transport (Van Rensburg *et al*., 1996; Van der Mescht *et al*., 1997; Lu and Zhang, 1999). These results have indicated that F_v/F_m of drought stressed trees was lower than the control trees, especially in the more drought intolerant trees. Van Rensburg *et al*. (1996) found that the decrease in F_v/F_m was due largely to an increase in F_o, an indication of permanent damage to the PSII. PSII appears to be particularly sensitive to a number of stress factors including freezing temperatures and drought (Öquist and Wass, 1988). Rolando and Little (2003) also showed a decrease in F_v/F_m of water stressed *Eucalyptus grandis* seedlings, resulting from a rise in F_o and a decrease in F_m. Since this ratio is a reflection of the maximum yield of primary photochemistry, F_v/F_m is also used as an indicator of tree or seedling vigour.

Water stress leads to several changes in the photosynthetic apparatus of plants. Low water potential has been observed to cause a decrease in the quantum yield of O_2 evolution in chloroplasts and leaves from sunflower plants, a decrease in the ability of the coupling factor isolated from spinach leaves to bind fluorescent nucleotides, and a decrease in the ratio of the maximum to the minimum fluorescence in the red algae *Porphyrs sanjuanesis* (Govindjee *et al*., 1981). Data presented on the relationship between maximum to minimum fluorescence ratios and the water potential of leaves of *Nerium oleander*, *Atriplex triangularis* and *Tolmiea menziesii* suggest that water stress blocks electron flow to the reaction center chlorophyll *a* of PSII (Govindjee *et al*. (1981). It was clear from these results that the ratio of maximum to minimum fluorescence decreases from a high value of 4.0 in well-watered *Nerium oleander* plants (water potential -0.8 MPa) to a low value of 1.1 in a severely stressed plant (water potential -3.9 MPa). In all cases examined, the ratio decreased as the water potential decreased. Because of these results, Govindjee *et al*. (1981) concluded that water stress inhibited electron flow of PSII in the three species examined, and that this ratio serves as a qualitative indicator of leaf water potential.

Chlorophyll fluorescence ratios have gained increased acceptance in recent years, and is commonly measured using hand-held relatively low-cost portable instruments which are

simple, rapid and non-destructive (Peterson *et al*., 2001; Strasser *et al*., 2001; Strasser and Tsmilli-Michael, 2001; Rolando and Little, 2003; Cifre *et al*., 2005; Lichtenthaler *et al*., 2007). With the development of an internal saturating light source in portable field fluorescence meters, chlorophyll fluorescence measurements can now be undertaken at any time of the day, from shaded or sunlit leaf samples.

Chlorophyll fluorescence measurements can be used in conjunction with other techniques as a relatively quick initial screening method for assessing plant stress within a localised area. There have also been significant advances in the application of chlorophyll fluorescence at larger spatial scales over the past decade, allowing for spatial detection of chlorophyll fluorescence parameters using laser-based fluorometers (Ounis *et al*., 2001; Cifre *et al*., 2005). Such technological improvements in chlorophyll fluorescence measurements may complement the ground-truthing of remote sensing imagery. However, further investigations are needed to establish its applicability for different crops growing under different conditions (Cifre *et al*., 2005). A disadvantage is that these instruments have not yet been designed for commercial or operational use.

3.4.3 Chlorophyll and carotenoid pigment concentration

Plant pigment concentrations vary with species, ecotype and phenology, and are also affected by season and various kinds of natural and anthropogenic stresses (Gitelson and Merzylak, 1997). Healthy plants, those capable of maximum growth, are generally expected to have higher chlorophyll pigment concentrations than unhealthy plants. Reduced chlorophyll concentrations are often associated with stressed plants, with variations in total chlorophyll to carotenoid ratios used as indicators of stress in plants (Netto *et al*., 2005; Lichtenthaler *et al*., 2007). Carotenoids play an important role in protecting the photosynthetic apparatus, and regulate the flow of energy into and out of the photosynthetic system (Sims and Gamon, 2002; Netto *et al*., 2005). Two commonly used approaches have been adopted to quantify chlorophyll and carotenoid pigment concentrations in plants, *viz*. conventional chemical methods and field chlorophyll meters. Conventional chemical methods of pigment quantification require destructive sampling and time-consuming laboratory analyses, compared to chlorophyll meters which are simple, portable field instruments which save time and resources. Both applications are more suited for localised

ground-based measurements, but have also been used to ground-truth remote sensing imagery.

Conventional laboratory methods used for estimating chlorophyll and carotenoid pigment concentrations are seen as the most accurate methods, provided correct sampling and laboratory procedures are followed. These methods make use of spectrophotometry for estimating pigment concentrations in plant extractions via the linear absorption characteristics of these pigments in polar extractants at specific wavelengths. Concentrations are calculated taking cognisance of the extractant and the specific extinction coefficients as described in Lichtenthaler (1987). Two precautions are recommended when sampling, and during laboratory analysis: rapid and efficient collection of samples which must be frozen immediately using liquid nitrogen to prevent pigment deterioration, and minimal loss of pigment during laboratory extraction and dilution procedures in order to reduce the variability of the results. If the research is taking place in remote areas, liquid nitrogen could be substituted with sufficient dry ice or ice packs.

Chlorophyll meters are portable field instruments that allow for non-destructive repetitive sampling, and have been used successfully to estimate the chlorophyll content of many plant species (Schaper and Chacko, 1991; Netto *et al*., 2005; Pinkard *et al*., 2006). A chlorophyll index derived from two peak reflectance wavelengths, 650 nm and 940 nm, is used to estimate the observed chlorophyll content in a sample. However, several factors affecting chlorophyll concentration such as the type of plant species, leaf weight, leaf age and growing conditions may influence the relationship between the chlorophyll index and actual chlorophyll concentration. Therefore, calibration curves are required for many species, site and experimental conditions (Pinkard *et al*., 2006).

3.4.4 Leaf water content

Relative leaf water content is an indirect and gross estimate of the changes in the water content in leaves through precise weight measurements (Canny and Huang, 2006). Most water in leaves reside in mesophyll cells. Volumetric changes in these cells occur as the balance shifts between the rate of evaporation from leaves and the rate of water supply to the leaves. Volumetric changes in the leaves of plants affect many internal plant conditions such

as tension in the cell walls, exchange of water and carbon dioxide across cell membranes, osmotic pressure of vacuole contents, cell and tissue turgor, cell-to-cell contact and transport of water.

Measurements of relative water content from leaf tissues are commonly used to assess the water status of plants (Barrs and Weatherley, 1962; Catsky, 1969; Turner, 1981; Joly, 1985; Yamasaki and Dillenburg, 1999; Shen *et al.*, 2005; Canny and Huang, 2006). The relative leaf water content is expressed as the ratio of three weight determinations, *viz.* fresh weight, dry weight and turgid weight of the leaf sample. It is calculated as the ratio of fresh weight minus dry weight to turgid weight minus dry weight. It is important that sampling procedures are meticulous to prevent evaporative losses of water from the leaf samples (Barrs and Weatherley, 1962; Catsky, 1969; Turner, 1981; Joly, 1985; Yamasaki and Dillenburg, 1999; Shen *et al.*, 2005; Canny and Huang, 2006). Samples must also be stored immediately in plastic bags and stored in a cool, dark place to reduce moisture loss prior to fresh weight measurements. Furthermore, the validity of relative water content measurements depends on the precision of the three weight determinations; a reliable estimate of turgid weight being the most critical (Joly, 1985).

A typical water absorption curve shows a high initial rate of absorption, followed by a prolonged period of slow absorption (Yamasaki and Dillenburg, 1999). The amount of water initially absorbed has been commonly interpreted as being the amount of water needed to compensate for the water deficit of the plant tissue. Further water absorption would be driven by cell expansion, so that mass changes occurring during this phase would not be used in the estimation of the relative water content of the sample. Therefore, an accurate measurement of turgid weight should be determined at the end of the first initial absorption of water (Yamasaki and Dillenburg, 1999).

Water absorption periods usually recommended for conifers range from 12 to 48 hours, which is much longer than the 4 hour period usually required for most broad leaved plants (Yamasaki and Dillenburg, 1999). To reduce water absorption periods, leaf disks are commonly used instead of whole leaves (Barrs and Weatherley, 1962). This method may however, also allow more water infiltration through intercellular spaces, thereby resulting in

a greater water absorption per unit of leaf mass and an underestimation of the relative water content when compared to whole leaves (Barrs and Weatherley, 1962; Joly, 1985).

Measuring the relative leaf water content of plants is a simple yet time consuming process. Comparative measurements between stressed and unstressed plants should be undertaken during the late morning, when differences in water potentials between plants would be the greatest. Due to these time constraints this method is most appropriate for localised ground-truthing measurements.

3.4.5 Comparison of ground-based measurement techniques of plant water stress

This review suggests that all four ground-based measurements, *viz.* predawn leaf water potentials, chlorophyll fluorescence, chlorophyll and carotenoid pigment concentrations and leaf water content, can be used successfully to measure or assess plant water stress. However, these four ground-based methods are not suitable for large spatial scale sampling, and would be most useful for localised studies or as ground-truthing techniques for remote sensing applications. Sampling protocols for ground-truthing applications are dependent upon the spatial scales at which the remote sensing studies are being undertaken, *viz.* leaf, canopy, stand or landscape scale and thus sample sizes will differ accordingly. A summary of some of the advantages and disadvantages of each ground-based method is listed in Table 3.2.

Table 3.2 Advantages and disadvantages of four ground-based methods for measuring plant water stress.

Ground-based Method for Measuring Plant Water Stress	Advantages	Disadvantages
Predawn leaf water potential	Simple, reliable, instantaneous measurement, low capital cost, portable, direct indication of plant water stress. All parts of plant at predawn should be at same water potential.	Slow and time-consuming for landscape-scale measurements; not suitable for use over large spatial scales; can be cumbersome when sampling sites not in close proximity to each other; destructive sampling. Pre-dawn sampling is inconvenient.
Leaf chlorophyll fluorescence	Hand-held portable, light weight field instruments, simple, rapid non-destructive sampling, relatively low capital cost, internal saturating light source present in latest models, measurements can be taken at any time of the day, technology advances for remote sensing applications using laser-based fluorometers.	Not designed for use over large spatial scales.

Chlorophyll and carotenoid pigment concentrations	*a. Conventional chemical methods* Foundations in well researched methodologies of spectrophotometry. *b. Chlorophyll meter* Simple, portable, non-destructive sampling, allow for repeated measurements on the same sample over time, instantaneous measurement.	Problem in keeping leaves fresh to avoid chlorophyll degradation. Destructive sampling, time consuming. Calibration required to obtain actual chlorophyll concentrations for different species and environments.
Leaf water content	Simple, low capital costs, low precision analytical measurements.	Validity dependent on precision of weight determinations, time-consuming, destructive sampling.

These four ground-based measurements vary in their practical use as well as in the physiological processes measured. Differences in these methods, as well as the processes measured may be affected by different sources of variability, which in turn may affect the strength of the relationship to spectral indices (Stimson *et al.*, 2005). As a result strong relationships may exist between certain ground measurements and spectral indices, while others may be poorer for a specific plant species. For example, the water band index derived by Gao (1995) focussed on water content of vegetation and therefore could be correlated more strongly to leaf water content measurements compared to plant pigment concentrations and vice versa.

Different ground-based measurements of plant water stress may be preferred, depending upon the research conditions under which a particular method is being applied. For airborne and satellite remote sensing vegetation studies, ground-truthing techniques which are cost effective, efficient and reliable and can be applied over large spatial scales within a reasonable time-frame of acquiring the remote sensing images, would be preferred. Under such research conditions, measurements of chlorophyll fluorescence or leaf water content would be more suited. On the other hand, measurements of predawn leaf water potential or chlorophyll pigment concentrations could be used for smaller-scale intensive sampling. However, should costs be a constraining factor, predawn leaf water potential measurements would be preferred over laboratory analyses of plant chlorophyll pigment concentrations.

In summary, it is recommended that a more complete but practical approach to assessing plant water stress is adopted through the use of at least one ground-based measurement, *viz.* plant pigment concentrations, chlorophyll fluorescence or relative leaf water content to identify gradients in plant stress, and to then undertake predawn leaf water content measurements along this gradient, specifically to identify the extremes in plant water stress.

3.5 CONCLUDING REMARKS

This review demonstrates that there has been extensive research on the detection and measurement of plant water stress using ground-based and remote sensing technologies.

Ground-based techniques are more suited for localised measurements and for ground-truthing of remotely sensed data. Remote sensing research has identified several individual spectral bands and vegetation spectral reflectance indices which have been used to detect plant water stress. Many of the earlier studies have focused on broad spectral bandwidths and it recommended that plant stress researchers utilise the spectral findings to investigate further the potential of narrow hyperspectral bandwidths to detect and interpret patterns of plant stress. Furthermore, the importance of the red edge, defined as the region between 690 and 740 nm, has gained increasingly more attention over the years, and is seen as one of the most important regions of the spectrum when investigating plant stress. It is also recommended that the results from hyperspectral studies should be incorporated in multispectral systems and technologies to allow for specialised high spectral resolution investigations to be undertaken with reduced data volumes in a cost-effective manner. Most spectral indices have been derived for a single species with constant leaf size and shape, leaf surface and internal structure, implying that their usefulness varies with respect to species and site conditions. Therefore, the most commonly used indices reported in the literature must be evaluated against ground-truthing data. Ground-truthing of remote sensing data is not an easy task, especially when considering different temporal and spatial scales. Depending upon the scale at which an investigation is being undertaken, it is recommended that a practical approach to assessing plant water stress is adopted through the use of at least one ground-based measurement, *viz.* plant pigment concentrations, chlorophyll fluorescence or relative leaf water content to identify gradients in plant stress, and to then undertake predawn leaf water content measurements along this gradient, specifically to identify the extremes in plant water stress.

CHAPTER 4. SPECTROSCOPY AS A TOOL FOR IDENTIFYING PLANT WATER STRESS AT THE LEAF-LEVEL

ABSTRACT

The purpose of this study was to investigate the potential of hand-held spectroscopy as a tool for identifying plant water stress at the leaf-level. Seventy seven spectral reflectance indices and specific individual spectral wavelengths useful for detecting plant water stress, plant pigment content, the presence of stress related pigments in vegetation, and changes in leaf cellular structure, were investigated in this study. The objective was to investigate relationships between leaf spectral reflectance data and ground-based measurements of plant water stress, such as predawn leaf water potential, leaf chlorophyll fluorescence, chlorophyll and carotenoid pigment content and relative leaf water content. Finally, spectral models which could be used to detect plant water stress in three tree species, *Eucalyptus camaldulensis, E. sideroxylon* and *Searia lancea* in the Welkom, Vaal River and West Wits mining districts were identified.

Four commonly used ground-truthing techniques; predawn leaf water potential, leaf chlorophyll fluorescence, leaf chlorophyll and carotenoid pigment content and leaf water content, were used to measure plant water stress in the 75 sample trees. Leaf spectral reflectance measurements were taken with a hand-held spectrometer, from which spectral reflectance indices were then calculated. Multiple linear regression was applied to investigate the interactions between the districts and species, and their respective spectral reflectance indices and plant water stress measurements. The "best" models for each plant water stress measurement and the best model across all combinations of spectral reflectance indices and plant water stress measurements resulting from the stepwise regression, were selected using the highest adjusted R^2 value and the significance of the F (ANOVA) and t (t-test) probability values.

The results of the ground-based measurements of plant water stressed revealed that predawn leaf water potential measurements ranged from -0.56 to -0.68 MPa at unstressed sites, and from -0.93 to -1.78 MPa at stressed sites. Predawn leaf water potential measurements revealed higher (more negative) values at West Wits, and lower (less negative) values at Vaal River. The median photochemical efficiency ratios of all three districts were similar ranging between 0.6 and 0.7. The distribution of the data measured for chlorophyll a, chlorophyll b, total chlorophyll content and carotenoid content followed a similar amplitudinal pattern for each mining district. For all four measurements the highest upper quartile and median values were measured at Welkom, and the lowest lower quartile values at Vaal River. Maximal multiple linear regression models were derived for all possible combinations of plant water stress measurements and the 77 spectral reflectance indices extracted from leaf-level spectral reflectance data. The results of the multiple linear regression models indicated that the (695/690) (Carter, 1994), (850-710)/(850-680) (Datt, 1999), near infra-red index (710/760) (Carter, 1994), and the water band index (900/970) (Penuelas *et al*., 1997)performed well and accounted for more than 50% of the variance in the data.

The principal conclusion was that the stepwise regression model derived between chlorophyll b content and the DATT index was selected as the "best" model, having the highest adjusted R^2 of 69.3%. This model has been shown to be the most robust model in this study, which could be used at different locations for different species to predict chlorophyll content at the leaf-level.

Keywords :carotenoid pigment content, leaf chlorophyll, leaf chlorophyll fluorescence, leaf water content, plant water stress, predawn leaf water potential, spectral reflectance indices, spectroscopy

4.1 INTRODUCTION

Numerous studies have yielded information on the use of spectral reflectance characteristics to describe plant water status and plant water stress (Gao, 1995; Gitelson and Merzlyak, 1996; Datt, 1999; Ceccato *et al*., 2001; Coops *et al*., 2003; Stimson *et al*., 2005; Eitel *et al*.,

2006). Several individual spectral reflectance wavelengths and vegetation spectral reflectance indices have been reported that are sensitive to changes in pigment content, leaf water content, leaf water potentials and chlorophyll fluorescence ratios (Ceccato *et al*., 2001; Sims and Gamon, 2002; Coops *et al*., 2003; Pu *et al*., 2003; Jackson *et al*., 2004; Stimson *et al*., 2005; Eitel *et al*., 2006). Commonly used vegetation spectral reflectance indices include the water band index (WBI) (Penuelas *et al*., 1995); normalised difference water index (NDWI) (Gao, 1995); the normalised difference vegetation index (NDVI) (Tucker, 1979); green NDVI and red edge NDVI (RENDVI) (Sims and Gamon, 2002); red edge position (REP) (Curran *et al*., 1990) and the plant senescence reflectance index (PSRI) (Merzlyak *et al*., 2003a). However, vegetation spectral reflectance indices have usually been derived for a specific species and specific sites (Datt, 1999; Eitel *et al.*, 2006). Therefore, caution is necessary when applying spectral indices over different vegetation types or biomes for which these relationships have not been established and might not be valid (Coops *et al*., 2003).

The aim of this study was to investigate the potential of hand-held spectroscopy as a tool for identifying plant water stress during the dry winter season in *E. camaldulensis, E. sideroxylon* and *S. lancea* in the Welkom, Vaal River and West Wits mining districts. The spectral responses to plant water stress in the three tree species were investigated by undertaking leaf-level spectral reflectance signatures and ground-based measurements of plant water stress undertaken at the same time on the same sample trees during the dry winter season. Relationships between individual spectral wavelengths and spectral reflectance indices derived from the leaf-level spectral data and the measurements of predawn leaf water potential, leaf chlorophyll fluorescence, chlorophyll and carotenoid pigment content and relative leaf water content were then investigated. Ultimately, leaf-level plant water stress spectral relationships valid for the three species studied were identified.

4.2 MATERIALS AND METHODS

Leaf spectral reflectance measurements and ground-based measurements of plant water stress were undertaken on the three species *E. camaldulensis* and *E. sideroxylon* and *S. lancea* in the Welkom, Vaal River and West Wits mining districts, during late July 2004. Details of the tree samples and the collection sites have been provided in Chapter 2.

The step by step details of the procedures of each ground-based plant water stress measurement used, *viz*. predawn leaf water potential, leaf chlorophyll fluorescence, chlorophyll and carotenoid pigment content (including equations), and relative leaf water content, are presented in Appendix 2.

4.2.1 Sampling design

Stands or blocks of trees within the study areas of the WBGs are limited, with some clumps or rows of indigenous and non-native tree species growing in close proximity to TSFs. Although tree plantations are rare in these mining districts, sample sites were selected from stands, single trees or rows of trees and small-plot species trials in each mining district (Dye, 2004; I. Weiersbye, 2005 pers comm.) and as illustrated in section 2.4. Fifteen sample sites each comprising of five sample trees, were selected across the three mining districts, totally 75 sample trees across the three mining districts.

The 75 sample trees selected represented the three species *E. camaldulensis*, *E. sideroxylon* and *S. lancea*, and these were sampled for plant water stress during the dry winter season in July 2004 using ground-based measurements of plant water stress and leaf spectroscopy. Sample trees were categorised as either stressed (low water availability), or unstressed (high water availability). Sample trees with lower water availability were differentiated from trees with higher water availability through visual inspection of leaf colour and canopy density using hazard tape and metal tags, and their coordinates recorded using a global positioning system. Thereafter, the categorisation of the trees was confirmed using predawn leaf water potential measurements. A threshold reading of -0.8 MPa was used as a criterion to separate stressed (more negative) from unstressed (less negative) trees (Cleary and Zaerr, 1984).

4.2.2 Ground measurements of plant water stress

Four commonly used ground-truthing techniques were used to measure plant water stress in the 75 sample trees.

4.2.2.1. Predawn leaf water potential

Predawn leaf water potential measurements provide a direct measurement of plant water stress. Measurement of predawn leaf water potential using a pressure chamber has gained wide acceptance among researchers, and is commonly used as a plant water stress indicator (Aranda *et al.*, 2005; Nortes *et al.*, 2005; Intrigliolo and Castel, 2006; Pellegrino *et al.*, 2006).

During late July 2004, leaf water potentials were measured each day before dawn (between 12:00 am and 5:30 am) using a PMS pressure chamber unit (PMS Instrument Company, 2750 N.W. Royal Oaks Drive, Corvallis, Oregon, USA). Five replicate leaf samples were excised from each sample tree, a total of 375 samples (five samples from each of seventy five trees) for the three mining districts. For each ground-based measurement, fully expanded leaves were sampled at a height of between 1.5 and 2 m above the ground at different points around the canopy to represent different aspects and daytime illumination. Leaf samples were immediately placed in plastic bags, sealed and kept cool until time of measurement, which occurred within one hour of sampling. Measurements were recorded to the nearest 0.05 MPa.

4.2.2.2. Leaf chlorophyll fluorescence

Photosynthetic efficiency is a good indicator of the degree of stress and stress adaptation in plants (Strasser and Tsmilli-Michael, 2001). The photochemical efficiency of photosynthetic system II is estimated by F_v/F_m, which is the ratio of variable fluorescence (F_v) to maximum fluorescence (F_m). Most healthy plants exhibit F_v/F_m values around 0.8 (Peterson *et al.*, 2001).

Leaf chlorophyll fluorescence was measured with a portable OS5-FL chlorophyll fluorometer (Opti-Sciences, 164 Westford Rd, Tyngsboro, MA01879), utilising an external light source. To standardise the sampling procedure, five replicate attached leaves were sampled from the same sample trees during daylight hours (between 8:30 am and 4:00 pm). A total of 375 chlorophyll fluorescence measurements (five samples from each of seventy five trees) were collected from the sample sites.

4.2.2.3. Leaf chlorophyll and carotenoid pigment content

A relative measure of plant chlorophyll and carotenoid pigment content has been used as an indicator of plant vigour and stress (Curran *et al*., 1990; Gitelson and Merzlyzak, 1996; Lichtenthaler *et al*., 1996; Zagolski *et al*., 1996), with the assumption that a decrease in chlorophyll content is indicative of some level of plant stress.

Five replicate leaf samples were excised from each sample tree, a total of 375 samples (five samples from each of seventy five trees) from all sites. Leaf samples were excised and sealed immediately in zip lock bags, and kept frozen using ice packs to prevent pigment degradation prior to laboratory analysis. Frozen leaf samples were transported to the laboratory and analysed within seven days. Pigments were extracted with 100% methanol and then quantified using a spectrophotometer, and their relative pigment contents were derived using the accepted equations developed by Lichtenthaler (1987).

4.2.2.4. Leaf water content

Measurements of the relative water content of leaf tissue are commonly used to assess the water status of plants (Yamasaki and Dillenburg, 1999; Shen *et al*., 2005; Canny and Huang, 2006). Relative leaf water content is commonly expressed as the ratio of fresh weight minus oven-dry weight to the turgid weight minus dry weight of the leaf sample.

The first trial measurements of relative leaf water content was undertaken at the Deelkraal site in the West Wits mining district during July 2004. *E. sideroxylon* trees were sampled at two locations at the Deelkraal site, near a farm dam (-26.43969; 27.32871) and further upslope within the same stand (-26.43899; 27.33024). Five replicate leaf samples were excised from each sample tree, a total of 50 samples (five samples from each of ten trees) for the Deelkraal site. Leaves were sampled for relative leaf water content measurements before midday, between 9 am and 11:30 am. Fresh weight measurements were undertaken immediately in the field after the leaf samples were cut and were then immersed in water. Turgid weight was obtained after samples had rehydrated to full turgidity, and was measured

at least 24 hours later. Samples were oven dried at 60ºC for 24 hours, after which the dry weight measurements were determined.

4.2.3 Leaf spectral reflectance measurements

Leaf spectral reflectance measurements were taken with a hand-held Analytical Spectral Device (ASD) spectrometer (Analytical Spectral Devices Inc, 5335 Sterling Drive, Suite A, Boulder, Colorado80301, USA). The ability of such field spectrometers to sample the electromagnetic spectrum at a high spectral resolution allows for narrow-band individual spectral wavelengths and several spectral indices associated with stress detection to be investigated at the leaf-level.

4.2.3.1. ASD hand-held spectral measurements at leaf-level

The ASD spectrometer measures contiguous spectral signatures from 350 nm to 2500 nm. Due to atmospheric effects, the instrument was calibrated with a white reference at each site and between sampling, depending on the prevailing cloud cover. All leaf spectral signatures were measured between 10:00 am and 2:00 pm, under clear skies and full sunlight. To minimise differences in background reflectance, attached leaf-bearing branches were bunched together to permit a solid target of overlapping leaves to be presented to the field spectrometer. Under conditions of poor sunlight resulting from canopy shading effects, branches were cut and immediately overlaid and sampled in an area of full sunlight. To obtain a representative leaf spectral measurement from each tree, five measurements each consisting of five replicate spectrometer readings (total of 375 readings across all three mining districts) were measured. Spectrometer measurements were undertaken at different points around the tree canopy to represent different aspects.

4.2.3.2. Vegetation spectral reflectance indices derived from leaf-level spectral measurements

Seventy seven spectral reflectance indices and specific individual spectral wavelengths useful for detecting plant water stress, plant pigment content, the presence of stress related pigments in vegetation, and changes in leaf cellular structure, were investigated in this study (Table 4.1). For each of the 75 sample trees, the individual spectral wavelengths were

extracted from the spectral reflectance signatures. Spectral indices were then calculated using ENVI 4.1 (Research Systems Inc., 2005) and Microsoft Excel.

Table 4.1 Spectral wavelengths and reflectance indices used in the leaf-level analysis.

Common name for spectral index or spectral region of the spectrum	Spectral Reflectance Ratio or Index (nm)	Reference
Carter index	(695/760)	Carter (1994)
Gamon and Surfus index	(600-700)/(500-600)	Gamon and Surfus (1999)
Datt (1999) index	(850-710)/(850-680)	Datt (1999)
Green peak index	(850-550)/(850-680)	Datt (1999)
Infrared red reflectance plateau	850	Gausman and Allen (1973)
Reflectance at 750 nm	750	Datt (1999)
Reflectance at 710 nm	710	Carter (1994)
Green reflectance peak	550	Strachan *et al*. (1999)
Reflectance at 680 nm	680	Strachan *et al*. (1999)
Reflectance ratio 750/710	(750/710)	Datt (1999)
Reflectance ratio 750/550	(750/550)	Lichtenthaler *et al*. (1996)
Reflectance ratio 850/550	(850/550)	Schepers *et al.* (1996)
Reflectance ratio 850/710	(850/710)	Datt (1999)
Reflectance ratio 865/552	(865/553)	Blackburn (2002)
Photochemical reflectance index (PRI)	(531-570)/(531+570)	Sims and Gamon (2002)
Red edge normalised difference vegetation index (RENDVI)	(750-705)/(750+705)	Sims and Gamon (2002)
Canopy normalised difference vegetation index	((800-900)-(671-674))/((800-900)+(671-674))	Stylinski *et al*. (2002)
Reflectance ratio 695/690	(695/690)	Carter (1994)
Reflectance ratio 695/420	(695/420)	Carter (1994)
Reflectance ratio 605/760	(605/760)	Carter (1994)
Reflectance ratio 710/760	(710/760)	Carter (1994)
Reflectance ratio 550/419	(550/420)	Carter (1994)
Reflectance ratio 710/419	(710/420)	Carter (1994)
Reflectance ratio 550/670	(550/670)	Carter (1994)
Reflectance ratio 710/670	(710/670)	Carter (1994)
Reflectance ratio 550/760	(550/760)	Carter (1994)
Reflectance ratio 520/420	(520/420)	Carter (1994)
Reflectance ratio 605/420	(605/420)	Carter (1994)
Reflectance ratio 520/760	(520/760)	Carter (1994)
Reflectance ratio 476	476	Blackburn (1999)
Reflectance ratio 632	632	Blackburn (1999)
Reflectance ratio 800	800	Blackburn (1999)
Reflectance index (800-476)	(800-476)	Blackburn (1999)
Reflectance index (800-550)	(800-550)	Blackburn (1999)
Reflectance index (800-632)	(800-632)	Blackburn (1999)
Reflectance index (800-680)	(800-680)	Blackburn (1999)
Reflectance ratio log(800)/476	log(800)/(476)	Blackburn (1999)
Reflectance ratio log(800)/550	log(800)/(550)	Blackburn (1999)
Reflectance ratio log(800)/632	log(800)/(632)	Blackburn (1999)
Reflectance ratio log(800)/680	log(800)/(680)	Blackburn (1999)
Reflectance ratio 476/800	(476/800)	Blackburn (1999)
Reflectance ratio 550/800	(550/800)	Blackburn (1999)
Reflectance ratio 632/800	(632/800)	Blackburn (1999)
Reflectance ratio 680/800	(680/800)	Blackburn (1998b)
Reflectance ratio (800-680)/(800+680)	(800-680)/(800+680)	Blackburn (1998b)
Inflection point	First value which crosses the x axis between 640 and 740 nm	Sims and Gamon (2002)

Common name for spectral index or spectral region of the spectrum	Spectral Reflectance Ratio or Index (nm)	Reference
Red edge position (REP)	Wavelength @ max derivative of red edge	Curran *et al*. (1990)
Derivative @ inflection wavelength	Derivative @ inflection wavelength derived between 640 to 740 nm	Curran *et al*. (1990)
Maximum derivative of red edge	Maximum derivative of red edge derived between 640 to 740 nm	Curran *et al*. (1990)
Slope of red edge	Slope between maximum and minimum derivatives and wavelengths between 640 and 740 nm	Curran *et al*. (1990)
Reflectance at 465 nm	465	Nagler *et al*. (2001)
Reflectance at 565 nm	565	Merzlyak *et al*. (2003b)
Reflectance at 664 nm	664	Porra (2002)
Reflectance at 870 nm	870	Blackburn (1999)
Reflectance ratio (870-664)/(870+664)	(870-664)/(870+664)	Porra (2002)
Reflectance ratio 664/870	(664/870)	Porra (2002)
Reflectance ratio 565/664	(565/664)	Merzlyak *et al*. (2003b)
Reflectance ratio 565/870	(565/870)	Merzlyak *et al*. (2003b)
Reflectance ratio (870-565)/(870-664)	(870-565)/(870-664)	Merzlyak *et al*. (2003b)
Reflectance ratio 465/565	(465/565)	Nagler *et al*. (2001)
Reflectance ratio 465/664	(465/664)	Nagler *et al*. (2001)
Reflectance ratio 465/870	(465/870)	Nagler *et al*. (2001)
Reflectance ratio 680/695	(680/695)	Datt (1998)
Reflectance ratio 680/690	(680/690)	Datt (1998)
Reflectance ratio 695/680	(695/680)	Datt (1998)
Reflectance ratio 850-710	(850-710)	Datt (1998)
Reflectance ratio 850-680	(850-680)	Sims and Gamon (2002)
Reflectance ratio 680/850	(680/850)	Sims and Gamon (2002)
Reflectance ratio 850/680	(850/680)	Sims and Gamon (2002)
Reflectance ratio 710/680	(710/680)	Datt (1998)
Reflectance ratio 680/710	(680/710)	Datt (1998)
Reflectance ratio 710/850	(710/850)	Datt (1999)
Reflectance ratio 850/710	(850/710)	Datt (1999)
Green normalised difference vegetation index (GNDVI)	(750-550)/(750+550)	Gitelson *et al*. (1996)
Normalised difference vegetation index (NDVI)	(750-676)/(750+676)	Tucker (1979)
Normalised difference water index (NDWI)	(857-1241)/(857+1241)	Gao (1995)
Water band index (WBI)	(900/970)	Penuelas *et al*. (1995)

4.2.4 Analysis of data

A statistical analysis of the plant water stress measurements collected in July 2004 was undertaken to produce a comparative summary for all species, across all three mining districts, per species for each mining district, and between species and mining districts for each of the ground-based methods used in this study. Spectral reflectance measurements obtained for each sample tree were averaged to produce average spectral reflectance signatures per species for each sampling site.

Simple linear regression has been the most accepted and more commonly used approach to investigate possible trends or relationships between spectral reflectance measurements and specific plant or environmental response variables (Blackburn, 1999; Datt, 1999; Champagne *et al.*, 2003; De Tar *et al.*, 2006; Blackburn, 2007). However, in many biological situations additive and interactive effects of predictor and response variables are anticipated (Quinn and Keough, 2002). Therefore linear regression is often used to investigate additive and interactive effects between variables, and to develop models for prediction. In this study, multiple linear regression was applied to investigate the interactions between the districts and species, and their respective spectral reflectance indices and plant water stress measurements, using Genstat (11th edition, 2008).

The general maximal multiple linear regression model, applied with the interactions can be illustrated as follows:

$$Y(i) = X(i) + L(i) + S(i) + L(i).X(i) + S(i).X(i) \quad (4.1)$$

where Y(i) represents the plant water stress measurements;
X(i) the spectral indices;
L(i) represents the districts and;
S(i) represents the species.

The maximal multiple regression model illustrated by Equation (4.1) was represented as follows:

$$Y(i) = b_o + b_1X(i) + a_1L_1 + a_2L_2 + g_1S_1 + g_2S_2 + d_1L_1X(i) + d_2L_2X(i) + e_1S_1X(i) + e_2S_2X(i) \quad (4.2)$$

where b_o represents the constant or intercept;
b_1 slope and;
a, g, d, e the regression coefficients.

The following statistical approach was adopted to select the best or most appropriate linear regression models and eliminate poor combinations of spectral reflectance indices (X) and plant water stress measurements (Y):

- Evaluation of maximal models identified at leaf-level
  - The maximal regression models for all combinations of X and Y variables were calculated using Equation (4.2) programmed in Genstat (11th edition, 2008).
  - For each maximal regression model the adjusted R^2 values were extracted into an Excel spreadsheet.
  - The adjusted R^2 values were ranked for each X and Y combination.
  - All plant water stress techniques (Y variables) with the adjusted R^2 value less than 50% were eliminated.
  - From the remaining X and Y combinations, the three highest adjusted R^2 maximal models were selected.
- Refinements to the models using stepwise regression
  - All subsets/stepwise regression methods were programmed in Genstat (11th edition, 2008) and used to determine the best statistical model for the selected X and Y combinations.
  - For each stepwise regression model the adjusted R^2 values were extracted into an Excel spreadsheet.
  - The adjusted R^2 values for the maximal models were compared with their corresponding stepwise regression models to determine any improvement in the models.
- Selection of the best model
  - The "best" models, i.e. best maximal model for each plant water stress measurement (Y), and the best model across all combinations of X and Y resulting from the stepwise regression, were selected using the highest adjusted R^2 value and the significance of the F (ANOVA) and t (t-test) probability values.
- Validation of the selected model in order to verify the robustness of the model parameters:
  - Three validation exercises were performed to assess the robustness of the model parameters.

- For each validation exercise, 10 random samples were excluded from the sample dataset, i.e. every 5th, 6thand 7th sample. Regressions models were fitted for each validation subset and these models were used to predict plant water stress measurements (Y) using the excluded spectral reflectance indices (X)
- Significant differences between Y predict and Y measured were determined using a t-test for paired samples.

4.3 RESULTS

4.3.1 Ground-based measurements of plant water stress and leaf spectral reflectance

Sample trees at the 15 sites that were initially categorised as either stressed (low water availability) or unstressed (high water availability) through visual inspection, and thereafter confirmed using predawn leaf water potential measurements, are presented in Table 4.2. Predawn leaf water potential measurements ranged from -0.56 to -0.68 MPa at unstressed sites, and from -0.93 to -1.78 MPa at stressed sites. At Vaal River, five *E. camaldulensis* sites were sampled, which comprised three stressed sites with predawn leaf water potential readings below -0.9 MPa, whereas at the two unstressed sites predawn leaf water potential readings were above -0.5 MPa. However, when corresponding measurements of leaf chlorophyll fluorescence, leaf chlorophyll content and leaf carotenoid content were compared between stressed and unstressed sites, these measurements did not follow the same pattern.

An assessment of comparative sampling sites, (sites within the same geographic location, in the same mining district and for the same species) revealed a relative increase in leaf chlorophyll fluorescence, leaf chlorophyll content and leaf carotenoid content for less stressed trees with relatively higher predawn leaf water potentials. An assessment of the comparative *E. camaldulensis* sampling sites 3 and 4in Vaal River and *E. sideroxylon* sampling sites 8 and 9 in West Wits demonstrate these differences.

Ground-based measurements of *E. camaldulensis* trees sampled near a tailing storage facility, sample sites 3 and 4 in Vaal River, showed significant differences between healthier (unstressed) and more stressed trees for total leaf chlorophyll content ($t = 2.43$, 8df, $P = 0.041$), chlorophyll a content ($t = 2.45$, 8df, $P= 0.040$), chlorophyll b content ($t = 2.34$, 8df, $P = 0.047$), carotenoid content ($t = 4.16$, 8df, $P = 0.006$), and predawn leaf water potential ($t = 3.03$, 8df, $P = 0.086$).

Similarly, healthier *E. sideroxylon* trees sampled close to a farm dam in the West Wits mining district, sampling sites 8 and 9, displayed significant differences in chlorophyll b content ($t = -1.92$, 8df, $P = 0.091$), chlorophyll fluorescence ($t = 1.95$, 8df, $P = 0.087$) and predawn leaf water potential ($t = 26.0$, 8df, $P < 0.001$) compared to stressed trees. Furthermore, the *E. sideroxylon* trees sampled near the farm dam were also found to have a mean relative leaf water content of 63% ± 0.066, in comparison to trees sampled further upslope away from the water source, which had a mean relative leaf water content of 54% ± 0.064 ($t = -5.31$, 48df, $P < 0.001$).

In contrast, *S. lancea* trees sampled near the pan, which had greater access to water but were exposed to higher concentrations of salts and inorganic contaminants, displayed significant differences in total chlorophyll content ($t = -4.38$, 8df, $P = 0.002$), chlorophyll a content ($t = -3.87$, 8df, $P = 0.005$), chlorophyll b content ($t = -5.90$, 8df, $P < 0.001$), chlorophyll fluorescence ($t = -3.02$, 8df, $P = 0.017$) when compared to trees sampled on farmland within the Welkom mining district. Measurements of plant water stress; total chlorophyll content, chlorophyll a content, chlorophyll b content and chlorophyll fluorescence; were higher for trees sampled on farmland compared to trees sampled near the pan.

An analysis of the mean values of predawn leaf water potential indicate that *E. sideroxylon* unstressed trees sampled in West Wits experienced greater plant water stress (-0.944 MPa ±0.03620($t = 26$, 8df, $P < 0.001$)compared to *E. camaldulensis* trees sampled in Vaal River which appeared to experience less plant water stress (-0.6949 MPa ± 0.0688 ($t = 3.03$, 2df, $P = 0.086$). Mean values of leaf chlorophyll fluorescence measurements per species per mining district were relatively similar, ranging from 0.550 to 0.687, indicating subtle differences

between species, mining districts, and stressed and unstressed sites. Unstressed sample sites also appeared to reflect a higher variance in carotenoid content (CV = 69.55 %) and less variance in total leaf chlorophyll content (CV = 36.01%).

Table 4.2/…

Table 4.2 Measurements of plant stress undertaken in the Welkom, Vaal River and West Wits mining districts during July 2004.

Site No.	Mining District	Tree Species	Geographic Coordinates (dd)	Site Classification according to Predawn Leaf Water Potential Measurements	Site Description	Predawn Leaf Water Potential (MPa)		Leaf Chlorophyll Fluorescence (ratio of variable to maximal fluorescence)		Leaf Chlorophyll (a+b) Content (mg/l)		Leaf Carotenoid Content (mg/l)	
						Mean	Std Dev.	Mean	Std. Dev	Mean	Std Dev.	Mean	Std. Dev
1	VR	EC	-26.95590; 26.69330	Stressed	Dolomite, meso- eutrophic soils, high TDS	-1.07	0.18	0.660	0.140	10.127	2.327	2.851	0.527
2	VR	EC	-26.99288; 26.78289	stressed	Dolomite, eutrophic soils, deep groundwater table ~ 20m	-0.93	0.26	0.817	0.025	10.655	2.036	2.812	0.475
3	VR	EC	-26.92922; 26.68182	Stressed	andesite, eutrophic soils, close to TSF	-0.96	0.25	0.503	0.074	2.050	0.507	0.946	0.154
4	VR	EC	-26.92970; 26.62100	Unstressed	andesite, eutrophic soils, close to TSF	-0.68	0.11	0.662	0.108	6.816	1.482	1.680	0.302
5	VR	EC	-26.99332; 26.78250	Unstressed	Dolomite, eutrophic soils, high water availability, water channel	-0.57	0.10	0.794	0.033	11.322	1.784	2.832	0.452
6	VR	SL	-26.92301; 26.69820	Stressed	Quartzite, meso- eutrophic soils, low TDS	-1.07	0.18	0.508	0.163	8.000	1.838	2.122	0.390
7	VR	SL	-26.93418; 26.69592	Stressed	Dolomite, meso- eutrophic soils, high TDS, higher water availability	-1.18	0.22	0.592	0.137	11.048	2.862	2.681	0.889
8	WW	ES	-26.43969; 27.32871	Stressed	shale, non calcarious soils, high water availability, farm dam, shallow groundwater table <~ 5m	-0.95	0.07	0.714	0.034	9.135	0.831	2.459	0.198
9	WW	ES	-26.43899; 27.33024	Stressed	shale, non calcarious soils, lower water availability	-1.78	0.25	0.637	0.116	8.565	0.986	2.423	0.210
10	WW	EC	-26.43207; 27.36888	-	shale, non calcarious soils, higher water availability, riparian zone	-	-	0.549	0.147	7.092	1.319	2.501	0.346
11	WW	EC	-26.43158; 27.36155	-	shale, non calcarious soils, low water availability	-	-	0.566	0.129	7.962	0.995	2.559	0.336
12	W	EC	-28.03052; 26.51879	Unstressed	shale, eutrophic soils, farmland	-0.56	0.08	0.699	0.059	9.305	1.520	2.792	0.464
13	W	EC	-27.96743; 26.55001	Stressed	shale, eutrophic and non calcarious soils, high water availability, near pan	-1.48	0.42	0.580	0.123	11.747	1.364	2.674	0.875
14	W	SL	-28.03361; 26.51199	Stressed	shale, eutrophic soils, farmland	-1.37	0.34	0.728	0.129	14.967	2.441	3.206	0.532
15	W	SL	-27.96695; 26.55075	Stressed	shale, non calcarious soils, high water availability, near pan	-1.31	0.25	0.577	0.129	9.049	3.028	2.799	0.835
Means per species per district													
Mean value for *E. camaldulensis* for Vaal River						-0.84	0.18	0.687	0.076	8.194	1.627	2.224	0.382
Mean value for *S. lancea* for Vaal River						-1.13	0.20	0.550	0.150	9.524	2.350	2.402	0.640

Site No.	Mining District	Tree Species	Geographic Coordinates (dd)	Site Classification according to Predawn Leaf Water Potential Measurements	Site Description	Predawn Leaf Water Potential (MPa)		Leaf Chlorophyll Fluorescence (ratio of variable to maximal fluorescence)		Leaf Chlorophyll (a+b) Content (mg/l)		Leaf Carotenoid Content (mg/l)	
						Mean	Std Dev.	Mean	Std. Dev	Mean	Std Dev.	Mean	Std. Dev
Mean value for *E. sideroxylon* for West Wits						-1.37	0.16	0.676	0.075	8.850	0.909	2.441	0.204
Mean value for *E. camaldulensis* for West Wits								0.558	0.138	7.527	1.157	2.530	0.341
Mean value for *E. camaldulensis* for Welkom						-1.02	0.25	0.640	0.091	10.526	1.442	2.733	0.670
Mean value for *S. lancea* for Welkom						-1.34	0.30	0.653	0.129	12.008	2.735	3.003	0.684

W = Welkom; VR = Vaal River, WW = West Wits; EC = *E. camaldulensis*; ES = *E. sideroxylon*; SL = *S. lancea*

Box plots were used to further represent the distributions of the plant water stress measurements for each technique within each mining district. Figure 4.1 illustrates the variability of predawn leaf water potential, photochemical efficiency ratio, chlorophyll a, chlorophyll b, total chlorophyll content and carotenoid content per mining district. Predawn leaf water potential measurements revealed higher (more negative) values at West Wits (-1.360 MPa ±0.4419), and lower (less negative) values at Vaal River(-0.843 MPa± 0.2538) (Figure 4.1a). The medians and upper quartiles of predawn leaf water potential measurements were higher (more negative) for Welkom and West Wits, indicating that trees which experienced higher plant water stress were located in these two districts, when compared to Vaal River. Conversely, the photochemical efficiency ratios measured at Vaal River were highly variable and incorporated the range of values recorded at Welkom and West Wits (Figure 4.1b). However, the median photochemical efficiency ratios of all three districts were similar ranging between 0.6 and 0.7. The highest upper quartile photochemical efficiency value was measured at Vaal River, in agreement with the less negative predawn leaf water potential measurements, indicating that healthier trees were experiencing lower plant water stress. The distribution of the data measured for chlorophyll a (Figure 4.1c), chlorophyll b (Figure 4.1d), total chlorophyll content (Figure 4.1e) and carotenoid content (Figure 4.1f) followed a similar amplitudinal pattern for each mining district. For all four measurements the highest upper quartile and median values were measured at Welkom, and the lowest lower quartile values were measured at Vaal River.

Figure 4.1/...

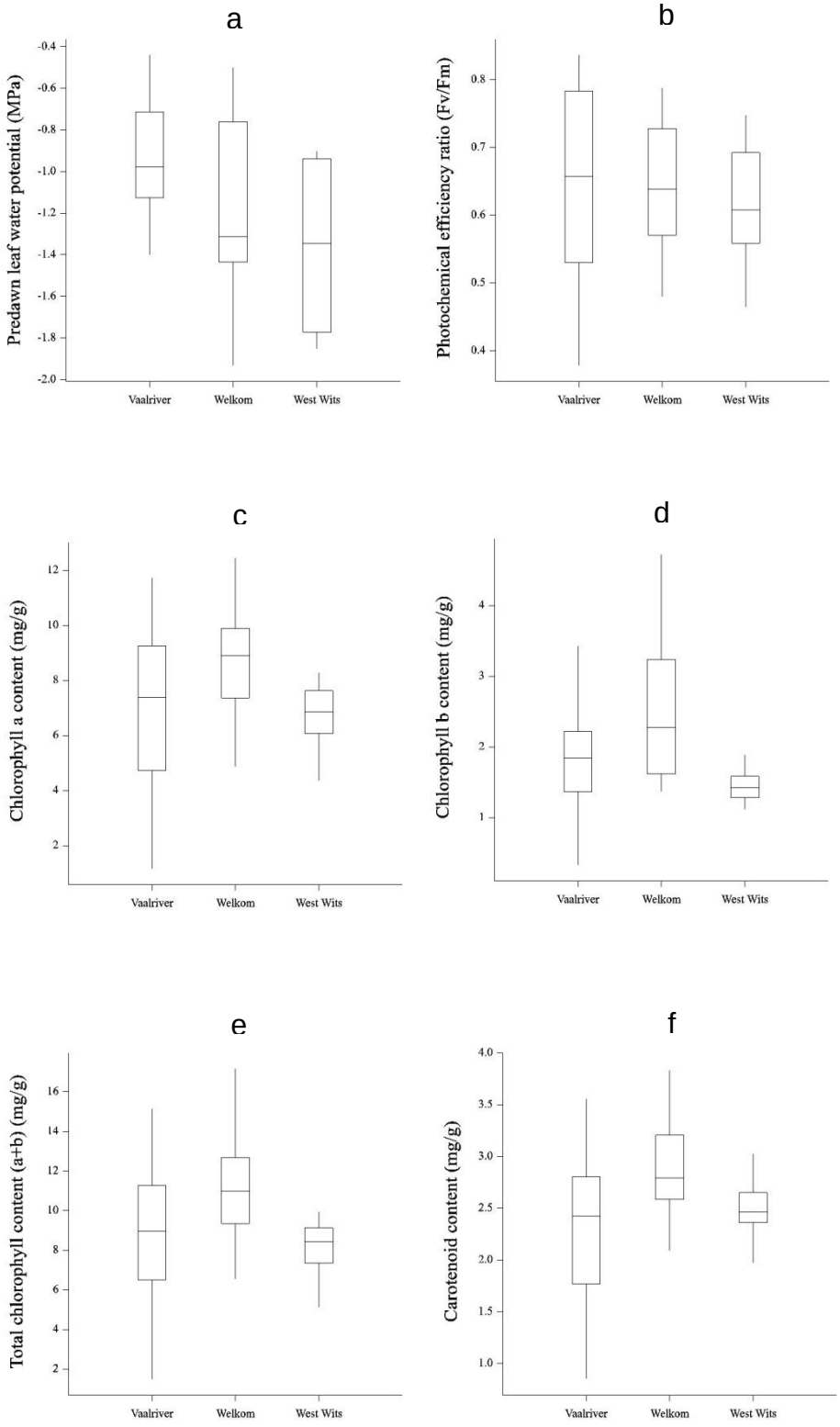


Figure 4.1 Box plots of plant water stress measurements a) predawn leaf water potential, b) photochemical efficiency, c) chlorophyll a content, d) chlorophyll b content e) total chlorophyll (a+b) content and f) carotenoid content for Vaal River, Welkom and West Wits.

The distributions of winter-time plant stress measurements collected per tree species were also investigated in this study. Box plots were used to illustrate similarities and differences of predawn leaf water potential, chlorophyll fluorescence, chlorophyll and carotenoid content measured for *E. camaldulensis*, *E. sideroxylon* and *S. lancea* (Figure 4.2). *E. sideroxylon* trees appeared to have the highest (more negative) upper quartile (-0.938 MPa) and median (-1.345 MPa), and largest variability (0.195 MPa) in predawn leaf water potentials (Figure 4.2a). However, this species displayed the least variation in photochemical efficiency (CV = 8.984)(Figure 4.2b), chlorophyll a (CV = 10.422)(Figure 4.2c), chlorophyll b (CV = 12.010)(Figure 4.2d), total chlorophyll content (CV = 9.467)(Figure 4.2e) and carotenoid content (CV = 6.284)(Figure 4.2f). The distribution of the data for chlorophyll a, chlorophyll b, total chlorophyll content and carotenoid content for each of the three tree species followed a similar amplitudinal pattern, with the highest values measured for *S. lancea* and the lowest values measured for *E. camaldulensis*. The range of median values for photochemical efficiency (0.643; 0.692; 0.626), total chlorophyll content (10.19; 9.107; 8.96) and carotenoid (2.575; 2.427; 2.684) were similar for all three species sampled.

Figure 4.2/...

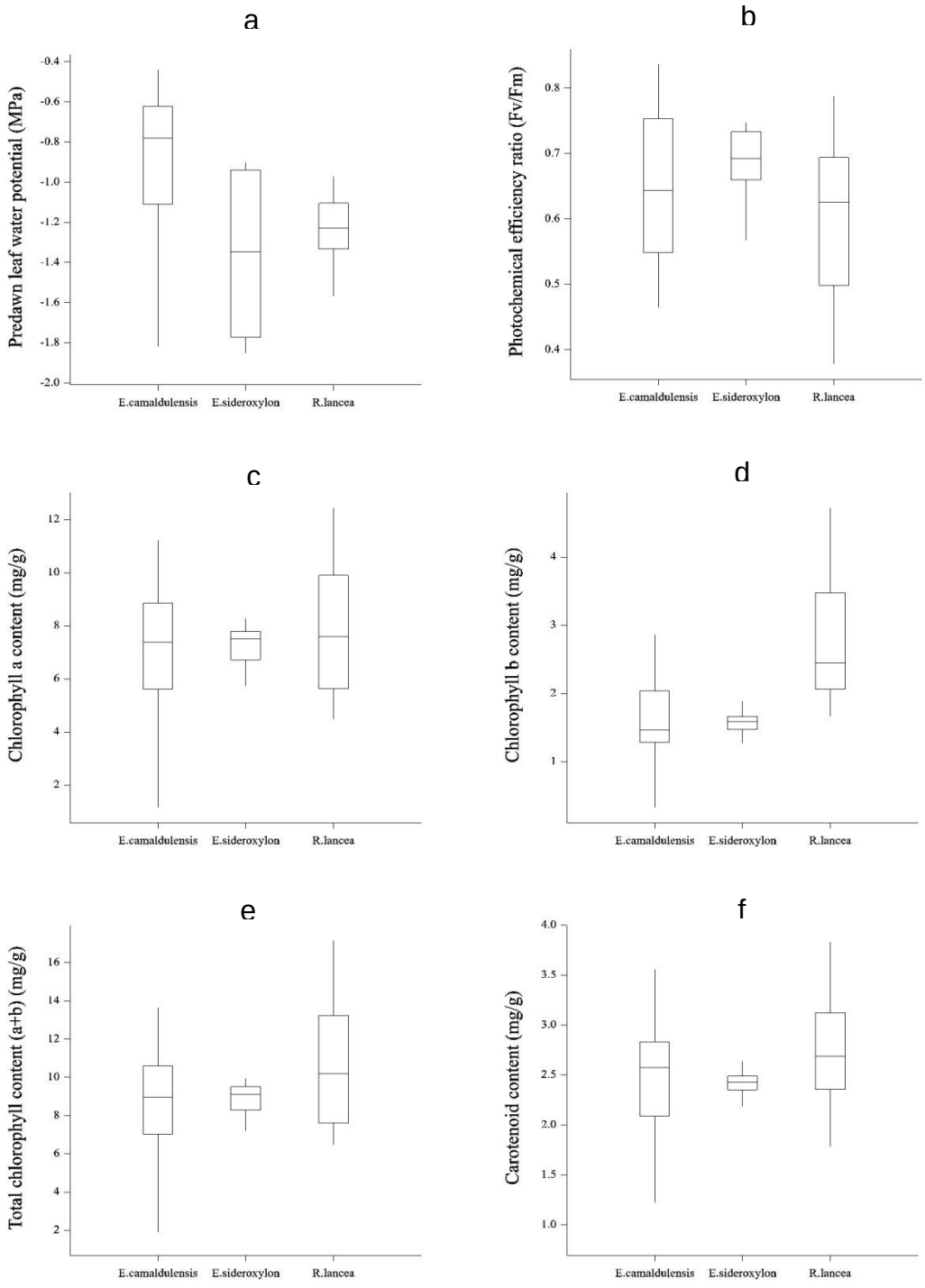


Figure 4.2 Box plots of plant water stress measurements a) predawn leaf water potential, b) photochemical efficiency, c) chlorophyll a content, d) chlorophyll b content e) total chlorophyll (a+b) content and f) carotenoid content for the three tree species E. camaldulensis, E. sideroxylon and S. lancea.

Average leaf spectral reflectance signatures were obtained for each of the fifteen sampling sites. In general, trees that were experiencing some degree of plant water stress displayed a higher leaf spectral reflectance curve across the spectrum compared to unstressed trees. Figure 4.3 demonstrates the spectral reflectance patterns observed at comparative sampling sites for *E. camaldulensis* near the Western Complex tailing storage facility in Vaal River, *E. sideroxylon* in West Wits and *S. lancea* in Welkom.

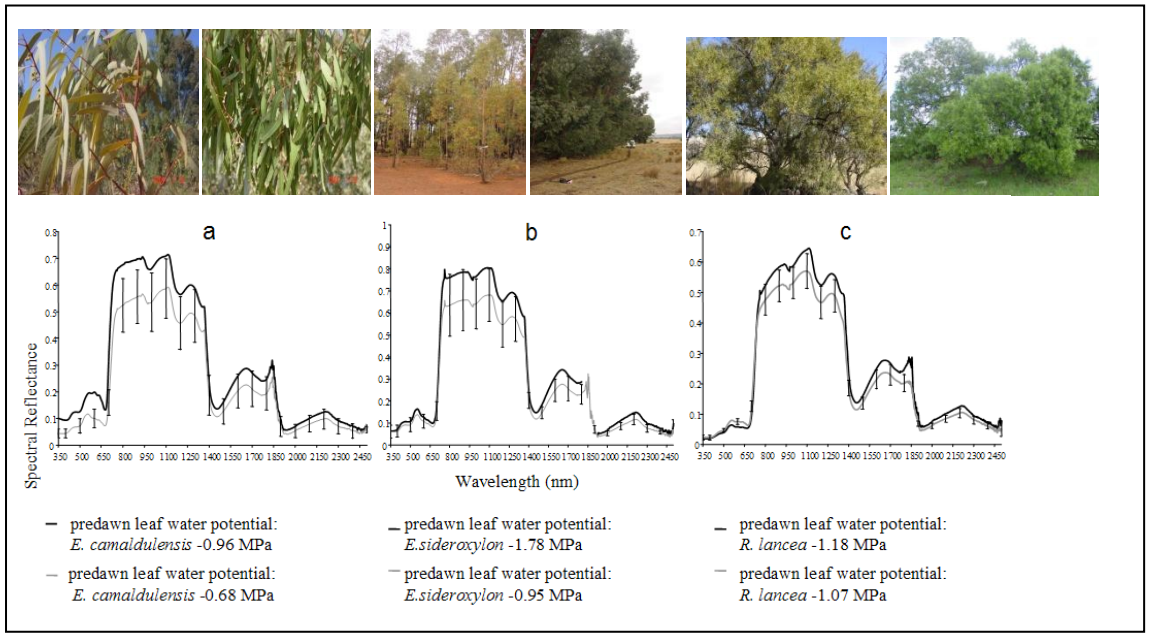


Figure 4.3 Typical average leaf reflectance spectra with standard deviation error bars (a) E. camaldulensis measured in Vaal River near the Western Complex tailing storage facility, (b) E. sideroxylon measured in West Wits and, (c) S. lancea measured in Welkom.

Leaf spectral reflectance signatures obtained for trees at a lower or more negative predawn leaf water potential (-0.96; -1.78; -1.31 MPa), also displayed a lower chlorophyll content, as presented in Table 4.2. Trees at lower or more negative predawn leaf water potential were considered to be experiencing some degree of plant water stress with the *E. camaldulensis* and *E. sideroxylon* trees (Figure 4.3a and 4.3b) visually displaying characteristics of yellow brown leaf colour, lower canopy density, greater distance from available water source when compared to trees with a higher predawn leaf water potential (-0.68; -0.95; -1.37 MPa).

4.3.2 Relationships identified at the leaf-level

Results from the multiple linear regressions were evaluated through the analysis of maximal models identified using leaf-level spectral reflectance data, refinements to the models using stepwise regression and the selection and validation of the "best" or most appropriate models.

4.3.2.1. Maximal models identified at leaf-level

Maximal multiple linear regression models were derived for all possible combinations of plant water stress measurements and the 77 spectral reflectance indices extracted from leaf-level spectral reflectance data, calculated using Equation (4.2) programmed in Genstat (11th edition, 2008). The maximal models, which included the interactions of district and species, were ranked in descending order for each plant water stress measurement (Table 4.3). The adjusted R^2 values ranged from a maximum of 68.0% for chlorophyll b content and (695/690) spectral reflectance index to a minimum of 2.8 for carotenoid content and (465/565) spectral reflectance ratio.

Table 4.3 Adjusted R^2 values ranked in descending order for each maximal model derived between plant water stress measurement (Y) and spectral reflectance index (X) resulting from leaf-level data.

Chlorophyll a (Y)		**Chlorophyll (a + b) (Y)**		**Chlorophyll b (Y)**		**Carotenoid (c+x) (Y)**		**Chlorophyll fluorescence (Fv/Fm) (Y)**		**Predawn leaf water potential (Y)**	
Spectral reflectance index (nm) (X)	**Adjusted R^2 for maximal model**	**Spectral reflectance index (nm) (X)**	**Adjusted R^2 for maximal model**	**Spectral reflectance index (nm) (X)**	**Adjusted R^2 for maximal model**	**Spectral reflectance index (nm) (X)**	**Adjusted R^2 for maximal model**	**Spectral reflectance index (nm) (X)**	**Adjusted R^2 for maximal model**	**Spectral reflectance index (nm) (X)**	**Adjusted R^2 for maximal model**
695/690	55.2	695/690	57.9	695/690	68.0	850-710	48.9	750/710	44.1	WBI	58.2
DATT	54.6	DATT	57.6	DATT	67.8	850-680	44.3	710/760	43.1	NDWI	39.5
710/760	51.7	710/760	54.6	710/760	65.5	800-476	44.0	RENDVI	41.9	710/760	36.5
850-710	50.8	REP	52.6	710/850	63.7	800-632	43.4	DATT	39.6	750/710	36.2
REP	50.2	850-710	51.8	Inflection l	62.8	800-550	43.3	REP	38.3	632	36.0
710/850	47.7	710/850	51.0	RENDVI	62.7	800-680	42.6	710/850	37.7	664	36.0
RENDVI	47.7	RENDVI	50.6	REP	62.6	870	41.7	PRI	37.6	DATT	35.8
750/710	45.9	750/710	49.1	750/710	62.5	850	41.1	CARTER	36.1	710/850	35.8
680/695	45.3	680/695	48.2	680/695	62.3	800	39.6	850/710	35.9	680	35.4
695/680	45.2	695/680	48.1	695/680	61.9	750	37.7	850/710	34.8	850/710	35.4
PRI	43.3	PRI	47.3	PRI	61.0	Maximum ∂ Red Edge	30.5	695/690	34.0	RENDVI	35.1
CARTER	42.1	CARTER	45.2	850/710	60.7	710	26.6	CNDVI	32.5	476	34.4
850/710	41.2	850/710	45.0	850-710	60.1	Slope Red Edge	26.5	605/760	32.3	565	34.4
CNDVI	39.1	CNDVI	42.5	CARTER	58.7	565	26.2	632/800	30.7	605/760	34.4
680/690	35.0	Inflection l	40.0	CNDVI	57.5	550	26.1	Inflection l	30.1	710	34.4
Inflection l	34.1	680/690	37.7	710/680	56.5	632	25.5	550/670	27.4	465	34.2
632/800	32.7	710/680	37.2	680/710	55.9	680	25.2	NDVI	26.5	870	34.1
710/680	32.7	632/800	36.9	605/760	55.8	664	24.8	664/870	26.2	800-550	34.1
WBI	32.6	605/760	36.8	632/800	55.4	∂ Inflection l	23.5	(870-664)/(870+664)	26.1	CARTER	34.0
605/760	32.4	680/710	35.2	680/690	53.9	WBI	21.9	565/664	25.8	850	34.0
680/710	30.4	WBI	34.8	NDWI	52.4	REP	19.3	GAMON and SURFUS	25.6	465/565	33.9
800-550	27.9	710/420	31.4	WBI	52.3	log (800/550)	18.6	695/680	24.5	550	33.8
850-680	27.5	695/420	31.1	710/670	52.0	log (800/476)	18.4	680/695	24.1	800	33.7
800-632	27.1	800-550	31.0	664/870	51.8	CNDVI	18.3	465/664	22.5	850-680	33.6
710/420	27.0	605/420	30.6	Slope Red Edge	51.6	DATT	18.2	565/870	21.9	800-476	33.6

Chlorophyll a (Y)		**Chlorophyll (a + b) (Y)**		**Chlorophyll b (Y)**		**Carotenoid (c+x) (Y)**		**Chlorophyll fluorescence (Fv/Fm) (Y)**		**Predawn leaf water potential (Y)**	
Spectral reflectance index (nm) (X)	**Adjusted R^2 for maximal model**	**Spectral reflectance index (nm) (X)**	**Adjusted R^2 for maximal model**	**Spectral reflectance index (nm) (X)**	**Adjusted R^2 for maximal model**	**Spectral reflectance index (nm) (X)**	**Adjusted R^2 for maximal model**	**Spectral reflectance index (nm) (X)**	**Adjusted R^2 for maximal model**	**Spectral reflectance index (nm) (X)**	**Adjusted R^2 for maximal model**
695/420	26.8	850-680	30.6	log (800/476)	51.6	476	17.7	680/800	21.8	632/800	33.5
605/420	25.7	664/870	30.4	605/420	51.2	695/690	17.1	(800-680)/(800+680)	21.8	476/800	33.2
664/870	25.5	800-632	30.2	710/420	50.8	465	17.0	800-550	21.6	850-710	33.1
800/476	25.2	(870-664)/(870+664)	29.9	695/420	50.2	710/760	17.0	GreenPeak	21.5	800-680	33.1
800/680	25.0	Slope Red Edge	29.4	800-550	50.0	710/850	17.0	800-632	21.5	(870-664)/(870+664)	33.1
(870-664)/(870+664)	24.9	NDWI	29.1	NDVI	49.6	NDWI	16.8	550-760	21.4	465/870	33.0
Slope Red Edge	24.1	800-476	28.5	850-680	49.6	log (800/680)	16.7	(870-565)/(870-664)	20.9	664/870	33.0
NDWI	24.0	800-680	28.4	800-632	49.2	Inflection l	16.6	680/850	20.7	520/760	32.9
710/670	22.8	710/670	28.2	680/800	49.1	RENDVI	16.6	850-680	20.6	750	32.9
870	21.8	NDVI	26.5	680/850	49.0	CARTER	16.5	850/680	19.9	800-632	32.9
NDVI	21.1	870	25.6	(870-565)/(870-664)	48.9	680/695	15.6	800-680	19.9	NDVI	32.8
850	21.0	680/800	25.4	(800-680)/(800+680)	48.6	695/680	15.6	695/420	19.8	550/760	32.5
680/800	19.8	680/850	25.1	800-476	48.5	log (800/632)	15.5	800-476	19.5	REP	32.4
680/850	19.5	R850	24.9	710	48.2	632/800	15.1	550/800	19.2	Slope Red Edge	32.1
(800-680)/(800+680)	19.3	(800-680)/(800+680)	24.9	800-680	48.2	750/710	14.9	605/420	19.2	680/800	32.0
465/664	19.2	465/664	24.3	565/870	48.1	680/690	14.3	GNDVI	18.6	680/850	32.0
800	18.9	800	23.1	550/670	47.3	850/710	14.3	520/760	18.3	(800-680)/(800+680)	32.0
750	16.6	550/670	21.7	870	47.3	605/760	13.9	710/420	18.1	850/680	31.8
550/670	15.7	565/870	21.5	850	47.1	710/680	13.1	WBI	17.5	Maximum ∂ Red Edge	31.7
565/870	15.5	750	20.9	850/680	47.1	PRI	12.7	750/550	17.4	565/664	31.4
565/664	14.5	565/664	20.4	465/664	46.9	GAMON and	12.5	465/870	17.0	550/420	31.3

Chlorophyll a (Y)		**Chlorophyll (a + b) (Y)**		**Chlorophyll b (Y)**		**Carotenoid (c+x) (Y)**		**Chlorophyll fluorescence (Fv/Fm) (Y)**		**Predawn leaf water potential (Y)**	
Spectral reflectance index (nm) (X)	**Adjusted R^2 for maximal model**	**Spectral reflectance index (nm) (X)**	**Adjusted R^2 for maximal model**	**Spectral reflectance index (nm) (X)**	**Adjusted R^2 for maximal model**	**Spectral reflectance index (nm) (X)**	**Adjusted R^2 for maximal model**	**Spectral reflectance index (nm) (X)**	**Adjusted R^2 for maximal model**	**Spectral reflectance index (nm) (X)**	**Adjusted R^2 for maximal model**
						SURFUS					
850/680	14.1	850/680	20.2	550/760	46.7	664/870	12.5	Slope Red Edge	16.6	565/870	31.3
550/420	12.7	550/760	19.0	565/664	46.3	(870-664)/(870+664)	12.3	476/800	16.5	GNDVI	31.1
550/760	12.7	550/420	18.6	800	46.3	680/710	11.3	680/690	16.1	550/670	31.0
465/565	12.4	465/565	18.5	632	46.0	710/670	11.1	865/553	16.0	550/800	30.9
Maximum ∂ Red Edge	12.2	Maximum ∂ Red Edge	17.7	465/565	45.7	680/850	10.1	850/550	15.8	750/550	30.7
520/420	11.4	∂ Inflection l	17.5	Maximum ∂ Red Edge	45.5	680/800	9.9	870	15.8	865/553	29.8
∂ Inflection l	11.3	520/420	17.2	550/420	45.5	(800-680)/(800+680)	9.8	465/565	15.6	850/550	29.7
550/800	10.2	550/800	16.6	865/553	45.5	NDVI	9.7	850	15.5	Inflection l	29.1
GNDVI	10.1	GNDVI	16.5	550/800	45.4	565/870	8.9	∂ Inflection l	15.4	520/420	28.8
GAMON and SURFUS	9.8	710	16.3	∂ Inflection l	45.2	710/420	8.5	800	14.8	CNDVI	28.6
520/760	9.8	GAMON and SURFUS	16.1	GNDVI	45.2	850/680	8.5	Maximum ∂ Red Edge	14.4	log (800/680)	28.3
710	9.1	520/760	16.1	750	45.2	550/760	7.1	750	14.2	PRI	28.2
log (800/476)	8.1	750/550	14.7	750/550	45.2	695/420	7.0	NDWI	13.4	log (800/632)	28.0
log (800/550)	8.1	632	14.5	850/550	45.2	550/800	6.8	log (800/476)	12.4	log (800/476)	27.8
750/550	7.8	865/553	14.5	520/760	44.6	GNDVI	6.6	log (800/550)	12.4	(870-565)/(870-664)	27.7
632	7.6	850/550	14.1	GAMON and SURFUS	44.4	520/760	6.5	710	11.9	log (800/550)	27.6
865/553	7.5	log (800/476)	13.9	520/420	44.3	750/550	5.6	710/680	11.9	GAMON and SURFUS	27.5
log (800/680)	7.5	log (800/550)	13.9	465/870	43.9	605/420	5.5	632	11.7	GreenPeak	27.4
850/550	7.1	log (800/680)	13.4	664	43.8	865/553	5.5	550/420	11.6	695/690	27.1

Chlorophyll a (Y)		**Chlorophyll (a + b) (Y)**		**Chlorophyll b (Y)**		**Carotenoid (c+x) (Y)**		**Chlorophyll fluorescence (Fv/Fm) (Y)**		**Predawn leaf water potential (Y)**	
Spectral reflectance index (nm) (X)	**Adjusted R^2 for maximal model**	**Spectral reflectance index (nm) (X)**	**Adjusted R^2 for maximal model**	**Spectral reflectance index (nm) (X)**	**Adjusted R^2 for maximal model**	**Spectral reflectance index (nm) (X)**	**Adjusted R^2 for maximal model**	**Spectral reflectance index (nm) (X)**	**Adjusted R^2 for maximal model**	**Spectral reflectance index (nm) (X)**	**Adjusted R^2 for maximal model**
476/800	6.6	476/800	13.2	476/800	43.2	465/870	5.3	log (800/632)	11.6	695/680	25.8
465/870	6.5	465/870	13.1	565	43.1	476/800	5.3	680/710	11.1	465/664	25.6
log (800/632)	6.2	log (800/632)	12.5	log (800/550)	43.1	850/550	5.3	log (800/680)	11.1	710/670	25.6
(870-565)/(870-664)	5.2	(870-565)/(870-664)	11.9	log (800/632)	43.0	550/670	4.8	520/420	10.4	680/695	25.1
465	4.8	664	11.7	GreenPeak	42.8	565/664	4.8	664	10.3	∂ Inflection l	24.6
476	4.8	GreenPeak	11.6	550	42.6	465/664	4.0	465	7.5	680/690	24.3
664	4.8	465	11.2	(870-664)/(870+664)	42.5	520/420	4.0	476	7.4	680/710	24.2
GreenPeak	4.7	476	11.1	log (800/680)	42.5	(870-565)/(870-664)	3.8	680	7.4	710/680	24.1
550	4.6	550	11.0	680	42.4	GreenPeak	3.5	550	7.3	695/420	23.4
565	4.1	565	10.9	465	42.1	550/420	3.5	565	7.3	605/420	23.3
680	4.0	680	10.7	476	42.1	465/565	2.8	710/670	7.0	710/420	22.7

Carotenoid content and chlorophyll fluorescence having a maximum of 48.9% and 44.1% respectively were eliminated. It is interesting to note that selected spectral reflectance indices (e.g. 695/690, DATT, 710/760, 750/710, 680/695, 695/680, PRI and 476/800 spectral reflectance indices) were ranked the same for total chlorophyll content, chlorophyll a and chlorophyll b content. For chlorophyll b content, twenty nine spectral reflectance models were derived which accounted for more than 50% variance in the data. However, only 1 model with an adjusted R^2 greater than 50% existed for predawn leaf water potential and therefore all remaining combinations for this measurement were eliminated. In general, the (695/690) index, DATT index (850-710)/(850-680), near infra-red index (710/760) and the water band (900/970) index performed better and accounted for more than 50% of the variance in the data.

4.3.2.2. Model refinements using stepwise regression

Stepwise regression used to refine the three selected maximal models resulted in predominant increases in adjusted R^2 values. Adjusted R^2 values for the stepwise regression ranged from a maximum of 69.3% for chlorophyll b DATT spectral reflectance index, to a minimum of 53.4% for chlorophyll a (710/760) spectral reflectance index (Table 4.4). There were no differences between the maximal and stepwise regression models for total chlorophyll (a+b) and (695/690) spectral index, and predawn leaf water potential and water band index.

Table 4.4 Comparison of the maximal and stepwise regression models obtained in the leaf-level analysis, for the three models with the highest adjusted R² values exceeding 50%.

Chlorophyll a (Y)			**Chlorophyll (a + b) (Y)**			**Chlorophyll b (Y)**			**Predawn leaf water potential (Y)**		
Spectral reflectance index (nm) (X)	**Adjusted R²**		**Spectral reflectance index (nm) (X)**	**Adjusted R²**		**Spectral reflectance index (nm) (X)**	**Adjusted R²**		**Spectral reflectance index (nm) (X)**	**Adjusted R²**	
	Maximal model	**Stepwise model**		**Maximal model**	**Stepwise model**		**Maximal model**	**Stepwise model**		**Maximal model**	**Stepwise model**
695/690	55.2	54.8	695/690	57.9	57.9	695/690	68.0	68.5	WBI	58.2	58.2
DATT	54.6	56.5	DATT	57.6	59.0	DATT	67.8	69.3			
710/760	51.7	53.4	710/760	54.6	55.6	710/760	65.5	67.1			

The DATT spectral reflectance index performed well across all three measurements of chlorophyll pigment content, resulting in the highest adjusted R^2values for chlorophyll a content (56.5%), total chlorophyll content (59.0%) and chlorophyll b content (69.3%). The

stepwise regression model derived between chlorophyll b content and the DATT index was selected as the "best" model, having the highest adjusted R^2 of 69.3%.

4.3.2.3. Selection of the best model

The multiple regression analysis using leaf-level spectral reflectance data resulted in chlorophyll b as the best "surrogate" measure of plant water stress. The general, multiple linear regression model resulted in three species-specific models as shown below:

Chlorophyll b = -1.449 + 4.6 (DATT) + 2.82 (S1) + (-1.90) (S2) + (-4.31)(S1)(DATT) +(3.80)(S2)(DATT)	*(4.3)*
($F_{5,69} \approx$ 34.34; Fprob <0.001; R_a^2 = 0.693%)	

For *E. camaldulensis* where S1=S2=0: Chlorophyll b = -1.449 + 4.6(DATT)	*(4.3.1)*

For *E. sideroxylon* where S1=1 and S2=0: Chlorophyll b = 1.371+ 0.29(DATT)	*(4.3.2)*

For *S. lancea* where S1=0 and S2=1: Chlorophyll b = -3.349 + 8.4(DATT)	*(4.3.3)*

Results of the complete regression analysis, which includes a summary of the analysis of variance and estimates of parameters for the multiple linear regression model from which Equation (4.3) was derived, is detailed in Appendix 3. Species-specific linear models depicted by Equations (4.3.1), (4.3.2) and (4.3.3) were characterised by positive slopes indicating that chlorophyll b content increases with an increase in the DATT spectral reflectance index. Regression models for *E. camaldulensis* and *S. lancea* included negative y intercepts.

Differences between the observed and predicted chlorophyll b content determined, using the model reported in Equation (4.3), were assessed using a standardised residual plot of predicted or fitted values of chlorophyll b content (Figure 4.4). The standardised residual plot indicated a slight curvature in the fitted values of chlorophyll b. The variability in the data increased midway relative to those at either extreme end of the plot. Residuals were smaller at lower fitted values of chlorophyll b, and were much higher as fitted values of chlorophyll b increased, resulting in a "funnel shaped" standardised residual plot.

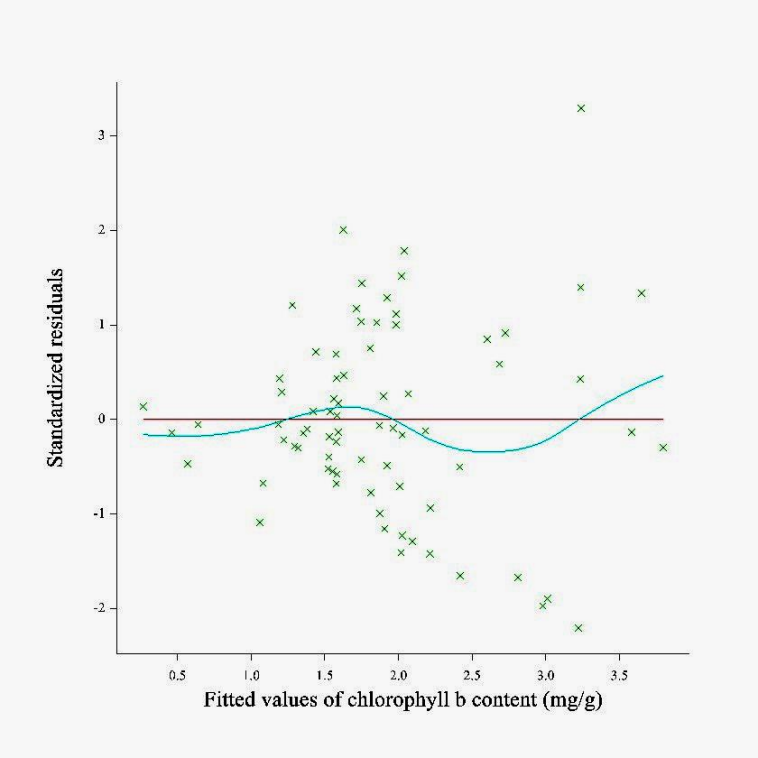


Figure 4.4 Standardised residual plot of fitted values of chlorophyll b content using the DATT spectral reflectance model.

The "funnel" shaped residual plot indicated that prediction errors could increase at higher values of chlorophyll b content. There appeared to be no apparent outliers in this data.

4.3.2.4. Validation of the selected model

The chlorophyll b DATT spectral reflectance model was validated using a practical and commonly used method of re-fitting the regression model with a certain percentage of data being excluded (Brieman and Spector, 1992). The validation process was repeated three

times, with 10 random samples excluded for each run. The randomly selected subsets of spectral reflectance data used to predict chlorophyll b content with actual corresponding measurements of chlorophyll b content are shown in Table 4.5. General multiple regression models for each validation dataset were not identical, and were represented by different slopes and intercepts for each tree species (Table 4.5). Thus, the robustness of the relationship identified between chlorophyll b and the DATT spectral reflectance index was also evaluated.

Table 4.5 Validation models used in the leaf-level analysis to predict chlorophyll b.

Species	Fitted Models	DATT index (X)	Chlorophyll b measured (Y)	Chlorophyll b Predicted (Y)
Run1				
S. lancea	1.087 + 8.882(DATT)	0.757040	2.146720	3.121029
		0.592559	1.822520	1.660109
		0.850549	3.673230	3.951576
		0.686441	1.668320	2.493969
E. camaldulensis	-1.283 + 4.302(DATT)	0.628253	1.774220	1.419744
		0.746743	2.500210	1.929488
		0.694845	2.228460	1.706223
		0.545473	0.559356	1.063625
		0.708332	2.158090	1.764244
E. sideroxylon	1.457 + 8.492(DATT)	0.707907	1.885000	1.536286
Run2				
S. lancea	-3.05 + 8.014(DATT)	0.753490	2.080180	2.988469
		0.833186	4.228290	3.627153
E. camaldulensis	-1.390 + 4.494(DATT)	0.722075	1.843630	1.855005
		0.727966	2.012290	1.881479
		0.694845	2.228460	1.732633
		0.709202	1.455560	1.797154
		0.755636	1.462090	2.005828
		0.758381	2.861890	2.018164
		0.601954	1.182100	1.315181
E. sideroxylon	1.31 + 8.634(DATT)	0.653175	1.660140	1.541224
Run3				
S. lancea	-3.394 + 8.398(DATT)	0.634649	2.420840	1.935782
		0.783957	3.866980	3.189671
		0.686153	2.189670	2.368313
E. camaldulensis	-1.414 + 4.568(DATT)	0.596656	1.166340	1.311525
		0.746743	2.500210	1.997122
		0.415406	0.402482	0.483575
		0.709202	1.455560	1.825635
		0.729556	1.371890	1.918612
E. sideroxylon	1.116 + 8.438(DATT)	0.566637	1.567940	1.511513
		0.728498	1.330390	1.624492

T-tests were used to determine if there were differences between measured and predicted values of chlorophyll b content. The statistical tests for all three validation runs confirmed that there were no significant differences between measured and predicted chlorophyll b content (Run1 ($t = -0.13$, 9df, $P = 0.902$, $r = 0.76$); Run2 ($t = 0.15$, 9df, $P = 0.885$, $r = 0.79$) and Run3 ($t = 0.08$, 9df, $P = 0.937$, $r = 0.92$). Furthermore, the Pearson correlation coefficients indicated a high correlation between measured and predicted values of chlorophyll b content ($r > 0.7$).

4.4 DISCUSSION

In this study, statistical relationships were derived between spectral reflectance indices derived from leaf-level spectral reflectance data, and physical ground-based measurements used as "surrogate" measures of plant water stress. An analysis of the multiple linear regression models indicated that four prominent and recurring spectral reflectance indices could be applied to identify plant water stress within the three mining districts. Two general trends were identified when using spectral reflectance indices derived from leaf-level spectral reflectance data to detect plant water stress:

- Three spectral indices derived from the red and near-infrared regions of the electromagnetic spectrum were identified as useful spectral indicators of plant water stress, and could be linked to plant chlorophyll content.
- A spectral index designed to capture changes in plant water content was correlated to measurements of predawn leaf water potential.

In this investigation, three spectral reflectance indices with a strong dependence on spectral changes in the red and near-infrared regions of the electromagnetic spectrum, namely (695/690) (Carter, 1994), (850-710)/(850-680) (Datt, 1999) and (710/760) (Carter, 1994), were correlated to chlorophyll a, chlorophyll b and total chlorophyll (a+b) content. All three relationships confirmed that a relationship exists between spectral bands extracted from the red and near-infrared regions (680, 695, 690, 710, 760, 800 nm), including the red-edge region defined from 690 to 740 nm. Furthermore, this finding corroborates previous studies in which it was found that reflectance bands within the red edge, and indices designed to

capture spectral differences in this region, move to shorter wavelengths as plant chlorophyll content decreases and *vice versa* (Curran *et al*. 1990; Clay *et al*. 2006; Campbell *et al*. 2007; Mutanga and Skidmore, 2007). Stepwise regression analyses (section 4.3.2.2 and 4.3.2.3) resulted in the chlorophyll b DATT spectral reflectance model being selected as the "best" or most appropriate model from this study, which could be used as a surrogate for identifying plant water stress.

The positive relationships that were established between plant chlorophyll content and the (850-710)/(850-680) spectral reflectance index for *Eucalyptus* trees confirmed the findings of Datt (1999) and Coops *et al*. (2003), and it was shown that this relationship was also valid for *S. lancea* in the selected mining areas. Such vegetation indices, or band ratios, have often been developed using a combination of reflectance bands which are both highly sensitive and insensitive to pigment content, in order to enhance the spectral effects of the highly sensitive bands (Datt, 1998). Most often near infrared bands are used as the insensitive bands, since pigments do not absorb near infrared radiation (Datt, 1998). Several studies have shown reflectance in the region of 550 and 700 nm to be most sensitive to a wide range of chlorophyll contents (Curran *et al*. 1990; Gitelson and Lichtenthaler *et al*. 1996; Gitelson and Merzlyak, 1996; Gitelson and Merzlyak, 1997; Datt, 1999), and reflectance at 850 nm to be most insensitive to chlorophyll content (Datt, 1999). According to Datt (1999), this index is fairly robust, being insensitive to the effects of leaf scattering on reflectance, and relates strongly to the variation in reflectance caused by chlorophyll absorption. It is thus recommended that this index be tested across other species as well, as it was significant across all species and all sites in this study.

The popular water band index, which was derived to capture changes in plant water content, was found to be correlated to measurements of predawn leaf water potential in plants. This finding corroborates the use of remote sensing technologies to detect spectral differences in plant water content specifically using spectral indices derived from leaf-level spectral reflectance data (Gao, 1995; Champagne *et al*., 2003; Zarco-Tejada *et al*., 2003; Jackson *et al*., 2004; Shen *et al*., 2005; Chun-Jiang *et al*., 2006). Furthermore, many studies have advanced the estimation of plant water content using hyperspectral remote sensing, and have investigated the use of narrow band spectral reflectance indices and specifically, the 970 nm

spectral band as a spectral indicator of plant water stress (Gao, 1995; Penuelas *et al*., 1997; Champagne *et al*., 2003). This study supports such research were subtle relationships between plant water content and spectral reflectance data were enhanced with the use of narrow-band or hyperspectral remote sensing data.

4.5 CONCLUSIONS

This study has shown that significant linear relationships (Fprob < 0.001) do exist between ground measurements of plant water stress, *viz.* predawn leaf water potential, leaf chlorophyll content and changes in spectral reflectance at the leaf-level. These changes were best illustrated using spectral reflectance indices such as (850-710)/(850-680), (695/690), (710/760) indices derived from the near infrared and red edge regions of the spectrum, and the water band index. In this investigation of hand-held spectral reflectance data, the spectral model derived between chlorophyll b pigment content and the (850-710)/(850-680) (Datt, 1999) spectral reflectance index was selected as the "best" model for detecting plant water stress in the three mining districts. This relationship confirmed that leaf spectral reflectance characteristics can be linked to plant water stress. Therefore, based on these relationships, which were derived for the three species *E. camaldulensis*, *E. sideroxylon* and *S. lancea* within the Welkom, Vaal River and West Wits mining districts, trees which access water during the dry winter period are expected to display significantly different spectral relationships compared to trees which do not access ground water. Multiple linear regressions were used to determine the interactions between species and the effects of the three locations of the mining districts. Species-specific relationships were produced which could be applied across all three mining districts. In general, the reflectance index (850-710)/(850-680) has been shown to be the most robust model in this study which could be used at different locations for different species to predict chlorophyll content at the leaf-level.

CHAPTER 5. EVALUATION OF MEDIUM TO HIGH RESOLUTION SATELLITE EARTH OBSERVATION DATA TO DETECT SPATIAL PATTERNS OF PLANT WATER STRESS

ABSTRACT

The purpose of this study was to evaluate the use of satellite remote sensing imagery of different spatial and spectral resolutions to predict spatial patterns of plant water stress over the same geographical areas.

Satellite earth observation data were acquired from two data sources for this investigation; the Hyperion hyperspectral sensor and the Proba Chris pseudo-hyperspectral sensor. The Hyperion sensor was selected to obtain high spatial and spectral resolution data, whereas the Proba Chris sensor provided high spatial and medium spectral resolution earth observation data. Twelve vegetation indices designed to capture changes in canopy water status, plant pigment content and changes in plant cellular structure, were selected and calculated from the satellite remote sensing imagery. Ground-based measurements of plant water stress, which included measurements of predawn leaf water potential, leaf chlorophyll fluorescence, chlorophyll and carotenoid pigment content and relative leaf water content, were undertaken on *Eucalyptus camaldulensis*, *E. sideroxylon* and *Searia lancea* in the Welkom, Vaal River and West Wits mining districts. Measurements undertaken during late July 2004 were used for ground-truthing the Hyperion image, while those undertaken during July 2005 and August 2005 were used for ground-truthing the Proba Chris images. Multiple linear regressions were derived to investigate the interactions between the districts and species and their respective spectral reflectance indices derived from the satellite images and the ground-based measurements of plant water stress.

Predawn leaf water potential measurements ranged from -0.42 to -0.78 MPa at unstressed sites, and -0.95 to -4.66 MPa at stressed sites. Predawn leaf water potentials measured for *E. camaldulensis* trees sampled on the species trials in Vaal River were significantly different between stressed and non stressed trees ($t = 3.39$, 8df, $P = 0.009$). In contrast, *E. camaldulensis* trees sampled near the pan within the Welkom mining district, which had greater access to water but were exposed to higher concentrations of salts and inorganic contaminants, displayed differences in total chlorophyll content ($t = -2.20$, 8df, $P = 0.059$), carotenoid content ($t = -5.68$, 8df, $P < 0.001$) and predawn leaf water potential ($t = 4.25$, 8df, $P = 0.011$) when compared to trees sampled on farmland. *E. sideroxylon* trees sampled close to a farm dam in the West Wits mining district displayed differences in predawn leaf water potential ($t = 69.32$, 8df, $P < 0.001$) and carotenoid content ($t = -2.13$, 8df, $P = 0.066$) compared to stressed trees further upslope away from the water source. Predawn leaf water potential together with greenness normalised difference vegetation index spectral reflectance index resulted in the "best" surrogate measure of plant water stress when using broad-band multispectral satellite data. The model selected using narrow-band hyperspectral satellite data indicated that strong relationships exists between predawn leaf water potential, which is a direct measure of plant water stress, and the water band index, which is designed to capture changes in plant water content.

It was concluded from this study that vegetation indices designed to capture changes in plant water content/plant water status and spectral changes in the red edge region of the spectrum performed well when applied to high spectral resolution remote sensing data. The greenness normalised difference vegetation index was considered to be a fairly robust index, which was highly correlated to chlorophyll fluorescence and predawn leaf water potential. It is recommended that this index has the potential to be used to map spatial patterns of winter-time plant stress for different genera/species and in different geographical locations.

Keywords : carotenoid pigment content, chlorophyll pigment content, leaf chlorophyll fluorescence, plant water stress, predawn leaf water potential, relative leaf water content, satellite imagery, spectral reflectance indices

5.1 INTRODUCTION

A spatial evaluation of sites where existing trees have access to groundwater during the dry winter season would provide valuable information for future tree plantings. Sites with similar site characteristics could then be targeted to ensure effective removal of large volumes of groundwater, and optimal containment of contaminated seepage water. In this study, alternative technologies for measuring the degree of water stress experienced by trees that are less time consuming and more practical for large scale spatial mapping, were considered.

Reliable estimation of agronomical and biophysical parameters such as leaf area index, absorbed photosynthetically active radiation, water content and the surface energy balance from local to regional scales is crucial for many applications including ecosystem assessments and crop management, weather forecasting, hydrological modelling, irrigation scheduling, water resource management, and climate change research. Numerous models have been developed using remote sensing, which permits spatially distributed mapping of the agronomical, biophysical and surface energy balance parameters over large areas, with the ambition of developing reliable, robust and cost-effective methods for land and vegetation assessments (Stark, 2001; Zarco-Tejada *et al*., 2003; Marignani *et al*., 2007; Zwart and Bastiaassen, 2007; Glenn *et al*., 2008; Choi *et al*., 2009; Hong *et al*., 2009; He and Mui, 2010). Ultimately, such methodologies and approaches could support the decision making process and which could add value in land use and catchment management.

Remote sensing data from satellite based sensors have the potential to provide detailed information on land surface and vegetation parameters, to assess the degradation of habitats and better manage natural resources at local to regional scales. One of the important vegetation parameters that has been successfully derived from remote sensing data is the spatial estimates of actual evapotranspiration required for sustainable management of water resources as well as for a better understanding of water exchange processes between the land surface and the atmosphere (Zwart and Bastiaassen, 2007; Hong *et al*., 2009). Ground measurements of evapotranspiration like many other land surface and vegetation parameters

over a range of space and time scales are difficult to obtain due to the time and cost involved. However, more widely available are large amounts of remotely sensed satellite data such as Land remote sensing satellite Enhanced Thematic Mapper Plus (Landsat ETM+), the Advanced Spaceborne Thermal Emission and Reflection Radiometer (ASTER), the Advanced Very High Resolution Radiometer (AVHRR), the Moderate Resolution Imaging Spectroradiometer (MODIS) and the Geostationary Orbiting Environmental Satellite (GOES) all of variable spatial, temporal, and spectral resolutions. Scaling of these datasets, up-scaling or aggregation and down-scaling or disaggregation has been employed in the application of satellite remote sensing data to estimate land surface and vegetation conditions (Bastiaanssen *et al*., 2005; Allen *et al*. ,2007). Hong *et al*. (2009) reported on the up-scaling of Landsat satellite data (30 m spatial resolution) to MODIS (250 m spatial resolution) as input into the Surface Energy Balance Algorithm for Land (SEBAL) to estimate regional estimates of evapotranspiration. This model was also extended to produce estimates of crop biomass production, so that crop yield, water use and water productivity can be obtained in an integrated way (Zwart and Bastiaanssen, 2007) using both the National Oceanic and Atmospheric Administration-Advanced Very High Resolution Radiometer (NOAA-AVHRR) at 1 km low spatial resolution and Landsat satellite images at a 30 m high spatial resolution. Remote sensing in combination with crop production models has been acknowledged to be a powerful tool for estimating crop yields at various spatial scales, within fields, between fields and on a regional scale. Up-scaling procedures were performed using simple averaging and nearest neighbour resampling techniques. The advantages of using different sensors are combined in this methodological framework where high and low resolution products are integrated to calculate total seasonal evapotranspiration and biomass production at field level (Zwart and Bastiaanssen, 2007).

Ground-based measurements can provide accurate and representative values of land surface or vegetation parameters such as chlorophyll content, water potential, biomass or evapotranspiration for different land cover types, but such point data cannot be easily extrapolated to produce accurate maps over a landscape or region, due to natural variability in the physical properties of the vegetation, soil and climatic conditions. To address this need, there has been a major effort over the past several years to develop and refine remote

sensing based models such as canopy reflectance and energy balance models that provide spatially distributed maps using satellite data (Choi *et al*., 2009). A few of these have been promoted as having operational capabilities.

A few widely accepted canopy reflectance models include SAILH and PROSPECT. Canopy reflectance models are also used for estimating biometric properties over large areas. Such models include assumptions about the leaf property data used as input, the geometry of the shrubs and trees in the field of view, and the nature of the surrounding environment, including climatic conditions. Examples of remote sensing based surface energy balance models include the Two-Source Energy Balance (TSEB) model, Mapping EvapoTranspiration at high Resolution using Internalized Calibration (METRIC), Trapezoid Interpolation Model and SEBAL. The above mentioned surface energy balance models have different levels of complexity and input requirements, but all have operational capabilities (Choi *et al*., 2009).

A significant benefit of using high resolution airborne or satellite remote sensing imagery is the relatively 'pure' smaller pixels of canopy, shadow and soil that can be obtained. Some remote sensing studies however, have successfully estimated the percentage of vegetative cover present in a pixel using leaf area index derived from higher resolution satellite imagery using the Normalized Difference Vegetation Index (NDVI), spectral un-mixing and textural analysis. Therefore, selecting the remote sensing data of an appropriate spatial resolution is certainly a determining factor, as the size of the vegetation patches in relation to the pixel size is extremely important.

Vegetation indices to monitor terrestrial landscapes by satellite sensors were first developed in the 1970s and have been highly successful in assessing vegetation condition, foliage, land cover, phenology, and processes such as evapotranspiration and primary productivity. Although many variations exist, many vegetation spectral reflectance indices are a ratio of the reflection of light in the red and near-infrared regions of the electromagnetic spectrum in order to separate the landscape into water, soil, and vegetation. Vegetation indices derived from robust satellite data products are computed the same way across all pixels in time and

space, regardless of surface conditions. As ratios, they can be easily cross-calibrated across sensor systems, ensuring continuity of data sets for long-term monitoring of the land surface and climate-related processes. A global record of NDVI data since 1981 from the NOAA AVHRR has contributed to significant global climate, ecosystem and agricultural studies. A new generation of vegetation index data derived from MODIS satellite data has been inter-calibrated with AVHRR NDVI, and provides near daily coverage of the earth at 250 m pixel resolution.

Vegetation indices are now indispensable tools in land cover classification, climate- and land use change detection, drought monitoring, and habitat loss, to name just a few applications. Vegetation indices have been used to combine ground data and vegetation indices to scale biophysical, biochemical and physiological processes over larger areas. When ground-based measurements are available, remote sensing data can also serve as a scaling tool rather than as a complete physical model. Many remote sensing applications have linked the spectral properties of vegetation to plant water status and plant water stress (Carter, 1993; Gao, 1995; Gitelson and Merzlyak, 1996; Lichtenthaler *et al*. 1996; Gitelson and Merzlyak, 1997; Blackburn, 1999; Datt, 1999).

In this study, the use of remote sensing data, which are commercially available and could potentially be operationally used in the future, were investigated. Over the past thirty years, significant progress has been made on the use of remotely sensed data from satellite-based sensors and cameras for retrieval of information useful for several environmental, agricultural and water management applications. This chapter investigates an approach of using satellite based images of different spatial and spectral resolutions to predict spatial patterns of plant water stress. This study provided a unique opportunity to investigate the importance of improved image resolution and spectral density over the same geographical districts.

Medium to high spatial and spectral resolution remote sensing datasets were selected to identify and provide detailed spectral information on small stands, rows or even clumps of trees characteristic of the mining districts. Imagery was obtained from the hyperspectral

Hyperion sensor and the pseudo-hyperspectral Proba Compact High Resolution Imaging Spectrometer (CHRIS) sensor. These data sources permitted mapping of a variety of vegetation spectral reflectance properties that were further enhanced using vegetation spectral reflectance indices, some of which have been correlated to plant water stress.

5.2 MATERIALS AND METHODS

A description of the tree species, mining districts and sampling sites selected for this study are discussed in Chapter 2. Sampling sites within the three mining districts, Welkom, Vaal River and West Wits, were used for ground-based measurements of plant water stress and as ground-truthing sites for the remote sensing surveys. Ground-based measurements of plant water stress were undertaken on the three species *E. camaldulensis*, *E. sideroxylon* and *S. lancea* in the Welkom, Vaal River and West Wits mining districts during late July 2004 (as presented and discussed in Chapter 4, section 4.3.1, Table 4.2), and was used for ground-truthing the Hyperion image, while measurements undertaken during July 2005 and August 2005 were used for ground-truthing the Proba Chris images. The field sampling procedures of each ground-based plant water stress measurement used, *viz*. predawn leaf water potential, leaf chlorophyll fluorescence, chlorophyll and carotenoid pigment content and relative leaf water content are described in Chapter 4, whereas the step by step details of the protocols are presented in Appendix 2.

5.2.1 Selection and requisition of satellite earth observation data

Large stands or blocks of trees and tree plantations are rare in these mining districts, therefore high spatial and spectral resolution remote sensing data was required to identify and provide detailed information for small stands, single trees or rows of trees and small-plot species trials in each mining district. There is currently very few commercially available satellite earth observation data sources which could provide remote sensing data of a high spatial and spectral resolution on a temporal scale that could be used in any future operational applications.

Satellite earth observation data were acquired from two data sources for this investigation; the Hyperion hyperspectral sensor (United States Geological Survey Earth Resources Observation Systems) and the Proba Chris pseudo-hyperspectral sensor (European Space Agency). The Hyperion sensor was selected to obtain high spatial and spectral resolution data, whereas the Proba Chris sensor provided high spatial and medium spectral resolution earth observation data. Free Proba Chris data were obtained through the European Space Agency, Tiger Initiative in Africa, which was established to promote the use of space technologies for improved water resources management in Africa.

The satellite earth observation data were acquired during 2004 and 2005. The Hyperion image was acquired for the West Wits mining district during early August 2004. This image was a 42 by 7.7 km scene, at a 30 m spatial resolution, and comprised of 242 calibrated and uncalibrated spectral bands ranging from 357 nm to 2576 nm. The 196 calibrated bands were converted to absolute radiance by applying a scaling factor of 40 and 80 to the visible and short-wave infrared spectral bands respectively (Beck, 2003).Calibrated wavelengths ranged from 498.04 to 993.17 nm for the visible and near infrared region and 1194.97 to 2395.5 nm for the short-wave infrared region.

Proba Chris data has been classified into five imaging modes, each model comprising of a list of pre-selected spectral bands. Mode 4 characterised as the chlorophyll band set was acquired in this study. Although a total of four Proba Chris images were planned for acquisition for the Welkom, Vaal River and West Wits mining districts during July and August 2005, only the Vaal River images were acquired, due to an increased demand for Proba Chris data from various countries participating in the Tiger initiative. Proba Chris images for Welkom were thus obtained during early October 2005, and for West Wits during late November 2005, and were flagged when correlating to ground truthing measurements undertaken during the dry-season months of July and August 2005. All Proba Chris images were characterised by 13 x 13 km scenes, at a 17 m spatial resolution, and comprised of 18 spectral bands ranging from 485.6 nm to 796.1 nm. These are most commonly used when requiring high spatial resolution data for vegetation studies.

Both the Hyperion and Proba Chris radiance images were atmospherically corrected by applying a flat field technique. This technique normalises the spectrum of each pixel in the respective image, using the average spectrum from a region of flat reflectance within the scene. The technique assumes that all the spectral features in the flat field region are due to the atmosphere and the solar spectrum. The respective radiance images were then divided by the flat field average spectrum, effectively removing the shape of the solar spectrum and atmospheric scattering and absorptions. The flat field atmospheric correction was applied to the Hyperion and Proba Chris images using the automated software options as provided in Spectral Analysis with ENVI 4.1 (2005).

Reflectance data were geometrically corrected, using georeferenced airborne imagery which extended across the research sites, and all images were projected to WGS 84, LO27 datum. All image processing was undertaken using ENVI 4.1 and Erdas Imagine 8.7 software packages.

5.2.2 Selection and derivation of vegetation spectral reflectance indices

Ten vegetation indices designed to capture changes in canopy water status, plant pigment content and changes in plant cellular structure, were selected for this investigation. Three of the ten indices were selected to describe the spectral changes in the plant water status and plant water content. The remaining seven indices provided a measure of the overall amount and quality of photosynthetic material present in the vegetation, the presence of stress related pigments in vegetation, and changes in leaf cellular structure. All ten selected indices reflect spectral changes in the visible, red and near infrared regions of the electromagnetic spectrum, which infer variability in plant physiological properties that might be indirectly caused by changes in plant water status. Table 5.1 provides a summary of the selected vegetation indices used in this study.

Table 5.1 Spectral wavelengths and reflectance indices derived from the satellite earth observation data.

Common name for spectral index or spectral region of the spectrum	Spectral Reflectance Ratio or Index (nm)	Reference	Closest wavelengths used to derive indices from Proba Chris data	Closest wavelengths used to derive indices from Hyperion data
Indices sensitive to changes in plant pigment content				
Green normalised difference vegetation index (GNDVI)	(750-550)/(750+550)	Gitelson *et al.* (1996)	(748.4-551.2)/(748.4+551.2)	
Normalised difference vegetation index (NDVI)	(750-676)/(750+676)	Tucker (1979)	(748.4-679.9)/(748.4+679.9)	
Red edge normalised difference vegetation index (RENDVI)	(750-705)/(750+705)	Sims and Gamon (2002)	(748.4-703.2)/(748.4+703.2)	(752.43-701.55)/(752.43+703.2)
Carter index	(695/760)	Carter (1994)	(697.2/755.3)	691.37/762.6)
Red edge position (REP)	Wavelength @ max derivative of red edge derived between 640 to 740 nm	Curran *et al.* (1990)		Wavelength @ max derivative of red edge derived between 640 to 740 nm
Modified Red Edge Simple Ratio (MRESR)	(750 – 445)/(705 – 445)	Sims and Gamon (2002)		(752.43-447.17)/(701.55-447.17)
Photochemical reflectance index (PRI)	(531-570)/(531+570)	Sims and Gamon (2002)		(528.57-569.27)/(528.57+569.27)
Indices sensitive to changes in plant water content/plant water status and plant cellular structure				
Water band index (WBI)	(900/970)	Penuelas *et al*. (1995)		(905.05/972.99)
Moisture stress index (MSI)	(1599/819)	Ceccato *et al.* (2001)		(1598.51/823.65)
Normalised Difference Infrared Index (NDII)	(819 – 1649)/(819 + 1649)	Jackson *et al*. (2004)		(823.65-1648.9)/(823.65+1648.9)

5.2.3 Analysis of data

A statistical analysis of the plant water stress measurements collected in July 2005 and August 2005 was undertaken to produce a comparative summary of the means for each sample site per species within each mining district, and per species for each mining district, and between species and mining districts for each of ground-based methods used in this study. Statistical averages were determined using a spreadsheet package, while graphical plots were produced using Genstat (11th edition, 2008).

Multiple linear regressions were derived to investigate the interactions between the districts and species and their respective spectral reflectance indices derived from the satellite images and the ground-based plant water stress measurements using Genstat (11th edition, 2008). The maximal regression model and the statistical procedure adopted in the selection of the "best" model while eliminating poor combinations of spectral reflectance indices (X) and plant water stress measurements (Y) as depicted in Chapter 4 (section 4.2.4),were applicable to this satellite remote sensing study. The highest adjusted R^2 value, and the significance of the F and t probability values were statistical measures used in the selection of the "best" multiple linear regression model. Significant differences between predicted and measured plant water stress measurements were determined using a t-test for paired samples.

5.3 RESULTS

5.3.1 Ground-based measurements of plant water stress

Because Proba Chris images were acquired at different times of the year, ground-truthing measurements were thus also undertaken at two different times, in order to increase the correlation between plant water stress measured on the ground and that observed using the satellite remote sensing data. The levels of plant water stress for the two datasets are presented in Table 5.2 and Table 5.3.

Measurements of predawn leaf water potential obtained in July 2005, were used to characterise sites, ranging from -0.42 to -0.78 MPa at unstressed sites, and -0.95 to -4.66 MPa at stressed sites. Corresponding measurements of leaf chlorophyll fluorescence, leaf chlorophyll content and leaf carotenoid content when compared between stressed and unstressed sites, did not follow the same pattern(Table 5.2 and Table 5.3).Instead, relative differences in ground-based measurements of plant water stress were identified to be a function of the locality and tree species under investigation.

An assessment of comparative sampling sites, sites within the same geographic location, in the same mining district and for the same species, revealed a relative increase in leaf

chlorophyll fluorescence, leaf chlorophyll content and leaf carotenoid content for less stressed trees with relatively higher predawn leaf water potential readings. These relative increases are illustrated, for example, by the comparative *E. camaldulensis* sampling sites 1 and 2in Vaal River, *E. sideroxylon* sampling sites 7 and 8 in West Wits (Table 5.2), and by the equivalent comparative sampling sites 1 and 2, and 5 and 6 in Table 5.3.

Table 5.2 Ground measurements of plant stress undertaken during July 2005 in the Welkom, Vaal River and West Wits mining districts.

Site No.	Mining District	Tree Species	Geographic Coordinates (dd)	Site Description	Site Classification according to Predawn Leaf Water Potential Measurements	Predawn Leaf Water potentials (MPa)		Relative Leaf Water Content (%)		Leaf Chlorophyll Fluorescence (Fv/Fm)		Leaf Chlorophyll Content (mg/l)		Leaf Carotenoid Content (mg/l)	
						Mean	Std Dev.	Mean	Std Dev.	Mean	Std. Dev.	Mean	Std Dev.	Mean	Std. Dev.
1	VR	EC	-26.98859; 26.77658	dolomite, meso-eutrophic soils, species trials, plot 3	unstressed	-0.67	0.17	66.34	15.00	0.666	0.094	11.029	1.752	1.599	0.257
2	VR	EC	-26.98896; 26.77676	dolomite, meso-eutrophic soils, species trials, plot 9	unstressed	-0.71	0.15	49.87	10.23	0.537	0.207	8.233	3.374	1.210	0.383
3	VR	EC	-26.92922; 26.68182	andesite, eutrophic soils, close to TSF	stressed	-1.97	0.33	57.04	5.27	0.462	0.212	8.039	2.187	1.224	0.249
4	VR	SL	-26.99185; 26.77592	dolomite, eutrophic soils, high water availability, water channel	stressed	-1.05	0.12	68.53	11.05	0.644	0.139	10.022	1.770	1.603	0.208
5	VR	SL	-26.92301; 26.69820	quartzite, meso- eutrophic soils, low TDS	stressed	-0.95	0.15	45.50	8.74	0.423	0.215	7.304	2.694	1.217	0.247
6	VR	SL	-26.93418; 26.69592	dolomite, meso- eutrophic soils, high TDS, higher water availability	stressed	-1.46	0.17	57.80	10.01	0.538	0.195	8.877	2.551	1.157	0.191
7	WW	ES	-26.43969; 27.32871	shale, non calcarious soils, high water availability, farm dam, shallow groundwater table <~ 5m	unstressed	-0.73	0.05	66.66	6.69	0.719	0.052	11.600	1.264	1.537	0.213
8	WW	ES	-26.43899; 27.33024	shale, non calcarious soils, lower water availability	stressed	-4.66	0.12	52.93	11.88	0.675	0.133	12.502	1.669	2.081	0.189
9	WW	EC	-26.43147; 27.36904	shale, non-calcarious soil, medala trial	unstressed	-0.51	0.06	82.56	11.94	0.700	0.089	11.407	1.552	1.504	0.161
10	WW	EC	-26.42508; 27.37172	shale, non-calcarious soil, trial near garage	unstressed	-0.78	0.05	72.75	15.35	0.524	0.176	14.033	1.377	1.978	0.169
11	WW	EC	-26.44070; 27.34495	shale, non-calcarious soil, trial	unstressed	-0.42	0.06	74.38	14.56	0.603	0.172	15.655	1.215	2.380	0.221
12	W	EC	-28.03052; 26.51879	shale, eutrophic soils, farmland	unstressed	-0.59	0.12	67.58	4.73	0.593	0.110	12.219	1.462	1.818	0.227
13	W	EC	-27.96743; 26.55001	shale, eutrophic and non calcarious soils, high water availability, near pan	stressed	-1.87	0.61	71.87	15.24	0.643	0.143	13.130	1.392	1.835	0.177
14	W	SL	-28.03361; 26.51199	shale, eutrophic soils, farmland	stressed	-1.67	0.27	59.98	3.56	0.315	0.115	10.729	2.818	1.931	0.327
15	W	SL	-27.96695; 26.55075	shale, non calcarious soils, high water availability, near pan	stressed	-1.12	0.19	68.15	12.04	0.481	0.181	9.019	1.827	1.594	0.284
Means per species per district															
Mean value for *E. camaldulensis* for Vaal River						-1.12	0.22	57.75	10.17	0.555	0.171	9.100	2.438	1.344	0.296
Mean value for *S. lancea* for Vaal River						-1.15	0.15	57.28	9.93	0.535	0.183	8.734	2.338	1.326	0.215
Mean value for *E. sideroxylon* for West Wits						-2.70	0.09	59.80	9.29	0.697	0.093	12.051	1.467	1.809	0.201

Site No.	Mining District	Tree Species	Geographic Coordinates (dd)	Site Description	Site Classification according to Predawn Leaf Water Potential Measurements	Predawn Leaf Water potentials (MPa)		Relative Leaf Water Content (%)		Leaf Chlorophyll Fluorescence (Fv/Fm)		Leaf Chlorophyll Content (mg/l)		Leaf Carotenoid Content (mg/l)	
						Mean	Std Dev.	Mean	Std Dev.	Mean	Std. Dev.	Mean	Std Dev.	Mean	Std. Dev.
Mean value for *E. camaldulensis* for West Wits						-0.57	0.06	76.56	13.95	0.609	0.146	13.698	1.381	1.954	0.184
Mean value for *E. camaldulensis* for Welkom						-1.23	0.37	69.73	9.99	0.618	0.127	12.675	1.427	1.827	0.202
Mean value for *S. lancea* for Welkom						-1.40	0.23	64.07	7.80	0.398	0.148	9.874	2.323	1.763	0.306

W = Welkom; VR = Vaal River, WW = West Wits; EC = E. camaldulensis; ES = E. sideroxylon; SL = S. lancea

Table 5.3 Ground measurements of plant stress undertaken during August 2005 in the Welkom, Vaal River and West Wits mining districts.

Site No.	Mining District	Tree Species	Geographic Coordinates (dd)	Site Description	Site Classification according to Predawn Leaf Water Potential Measurements undertaken in July 2005	Relative Leaf Water Content (%)		Leaf Chlorophyll Fluorescence (Fv/Fm)		Leaf Chlorophyll Content (mg/l)		Leaf Carotenoid Content (mg/l)	
						Mean	Std Dev.	Mean	Std. Dev	Mean	Std Dev.	Mean	Std. Dev
1	VR	EC	-26.98859; 26.77658	dolomite, meso-eutrophic soils, species trials, plot 3	unstressed	79.48	5.72	0.603	0.136	12.517	1.572	1.838	0.125
2	VR	EC	-26.92922; 26.68182	andesite, eutrophic soils, close to TSF	stressed	58.16	6.26	0.409	0.166	6.996	1.483	0.927	0.140
3	VR	SL	-26.92301; 26.69820	quartzite, meso- eutrophic soils, low TDS	stressed	65.21	9.64	0.490	0.163	7.311	1.692	1.134	0.186
4	VR	SL	-26.93418; 26.69592	dolomite, meso- eutrophic soils, high TDS, higher water availability	stressed	78.59	12.06	0.435	0.173	7.871	2.302	1.127	0.217
5	WW	ES	-26.43969; 27.32871	shale, non calcarious soils, high water availability, farm dam, shallow groundwater table <~ 5m	unstressed	63.68	6.08	0.748	0.031	11.814	1.956	1.691	0.373
6	WW	ES	-26.43899; 27.33024	shale, non calcarious soils, lower water availability	stressed	53.92	12.15	0.446	0.188	11.247	1.641	2.181	0.336
7	W	EC	-28.03052; 26.51879	shale, eutrophic soils, farmland	unstressed	64.75	7.24	0.647	0.096	12.231	2.589	1.389	0.178
8	W	EC	-27.96743; 26.55001	shale, eutrophic and non calcarious soils, high water availability, near pan	stressed	62.05	12.57	0.664	0.106	15.059	0.991	2.105	0.216
9	W	SL	-28.03361; 26.51199	shale, eutrophic soils, farmland	stressed	62.75	4.14	0.497	0.144	12.599	2.017	1.888	0.170
Means per species per district													
Mean value for *E. camaldulensis* for Vaal River						68.82	5.99	0.506	0.151	9.757	1.528	1.383	0.133
Mean value for *S. lancea* for Vaal River						71.90	10.85	0.463	0.168	7.591	1.997	1.131	0.202
Mean value for *E. sideroxylon* for West Wits						58.80	9.12	0.597	0.110	11.531	1.799	1.936	0.355
Mean value for *E. camaldulensis* for Welkom						63.40	9.91	0.656	0.101	13.645	1.790	1.747	0.197
Mean value for *S. lancea* for Welkom						62.75	4.14	0.497	0.144	12.599	2.017	1.888	0.170

W = Welkom; VR = Vaal River, WW = West Wits; EC = E. camaldulensis; ES = E. sideroxylon; SL = S. lancea

Statistical tests confirmed that significant differences in plant water stress measurements did exist between selected comparative sampling sites. Predawn leaf water potentials measured for *E. camaldulensis* trees sampled on the species trials in Vaal River were significantly different between stressed and unstressed trees ($t = 3.39$, 8df, $P = 0.009$). In contrast, *E. camaldulensis* trees sampled near the pan in the Welkom mining district, which had greater access to water but were exposed to higher concentrations of salts and inorganic contaminants, displayed significant differences in total chlorophyll content ($t = -2.20$, 8df, $P = 0.059$), carotenoid content ($t = -5.68$, 8df, $P < 0.001$) and predawn leaf water potential ($t = 4.25$, 8df, $P = 0.011$) when compared to trees sampled on farmland within the same district. *E. sideroxylon* trees sampled close to a farm dam in the West Wits mining district displayed significant differences in predawn leaf water potential ($t = 69.32$, 8df, $P < 0.001$) and carotenoid content ($t = -2.13$, 8df, $P = 0.066$) when compared to stressed trees further upslope away from the water source.

Box plots were used to represent the distributions of the plant water stress measurements undertaken in July 2005. Figure 5.1 illustrates the variability of predawn leaf water potential, photochemical efficiency ratio, total chlorophyll and carotenoid content and relative leaf water content per mining district. The highest (more negative) predawn leaf water potential measurements measured at West Wits (>4MPa) were classed as outliers in Genstat 11 (2008), compared to lower negative values recorded at Vaal River and Welkom (Figure 4.1a). The median photochemical efficiency ratios were similar for Vaal River and Welkom, ranging between 0.5 and 0.6, while the highest upper quartile photochemical efficiency value was measured at West Wits, which indicated healthier trees experiencing lower plant water stress (Figure 4.1b). Total chlorophyll and carotenoid content measurements followed a similar pattern for each mining district, with the highest upper quartile values measured at West Wits, and the lowest lower quartile values measured at Vaal River (Figure 4.2c and d). The ranges in relative leaf water content values were smallest for Welkom when compared to Vaal River and West Wits (Figure 4.1e). However, median values of relative leaf water content were similar for all three mining districts.

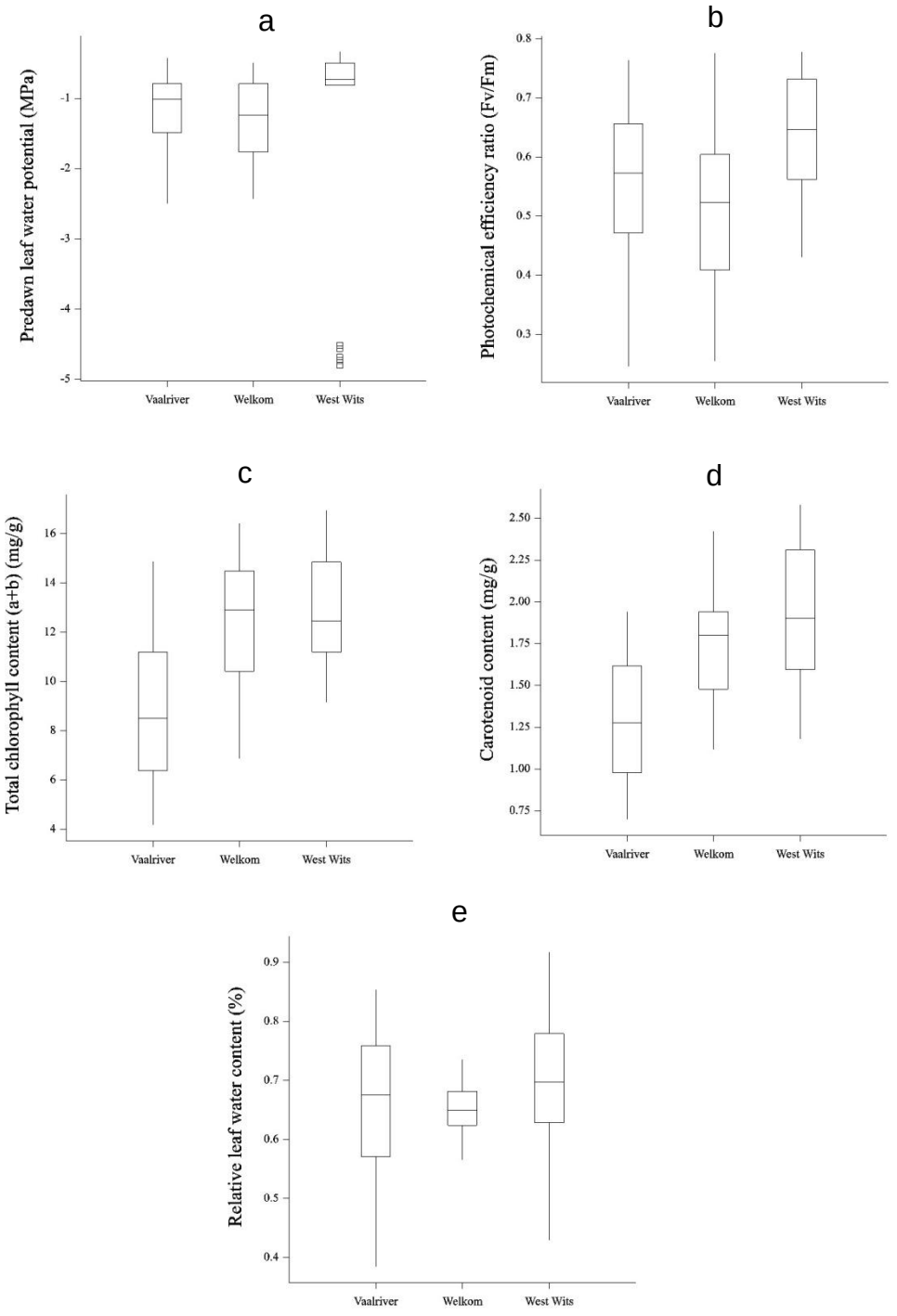


Figure 5.1 Box plots of plant water stress measurements a) predawn leaf water potential, b) photochemical efficiency, c) total chlorophyll (a+b) content, d) carotenoid content and e) relative leaf water content undertaken for Vaal River, Welkom and West Wits in July 2005.

Similarities and differences in plant water stress measurements undertaken for the three tree species were also investigated. The box plots in Figure 5.2 represent the range, upper and

lower quartiles and medians measured for predawn leaf water potential, chlorophyll fluorescence, chlorophyll and carotenoid content and leaf water content measured per tree species in July 2005. *E. sideroxylon* trees appeared to have the highest (more negative) upper quartile and median, and largest variability in predawn leaf water potentials (Figure 5.2a). However, this species displayed the least variation in photochemical efficiency (Figure 5.2b) and total chlorophyll content (Figure 5.2c). The range in predawn leaf water potentials measured for *E. camaldulensis* and *S. lancea* was smaller, with the lowest values recorded for *E. camaldulensis*. In contrast, the highest upper quartile values for total chlorophyll content were measured for *E. camaldulensis* and the lowest lower quartile values for *S. lancea*. The distribution of carotenoid content measurements were similar, with the highest upper quartile measured for *E. sideroxylon*, and the lowest lower quartile measured for *S. lancea* (Figure 5.2d). Median values for carotenoid content for all three species ranged between 1.25 and 2 mg per g. Median values of relative leaf water content ranged between 0.6 and 0.7 for all three species (Figure 5.2e). However, the highest value was measured for *E. camaldulensis*, and the lowest value for *E. sideroxylon*.

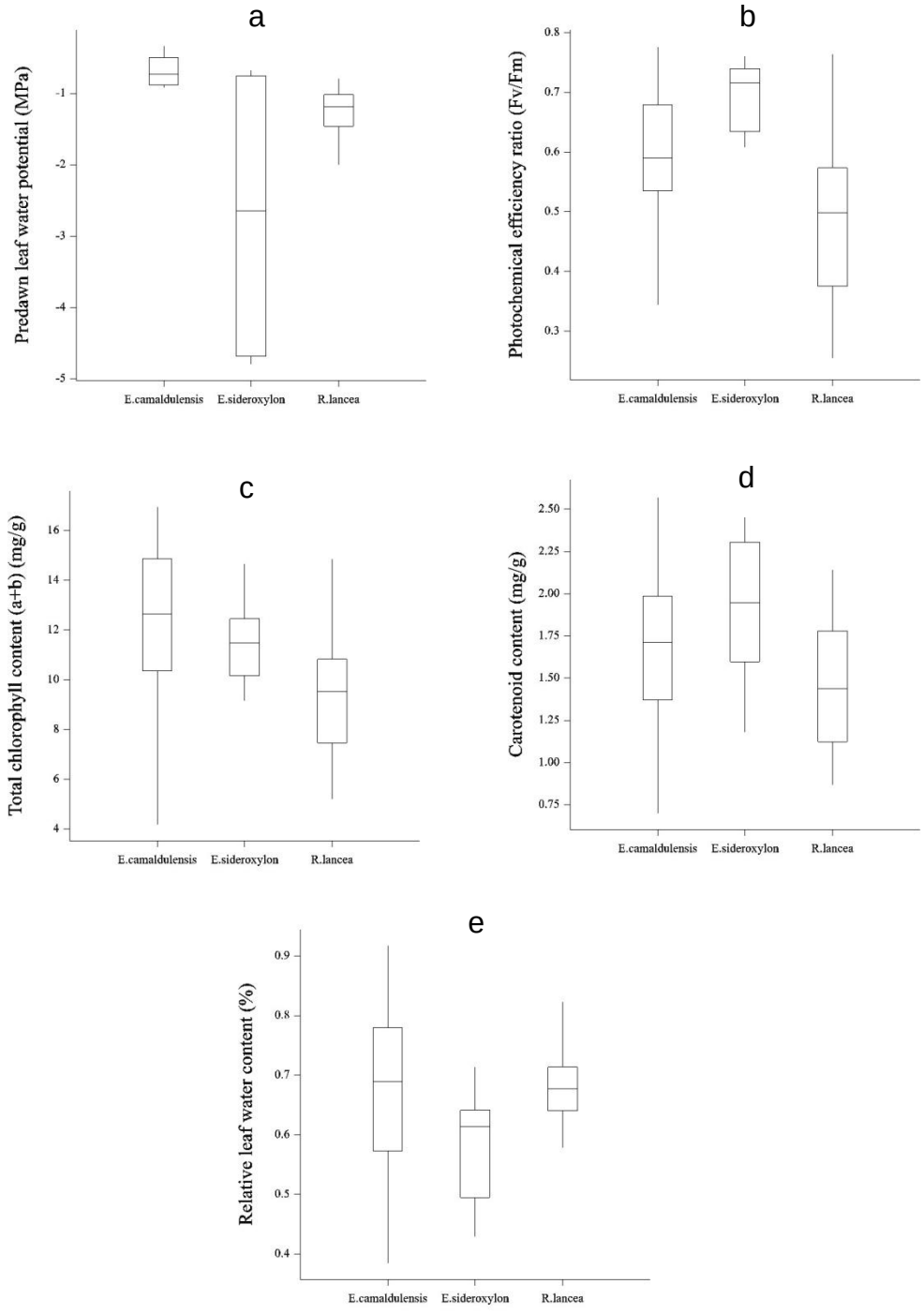


Figure 5.2 Box plots of plant water stress measurements a) predawn leaf water potential, b) photochemical efficiency, c) total chlorophyll (a+b) content, d) carotenoid content and e) relative leaf water content measured for E. camaldulensis, E. sideroxylon and S. lancea in July 2005.

5.3.2 Relationships identified using multispectral satellite data

Multiple linear regression analyses between plant water stress measurements and spectral indices derived from high spatial and medium spectral resolution Proba Chris satellite images were investigated.

5.3.2.1. Maximal models identified using multispectral satellite data

Maximal regression models were derived between measurements of plant water stress and the four spectral reflectance indices, normalised difference vegetation index (NDVI), green (GNDVI) and red edge (RENDVI) normalised difference vegetation indices, and the Carter index derived from Proba Chris multispectral imagery (Table 5.4). Adjusted R^2 values, which were ranked for plant water stress measurement, ranged from a maximum of 84.8% for predawn leaf water potential and green normalised difference vegetation index to a minimum of 20.0% for chlorophyll fluorescence and the Carter index.

Table 5.4 Adjusted R^2 values, ranked in descending order, for each maximal model determined between plant water stress methods (Y) and spectral reflectance index (X) derived from Proba Chris satellite data.

Chlorophyll (a + b) (Y)		**Leaf water content (Y)**		**Carotenoid (c+x) (Y)**		**Chlorophyll fluorescence (Fv/Fm) (Y)**		**Predawn leaf water potential (Y)**	
Spectral reflectance index (nm) (X)	**Adjusted R^2 for maximal model (%)**	**Spectral reflectance index (nm) (X)**	**Adjusted R^2 for maximal model (%)**	**Spectral reflectance index (nm) (X)**	**Adjusted R^2 for maximal model (%)**	**Spectral reflectance index (nm) (X)**	**Adjusted R^2 for maximal model (%)**	**Spectral reflectance index (nm) (X)**	**Adjusted R^2 for maximal model (%)**
RENDVI	47.6	GNDVI	34.1	NDVI	49.9	GNDVI	63.5	GNDVI	84.8
NDVI	45.4	NDVI	32.9	CARTER	46.4	NDVI	39.9	NDVI	53.9
CARTER	44.2	RENDVI	27.9	GNDVI	41.2	RENDVI	35.6	RENDVI	50.5
GNDVI	40.8	CARTER	26.1	RENDVI	39.4	CARTER	20.0	CARTER	35.7

Maximal regression models derived with chlorophyll (a+b) content, leaf water content and carotenoid content did not account for at least 50% of the variance in the data, and were therefore excluded from further analyses. Four models remained after this elimination process. These included the chlorophyll fluorescence and GNDVI (adjusted R^2= 63.5%), and predawn leaf water potential and GNDVI (adjusted R^2= 84.8%), RENDVI (adjusted $R^{2=}$ 50.5%) and NDVI (adjusted $R^{2=}$ 53.9%).

5.3.2.2. Model refinements using stepwise regression

Stepwise regression was used to refine the four remaining maximal regression models. The adjusted R^2 value for chlorophyll fluorescence and GNDVI increased from 63.5% to 64.8%. Similarly, for predawn leaf water potential and NDVI, the adjusted R^2 value increased from 53.9 to 54.5%.

Table 5.5 Comparison of the maximal and stepwise regression models derived using Proba Chris satellite data.

Chlorophyll fluorescence (Fv/Fm) (Y)			**Predawn leaf water potential (Y)**		
Spectral reflectance index (nm) (X)	**Adjusted R^2 (%)**		**Spectral reflectance index (nm) (X)**	**Adjusted R^2 (%)**	
	Maximal model	**Stepwise model**		**Maximal model**	**Stepwise model**
GNDVI	63.5	64.8	GNDVI	84.8	84.8
			NDVI	53.9	54.5
			RENDVI	50.5	50.5

For the stepwise regression modeling, the GNDVI index performed well for both measurements of plant water stress. The maximal regression model derived between predawn leaf water potential and GNDVI with the highest adjusted R^2 of 84.8% was selected at the "best" model resulting from the multispectral satellite data.

5.3.2.3. Selection of the best multispectral satellite model

Predawn leaf water potential together with GNDVI spectral reflectance index resulted in the "best" surrogate measure of plant water stress when using broad-band multispectral satellite

data. The general statistical model which resulted in six site- and species-specific models are reported below:

Predawn leaf water potential = -4.169 + 28.22(GNDVI) + 5.025 (S1) + 2.798 (S2) + (-60.29)(S1)(GNDVI)+(-23.54)(S2)(GNDVI)+ (0.690)(L1) + (3.239)(L2) +(-13.58)(L1)(GNDVI) + (-25.39)(L2)(GNDVI)	*(5.1)*
($F_{9,65} \approx 46.73$; $F_{prob} < 0.001$; $R_a^2 = 84.8$)	

For *E. camaldulensis* in Vaal River where L1=L2=0 and S1=S2=0: Predawn leaf water potential = -4.169 + 28.22(GNDVI)	*(5.1.1)*

For *S. lancea* in Vaal River where L1=L2=0, S1=0 and S2=1: Predawn leaf water potential = -1.371 + 4.68(GNDVI)	*(5.1.2)*

For *E. camaldulensis* in Welkom where L1=1, L2=0 and S1=S2=0: Predawn leaf water potential = -3.479 + 14.64(GNDVI)	*(5.1.3)*

For *S. lancea* in Welkom where L1=1, L2=0, S1=0 and S2=1: Predawn leaf water potential = -0.681 + (-8.9)(GNDVI)	*(5.1.4)*

For *E. camaldulensis* in West Wits where L1=0, L2=1 and S1=S2=0: Predawn leaf water potential = -0.93 + (2.83)(GNDVI)	*(5.1.5)*

For *E. sideroxylon* in West Wits where L1=0, L2=1, S1=1 and S2=0: Predawn leaf water potential = 4.095 + (-57.46)(GNDVI)	*(5.1.6)*

The full regression analysis depicted by Equation (5.1), which includes a summary of the analysis of variance and estimate of parameters for the multiple regression model is illustrated in Appendix 3.

Differences between the observed and predicted predawn leaf water potential, using Equation (5.1), were assessed using a standardised residual plot of fitted values of predawn leaf water potential (Figure 5.3). The standardised residual plot indicates a cluster of fitted values at the lower and higher predawn leaf water potentials. However, the majority of the fitted values are clustered at lower predawn leaf water potential, indicating that the data could be skewed. Residuals tend to be smaller at higher predawn leaf water potentials (more negative), and larger at lower predawn leaf water potentials (less negative).

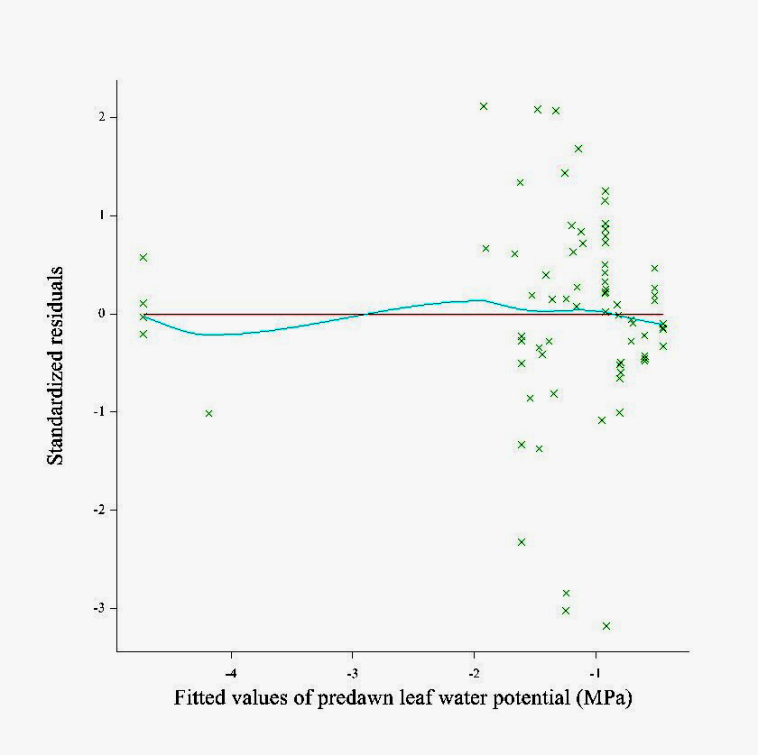


Figure 5.3 Standardised residual plot of fitted values of predawn leaf water potential using the green normalised difference vegetation spectral reflectance model.

5.3.2.4. Validation of the best model using multispectral satellite data

The predawn leaf water potential GNDVI spectral reflectance model was validated using the method of re-running the fitted regression model with a percentage of the data excluded. Three validation runs were used, with 10 random samples excluded from each run. Subsets of data which were used in the validation exercise are listed in Table 5.6.

Table 5.6 Validation models derived from multispectral satellite data used to predict predawn leaf water potential.

Mining District	Species	Fitted Models	GNDVI index (X)	Predawn leaf water potential measured (Y)	Predawn leaf water potential predicted (Y)
Run 1					
Vaal River	*E. camaldulensis*	-4.280+29.04(GNDVI)	0.091	-1.698	-1.645
			0.115	-0.832	-0.936
			0.115	-0.606	-0.936
Vaal River	*S. lancea*	-1.37+4.9(GNDVI)	0.053	-0.788	-1.108
			0.122	-1.184	-0.774
			-0.014	-1.590	-1.440
Welkom	*E. camaldulensis*	-3.177+12.03(GNDVI)	0.175	-0.818	-1.068
			0.160	-0.488	-1.257
Welkom	*S. lancea*	-0.267-12.11(GNDVI)	0.088	-2.000	-1.332
			0.030	-1.292	-0.629
Run 2					
Vaal River	*E. camaldulensis*	-4.647+32.66(GNDVI)	0.115	-0.722	-0.886
			0.115	-0.632	-0.886
Vaal River	*S. lancea*	-1.338+3.95(GNDVI)	0.123	-1.020	-0.851
			-0.003	-1.490	-1.349
Welkom	*E. camaldulensis*	-3.743+15.97(GNDVI)	0.175	-0.818	-0.943
Welkom	*S. lancea*	-0.434-12.74(GNDVI)	0.095	-1.450	-1.641
			0.139	-1.190	-2.208
West Wits	*E. camaldulensis*	-0.931+2.74(GNDVI)	0.172	-0.482	-0.460
			0.147	-0.330	-0.527
West Wits	*E. sideroxylon*	3.802+-55.76(GNDVI)	0.097	-0.684	-1.605
Run 3					
Vaal River	*E. camaldulensis*	-4.121+27.28(GNDVI)	0.115	-0.424	-0.980
			0.115	-0.838	-0.980
Vaal River	*S. lancea*	-1.384+5.07(GNDVI)	0.037	-0.842	-1.196
			0.122	-1.050	-0.768
			-0.014	-1.590	-1.457
Welkom	*E. camaldulensis*	-3.626+15.04(GNDVI)	0.147	-0.512	-1.943
Welkom	*S. lancea*	-0.889-7.17(GNDVI)	0.095	-1.450	-1.568
			0.048	-0.850	-1.231
West Wits	*E. camaldulensis*	-0.938+2.97(GNDVI)	0.078	-0.730	-0.705
			0.172	-0.570	-0.427

Significant differences between measured and predicted values of predawn leaf water potential were assessed using a t-test. The results of the t-test for Run1 (t = -0.12, 9df, P = 0.911, r = 0.43) and Run3 (t = 1.62, 9df, P = 0.139, r = 0.53) were not significant, compared to Run3 (t = 1.99, 9df, P = 0.078, r = 0.68), which was significant at the 10% level.

5.3.3 Relationships identified using hyperspectral satellite data

Spectral relationships were investigated between measurements of plant water stress and spectral indices derived from Hyperion satellite imagery. This study provided a unique opportunity to compare the results obtained from the multiple linear regression analyses, using broad multispectral bands compared with narrow-hyperspectral bands.

5.3.3.1. Maximal models identified using hyperspectral satellite data

Maximal regression models were determined between plant water stress measurements and eight vegetation spectral reflectance indices derived from Hyperion hyperspectral imagery (Table 5.7). Adjusted R^2 values were ranked for each plant water stress measurement, and ranged from a maximum of 90.5% for predawn leaf water potential and water band index to a minimum of 1.7% for chlorophyll (a+b) content and the normalised difference vegetation index. Models missing in Table 5.7 were a result of sampling points which were clustered at the edge of the image, and which did not contain the full complement of spectral bands. Therefore certain vegetation spectral reflectance indices could not be derived due to the missing spectral values.

Table 5.7/...

Table 5.7 Adjusted R^2 values, ranked in descending order, for each maximal model derived between plant water stress measurement (Y) and spectral reflectance index (X) derived from Hyperion satellite data.

Chlorophyll (a + b) (Y)		**Leaf water content (Y)**		**Carotenoid (c+x) (Y)**		**Chlorophyll fluorescence (Fv/Fm) (Y)**		**Predawn leaf water potential (Y)**	
Spectral reflectance index (nm) (X)	**Adjusted R^2 for maximal model (%)**	**Spectral reflectance index (nm) (X)**	**Adjusted R^2 for maximal model**	**Spectral reflectance index (nm) (X)**	**Adjusted R^2 for maximal model**	**Spectral reflectance index (nm) (X)**	**Adjusted R^2 for maximal model**	**Spectral reflectance index (nm) (X)**	**Adjusted R^2 for maximal model**
MSI	27.9	REP	63.0	WBI	14.3	MSI	13.7	WBI	90.5
RENDVI	26.4	PSRI	53.4	NDVI	5.4	MRESR	13.2	REP	33.6
NDII	18.0	CARTER	49.2	MRESR	4.6	NDII	11.5	PSRI	25.1
PSRI	12.6	RENDVI	41.6	MSI	3.7	RENDVI	10.5	RENDVI	21.6
CARTER	10.2	MRESR	34.1	NDII	2.3	CARTER	3.8	MRESR	17.6
REP	3.9	MSI	31.9			PSRI	3.6	CARTER	17.5
NDVI	1.7	WBI	28.7			NDVI	2.3	MSI	11.1
		NDII	28.5					NDII	2.7

Vegetation spectral reflectance models which did not account for at least 50% of the variance in the data were excluded from further analyses. Measurements of chlorophyll (a+b), carotenoid content and chlorophyll fluorescence which achieved maximum adjusted R^2 of 27.9%, were eliminated. Three maximal regression models were selected from this investigation for the stepwise regression analysis.

5.3.3.2. Model refinements using stepwise regression

The stepwise regression modeling in this investigation resulted in no further refinements to the existing maximal models. The adjusted R^2 values remained the same as shown in Table 5.8. The maximal model determined between predawn leaf water potential and the water band index which obtained the highest adjusted R^2 of 90.5%, was selected as the "best" model derived using hyperspectral satellite data.

Table 5.8/...

Table 5.8 Comparison of the maximal and stepwise regression models, obtained in the Hyperion satellite data analysis for the three models with the highest adjusted R^2 values exceeding 50%.

Leaf water content (Y)			**Predawn leaf water potential (Y)**		
Spectral reflectance index (nm) (X)	**Adjusted R^2 (%)**		**Spectral reflectance index (nm) (X)**	**Adjusted R^2 (%)**	
	Maximal model	**Stepwise model**		**Maximal model**	**Stepwise model**
REP	63.0	63.0	WBI	90.5	90.5
PSRI	53.4	53.4			

The selected model indicates that strong relationships exists between predawn leaf water potential, which is a direct measure of plant water stress, and the water band index, which is designed to capture changes in plant water content.

5.3.3.3. Selection of the"best" model derived from hyperspectral satellite data

The multiple regression analysis using hyperspectral satellite data resulted in a simple linear model between predawn leaf water potential and the water band spectral index. This model did not include any interactions between species or districts can be reported as follows, with detailed regression analysis listed in Appendix 3:

Predawn leaf water potential = 21.20 - 23.0(WBI)	*(5.2)*
($F_{1,18} \approx 182.07$; $F_{prob} < 0.001$; $R_a^2 = 90.5\%$)	

Differences in observed and predicted values of predawn leaf water potential when using the spectral model represented by Equation (5.2) were investigated using a standardised residual plot of fitted values of predawn leaf water potential. The plot of residuals against fitted values of predawn leaf water potential indicated that there seems to be four clusters of sample groups (Figure 5.4). The residuals indicate a non-random distribution of sample points, with one sample group at higher (more negative) predawn leaf water potential and three sample groups at lower (less negative) predawn leaf water potentials.

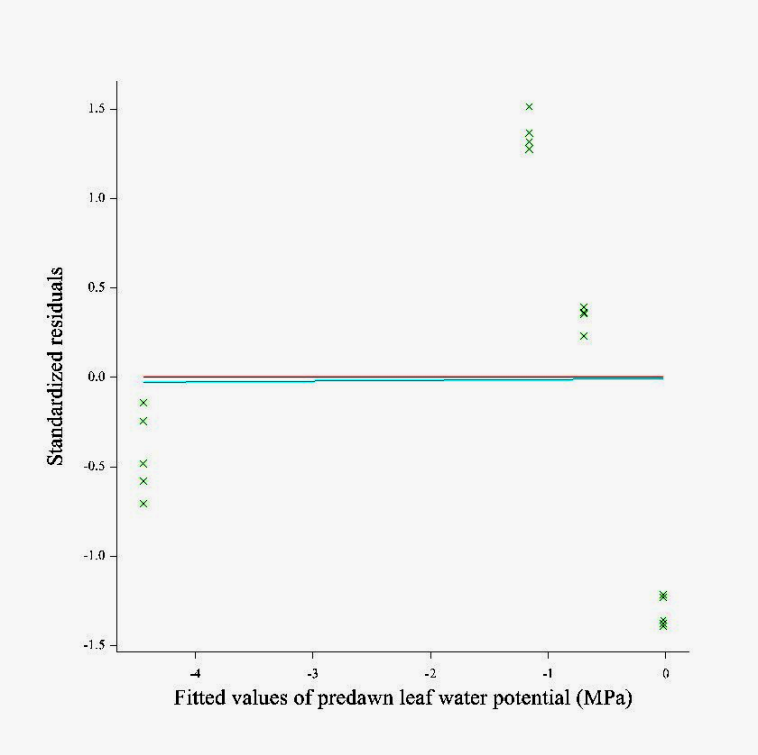


Figure 5.4 Standardised residual plot of fitted values of predawn leaf water potential using water band spectral reflectance model

There appeared to be no apparent outliers in the data. However the residual plot of fitted values of predawn leaf water potential indicated that the linear regression model may inadequately represent the data.

5.3.3.4. Validation of the "best" model derived from hyperspectral satellite data

The predawn leaf water potential and water band index spectral reflectance model for the West Wits mining district was validated, using the method of repeatedly re-running the fitted regression model with a percentage of the data excluded. Three validation runs were used, with 4 random samples excluded from each run. Subsets of data which were used in the validation exercise are listed in Table 5.9.

Table 5.9 Validation models, derived from hyperspectral satellite data, used to predict predawn leaf water potential in the West Wits mining district.

Species	Fitted Models	WBI index (X)	Predawn leaf water potential measured (Y)	Predawn leaf water potential predicted (Y)
Run 1				
E. camaldulensis	20.03 – 2.85 (WBI)	0.95152	-0.482	-0.712
		0.97191	-0.41	-1.178
E. sideroxylon	20.03 – 2.85 (WBI)	0.92197	-0.676	-0.037
		1.11607	-4.566	-4.472
Run 2				
E. camaldulensis	21.2 – 23 (WBI)	0.95152	-0.498	-0.685
		0.97191	-0.438	-1.154
E. sideroxylon	21.2 – 23.0 (WBI)	0.92197	-0.77	-0.005
		1.11607	-4.514	-4.470
Run 3				
E. camaldulensis	20.81 – 2.59 (WBI)	0.95152	-0.502	-0.685
		0.97191	-0.46	-1.145
E. sideroxylon	20.81 – 2.59 (WBI)	0.92197	-0.752	-0.017
		1.11607	-4.8	-4.402

T-tests were used to determine if there were differences between measured and predicted values of predawn leaf water potential. The statistical tests for all three validation runs confirmed that there were no significant differences between measured and predicted predawn leaf water potential (Run 1 ($t = 0.23$, 3df, $P = 0.836$, $r = 0.957$); Run 2 ($t = 0.08$, 3df, $P = 0.944$, $r = 0.952$) and Run 3 ($t = -0.21$, 3df, $P = 0.847$, $r = 0.956$)). Pearson correlation coefficients indicated a high correlation between measured and predicted values of predawn leaf water potential ($r > 0.7$).

5.4 DISCUSSION

The multiple linear regression modeling identified significant (Fprob < 0.001) spectral relationships which represented at least 50% of the variation in the data, for predawn leaf water potential, carotenoid content, chlorophyll fluorescence and leaf water content. Potential spectral reflectance indices derived using the satellite remote sensing data, which were highlighted from this investigation, included the NDVI, GNDVI, RENDVI, WBI, REP and PSRI.

Three vegetation indices, which are sensitive to changes in plant pigment content and reflect spectral differences in the visible region of the spectrum, performed well when applied to the multispectral satellite data, represented by high spatial and medium resolution Proba Chris data. These indices included the normalised difference vegetation index, the greenness normalised difference vegetation index and the red edge normalised difference vegetation index, and are often grouped as broadband greenness vegetation indices. In this study these indices have performed better when applied to broader or lower level spectral resolution data. The importance of the spectral wavelengths 550, 676, 705, 750, 760 nm that were used to derive the indices, have been highlighted in this investigation by their linkage to changes in plant pigment contents and the inference of plant stress (Curran *et al.*, 1990; Carter, 1993; Baret *et al.*, 1994; Filella and Penuelas 1994; Gitelson and Merzlyak, 1996; Lichtenthaler *et al*., 1996; Blackburn, 1998b; Lelong *et al*., 1998; Blackburn, 1999; Gitelson *et al*., 2002).

Three vegetation indices performed well when applied to the hyperspectral satellite data obtained for the West Wits mining district, which was represented by the Hyperion high spatial and spectral resolution image. The water band index, which reflects spectral changes in the near-infrared regions of the electromagnetic spectrum, has been characterised as being sensitive to changes in plant water content, was linked to changes in predawn leaf water potentials. While the REP and PSRI indices have been characterised as being sensitive to changes in plant pigment content, were linked to changes in leaf water content. These results support the findings of recent studies which have utilised high spectral resolution remote sensing data and have highlighted the importance of specific regions of the spectrum such as

the red edge when investigating plant stress (Clay *et al*. 2006; Fitzgerald *et al*. 2006; Blackburn 2007; Campbell *et al*. 2007). Therefore, the results from the Hyperion high spectral resolution study, which has shown a link between the red edge position and measurement of leaf water content, corroborates the importance of this region of the spectrum for plant water stress studies.

In this study, a subset of the spectral reflectance indices, which were investigated using hand-held spectral reflectance data as shown in Chapter 4, were successfully applied to high spatial and medium to high spectral resolution satellite data. Some general trends which were identified from the use of satellite data to detect possible relationships with plant water stress were:

- Vegetation indices designed to capture changes in plant water content/plant water status and spectral changes in the red edge region of the spectrum performed well when applied to high spectral resolution remote sensing data.
- The greenness normalised difference vegetation index was considered to be a fairly robust index, which was highly correlated to chlorophyll fluorescence and predawn leaf water potential.
- The broadband vegetation indices, which capture changes in the visible region of the electromagnetic spectrum and are sensitive to changes in plant pigment content, performed well when applied to the medium spectral resolution remote sensing data.
- The greenness normalised difference vegetation index has the potential to be used to map spatial patterns of winter-time plant stress for different genera/species and in different geographical locations.
- Predawn leaf water potential measurements were found to be strongly correlated to spectral indices derived from high and medium spectral resolution satellite data.

These satellite investigations together with the findings from the hand-held spectral reflectance data, confirm that a range of broadband and narrowband spectral reflectance indices performed differently when applied to various forms of multispectral and hyperspectral remote sensing datasets.

5.5 CONCLUSIONS

These results demonstrate the potential for using satellite remote sensing imagery to detect and map spatial patterns of plant water stress within the Welkom, Vaal River and West Wits mining districts. Several spectral relationships, which are sensor, site- and tree species-specific, have been identified and could be used to map plant water stress over the vegetated areas within each district. Furthermore, the degree of stress can be ascertained using the predictive relationships derived between ground-based measurements of plant water stress; predawn leaf water potential, leaf chlorophyll fluorescence, and leaf water content and respective vegetation spectral reflectance indices. The investigation of high spatial and medium to high spectral resolution satellite data has highlighted the importance of the visible and near-infrared and red-edge region of the electromagnetic spectrum. A key finding is that vegetation indices, which are sensitive to spectral differences in vegetation as a result of changes in plant water content/plant water status and plant pigment content, are important when investigating plant water stress using satellite remote sensing data.

CHAPTER 6. EVALUATION OF AIRBORNE MULTISPECTRAL AND HYPERSPECTRAL REMOTE SENSING DATA TO DETECT SPATIAL PATTERNS OF PLANT WATER STRESS

ABSTRACT

The aim of this study was to evaluate the potential of using multispectral and hyperspectral airborne remote sensing imagery to detect plant water stress. The benefits of different platforms of remote sensing technologies have been recognised and therefore their various capabilities for detecting and mapping spatial patterns of plant water stress in the mining areas have been investigated.

Remote sensing airborne surveys were conducted by Land Resource International (PTY) Ltd, South Africa and Bar-Kal Systems Engineering Ltd, Israel, to respectively investigate the application of multispectral and hyperspectral airborne imagery to detect plant water stress. Ground-based measurements of plant water stress, predawn leaf water potential, leaf chlorophyll fluorescence, chlorophyll and carotenoid pigment content and relative leaf water content were carried out during July and August 2005. Ten individual spectral bands and vegetation spectral reflectance indices which are sensitive to changes in plant pigment content and plant water status/content were calculated from the airborne remote sensing imagery. Multiple linear regressions were used to investigate the interactions between the districts and species, and their respective spectral reflectance indices and plant water stress measurements.

The results of the multispectral airborne study revealed that carotenoid content together with the green spectral waveband resulted in the "best" surrogate measure of plant water stress when using broad-band multispectral airborne data. However, when using airborne

hyperspectral data, predawn leaf water potential with the normalized difference water index was selected as the most appropriate model. Upon evaluation of the multiple linear regression models, it was concluded, that the airborne hyperspectral data produced several more regression models with higher adjusted R^2 values (R_a^2 range 6.2 - 76.2%) compared to the airborne multispectral data (R_a^2 range 6 - 50.1). Therefore, preference was given to hyperspectral airborne data sources based on the many stronger multiple linear relationships which were derived in this study.

Keywords : airborne remote sensing data, carotenoid pigment content, hyperspectral, multispectral, plant water stress, predawn leaf water potential, spectral reflectance indices

6.1 INTRODUCTION

The relevance of remote sensing technologies in southern Africa has grown over the past two decades, and has become a vital component of several research and commercial applications, including mining exploration, environmental monitoring, geological mapping, agriculture management, energy efficiency and other applications. Several different types of platforms and sensors have been tested and utilised including digital photography, multispectral or hyperspectral satellite and airborne sensors, radar and lidar scanners and magnetic sensors. Multispectral sensor systems commonly collect data in four to seven broad spectral bands from the visible (VIS) and near-infrared (NIR) regions of the spectrum, while hyperspectral sensor systems allow the collection of several hundred narrow spectral bands across the spectrum. Advancements in airborne remote sensing technologies have allowed for both multispectral and hyperspectral images to be acquired at much higher spatial resolutions of less than 5m, when compared to satellite systems. Therefore, even though the spectral resolutions of airborne and satellite systems are similar, differences in these two platforms are strongly dependent on the spatial resolutions at which the remotely sensed images are acquired. However, it is important to note that airborne remote sensing systems are costly to obtain for research applications. Currently in South Africa, a platform exists only for multispectral airborne imagers such LREye (Land Resource International (PTY) Ltd, South Africa) or ArcEagle (Agricultural Research Council, South Africa), while hyperspectral

airborne imagers such as AISA-ES sensor (Bar-Kal Systems Engineering Ltd, Israel), CASI (Hyperspectral Imaging Ltd, Canada) and HYPMAP (HyVista Cooperation, Australia) must be sourced from international organisations or consultants.

Considerable effort has been put into interpreting spectral data used to calculate vegetation indices for remotely mapping temporal and spatial variations in vegetation structure, as well as certain biophysical parameters. As mentioned in the previous chapters many indices are based on the principle of combining information contained in the red and near infrared region exploiting the spectral differences between these two regions of the spectrum. However, indices do perform differently as a result of band selection or width, changes in near infrared reflectance due to canopy geometry, phenological conditions or due to non-photosynthetic background contribution, essentially being factors influenced by the spectral and spatial resolutions of the remote sensing data (Tucker *et al.,* 1980; Gitelson *et al.,* 2002; Jackson *et al.,* 2004). As a result relationships based on near infrared reflectance are usually species-specific, due to the dependence on factors such as canopy architecture, cell structure and leaf inclination. In contrast, reflectance in the visible region is less species-specific, because it is governed mainly by pigment content and composition such as chlorophyll content (Chappelle *et al.*,1992; Gitelson and Merzlyak, 1996). Canopy reflectance is influenced by a number of factors, such as variation in soil properties (Bannari *et al.,* 2008), canopy geometry (Curran *et al*., 1990), and leaf distribution, density and structure. With the use of reference end-members, spectral un-mixing has been employed to model reflectance data as mixtures of green vegetation, non-photosynthetic vegetation, soils and shade, essentially modelling the combination of spectra of components in the field of view (Baret *et al*., 1994).

In this study, the benefits of different platforms of remote sensing technologies have been recognised and therefore their various capabilities for detecting and mapping spatial patterns of plant water stress in the mining areas have been investigated. In chapters 4 and 5, the use of hand-held and satellite remote sensing data at different spatial and spectral resolutions were evaluated. This study (chapter 6) presented a unique opportunity to undertaken both a

multispectral and hyperspectral airborne remote sensing campaign, and to investigate potential linkages with plant water stress in the mining areas.

6.2 MATERIALS AND METHODS

A detailed description of the tree species, mining districts and sampling sites selected for this study are discussed in Chapter 2. Sampling sites within the three mining districts, Welkom, Vaal River and West Wits, were used for ground-based measurements of plant water stress and as ground-truthing sites for the remote sensing surveys. Ground-based measurements of plant water stress were undertaken on the three species *E. camaldulensis*, *E. sideroxylon* and *S. lancea* in the Welkom, Vaal River and West Wits mining districts during July 2005 and August 2005 (as presented and discussed in Chapter 5, section 5.3.1, Table 5.2 and Table 5.3) were used for ground-truthing the airborne multispectral and hyperspectral remote sensing images. Measurements of plant water stress were undertaken within 10 days of acquiring the respective airborne remote sensing images. The field sampling procedures of each ground-based plant water stress measurement used, *viz*. predawn leaf water potential, leaf chlorophyll fluorescence, chlorophyll and carotenoid pigment content and relative leaf water content, are described in Chapter 4, whereas the step by step details of the protocols are presented in Appendix 2.

6.2.1 Airborne remote sensing surveys

Two airborne remote sensing surveys took place during July and August 2005. The multispectral campaign was undertaken between 16 and 22 of July, while the hyperspectral campaign was undertaken between 22 and 25 of August 2005. The survey areas of the multispectral and hyperspectral remote sensing campaigns are illustrated in Figure 6.1.

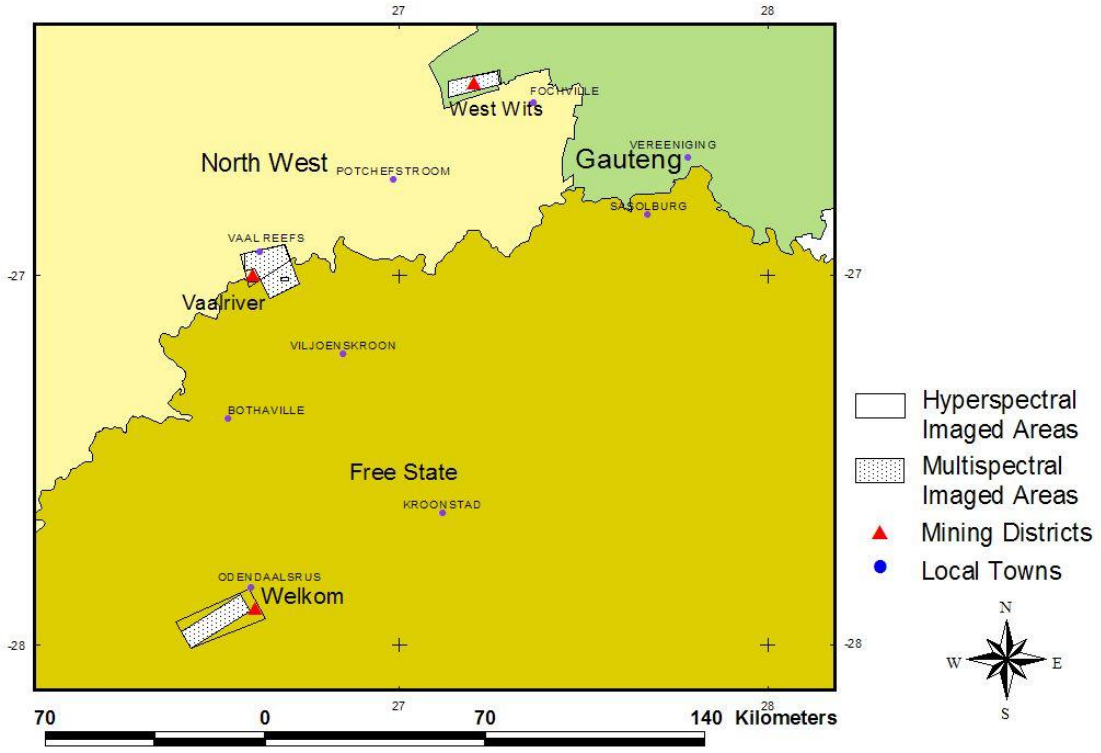


Figure 6.1 Location of multispectral and hyperspectral surveys in the Welkom, Vaal River and West Wits mining districts. Multispectral survey areas are patterned, while hyperspectral survey areas are unshaded.

The multispectral survey was undertaken by Land Resource International (PTY) Ltd at a spatial resolution of 0.75 m. Approximately 12 000 ha, 17 200 ha and 5 200 ha were imaged across the Welkom, Vaal River and West Wits mining districts respectively, at an altitude of 1829 m (6000 ft) ASL (Figure 6.1). Four multispectral bands were acquired from the visible and near infrared regions of the electromagnetic spectrum. The centre wavelengths, at which the red, green, blue and near-infrared filters operated, were 664.7 nm, 568.4 nm, 465.9 nm and 870.5 nm respectively. All four multispectral bands were ortho-rectified and geo-registered to WGS84 L027, datum Transverse Mercator.

The hyperspectral survey was undertaken by Bar-Kal Systems Engineering Ltd, from Israel. The survey was conducted with the AISA-ES hyperspectral push broom sensor, which was composed of two cameras covering the visible and near infrared (400 to 963 nm) and

shortwave infrared (968 to 2372 nm) regions of the electromagnetic spectrum. One hundred and eighty narrow spectral bands were acquired at a spatial resolution 3.3 to 3.5 m across the Welkom, Vaal River and West Wits mining districts (Figure 6.1). A total of 52 strips were flown across the three mining districts including one calibration strip at 7620 m (25 000ft) ASL in each mining district. All images acquired from the hyperspectral survey were radiometrically and geometrically corrected and projected to UTM 35 S, datum WGS84 (Bar-Kal Systems Engineering Ltds, 2005). Atmospheric correction was performed using the "empirical line" method in which radiance values coming back from the surface were compared to reflectance values measured on the ground with a calibrated hand-held spectrometer (Bar-Kal Systems Engineering Ltds, 2005).

Spectral signatures of several targets were collected for atmospheric calibration. In order to ensure the quality of the ground-truth data all measurements were done in-situ and in-vivo, and thus removing any time related effects on the targets. The instrument was routinely calibrated in the field every 10 to 20 measurements. In addition, in order to reduce noise, forty measurements were obtained at each spot and the average value was used (Bar-Kal Systems Engineering Ltds, 2005).

Calibration sites used for atmospheric correction in Welkom consisted of a salt pan area characterised by very bright, very dark and gray locations; Vaal River included a tennis court, wet tailing surface, tailing covered with dark soil; West Wits included a tailing storage facility, paved road side, a tilled soil plot and tarred area at a petrol station.

The images were atmospherically corrected using the empirical lines method using four ground targets (namely tennis court, wet tailing surface, tailing covered with dark soil). The atmospheric correction was applied to the calibration strip and generated a gain and offset. The gain and offset that were generated for the calibration strip were then applied to all of the images. Because the calibration strip crosses all of the other images, it was used as the reflectance reference for the other images to improve their reflectance accuracy. This was done by identifying targets in the calibration strip with those in the other strips and correcting their reflectance.

6.2.2 Spectrometer measurements

Spectral reflectance signatures were collected using an ASD hand-held field spectrometer (Analytical Spectral Devices Inc, 5335 Sterling Drive, Suite A, Boulder, Colorado 80301, USA) during late August 2005. Hand-held spectral signatures were recorded for the three tree species investigated and of specific ground targets for the calibration of the airborne hyperspectral remote sensing images using a bare optic fibre with 25º field of view. When atmospheric conditions were not conducive to bare optic fibre measurements, all spectral signatures were acquired with a high intensity contact probe which has an internal calibrated illumination source. A total of 36 calibration sites such as dry grass, parking lots, wet and dry tailing surfaces, soil plots, bright and dark surfaces of stones, tarred roads were recorded across the three mining districts.

6.2.3 Selection and derivation of the vegetation spectral reflectance indices

A total of ten individual spectral bands and vegetation spectral reflectance indices investigated in Chapter 4 were selected and derived from the multispectral and hyperspectral airborne remote sensing data (Table 6.1). Four individual spectral bands and two vegetation spectral reflectance indices, which are sensitive to changes in plant pigment content, were derived from the processed multispectral images *viz*. red, green, blue and near-infrared spectral bands and the normalised difference vegetation index (NDVI) and greenness normalised difference vegetation index (GNDVI). The two vegetation spectral reflectance indices used in the multispectral analysis, together with four additional vegetation spectral reflectance indices designed to capture changes in plant pigment and plant water status/content, were derived from the processed hyperspectral images.

Table 6.1 Spectral wavelengths and reflectance indices derived from the airborne multispectral and hyperspectral remote sensing data.

Multispectral (MS) or Hyperspectral (HS) Airborne Survey	Common name for spectral index or spectral region of the spectrum	Spectral Reflectance Ratio or Index (nm)	Reference	Closest wavelengths used to derive indices from MS imagery	Closest wavelengths used to derive indices from HS imagery
Indices sensitive to changes in plant pigment content					
MS survey	Red	664.67	Land Resource International (PTY) Ltd (2005)	664.67	
MS survey	Green	568.42	Land Resource International (PTY) Ltd (2005)	568.42	
MS survey	Blue	465.88	Land Resource International (PTY) Ltd (2005)	465.88	
MS survey	Near infrared	870.53	Land Resource International (PTY) Ltd (2005)	870.53	
MS and HS survey	Green normalised difference vegetation index (GNDVI)	(750-550)/(750+550)	Gitelson *et al.* (1996)	(870.53 - 568.42)/(870.53 + 568.42)	(750-550)/(750+550)
MS and HS survey	Normalised difference vegetation index (NDVI)	(750-676)/(750+676)	Tucker (1979)	(870.53 - 664.67)/(870.53 + 664.67)	(750-676)/(750+676)
HS survey	R695/R670	(695/670)	Carter (1997)		(695/670)
HS survey	Datt index	(850 – 71)/(850 - 680)	Datt (1999)		(850 – 71)/(850 - 680)
HS survey	Plant senescence reflectance index (PSRI)	(680-500)/(750)	Merzlyak *et al*. (2003a)		(680-500)/(750)
Indices sensitive to changes in plant water content/plant water status and plant cellular structure					
HS survey	Normalised difference water index (NDWI)	(857-1241)/(857+1241)	Gao (1995)		(980-1241)/(980+1241)

6.2.4 Analysis of data

Multiple linear regressions were used to investigate the interactions between the districts and species, and their respective spectral reflectance indices and plant water stress measurements using GenStat (11th edition, 2008). The general maximal multiple linear regression model applied with the interaction factors in Chapter 4 (section 4.2.4) has been used:

$$Y(i) = b_o + b_1X(i) + a_1L_1 + a_2L_2 + g_1S_1 + g_2S_2 + d_1L_1X(i) + d_2L_2X(i) + e_1S_1X(i) + e_2S_2X(i) \quad (6.1)$$

where Y(i) represents the plant water stress measurements;
X(i) the spectral indices;
L(i) represents the districts;
S(i) represents the species;
b_o represents the constant or intercept;
b_1 slope and;
a, g, d, e the regression coefficients.

The same statistical approach used in the analysis of the hand-held spectral reflectance data and the multispectral and hyperspectral satellite remote sensing data was applied in this study. Statistical procedures to select the "best" or most appropriate linear regression models and eliminate poor combinations of spectral reflectance indices (X) and plant water stress measurements (Y) are briefly summarised below:

- Maximal models were derived from multispectral and hyperspectral airborne remote sensing images and ground based measurements of plant water stress. Models were ranked, screened, and the three highest adjusted R^2 maximal models which accounted for more than 50% of the variance in the data, were selected.
- Model refinements included the use of stepwise regression. The adjusted R^2 values for the maximal models were compared with their corresponding stepwise regression models to determine any improvement in the models.
- The "best" models i.e. best maximal model for each plant water stress measurement (Y) and the "best" model across all combinations of X and Y resulting from the

stepwise regression, were selected, using highest adjusted R^2 value and the significance of the F and t probability values.

- Validation was performed for "best" model with significant differences between predicted and measured Y values determined using a t-test for paired samples.

6.3 RESULTS

Multiple linear regressions between vegetation indices and ground based measurements of plant water stress were evaluated to ascertain which spectral models performed best when applying vegetation indices derived from the airborne multispectral and hyperspectral spectral data. The results are discussed the subsequent sections.

6.3.1 Relationships identified using airborne multispectral data

6.3.1.1. Maximal models identified using airborne multispectral data

The maximal multiple linear regression models determined between ground based measurements of plant water stress undertaken in July and August 2005, and the six vegetation spectral reflectance indices derived from airborne multispectral data, were ranked to ascertain which were the better performing models (Table 6.2). Six methods of plant water stress were obtained in July 2005, five of which were repeated in August 2005. Adjusted R^2 values, which were ranked for each method, ranged from a maximum of 50.1% for the green spectral waveband (568.4 nm) and carotenoid content, to a minimum of 10.1% for NDVI and chlorophyll fluorescence undertaken in July 2005. Similarly, adjusted R^2 values ranged from a maximum of 51.1% for blue spectral waveband (465.88 nm) and carotenoid content, to a minimum of 6.0% for NDVI and chlorophyll fluorescence measurements undertaken in August 2005.

Five plant water stress measurements which did not attain adjusted R^2 values greater than 50% were excluded from further analyses. These included total chlorophyll (a+b) content, chlorophyll fluorescence, leaf water content and predawn leaf water potential. Potential

relationships between carotenoid content and the green and blue spectral wavebands were investigated further.

Table 6.2/...

Table 6.2 Adjusted R^2 values, ranked in descending order, for each maximal model derived between plant water stress measurement (Y) and spectral reflectance indices (X)derived from airborne multispectral data.

July 2005										August 2005							
Chlorophyll (a + b) (Y)		Carotenoid (c+x) (Y)		Chlorophyll fluorescence (Fv/Fm) (Y)		Leaf water content (Y)		Predawn leaf water potential (Y)		Chlorophyll (a + b) (Y)		Carotenoid (c+x) (Y)		Chlorophyll fluorescence (Fv/Fm) (Y)		Leaf water content (Y)	
Spectral reflectance index (nm) (X)	**Adjusted R^2 for maximal model**	**Spectral reflectance index (nm) (X)**	**Adjusted R^2 for maximal model**	**Spectral reflectance index (nm) (X)**	**Adjusted R^2 for maximal model**	**Spectral reflectance index (nm) (X)**	**Adjusted R^2 for maximal model**	**Spectral reflectance index (nm) (X)**	**Adjusted R^2 for maximal model**	**Spectral reflectance index (nm) (X)**	**Adjusted R^2 for maximal model**	**Spectral reflectance index (nm) (X)**	**Adjusted R^2 for maximal model**	**Spectral reflectance index (nm) (X)**	**Adjusted R^2 for maximal model**	**Spectral reflectance index (nm) (X)**	**Adjusted R^2 for maximal model**
BLUE	43.3	GREEN	50.1	GREEN	20.9	GNDVI	43.9	GREEN	39.5	BLUE	46.5	BLUE	51.0	GREEN	24.0	NDVI	32.8
GREEN	42.7	BLUE	47.3	GNDVI	20.7	NDVI	41.5	RED	36.7	GREEN	42.8	GREEN	47.3	RED	11.3	GNDVI	31.2
RED	40.2	RED	42.8	BLUE	18.6	BLUE	40.5	BLUE	35.3	GNDVI	41.9	GNDVI	45.3	BLUE	11.2	IR	29.8
IR	39.7	IR	41.6	RED	14.4	RED	39.3	NDVI	35.2	IR	40.1	IR	41.4	IR	7.9	GREEN	28.7
NDVI	37.6	NDVI	40.3	IR	13.5	GREEN	38.9	GNDVI	32.4	NDVI	39.2	NDVI	39.8	GNDVI	7.8	BLUE	25.6
GNDVI	36.2	GNDVI	39.8	NDVI	10.1	IR	36.1	IR	30.4	RED	38.9	RED	39.3	NDVI	6.0	RED	25.0

6.3.1.2. Model refinements using stepwise regression

Stepwise regression was used to refine two maximal models which were selected based on their adjusted R^2 values. These included carotenoid content measured in July and August 2005, and the green and blue spectral wavebands respectively. The stepwise regression modeling did not result in further improvements to the maximal models. Adjusted R^2 of 50.1% obtained between carotenoid content and the green spectral waveband (July 2005) remained the same for the stepwise regression model. However, the adjusted R^2 obtained between carotenoid content and the blue spectral waveband (August 2005) decreased by 0.1% for the stepwise regression model. Based on these results, the maximal model derived between carotenoid content and the green spectral waveband with the highest adjusted R^2 of 50.1% was selected as the "best" model.

6.3.1.3. Selection of the best model derived from airborne multispectral data

Carotenoid content together with the green spectral waveband resulted in the "best" surrogate measure of plant water stress when using broad-band multispectral airborne data. The general statistical model which resulted in six site- and species-specific models are reported below:

Carotenoid content = 2.262 + (-0.01164)(GREEN) + (-0.227)(L1) + (1.699)(L2) + (-4.70)(S1) + (0.083)(S2) + (0.0672)(GREEN)(S1) + (-0.00315)(GREEN)(S2) + (0.00792)(GREEN)(L1) + (-0.0156)(GREEN)(L2)	*(6.1)*
($F_{9,65} \approx 9.26$; $F_{prob} < 0.001$; $R_a^2 = 50.1$)	

For *E. camaldulensis* in Vaal River where L1=L2=0; S1=S2=0: Carotenoid content = 2.262 + (-0.01164)(GREEN)	*(6.1.1)*

For *S. lancea* in Vaal River where L1=L2=0; S1=0; S2=1: Carotenoid content = 2.345 + (-0.01479)(GREEN)	*(6.1.2)*

For *E. camaldulensis* in Welkom where L1=1; L2=0; S1=S2=0: Carotenoid content = 2.035 + (-0.00372)(GREEN)	*(6.1.3)*

For *S. lancea* in Welkom where L1=1; L2=0; S1=0; S2=1: Carotenoid content = 2.118 + (-0.00687)(GREEN)	*(6.1.4)*

For *E. camaldulensis* in West Wits where L1=0; L2=1; S1=S2=0: Carotenoid content = 3.961 + (-0.02724)(GREEN)	*(6.1.5)*

For *E. sideroxylon* in West Wits where L1=0, L2=1; S1=1; S2=0: Carotenoid content = -0.739 + (0.03996)(GREEN)	*(6.1.6)*

The full regression analysis, depicted by Equation (6.1) which includes a summary of the ANOVA and estimate of parameters for the multiple linear regression model, is illustrated in Appendix 3. Site- and species-specific models represented by Equations (6.1.1 to 6.1.5) are all characterised by negative slopes, except for the model derived for *E. sideroxylon* in West Wits mining district.

A standardised residual plot of fitted values of carotenoid content was determined to assess differences between measured and predicted values of carotenoid when using the model represented by Equation (6.1). The residual plot indicated that the model adequately represented the data, and there appeared to be no distinct pattern in the data. The residuals appeared to be normally distributed and independent.

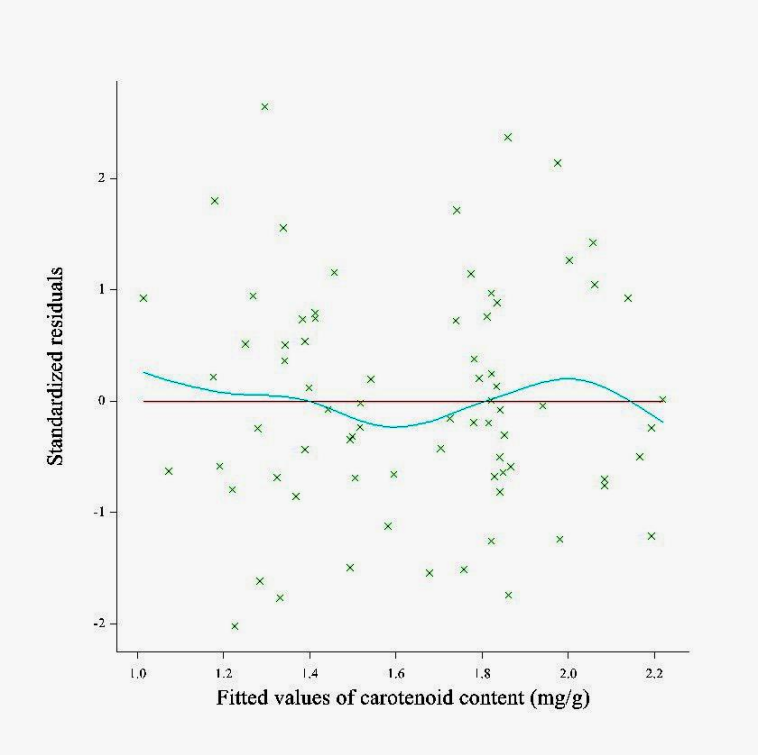


Figure 6.2 Standardised residual plot of fitted values of carotenoid content using the green waveband spectral reflectance model.

6.3.1.4. Validation of the best airborne multispectral data

The carotenoid content and green waveband spectral reflectance model was validated using the method of re-fitting the regression model with a subset of the data being excluded for each validation run. The validation process was repeated three times, with 10 random samples excluded for each run. The subsets of measured and predicted datasets for each validation model are shown in Table 6.3.

Table 6.3 Validation models used to predict carotenoid content using airborne multispectral data.

Mining District	Species	Fitted Models	Green band (X)	Carotenoid measured (Y)	Carotenoid predicted (Y)
Run 1					
Vaal River	*E. camaldulensis*	2.198 + (-0.01017)(GREEN)	80	0.84257	1.3844
			66	1.39785	1.52678
			64	1.45321	1.54712
Vaal River	*S. lancea*	2.21 + (-0.01234)(GREEN)	76	1.00032	1.27216
			61	1.42213	1.45726
			86	0.91211	1.14876
Welkom	*E. camaldulensis*	2.196 + (-0.00622)(GREEN)	54	1.87015	1.86012
			52	1.70476	1.87256
Welkom	*S. lancea*	2.208 + (-0.00839)(GREEN)	43	1.48322	1.84723
			55	1.9384	1.74655
Run 2					
Vaal River	*E. camaldulensis*	2.8 + (-0.01955)(GREEN)	93	1.62998	0.98185
			75	1.53891	1.33375
Vaal River	*S. lancea*	2.836 + (-0.02196)(GREEN)	64	1.43171	1.43056
			90	1.23707	0.8596
Welkom	*E. camaldulensis*	2.144 + (-0.00535)(GREEN)	54	1.87015	1.8551
			49	1.77191	1.88185
Welkom	*S. lancea*	2.18 + (-0.00776)(GREEN)	42	1.64729	1.85408
West Wits	*E. camaldulensis*	3.781 + (-0.02495)(GREEN)	87	1.42534	1.61035
			72	2.35466	1.9846
West Wits	*E. sideroxylon*	-0.949 + (0.04315)(GREEN)	57	1.58582	1.51055
Run 3					
Vaal River	*E. camaldulensis*	2.139 + (-0.01049)(GREEN)	83	2.01695	1.26833
			84	0.84653	1.25784
Vaal River	*S. lancea*	2.099 + (-0.0114)(GREEN)	65	1.58658	1.3580
			63	1.61668	1.3808
			86	0.91211	1.1186
Welkom	*S. lancea*	2.047 + (-0.00499)(GREEN)	43	1.82382	1.83243
			64	1.26194	1.72764
Welkom	*E. camaldulensis*	2.087 + (-0.00408)(GREEN)	49	1.77191	1.88708
West Wits	*E. camaldulensis*	4.512 + (-0.03499)(GREEN)	64	2.22451	2.27264
			99	1.45597	1.04799

T-tests were used to determine if there were differences between measured and predicted values of carotenoid content. The statistical test for Run 1 was significant at the 5% level (Run1 ($t = -2.52$, 9df, $P = 0.033$, $r = 0.866$)), while the t-test for the second and third validation runs were not significant (Run 2 ($t = 0.08$, 3df, $P = 0.944$, $r = 0.952$) and Run 3 ($t = -0.21$, 3df, $P = 0.847$, $r = 0.956$)).

6.3.2 Relationships identified using airborne hyperspectral data

6.3.2.1. Maximal models identified using airborne hyperspectral data

The maximal multiple linear regression models determined between ground-based measurements of plant water stress undertaken in August 2005, and the six vegetation spectral reflectance indices derived from airborne hyperspectral data, were ranked to ascertain which were the better performing models (Table 6.4). Predawn leaf water potential measurements, which have been identified as an important measurement of plant water stress (Chapter 2), was also included in the airborne hyperspectral analysis. Adjusted R^2 values which were ranked for each method, ranged from a maximum of 76.2% for predawn leaf water potential with the normalised difference water index (NDWI) and a minimum of 6.2% for chlorophyll fluorescence with the (695/670) spectral reflectance ratio. Two groups of plant water stress measurements, chlorophyll (a+b) and leaf water content, which did not obtain adjusted R^2 values greater than 50%, were excluded from further analyses.

Table 6.4 Adjusted R^2 values, ranked in descending order, for each maximal model determined between plant water stress measurement (Y) and the spectral reflectance indices(X) derived from airborne hyperspectral data.

Chlorophyll (a + b) (Y)		**Carotenoid (c+x) (Y)**		**Chlorophyll fluorescence (Fv/Fm) (Y**		**Leaf water content (Y)**		**Predawn leaf water potential (Y)**	
Spectral reflectance index (nm) (X)	**Adjusted R^2 for maximal model**	**Spectral reflectance index (nm) (X)**	**Adjusted R^2 for maximal model**	**Spectral reflectance index (nm) (X)**	**Adjusted R^2 for maximal model**	**Spectral reflectance index (nm) (X)**	**Adjusted R^2 for maximal model**	**Spectral reflectance index (nm) (X)**	**Adjusted R^2 for maximal model**
PSRI	45.6	PSRI	56.6	DATT	70.7	NDVI	34.3	NDWI	76.2
GNDVI	43.7	GNDVI	49.5	NDWI	37.9	R695_670	32.6	DATT	74.0
NDWI	39.2	DATT	49.2	GNDVI	30.0	GNDVI	32.4	GNDVI	73.7
DATT	38.2	NDWI	47.2	NDVI	22.8	DATT	32.0	NDVI	64.2
NDVI	38.0	NDVI	44.6	PSRI	8.9	PSRI	31.2	R695_670	48.8
R695_670	37.8	R695_670	40.4	R695_670	6.2	NDWI	30.1	PSRI	39.4

Six spectral reflectance models, which accounted for more than 50% of the variance in the data, were found for the airborne hyperspectral analysis. These models included the measurements of carotenoid content, chlorophyll fluorescence and predawn leaf water potential, with adjusted R^2 values ranging from 56.6 to 76.2%. Potential indices highlighted from this analysis included the PSRI, DATT, NDWI, GNDVI and NDVI.

6.3.2.2. Model refinements using stepwise regression

Stepwise regression models resulted in slight changes to the maximal models which were selected for predawn leaf water potential and the NDWI, DATT and NDVI. The adjusted R^2 values for the six maximal and the stepwise regression models compared in Table 6.5, ranged from 76.8 to 56.6%. There were no differences resulting from the stepwise regression modeling for carotenoid content and chlorophyll fluorescence.

Table 6.5 Comparison of the maximal and the step-wise regression models, derived from the airborne hyperspectral data, with the highest adjusted R^2 values exceeding 50%.

Carotenoid (c+x) (Y)			**Chlorophyll fluorescence (Fv/Fm) (Y)**			**Predawn leaf water potential (Y)**		
Spectral reflectance index (nm) (X)	**Adjusted R^2 (%)**		**Spectral reflectance index (nm) (X)**	**Adjusted R^2 (%)**		**Spectral reflectance index (nm) (X)**	**Adjusted R^2 (%)**	
	Maximal model	**Stepwise model**		**Maximal model**	**Stepwise model**		**Maximal model**	**Stepwise model**
PSRI	56.6	56.6	DATT	70.1	70.1	NDWI	76.2	76.8
						DATT	74.0	74.7
						GNDVI	73.7	73.7
						NDVI	64.2	64.6

The DATT spectral reflectance model performed well when correlated to measurements of both chlorophyll fluorescence and predawn leaf water potential. Similarly, the GNDVI and NDVI index was also well correlated to predawn leaf water potential. The stepwise regression model derived between predawn leaf water potential and the NDWI with the highest adjusted R^2 value of 76.8% was selected as the "best" resulting from the airborne hyperspectral analysis.

6.3.2.3. Selection of the best model derived from airborne hyperspectral data

Predawn leaf water potential was selected as the "best" surrogate measure of plant water stress when using the airborne hyperspectral data. The general model, derived between predawn leaf water potential and the normalised difference water index, represented by Equation (6.2) below, included the interactions of different mining sites and species investigated in this study.

Predawn leaf water potential = 2.43 + (-3.15)(NDWI) + (4.34)(L1) + (-3.10)(L2) + (-1.882)(S1) + (0.740)(S2) + (27.60)(NDWI)(S1) + (-0.641)(NDWI)(S2)	*(6.2)*
($F_{7,65} \approx$ 34.96; $F_{prob} <$ 0.001; R_a^2 = 76.8)	

For *E. camaldulensis* in Vaal River where L1=L2=0 and S1=S2=0: Predawn leaf water potential = 2.43 + (-3.15)(NDWI)	*(6.2.1)*

For *S. lancea* in Vaal River where L1=L2=0 and S1=0; S2=1: Predawn leaf water potential = 3.17 – (3.791)(NDWI)	*(6.2.2)*

For *E. camaldulensis* in Welkom where L1=1; L2=0 and S1=S2=0: Predawn leaf water potential = 6.77 + (-3.15)(NDWI)	*(6.2.3)*

For *S. lancea* in Welkom where L1=1; L2=0; S1=0 and S2=1: Predawn leaf water potential = 7.51 + (-3.791)(NDWI)	*(6.2.4)*

For *E. camaldulensis* in West Wits where L1=0; L2=1 and S1=S2=0: Predawn leaf water potential = -0.67 + (-3.15)(NDWI)	*(6.2.5)*

For *E. sideroxylon* in West Wits where L1=0; L2=1; S1=1 and S2=0: Predawn leaf water potential = -2.552 + (24.45)(NDWI)	*(6.2.6)*

Six site- and species-specific models, represented by Equations (6.2.1 to 6.2.6), were derived using the airborne hyperspectral data. A residual plot of fitted values of predawn leaf water potential (Figure 6.3) was used to evaluate differences between measured and predicted values of predawn leaf water potential, as determined with the model represented by Equation (6.2).

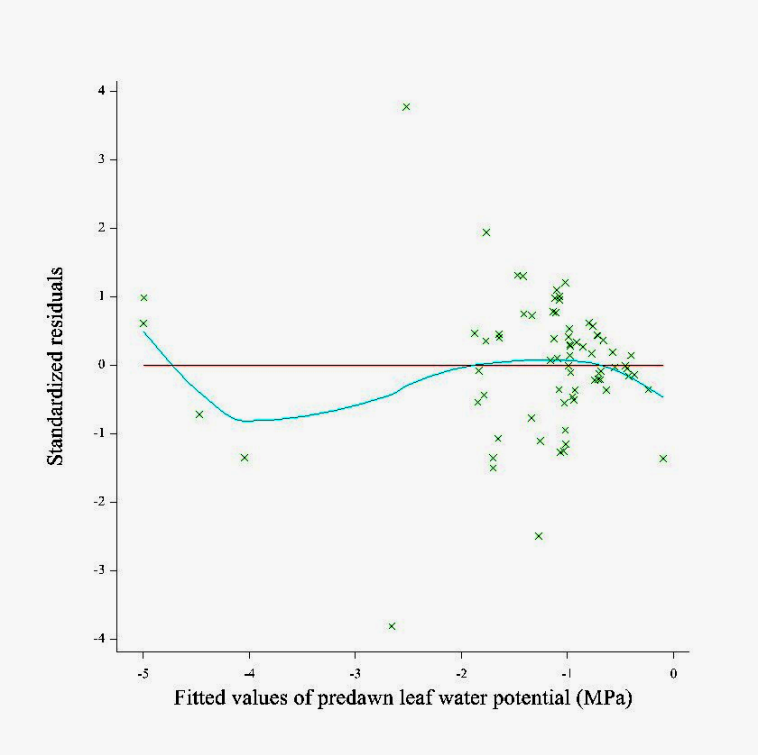


Figure 6.3 Standardised residual plot of fitted values of predawn leaf water potential spectral reflectance model.

The standardised residual plot indicated a cluster of points towards less negative predawn leaf water potentials, representing a typical skewed distribution. A detailed regression analysis is illustrated in Appendix 3.

6.3.2.4. Validation of the best model derived from airborne hyperspectral data

Validation exercises were undertaken to test robustness of the model derived between predawn leaf water potential and the normalised difference water index. Table 6.6 includes a listing of the three subsets of data used for each validation run, comprising of district and species for which the models were valid with corresponding measurements and predictions of predawn leaf water potential and NDWI values.

Table 6.6 Validation models used to predict predawn leaf water potential, using airborne hyperspectral data.

Mining District	Species	Fitted Models	NDWI (X)	Predawn leaf water potential measured (Y)	Predawn leaf water potential predicted (Y)
Run 1					
Vaal River	*E. camaldulensis*	3.02+(-3.66)(NDWI)	1.111	-1.698	-1.045
			1.083	-0.832	-0.943
			1.115	-0.606	-1.059
Vaal River	*S. lancea*	3.81+(-4.339)(NDWI)	1.211	-0.788	-1.444
			1.088	-1.184	-0.912
			1.106	-1.590	-0.987
Welkom	*E. camaldulensis*	-2.02+(-3.66)(NDWI)	-0.044	-0.818	-1.857
			-0.037	-2.000	-1.884
Welkom	*S. lancea*	-1.23+(-4.339)(NDWI)	-0.133	-0.488	-0.652
West Wits	*E. camaldulensis*	-0.67+(-3.66)(NDWI)	-0.013	-0.816	-0.624
Run 2					
Vaal River	*E. camaldulensis*	2.55+(-3.31)(NDWI)	1.085	-0.722	-1.040
			1.127	-0.632	-1.180
Vaal River	*S. lancea*	3.423+(-3.982)(NDWI)	1.092	-1.020	-0.925
			1.106	-1.490	-0.982
Welkom	*E. camaldulensis*	-2.06+(-3.31)(NDWI)	-0.044	-0.818	-1.913
			-0.083	-1.450	-1.785
West Wits	*E. camaldulensis*	-0.71+(-3.31)(NDWI)	0.058	-0.730	-0.901
			0.014	-0.502	-0.755
			-0.076	-0.460	-0.460
West Wits	*E. sideroxylon*	-2.353+(24.51)(NDWI)	-0.004	-4.514	-2.454
Run 3					
Vaal River	*E. camaldulensis*	2.71+(-3.44)(NDWI)	1.096	-0.424	-1.060
			1.082	-0.838	-1.012
Vaal River	*S. lancea*	3.455+(-4.051)(NDWI)	1.225	-0.842	-1.508
			1.127	-1.050	-1.110
			1.106	-1.590	-1.024
Welkom	*S. lancea*	-1.195+(-4.051)(NDWI)	-0.117	-0.512	-0.721
			-0.111	-0.850	-0.745
Welkom	*E. camaldulensis*	-1.94+(-3.44)(NDWI)	-0.083	-1.450	-1.654
West Wits	*E. camaldulensis*	-0.68+(-3.44)(NDWI)	-0.031	-0.482	-0.572
			-0.096	-0.438	-0.349

T-tests for paired samples were used to determine if there were differences between measured and predicted values of predawn leaf water potential. The statistical tests for all three validation runs confirmed that there were no significant differences between measured and predicted predawn leaf water potential (Run 1 ($t = 0.34$, 9df, $P = 0.739$, $r = 0.369$); Run 2 ($t = 0.02$, 9df, $P = 0.983$, $r = 0.763$) and Run 3 ($t = 1.13$, 9df, $P = 0.288$, $r = 0.616$)).

Pearson correlation coefficients for Run 2 and Run 3 indicated a reasonably good correlation between measured and predicted values of predawn leaf water potential($r > 0.6$).

6.4 DISCUSSION

Vegetation spectral reflectance indices, which were previously tested using hand-held spectral reflectance measurements (Chapter 4) and satellite medium and high resolution remote sensing data (Chapter 5), were successfully applied to the airborne multispectral and hyperspectral remote sensing data. Several significant spectral relationships ($Fprob < 0.001$) were identified between carotenoid content, chlorophyll fluorescence and predawn leaf water potential and various vegetation indices derived from airborne multispectral and hyperspectral remote sensing data. Some common trends identified when using the airborne multispectral and hyperspectral remote sensing data to detect spatial patterns of plant water stress included:

- Vegetation indices designed to capture changes in plant pigment content performed well when applied to both the multispectral and hyperspectral remote sensing data.
- The DATT (1999) spectral reflectance model (850 – 710)/(850 – 680) is considered to be a fairly robust index which was correlated to ground based measurements of chlorophyll fluorescence and predawn leaf water potential.
- Predawn leaf water potential measurements were found to be strongly correlated to spectral indices derived from the visible, near-infrared and short-wave infrared region of the airborne hyperspectral data.

The green and blue individual spectral wavebands extracted from the visible region of the airborne multispectral data, and which are sensitive to changes in plant pigment content were correlated to total carotenoid pigment content. The spectral reflectance model derived between carotenoid content and green spectral waveband resulted in six site- and species-specific spectral models. These relationships were in accordance with several studies reported on the sensitivities of plant pigments within the visible and infrared region of the

spectrum (Gaussman, 1977; Lichtenthaler, 1987; Curran *et al*., (1995); Gitelson and Merzylak, 1996; Blackburn, 1999; Datt, 1999).

Several more useful relationships were identified between vegetation indices derived from the airborne hyperspectral data and ground measurements of plant water stress, as compared to the multispectral analysis discussed in section 6.3.1.3. Six potential spectral reflectance models were highlighted from the airborne hyperspectral analysis for carotenoid content, chlorophyll fluorescence and predawn leaf water potential. Spectral reflectance indices designed to capture changes in plant pigment content (PSRI, GNDVI, NDVI, DATT) and changes in plant water content (NDWI) were identified as useful spectral indices resulting from the airborne hyperspectral analysis.

It may also be concluded, upon evaluation of the multiple linear regression models, that the airborne hyperspectral data produced several more regression models with a higher adjusted R^2 values (R_a^2 range 6.2 - 76.2%) when compared to the airborne multispectral data (R_a^2 range 6 - 50.1). These differences could be attributed to the hyperspectral sensor acquiring more detailed information on the plant spectral properties at a higher spatial and spectral resolution. Furthermore, it can also be concluded that the four central wavelengths (465.88; 568.42; 664.67 and 870.53 nm) acquired from the visible and near-red region of the spectrum using the multispectral sensor displayed a lower spectral relationship to plant water stress.

6.5 CONCLUSIONS

From this study it can be concluded that airborne multispectral and hyperspectral remote sensing technologies can be used to detect plant water stress for the three species *E. camaldulensis, E. sideroxylon* and *S. lancea*, within the Welkom, Vaal River and West Wits mining districts. Preference is given to hyperspectral data sources based on the many stronger multiple linear relationships which were derived in this study, and resulted from the narrow bandwidth characteristics of the hyperspectral imagery. In general, there will always be a trade-off between multispectral and hyperspectral systems between spectral and spatial

resolutions. High spatial and spectral resolution imagery is more expensive to acquire and process than broad-scale low resolution imagery. While it may be easier to map plant water stress more accurately from airborne imagery, certain applications may warrant the use of satellite data due to the higher relative costs associated with airborne systems. Furthermore, technologies must be repeatable and cost effective for operational use.

CHAPTER 7. CORRELATION OF PLANT STRESS PATTERNS TO SITE CHARACTERISTICS IN THREE GOLD MINING DISTRICTS IN CENTRAL SOUTH AFRICA

ABSTRACT

The objective of this study was to correlate spatial patterns of trees which were not experiencing winter-time water stress (unstressed areas) to site characteristics such as geology, soils, groundwater chloride and sulphate, total dissolved solids, electrical conductivity and groundwater water level within the Welkom, Vaal River and West Wits mining districts.

The spectral reflectance model derived between predawn leaf water potential and the green normalised difference vegetation index using broad-band multispectral Proba Chris satellite data was used to map spatial patterns of unstressed trees across three mining districts. Very high resolution (75 cm) multispectral airborne images acquired by LRI in 2005 were used to demarcate and classify vegetation. Four commonly used statistical classifying techniques were used in the classification process which included maximum likelihood, minimum distance, Mahalanobis distance and parallelepiped. The maximum likelihood supervised classification technique achieved the highest kappa coefficients and overall accuracies, and was therefore selected as the most appropriate method for classifying vegetation and different landcovers.

Spatial maps of average soil depth and average percentage clay in the topsoil and interpolated surfaces of groundwater chloride and sulphate concentrations, total dissolved solids, electrical conductivity, pH and groundwater table levels were created using the kriging geostatistical interpolation technique. Spatial interpolation is widely used for creating continuous data from discrete or point data. Spatial interpolation has also been well

accepted amongst GIS developers and specialists, with the inclusion of interpolation techniques in well renowned GIS software packages such as ESRI Arc Info and ArcGIS packages. In this study ordinary kriging which is commonly used in GIS studies was applied. The default spherical model with a variable radius was selected due to the sparse and irregular location of the observation points. Random sample analyses between stressed and unstressed trees were extracted in order to determine whether site characteristics were significantly different (using t-tests).

The interpolated site characteristic surfaces which were significantly different from stressed areas were spatially linked to trees which were not experiencing winter-time plant water stress, in order to recommend and prioritise sites for the establishment of future block plantings. Groundwater table levels were not significantly different between stressed and unstressed areas at all sites. This implies that unstressed sites which have been identified in each mining district do have access to groundwater during the drier winter season, and other factors could be contributing to plant stress As has been reported at the beginning of the thesis, this research project was heavily dependent on trees growing singly, in rows or in small groups, which experienced lower levels of competition from neighbouring plants. Therefore, these trees would have had a greater opportunity for extending root systems laterally, and the link between dry season tree water stress and groundwater accessibility could be have been influenced.

Earlier studies have reported on the surrounding lands and water systems of the Welkom, Vaal River and West Wits mining district to show increasing salinity levels over the years (Roos and Pieterse, 1995; Viver *et al*., 2001; Naicker *et al*., 2003; Winde *et al*., 2004a,b,c). An evaluation of the site characteristic data indicates that salinity levels possibly do affect whether trees are stressed or unstressed, as these characteristics such as groundwater chloride and sulphate concentrations, total dissolved solids and electrical conductivity displayed significant differences between stressed and unstressed areas in the three mining districts.

Larger areas of unstressed sites were identified and are recommended for future plantings of trees in the West Wits mining region compared to smaller areas recommended in the Welkom and Vaal River districts. The resistivity surveys clearly highlight areas of groundwater saturation, shallow groundwater tables in some areas, and possibly higher salinity levels. In such areas trees could thrive, access contaminated water seeping from TSFs and reduce lateral flows into groundwater river systems. Also, the high salinity values are indicative of the contaminant flows from the TSFs, where again trees could possibly sequester contaminants in the area and reduce lateral pollution into surrounding areas over time.

Keywords : geostatistical interpolation, site characteristics, spectral reflectance model, supervised classification, unstressed trees

7.1 INTRODUCTION

In previous chapters, spectral plant water stress relationships were investigated using various sources of remote sensing data *viz.* leaf-level spectroscopy (Chapter 4), medium to high resolution satellite earth observation data (Chapter 5), and multispectral and hyperspectral airborne remote sensing imagery (Chapter 6). From these investigations it is now possible to distinguish sites at which trees show winter-time water stress (stressed areas), from those where the trees show no such water stress(unstressed areas) within each mining district. Furthermore, within each mining district, the site characteristics such as geology, soils, salinity (groundwater chloride and sulphate, total dissolved solids, electrical conductivity) and groundwater table level (Weiersbye, 2008), which are important in distinguishing unstressed areas and which are significantly different from stressed areas, were investigated. In this chapter the methodology for **mapping spatial patterns of unstressed areas** and their site characteristics are recommended for future plantings in each mining district, to assist in containing and reducing contaminated seepage water from the TSFs.

7.2 MATERIALS AND METHODS

In this chapter **spatial patterns of unstressed areas** and their site characteristics which could be recommended for future block plantings were identified. High resolution mulitispectral remote sensing imagery was used to classify vegetation per tree species investigated in each mining district i.e. Vaal River (*E. camaldulensis*; *S. lancea*), Welkom (*E. camaldulensis*; *S. lancea*) and West Wits (*E. camaldulensis*; *E. sideroxylon*). These high resolution classified vegetation maps were then used to clip unstressed tree species modelled using the spectral model reported on in section 5.3.2.3 i.e. PLWP and the green normalised difference vegetation index (GNDVI). To obtain a spatial distribution of site characteristics within each mining district, a geostatistical interpolation technique was used to create raster layers of groundwater chloride and sulphate concentrations, total dissolved solids, electrical conductivity, pH, groundwater table levels, soils and geology for each sampling area. The spatial distribution of **unstressed trees** was then correlated to particular site characteristics that may be recognised and used to prioritise sites for the establishment of future block plantings.

7.2.1 Vegetation classification

Very high resolution (75cm) multispectral airborne images acquired by LRI in July 2005 were used to demarcate and classify vegetation across the three mining districts. These multispectral airborne images were selected to classify the vegetation due to their very high spatial resolution, allowing for spatial discrimination between different spectral features and objects on the ground. The near-infrared band was specifically used to highlight trees and other landcover classes in these districts. Regions of interest (ROIs) which were ground-truth in the field, were created for each tree species investigated in this study per mining district i.e. Vaal River (*E. camaldulensis*; *S. lancea*), Welkom (*E. camaldulensis*; *S. lancea*) and West Wits (*E. camaldulensis*; *E. sideroxylon*) and the three common landcover classes characteristic of the mining areas, namely tailing storage facilities, grassland/open woodlands and rivers. These ROIs spatially represented the dominant spectral features of each mining district.

Regions of interest may be defined within the context of remote sensing as areas of an image which contain pixels of the same spectral characteristics which represent the same landcover or vegetation type. Regions of interest were selected using ground control points and high resolution aerial photos, which were verified during field surveys undertaken in 2005. Several studies on vegetation classification using different sources of remote sensing data have shown that the performance of statistical classifiers can vary with vegetation types (Kruce *et al*., 1993; Lillesand and Kiefer, 1999; Castro-Esau, 2004; Govender *et al*., 2008). Due to this variability, four commonly used statistical classifying techniques were used in the classification process. These techniques included maximum likelihood, minimum distance, Mahalanobis distance and parallelepiped (Foody, 2004; Foody and Mathur, 2006).

In remote sensing applications the term classification accuracy is used to express the degree to which a classified remote sensing image represents reality (Foody, 2004). Accuracy assessments are important not only for evaluating the suitability of different classification techniques but also for providing an indication of the quality of maps produced (Foody, 2004). Thomlinson *et al*. (1999) suggested an overall accuracy of greater than 85% as an indicator of superior classification. A confusion or error matrix forms the building blocks of an accuracy assessment (Congalton and Green, 1993; Congalton, 1994; Foody, 2004). The confusion or error matrix can be described as a square array of numbers set out in rows and columns which express the number of sampling units (pixels) assigned to a particular class, relative to the actual class verified on the ground (Congalton and Green, 1993).

Accuracy assessments were used to determine which statistical classifier produced the best classification results. Three measures of a classification accuracy analysis *viz.* kappa coefficient of agreement, overall accuracy and user accuracy, were used in this study. The kappa coefficient of agreement is a statistical measure used to describe the accuracy of spatial data sets (Foody, 2004; Congalton and Mead, 1983). Landis and Koch (1977) categorised the possible ranges of the kappa coefficient of agreement into three groups, where a value greater than 0.8 represents strong agreement; a value between 0.8 and 0.4 represents moderate agreement and a value below 0.4 represents poor agreement. The overall

accuracy is the number of correctly allocated classes, which is most commonly used in vegetation studies, as a measure of how accurately a remote sensing image has been classified. The kappa coefficient of agreement and the overall accuracy (>85%) reported by Foody and Mathur (2006) which are two commonly used measures of a classification accuracy analysis, were used to select the most suitable statistical classifier for vegetation classification in this study. The user's accuracy indicates the probability with which a pixel classified on the map represents the same category or class on the ground. Therefore, the user's accuracy was used to evaluate how well an individual vegetation class was classified for a specific statistical classifier method.

The results of each supervised classification performed for each mining district are shown in Tables7.1 to 7.3. The maximum likelihood supervised classification technique achieved the highest kappa coefficients and overall accuracies, and was therefore selected as the most appropriate method for classifying vegetation and different landcovers across all three mining districts.

Table 7.1 Accuracy assessments of the supervised classifications for the Vaal River mining district.

Supervised classification methods and % Ground truthing pixels	**User Accuracy (%)**	**Kappa coefficient**	**Overall accuracy (%)**
Mahalanobis distance		0.90	94.02
Searsia lancea- (1.03 %)	48.96		
Eucalyptus camaldulensis- (0.69%)	62.19		
Grassland/open woodlands- (36.51%)	87.21		
Tailing storage facility- (41.02%)	100		
River- (20.76)	100		
Maximum likelihood		0.99	99.35
Searsia lancea	52.61		
Eucalyptus camaldulensis	81.80		
Grassland/open woodlands	100		
Tailing storage facility	99.93		
River	100		
Minimum distance		0.93	95.97
Searsia lancea	50.31		
Eucalyptus camaldulensis	67.41		
Grassland/open woodlands	91.56		
Tailing storage facility	100		
River	99.65		
Parallelepiped		0.45	56.84

Searsia lancea	1.69		
Eucalyptus camaldulensis	2.46		
Grassland/open woodlands	0		
Tailing storage facility	100		
River	72.52		

Table 7.2 Accuracy assessments of the supervised classifications for the Welkom mining district.

Supervised classification methods and % Ground truthing pixels	**User Accuracy (%)**	**Kappa coefficient**	**Overall accuracy (%)**
Mahalanobis distance		0.91	94.26
Searsia lancea- (1.05%)	20.83		
Eucalyptus camaldulensis- (1.3%)	37.52		
Ploughed lands/veld - (30.6%)	99.92		
Tailing storage facility- (45.2%)	99.96		
Pan (dry)- (21.85%)	99.39		
Maximum likelihood		0.96	97.55
Searsia lancea	24.91		
Eucalyptus camaldulensis	88.13		
Ploughed lands/veld	100		
Tailing storage facility	99.99		
Pan (dry)	99.88		
Minimum distance		0.90	93.46
Searsia lancea	22.18		
Eucalyptus camaldulensis	62.71		
Ploughed lands/veld	91.39		
Tailing storage facility	99.96		
Pan (dry)	99.95		
Parallelepiped		0.47	55.96
Searsia lancea	2.13		
Eucalyptus camaldulensis	0		
Ploughed lands/veld	0		
Tailing storage facility	100		
Pan(dry)	95.76		

Table 7.3 Accuracy assessments of the supervised classifications for the West Wits mining district.

Supervised classification methods and % Ground truthing pixels	**User Accuracy (%)**	**Kappa coefficient**	**Overall accuracy (%)**
Mahalanobis distance		0.86	89.97
Eucalyptus camaldulensis - (4.42%)	1.15		
Eucalytpus sideroxylon- (24.47%)	99.02		
Grassland/open woodlands- (29.87%)	91.59		
Tailing storage facility- (21.10%)	100		
River- (20.14)	99.83		
Maximum likelihood		0.94	95.58
Eucalyptus camaldulensis	1.95		

Supervised classification methods and % Ground truthing pixels	User Accuracy (%)	Kappa coefficient	Overall accuracy (%)
Eucalytpus sideroxylon	99.81		
Grassland/open woodlands	99.99		
Tailing storage facility	99.87		
River	100		
Minimum distance		0.90	93.12
Eucalyptus camaldulensis	1.45		
Eucalytpus sideroxylon	98.76		
Grassland/open woodlands	99.66		
Tailing storage facility	100		
River	97.64		
Parallelepiped		0.49	56.35
Eucalyptus camaldulensis	0.29		
Eucalytpus sideroxylon	0		
Grassland/open woodlands	100		
Tailing storage facility	99.98		
River	100		

In Table 7.3, extremely low user accuracies were determined for *E. camaldulensis* when using the Mahalanobis distance, maximum likelihood and minimum distance statistical classifiers, while parallelepiped resulted in low user accuracies for both *E. camaldulensis* and *E. sideroxylon*. Only one *Eucalyptus* species could be mapped more accurately than the other as shown with the maximum likelihood and minimum distance methods, while both *Eucalyptus* species were not classified well when applying the parallelepiped method. These results imply that the spectral characteristics of the two *Eucalyptus* species, *E. camaldulensis* and *E. sideroxylon*, were similar in this remote sensing data set and therefore separation during the vegetation classification process was difficult.

The maximum likelihood supervised classification technique was then used to produce high resolution vegetation maps for each tree species investigated in each mining district i.e. Vaal River (*E. camaldulensis*; *S. lancea*), Welkom (*E. camaldulensis*; *S. lancea*) and West Wits (*E. camaldulensis*; *E. sideroxylon*). These high resolution classified vegetation maps were then used to clip unstressed tree species modelled using the spectral model reported on in section 5.3.2.3 i.e. PLWP and the green normalised difference vegetation index (GNDVI).

7.2.2 Mapping spatial patterns of unstressed trees

The principal aim of this study was to correlate the spatial distribution of **unstressed trees** to particular site characteristics that may be recognised and used to prioritise sites for the establishment of future block plantings. Therefore the geographic information system workflow processing focussed on producing spatial maps of **unstressed trees** which are illustrated in subsequent maps in this chapter. It is noted that areas not categorised as unstressed are considered stressed by the spectral reflectance model.

Several vegetation spectral reflectance models were investigated using different types of remote sensing data, as shown in Chapters 4, 5 and 6. A summary of the "best" models which were selected from each study is shown in Table 7.4.

Table 7.4 Best performing spectral reflectance models derived from leaf, satellite and airborne remote sensing data.

Type of Remote Sensing Data	Surrogate Measurement of Plant Water Stress	Spectral Reflectance Ratio or Index	Reference to Model(s)	Adjusted R^2 (%)
ASD spectrometer: leaf-level spectral reflectance signatures	Chlorophyll b	DATT index	Section 4.3.2.3	69.3
Satellite: multispectral imagery	Predawn leaf water potential	Green normalised difference vegetation index (GNDVI)	Section 5.3.2.3	84.8
Satellite: hyperspectral imagery	Predawn leaf water potential	Water band index (WBI)	Section 5.3.3.3	90.5*
Airborne: multispectral imagery	Carotenoid content	GREEN	Section 6.3.1.3	50.1
Airborne: hyperspectral imagery	Predawn leaf water potential	Normalised difference vegetation index (NDVI)	Section 6.3.2.3	76.8

**model derived for the West Wits mining district*

The adjusted R^2 values were used as a criterion for selecting a common model for mapping spatial patterns of plant water stress across all three mining districts. The highest adjusted R^2 value (90.5%) was obtained for the model derived between predawn leaf water potential

(PLWP) and the water band index (WBI) when using hyperspectral satellite imagery. However, this model was derived only for the West Wits mining district and, as this study has clearly illustrated, that reflectance models are site- and species-specific, this model should not be applied across the Vaal River and Welkom mining districts.

The model with the next highest adjusted R^2 (84.8%) was derived between PLWP and the green normalised difference vegetation index (GNDVI) using broad-band multispectral Proba Chris satellite data. Six site- and species-specific models reported on in section 5.3.2.3 resulted from this study, and were selected to map spatial patterns of **unstressed trees**. High resolution classified vegetation maps were used to clip unstressed trees per tree species investigated in each mining district during the dry winter season, as shown in Figure 7.1 to 8.6.Tree plantations are rare in these mining districts; hence vegetation in the landscape is very patchy. Sample sites used in the derivation of the site- and species-specific models reported in section 5.3.2.3 were selected from stands, single trees or rows of trees and small-plot species trials growing in each mining district as illustrated by Figure 2.4(Chapter 2). Therefore the spatial patterns of unstressed trees which are illustrated in Figures 7.1 to 7.6 are very patchy. Is noted though that areas not categorised as unstressed are considered stressed by the PLWP GNDVI model.

It is important to remember that even though the PLWP GNDVI was selected as the most appropriate model to identify where trees would most likely not experience stress during the dry season (R_a^2 of 84.8%) the time of year upon which these analysis are based must be considered in the interpretation of the results. Plant water stress measurements undertaken during July 2005 and August 2005 were used for ground-truthing the Proba Chris images. As discussed previously in Chapter 5, although a total of four Proba Chris images were planned for acquisition for the Welkom, Vaal River and West Wits mining districts during July and August 2005, only the Vaal River images were acquired during the dry winter season, due to an increased demand for Proba Chris data from various countries participating in the Tiger initiative. Proba Chris images for Welkom were obtained during early October 2005, and for West Wits during late November 2005. These images were correlated to predawn leaf water potential measurements undertaken during July and August 2005. However, a strong

correlation between remote sensing satellite imagery and the ground truthing measurements were still found (R_a^2 of 84.8%).

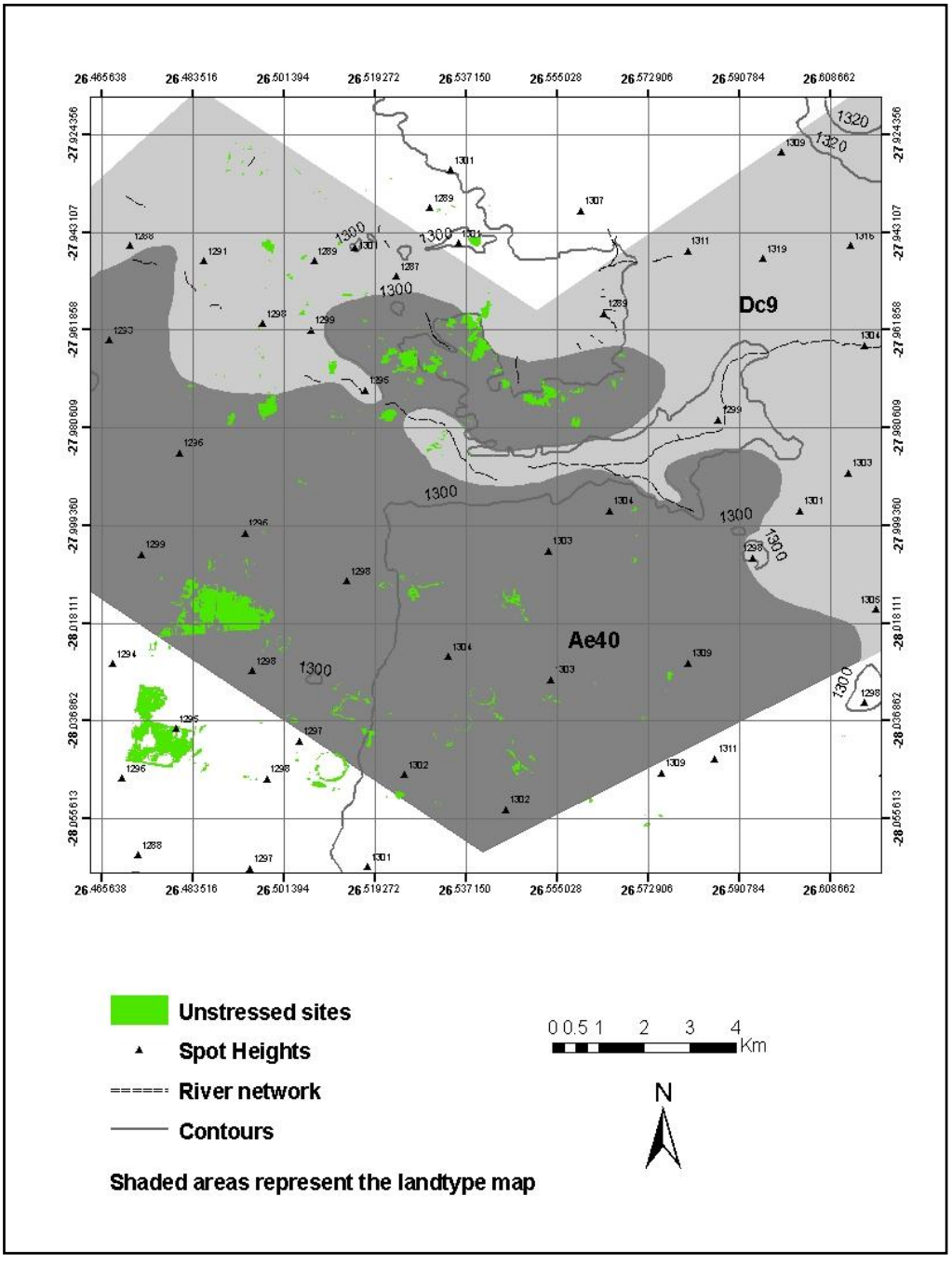


Figure 7.1 *Spatial patterns of unstressed Eucalyptus camaldulensis sites mapped in the Welkom mining district using the Predawn leaf water potential and the Green normalized difference vegetation index derived from Proba Chris satellite imagery.*

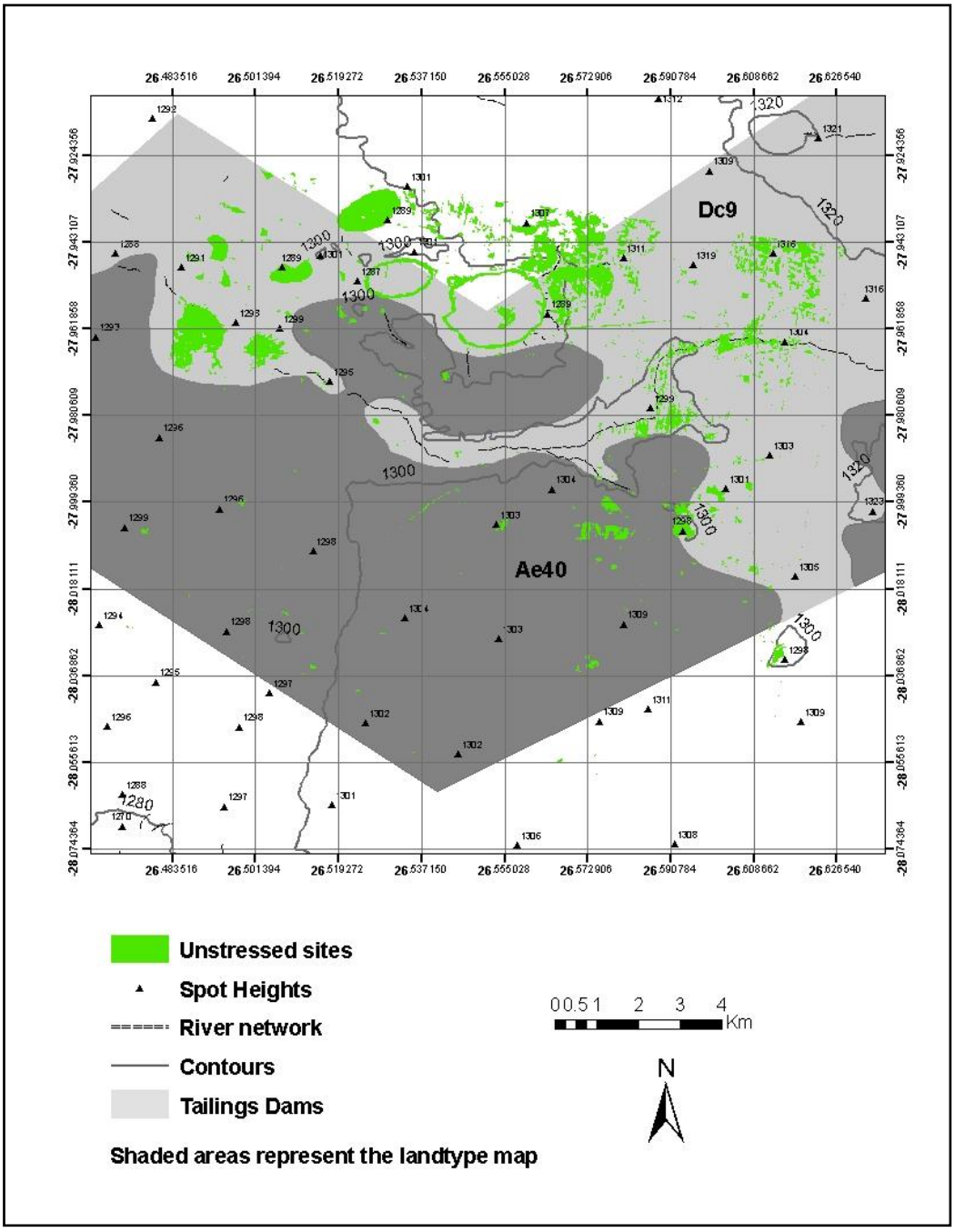


Figure 7.2 *Spatial patterns of unstressed Searsia lancea sites mapped in the Welkom mining district using the Predawn leaf water potential and the Green normalized difference vegetation index derived from Proba Chris satellite imagery.*

Figure 7.1 and 7.2 highlight the spatial patterns of unstressed trees mapped in the Welkom mining district using the predawn leaf water potential and the green normalized difference

vegetation index. It is noted that these patterns were determined using Proba Chris images obtained during early October 2005, which could have an effect on the spatial patterns required for the dry winter season when trees may not be accessing groundwater. The area is also fairly flat with altitudinal difference of approximately 2.7%. The river network shown in the map is fairly disconnected, which is common for flat areas, as the digital elevation model which is normally used to derive river networks would have sinks, making it difficult to map river flow paths. Unstressed trees mapped do not follow any specific river network. The *E. camaldulensis* trees are dominant on the Ae40 land type. Areas where irrigation centre pivots exist were mapped, indicating that the spectral model could be sensitive to vegetation and water present in these areas. *S. lancea* sites were mapped predominantly on the Dc9 land type. The *S. lancea* also highlighted areas around the pans, which could once again be an indication of the model being sensitive to higher water content in the soil.

Spatial patterns of unstressed *E. camaldulensis* and *S. lancea* sites were mapped in the Vaal River mining district using the predawn leaf water potential and the green normalized difference vegetation index derived. The spatial patterns of unstressed trees were mapped for Vaal River using Proba Chris satellite imagery which was acquired during the dry winter season. However, as is shown is Figure 7.3 and 7.4 unstressed trees are sparse and are dominant in the north west and south east areas of the map. It is surprising that spatial patterns of unstressed trees were not identified downstream of the TSFs. Unstressed trees mapped in the north west areas of the mining district are located along the river network. However, it is interesting to note that there are not many unstressed trees mapped along the main Vaal River channel, except for a few *S. lancea* sites. Figure 7.3 and 7.4 imply that there are very few sites where trees would access water during the drier winter months. Alternatively these results could be affected by the lack of *E. camaldulensis* and *S. lancea* sites currently growing in the Vaal River mining district. However, if this assumption were accepted then the same would apply to the Welkom and West Wits mining district.

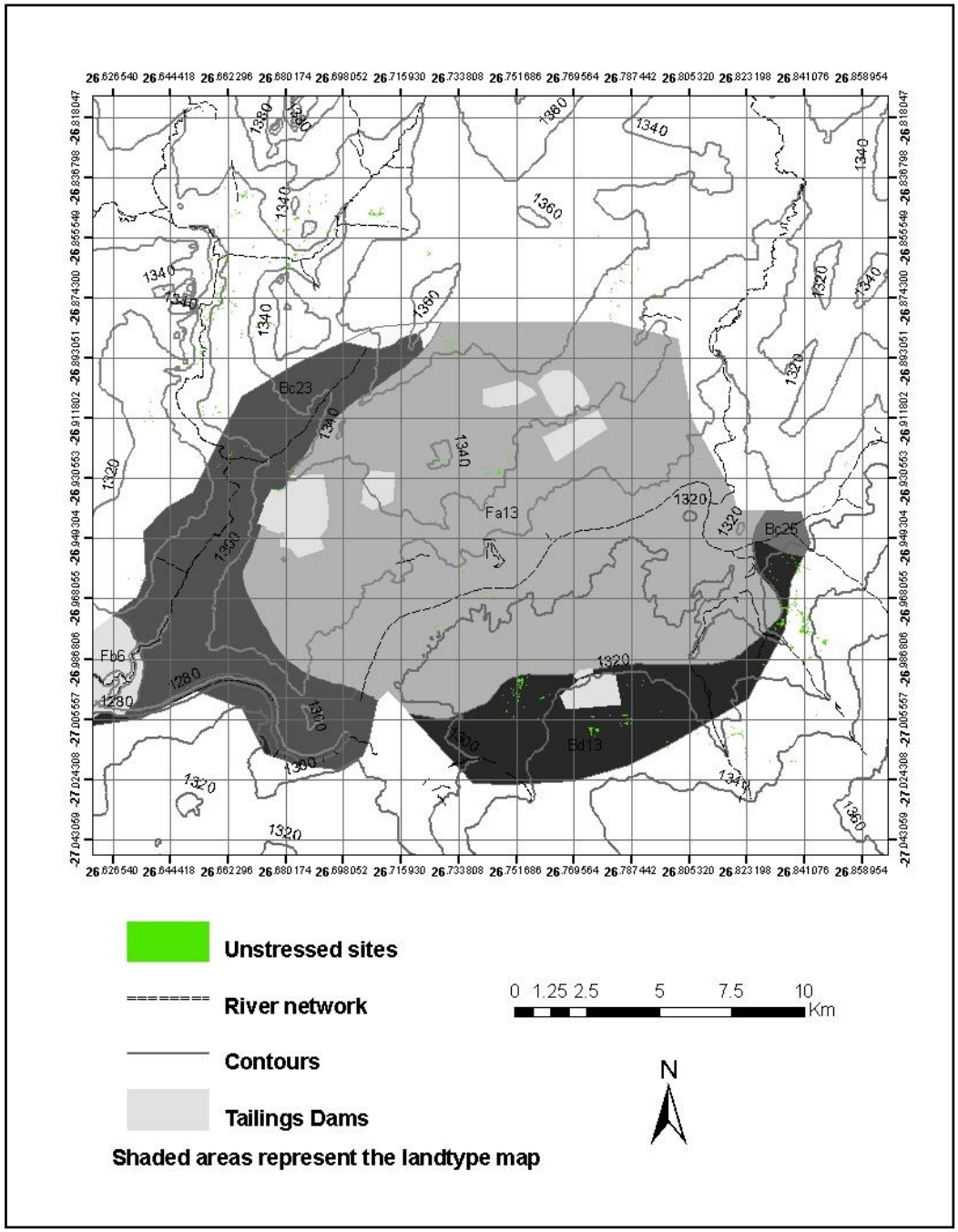


Figure 7.3 *Spatial patterns of unstressed <u>Eucalyptus camaldulensis</u> sites mapped in the Vaal River mining district using the Predawn leaf water potential and the Green normalized difference vegetation index derived from Proba Chris satellite imagery.*

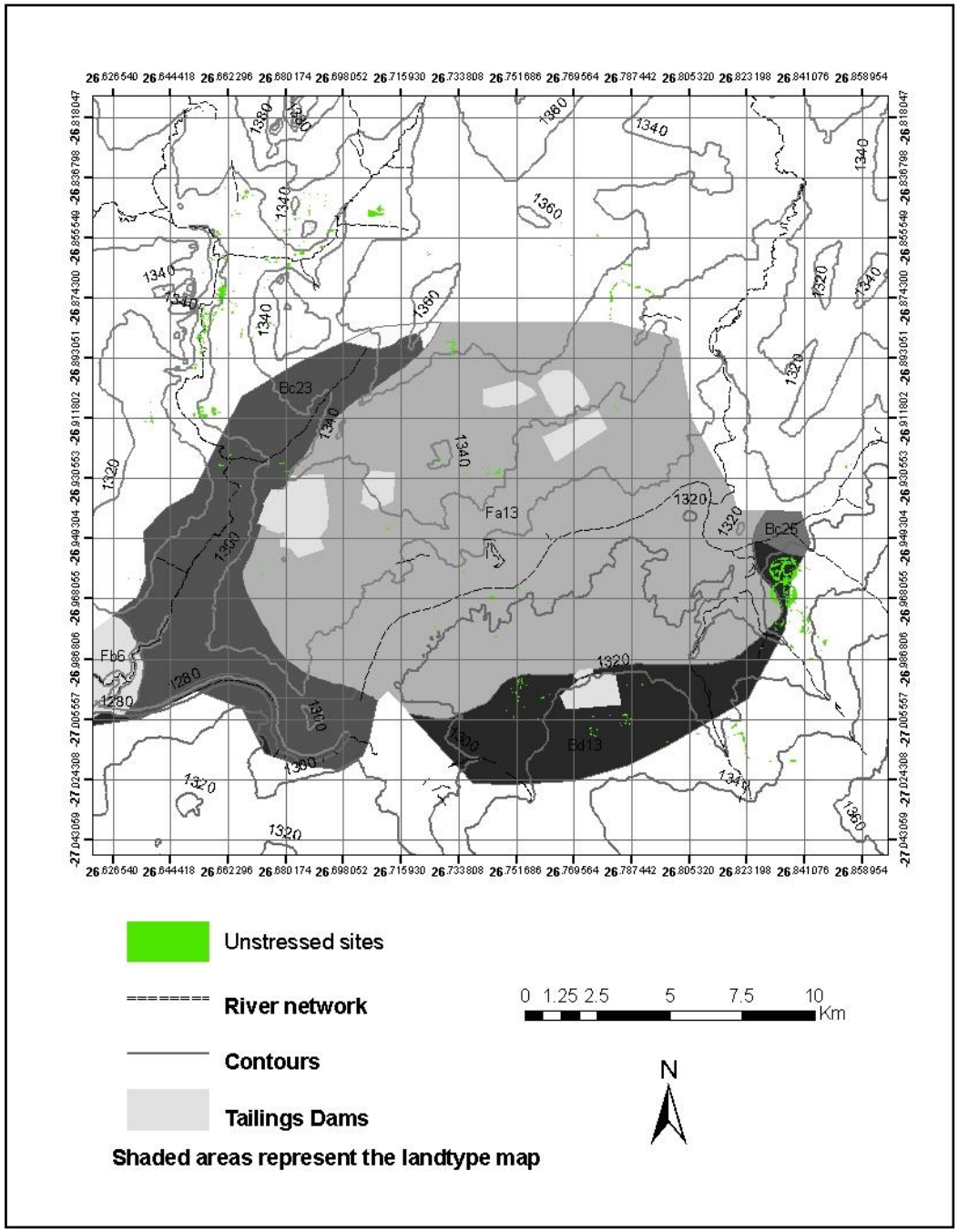


Figure 7.4 *Spatial patterns of unstressed <u>Searsia lancea</u> sites mapped in the Vaal River mining district using the Predawn leaf water potential and the Green normalized difference vegetation index derived from Proba Chris satellite imagery.*

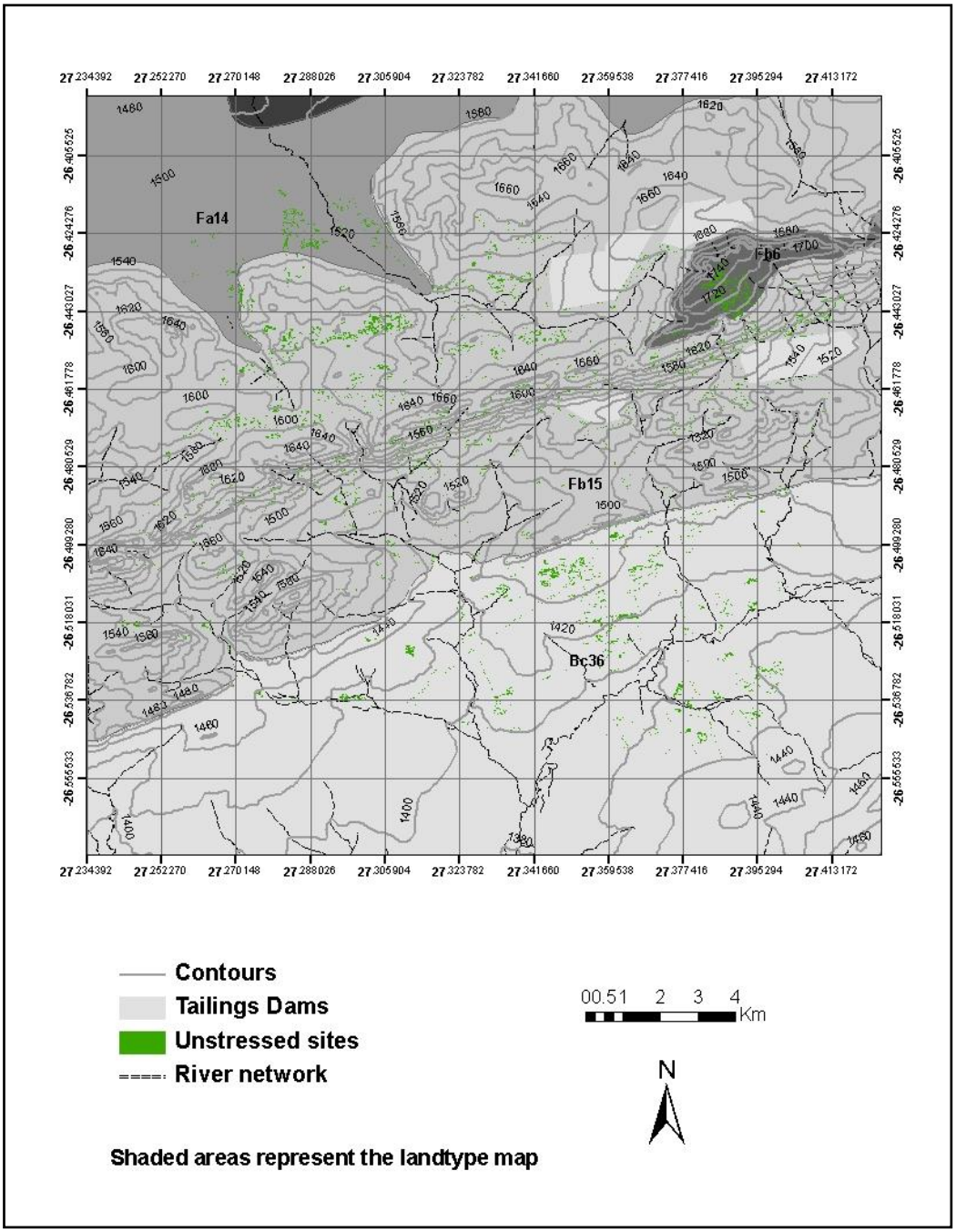


Figure 7.5 *Spatial patterns of unstressed Eucalyptus camaldulensis sites mapped in the West Wits mining district using the Predawn leaf water potential and the Green normalized difference vegetation index derived from Proba Chris satellite imagery.*

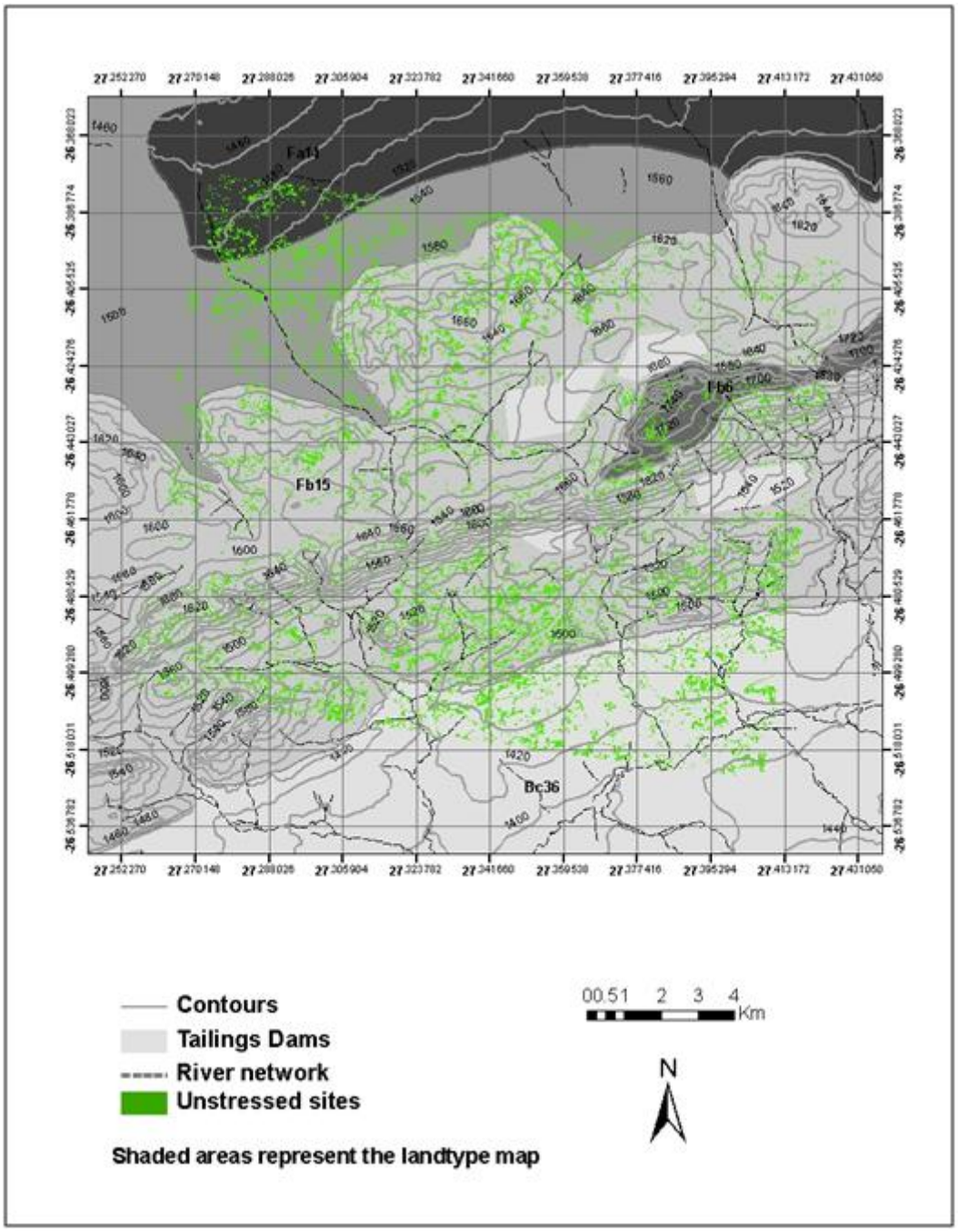


Figure 7.6 *Spatial patterns of unstressed Eucalyptus sideroxylon sites mapped in the West Wits mining district using the Predawn leaf water potential and the Green normalized difference vegetation index derived from Proba Chris satellite imagery.*

Figure 7.5 and 7.6 display the spatial patterns of *E. camaldulensis* and *E. sideroxylon* sites mapped in the West Wits mining district respectively. A high mean annual rainfall is characteristic of the region when compared to the Welkom and Vaal River mining districts.

Furthermore, the area has a denser river network as is clearly shown in Figures 7.5 and 7.6. Unstressed sites are also identified along the riparian zones. Unstressed trees were identified across the West Wits mining district and also around the TSFs. It is also noted a maximum number of unstressed sites was mapped in this district which also coincides with the *Eucalyptus* plantations currently growing in this area.

7.2.3 Creation of spatial layers of site characteristic data

Existing site characteristic datasets were obtained for each mining district for periods which overlapped with the remote sensing data analyses, according to the acquisition periods detailed in section 5.2.1. Measurements of groundwater chloride and sulphate concentrations, total dissolved solids, electrical conductivity, pH, groundwater table levels, soils and geology data, which were undertaken by Africa Geo-Environmental Services (AGES), School of Animal Plant and Environmental Sciences (APES) at the University of the Witwatersrand and Anglogold Ashanti, were sourced from Weiersbye (2008). Additional soils data were obtained from an Agricultural Research Council land-type database developed for South Africa (ISCW, 1993). Land-type data for the three mining districts included the average soil depth, depth classes per land-type, average topsoil clay percentage and the clay content class per land-type for the soil profile (ISCW, 1993). According to the ISCW, soil surveys used to produce the land-type database were undertaken during the cooler winter months, using standard soil augers and with samples taken to a maximum depth of 1.2 m (ISCW, 1993).

To obtain a spatial distribution of site characteristics within each mining district, a geostatistical interpolation technique was used to create raster layers for each sampling area for which data were available. Interpolation techniques are useful as they can be used to predict information for any geographical location by making the assumption that spatially distributed objects are spatially correlated and therefore would tend to have similar characteristics (Juang *et al*., 2001).

The kriging method was selected as the most appropriate interpolation technique for this study as it utilises the statistical properties of the measured sample points, thereby incorporating the statistical properties of the measured data in the created interpolated surface or raster layer. Interpolated surfaces of groundwater measurements included groundwater chloride and sulphate concentrations, total dissolved solids, electrical conductivity, pH and groundwater table levels were created within each mining district using the ArcGIS (version 9.3, 2009) software package.

A listing of all observation points which were used to create the interpolated groundwater hydrochemistry and groundwater table level surfaces for each mining district is shown in Appendix 3. In the Welkom mining district, 23 observation sampling points were used to interpolate 83.21 km² to create a spatial representation of groundwater chloride and sulphate concentrations, electrical conductivity, pH and total dissolved solids, while eight observation points were used to interpolate 51.27 km² to create a spatial representation of the groundwater table level. Similarly, in the Vaal River and West Wits mining districts, 19 and 23 observations were used to create 92.42 km² and 64.48 km² interpolated surfaces for groundwater chloride and sulphate concentrations, electrical conductivity, pH and total dissolved solids, while 15 and 9 observation points were used to create 16.94 km² and 24.71 km² groundwater table level surfaces respectively. It must be acknowledged that site characteristic data i.e. sampling point data obtained for these areas, and especially groundwater table level data were minimal. Hence the spatial extent of interpolated surfaces and subsequent analyses were constrained by these datasets.

7.3 RESULTS

7.3.1 Differences between the site characteristic data of stressed and unstressed sites

For each mining district, spatial patterns of stressed and unstressed sites were mapped, using the six site- and species-specific models reported on in section 5.3.2.3, derived between PLWP and GNDVI, using broad-band multispectral Proba Chris satellite data. As a specific aim of this study was to correlate the spatial distribution of **unstressed trees** to particular

site characteristics that may be recognised and used to prioritise sites for the establishment of future block plantings, spatial patterns of **unstressed trees** have been illustrated in subsequent maps in this chapter and in Figures 7.1 to 7.6. It is noted though that areas not categorised as unstressed are considered stressed by the PLWP GNDVI model.

In order to test for significant differences between site characteristic data for these stressed and unstressed trees, a random sample of one hundred points was selected per tree species for each mining district for stressed and unstressed areas. Site characteristic information was then extracted for the two hundred sample points (stressed and unstressed points) per mining district. This included information on the average percent clay in the topsoil, average soil depth, groundwater measurements of chloride concentration, electrical conductivity, pH, sulphate concentration, total dissolved solids and the groundwater table level. These variables were considered as important site characteristics for each region and for which data were available (Weiersbye, 2006; 2008). Geographical information system analyses were performed using the ArcGIS (version 9.3, 2009) software package.

A t-test was then used to test for statistically significant differences in the average percent clay in the topsoil, average soil depth, groundwater measurements of chloride concentration, electrical conductivity, pH, sulphate concentration, total dissolved solids and groundwater table level, between stressed and unstressed trees per species for each mining district using the Genstat (11th edition, 2008) statistical software package. Results from the t-tests are shown in Tables7.5, 7.6 and 7.7 for the Welkom, Vaal River and West Wits mining districts respectively.

Table 7.5 Comparisons (mean+standard deviation) of the site characteristics geology, soils, salinity and groundwater table level between stressed and unstressed trees of Eucalyptus camaldulensis and Searsia lancea in the Welkom mining district. Differences between stressed and unstressed trees per species were tested using t-tests (P<0.05.

Mining district	Tree Species	Site Data	Plant water stress	Sample size	Mean	Standard deviation	T test	Degree of freedom (df)	Probability value (P)
Welkom	*Eucalyptus camaldulensis*	Topsoil clay (%)	Unstressed	100	10.32	2.910	-2.13	187	0.035
			Stressed	89	11.27	3.258			
		Soil depth (mm)Soil	Unstressed	100	1116	219.1	2.13	187	0.035
			Stressed	89	1044	245.4			

Mining district	Tree Species	Site Data	Plant water stress	Sample size	Mean	Standard deviation	T test	Degree of freedom (df)	Probability value (P)
		depth (mm)							
		Chloride (mg/l)	Unstressed	100	4811	2969	6.31	198	< 0.001
			Stressed	100	2259	2746			
		Electrical conductivity (mS/cm)	Unstressed	100	1252.9	714.8	6.39	198	< 0.001
			Stressed	100	628.5	667			
		pH	Unstressed	100	8.244	0.1358	2.20	166	0.029
			Stressed	100	8.188	0.2169			
		Sulphate (mg/l)	Unstressed	100	1244.7	721.7	6.39	198	< 0.001
			Stressed	100	614.6	671.4			
		Total dissolved solids (mg/l)	Unstressed	100	10983	6383	6.50	198	< 0.001
			Stressed	100	5325	5926			
		Water level (mbgl)	Unstressed	91	6.784	1.831	-1.12	152	0.266
			Stressed	63	7.110	1.705			
	Searsia lancea	Topsoil clay (%)	Unstressed	65	15.20	0.000	9.72	152	< 0.001
			Stressed	89	11.27	3.258			
		Soil depth (mm)	Unstressed	65	748.3	0.000	9.72	152	< 0.001
			Stressed	89	1044.3	245.4			
		Groundwater chloride (mg/l)	Unstressed	100	1439	1147	-2.76	132	0.007
			Stressed	100	2259	2746			
		Electrical conductivity (mS/cm)	Unstressed	100	467.3	272.5	-2.24	131	0.027
			Stressed	100	628.5	667.0			
		pH	Unstressed	100	8.626	0.0719	19.18	120	< 0.001
			Stressed	100	8.188	0.2169			
		Groundwater sulphate (mg/l)	Unstressed	100	631.4	256.2	0.23	127	0.816
			Stressed	100	614.6	671.4			
		Total dissolved solids (mg/l)	Unstressed	100	3744	2462	-2.46	132	0.015
			Stressed		5325	5926			
		Water level (mbgl)	Unstressed	98	9.958	1.700	10.36	159	< 0.001
			Stressed	63	7.110	1.705			

An analysis of the means extracted for *E. camaldulensis* in the Welkom mining district indicated that all **site variables** listed in Table 7.5 were higher in unstressed sites, except for topsoil clay (%) and groundwater table level which showed a higher mean value in the stressed sites. However, site variables which displayed significant differences between stressed and unstressed sites for the Welkom mining district for *E. camaldulensis* included the average percentage clay in the topsoil, average soil depth, groundwater chloride concentration, electrical conductivity, pH, groundwater sulphate concentration and total dissolved solids.

For *S. lancea* sites in the Welkom mining district, the mean values for the average percentage clay in the topsoil, pH, sulphate concentration and water level were higher for the unstressed sites, while the mean values for average soil depth, groundwater chloride concentration, electrical conductivity and total dissolved solids were higher in stressed sites. Furthermore, significant differences were found in the site variables between stressed and unstressed sites for the topsoil clay (%), soil depth, groundwater chloride concentration, electrical conductivity, pH, total dissolved solids and the groundwater table level.

Table 7.6 Comparisons (mean+standard deviation) of the site characteristics geology, soils, salinity and groundwater table level between stressed and unstressed trees of Eucalyptus camaldulensis and Searsia lancea in the Vaal River mining district. Differences between stressed and unstressed trees per species were tested using t-tests (P<0.05).

Mining district	Tree Species	Site Data	Plant water stress	Sample size	Mean	Standard deviation	T test	Degree of freedom (df)	Probability value (P)
Vaal River	*Eucalyptus camaldulensis*	Topsoil clay (%)	Unstressed	100	16.42	1.0250	0.70	198	0.484
			Stressed	100	16.32	0.9518			
		Soil depth (mm)	Unstressed	100	423.9	50.81	-0.34	198	0.733
			Stressed	100	426.3	49.80			
		Groundwater chloride (mg/l)	Unstressed	99	362.5	34.24	1.09	197	0.276
			Stressed	100	356.7	39.47			
		Electrical conductivity (mS/cm)	Unstressed	99	22912	8167	2.42	197	0.017
			Stressed	100	20018	8712			
		pH	Unstressed	99	7.552	0.2909	-3.16	175	0.002
			Stressed	100	7.664	0.2030			
		Groundwater sulphate (mg/l)	Unstressed	99	1765	713.9	-0.77	154	0.443
			Stressed	100	1829	403.6			
		Total dissolved solids (mg/l)	Unstressed	99	3862	771.3	1.44	197	0.151
			Stressed	100	3696	860.5			
		Water level (mbgl)	Unstressed	3	4.228	0.4203	0.07	18	0.947
			Stressed	17	4.208	0.4718			
	Searsia lancea	Topsoil clay (%)	Unstressed	100	16.55	0.4403	2.23	139	0.027
			Stressed	100	16.32	0.9518			
		Soil depth (mm)	Unstressed	100	417.9	10.91	-1.65	108	0.101
			Stressed	100	426.3	49.80			
		Groundwater chloride (mg/l)	Unstressed	100	366.3	32.87	1.87	198	0.063
			Stressed	100	356.7	39.47			
		Electrical conductivity (mS/cm)	Unstressed	100	22858	8330	2.36	198	0.019
			Stressed	100	20018	8712			
		pH	Unstressed	100	7.576	0.2810	-2.55	180	0.012

Mining district	Tree Species	Site Data	Plant water stress	Sample size	Mean	Standard deviation	T test	Degree of freedom (df)	Probability value (P)
			Stressed	100	7.664	0.2030			
		Groundwater sulphate (mg/l)	Unstressed	100	1818	916.1	-0.10	136	0.917
			Stressed	100	1829	403.6			
		Total dissolved solids (mg/l)	Unstressed	100	3916	784.0	1.89	198	0.060
			Stressed	100	3696	860.5			
		Water level (mbgl)	Unstressed	6	4.713	0	2.58	21	0.017
			Stressed	17	4.208	0.4718			

Comparison of the site variables for *E. camaldulensis* trees in Vaal River indicated higher mean values in the topsoil clay percent, groundwater chloride concentration, electrical conductivity, total dissolved solids and the groundwater table level in unstressed sites; while the average soil depth, pH and groundwater sulphate concentrations were higher in stressed sites. However, significant differences were identified for electrical conductivity and the pH between stressed and unstressed *E. camaldulensis* sites.

For *S. lancea*, mean values of the average percent of clay in topsoil, groundwater chloride concentration, electrical conductivity, total dissolved solids and groundwater table level were higher in unstressed sites; while the mean values in average soil depth, pH, and groundwater sulphate concentration were higher in stressed sites. Statistically significant differences were determined in the average percent of clay in topsoil, electrical conductivity, pH and water level of stressed and unstressed *S. lancea* sites in Vaal River.

Table 7.7 Comparisons (mean+standard deviation) of the site characteristics such as geology, soils, salinity and groundwater table level between stressed and unstressed trees of Eucalyptus camaldulensis and Eucalyptus sideroxylon in the West Wits mining district. Differences between stressed and unstressed trees per species were tested using t-tests (P<0.05).

Mining district	Tree Species	Site Data	Plant water stress	Sample size	Mean	Standard deviation	T test	Degree of freedom (df)	Probability value (P)
West Wits	*Eucalyptus camaldulensis*	Topsoil clay (%)	Unstressed	100	*same value				
			Stressed	100					
		Soil depth (mm)	Unstressed	100	*same value				
			Stressed	100					
		Groundwater chloride (mg/l)	Unstressed	100	132.2	15.22	9.36	125	< 0.001
			Stressed	100	90.9	41.47			
		Electrical conductivity (ms/cm)	Unstressed	100	16897	5854	4.28	166	< 0.001
			Stressed	100	12183	9329			

Mining district	Tree Species	Site Data	Plant water stress	Sample size	Mean	Standard deviation	T test	Degree of freedom (df)	Probability value (P)
		pH	Unstressed	100	7.315	0.0943	-1.76	136	0.081
			Stressed	100	7.355	0.2111			
		Groundwater sulphate (mg/l)	Unstressed	100	498.4	185.5	6.21	190	< 0.001
			Stressed	100	316.3	227.4			
		Total dissolved solids (mg/l)	Unstressed	100	954.8	324.3	6.01	198	< 0.001
			Stressed	100	662.6	362.5			
		Groundwater level (mbgl)	Unstressed	90	11.36	2.411	-2.57	34	0.015
			Stressed	27	13.18	3.432			
	Eucalyptus sideroxylon	Topsoil clay (%)	Unstressed	100	*same value				
			Stressed	100					
		Soil depth (mm)	Unstressed	100	*same value				
			Stressed	100					
		Groundwater chloride (mg/l)	Unstressed	100	137.6	13.09	10.75	118	< 0.001
			Stressed	100	90.9	41.47			
		Electrical conductivity (ms/cm)	Unstressed	100	19401	5286	6.73	156	< 0.001
			Stressed	100	12183	9329			
		pH	Unstressed	100	7.259	0.0758	-4.30	124	< 0.001
			Stressed	100	7.355	0.2111			
		Groundwater sulphate (mg/l)	Unstressed	100	558.5	146.6	8.95	169	< 0.001
			Stressed	100	316.3	227.4			
		Total dissolved solids (mg/l)	Unstressed	100	1059.4	267.0	8.81	181	< 0.001
			Stressed	100	662.6	362.5			
		Groundwater level (mbgl)	Unstressed	90	11.29	2.623	-3.01	110	0.003
			Stressed	27	13.18	3.432			

**data obtained for this area were coarse and did not vary between sites*

In the West Wits mining area, higher mean values in the groundwater chloride and sulphate concentrations, electrical conductivity and total dissolved solids were identified at unstressed *E. camaldulensis* sites, while the pH and water level were higher at stressed sites. Significant differences were found in groundwater chloride concentrations, electrical conductivity, groundwater sulphate concentrations, total dissolved solids and the water level between stressed and unstressed *E. camaldulensis* sites.

For *E. sideroxylon* sites in the West Wits mining district, the mean values for groundwater chloride concentration, electrical conductivity, groundwater sulphate concentration and total dissolved solids were higher in unstressed sites, while the pH and water level were higher in stressed sites. The average percent of clay in the topsoil and the average soil depth displayed little or no variation across the stressed and unstressed sites. Furthermore, statistically

significant differences were also identified for groundwater chloride concentration, electrical conductivity, pH, groundwater sulphate concentration, total dissolved solids and the groundwater level between stressed and unstressed *Eucalyptus sideroxylon* sites.

7.4 DISCUSSIONSAND RECOMMENDATIONS FOR FUTURE PLANTINGS

A summary of the characteristics of unstressed sites which were identified within each mining district for each tree species is shown below (Table 7.8). Only those site characteristics which displayed significant differences between stressed and unstressed areas were selected, of which their interpolated surfaces are shown in Appendix 5.

Table 7.8 Descriptive statistics (minimum, maximum, mean, standard deviation) of the site variables geology, soils, salinity and groundwater table level used to characterise unstressed trees per species in each mining district.

Mining district	Tree Species	Site Data	Minimum	Maximum	Mean	Standard deviation
Welkom	*Eucalyptus camaldulensis*	Topsoil clay (%)	8.00	8.00	8.00	8.00
		Soil depth (mm)	748.29	1245.40	1214.33	120.32
		Groundwater chloride (mg/l)	31.78	12417.88	4064.92	3048.11
		Electrical conductivity (mS/cm)	78.22	3081.85	1070.93	736.86
		pH	7.86	8.61	8.23	0.15
		Groundwater sulphate (mg/l)	47.03	3056.84	1057.52	753.21
		Total dissolved solids (mg/l)	729.31	27253.27	9286.92	6631.00
Welkom	*Searsia lancea*	Topsoil clay (%)	8.6	15.19	13.90	2.61
		Soil depth (mm)	748.29	1245.40	845.55	197.20
		Groundwater chloride (mg/l)	50.55	14524.92	2137.32	2325.27
		Electrical conductivity (mS/cm)	82.16	3586.32	616.59	557.32
		pH	7.78	8.68	8.33	0.27
		Total dissolved solids (mg/l)	664.07	31755.84	5116.94	4991.87
		Groundwater level (mbgl)	2.64	13.00	7.98	2.26
Vaal River	*Eucalyptus camaldulensis*	Electrical conductivity (mS/cm)	6185.52	43253.38	21721.77	7056.23
		pH	6.75	8.04	7.59	0.23
Vaal River	*Searsia lancea*	Topsoil clay (%)	7.00	17.79	10.36	4.77
		Electrical conductivity (mS/cm)	6185.52	43679.29	21753.55	8024.30
		pH	6.74	8.04	7.57	0.27
		Groundwater level (mbgl)	3.98	5.02	4.71	0.43
West Wits	*Eucalyptus camaldulensis*	Groundwater chloride (mg/l)	24.84	214.89	92.47	36.58
	Eucalytpus sideroxylon	Electrical conductivity (mS/cm)	9972.05	49689.69	11462.43	7027.03
		pH	6.51	8.44	7.35	0.19
		Groundwater sulphate (mg/l)	20.92	1834.96	313.98	180.55

		Total dissolved solids (mg/l)	19.17	2625.17	664.10	286.92
		Groundwater level (mbgl)	4.92	19.94	12.60	2.147

The interpolated site characteristic surfaces shown in Appendix 5, and listed in Table 7.8 above were spatially linked to trees which were not experiencing winter-time plant water stress, mapped using the predawn leaf water potential and the green normalized difference vegetation index derived from Proba Chris imagery shown in Figures 7.1 to 7.6. The spatial distribution of these unstressed areas for which **site characteristic data were available**, were mapped using ArcGIS (version 9.3, 2009), and illustrated for each mining district in Figures 7.7to 7.9.

The recommended unstressed areas proposed for planting *Eucalyptus camaldulensis* and *S. lancea* in the Welkom mining district are shown in Figure 7.7. Quantitative site characteristics, which were found to be significantly different ($p < 0.05$; Table 7.5) from stressed sites for *E. camaldulensis*, included the average soil depth, groundwater chloride concentration, electrical conductivity, pH, groundwater sulphate concentration and total dissolved solids and, for *S. lancea*, the average % clay in the topsoil, average soil depth, groundwater chloride concentration, electrical conductivity, pH, total dissolved solids and the groundwater table level.

The geological formations characteristic of these unstressed areas mapped within the Welkom mining district are commonly referred to as Ecca Shales (Vegter, 1995). Two dominant soil land-types are found in this area, Ae40 land-type comprised of eutrophic, red massive or weak structured soils with a high base status, and the Dc9 land-type with non-calcarious soils, high clay accumulation, strongly structured soil of a non-reddish colour and the presence of one or more of the vertic, melanic or plinthic soils (ISCW, 1993). The natural vegetation is categorised primarily as the grassland biome within the Dry Highveld Grassland bioregion, with patches of the Azonal Vegetation biome forming part of the Inland Saline Vegetation bioregion (Mucina and Rutherford, 2006).

Spatial patterns of unstressed *E. camaldulensis* and *Searsia lancea* sites shown in Figure 7.7extend across a relatively flat area, with an altitude ranging from 1290 to 1300 m and

dominated by Ae40 and Dc9 landtype respectively. River networks are disconnected, as is common in relatively flat areas, were the digital elevation models used which include sinks in the area. The *S. lancea* sites also highlight the edges of the Pan, indicating that during the dry season trees could access water from the Pan and are therefore categorised as unstressed by the model.

To obtain more detailed subsurface information at selected sampling sites in the three mining districts, resistivity measurements were acquired by geophysical specialists from the CSIR using an ABEM Terrameter SAS1000. Geophysical studies have shown that resistivity measurements have been successfully applied to detect subsurface lithologies, groundwater depths, potential groundwater sources and plume contamination (Okereke *et al*., 1998; Salem, 2000; Tabbagh *et al*., 2000). Resistivities measurements undertaken in the Welkom mining district are illustrated in Figures 7.8a and 7.8b.

Figure 7.7/...

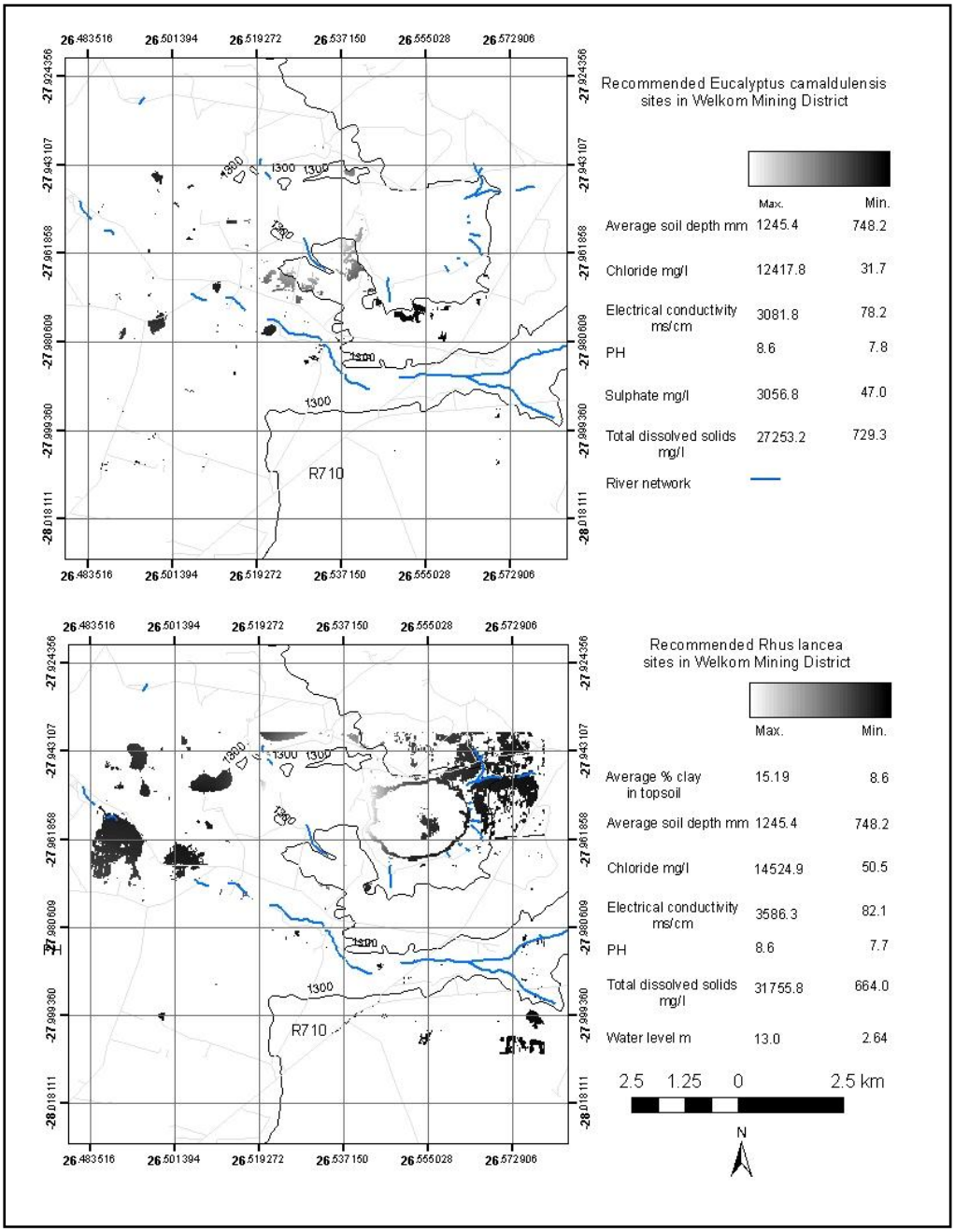


Figure 7.7 *A shaded selection of unstressed areas in the Welkom mining district recommended for planting <u>Eucalyptus camaldulensis</u> and <u>Searsia lancea</u> tree species. The graded scale represents the maximum (light grey) and minimum (black) values of site characteristic data representative of these unstressed areas.*

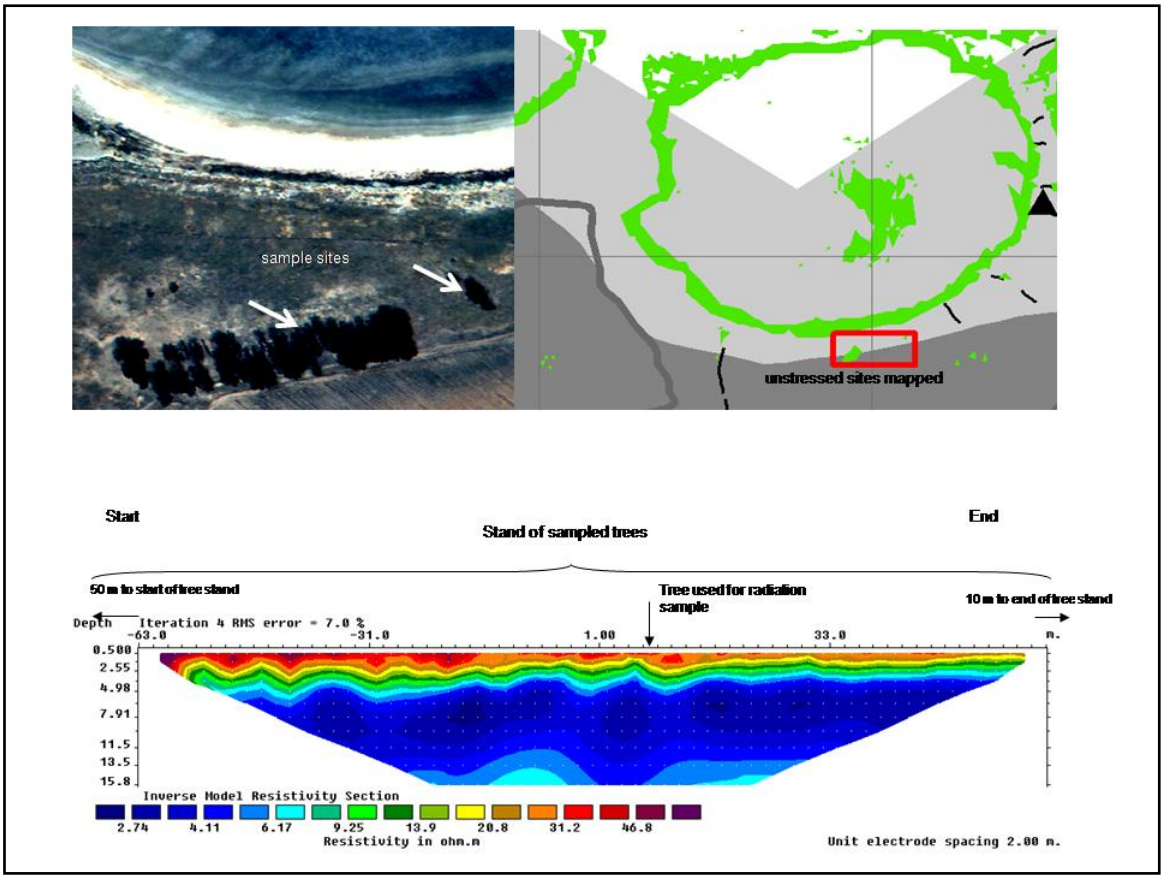


Figure 7.8a *Dankbaar Pan resistivity sampling site in the Welkom mining district, (clockwise) arrows in the picture represent the location of trees at each sampling site; the block demarcated in red represents the resistivity sampling area; unstressed areas mapped in green and the resistivity profile observed at the sampling site.*

The Dankbaar Pan is located on farmland within the Welkom mining district. The area is very flat and the groundwater is reported to have very high salinity concentrations, being influenced by drainage pathways from mining activities in the area. An older stand of *E.camalduensis* trees and scattered *S. lancea* trees approximately 100m from the edge were selected for ground-truthing measurements as shown in Figure 7.8a. The soils in the area appear well developed and deep. The resistivity transect extends through most of the length of the stand of *Eucalyptus* trees. The dark blue layers have a very low resistivity and is an indication of groundwater saturation from approximately 4.9 m below the surface, as the lower the resistivity the greater the moisture content or the higher the concentration of salts. With salts from the Pan being visually evident, the very low resistivity indicates the high

salinity of the groundwater. Even the resistivity of the drier topsoil layers are fairly low (30-50 ohms), indicating that the shallower soils are saline as well (Okereke *et al*., 1998; Salem, 2000; Tabbagh *et al*., 2000).

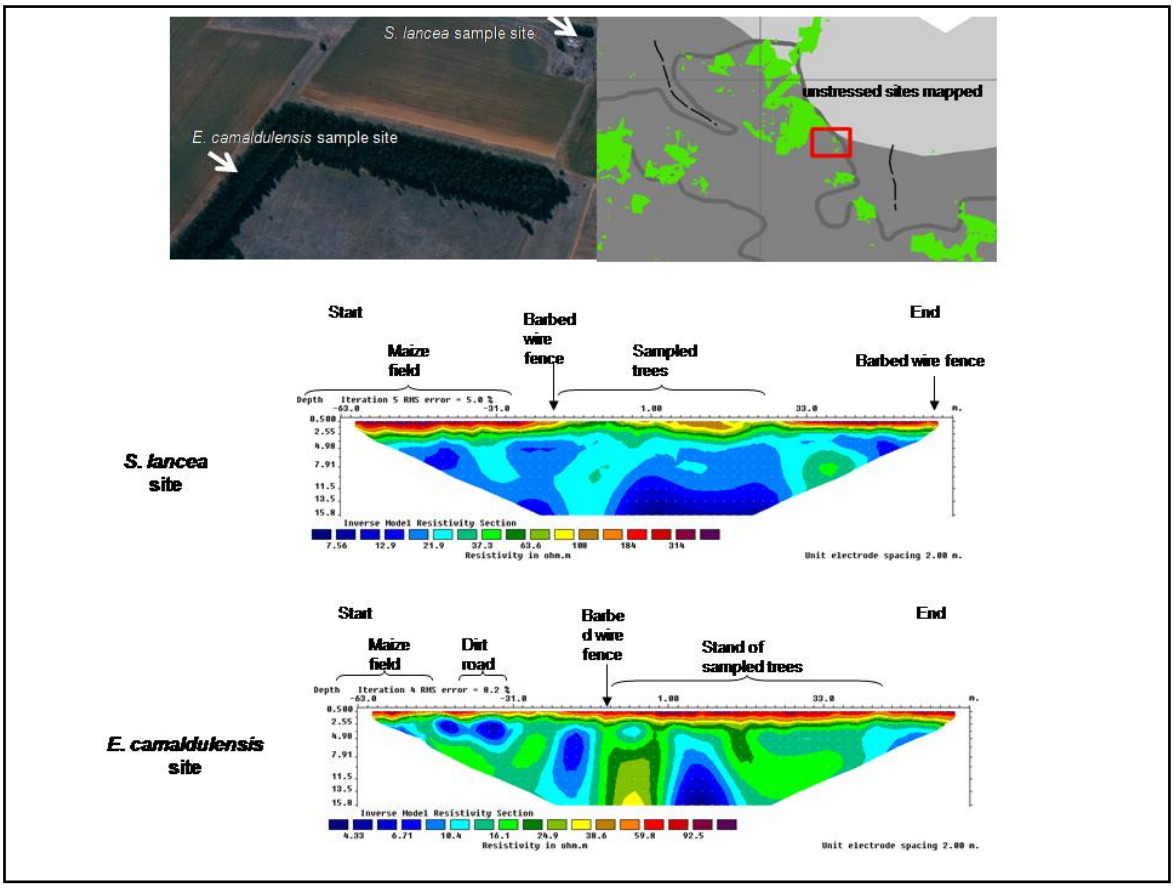


Figure 7.8b *Boet Van Der Berg Farmresistivity sampling site in the Welkom mining district, (clockwise) arrows in the picture represent the location of trees at each sampling site; block demarcated in red represents the resistivity sampling area; unstressed areas mapped in green and the resistivity profiles observed on the farm at the S. lancea and E. camaldulensis sampling areas.*

Sample sites on Mr. Boet Van Der Berg's Farm were selected for comparison with the Dankbaar Pan sampling sites. Two locations were surveyed, a site consisting of a row of *S. lancea* trees and a stand of older *E. camaldulensis* trees as shown in Figure 7.8b. These sites are characterized by red and yellow apedals, freely drained deep soils with a high base status. The predominant lithology group is Shale. Figure 7.8b illustrates lower resistivity

materials from a depth of 5m, which could be a result of deep drainage, hence saturated conditions of the weathered shale, resulting in a clay horizon and shallow groundwater sources. Topsoil layers (<1m) in both inverted sections are represented by much higher resistivities compared to the deep layers, usually indicating drier soils were electricity is not easily conducted. The intermediate resistivity zones (greens) probably indicate areas of fractured shale rather than fully developed clay zones.

Sampling sites selected on Mr. Boet Van Der Berg's Farm in comparison to the Dankbaar Pan sites, indicated different subsurface groundwater depths and soil formations according to the resistivity surveys. Soils in the area appear to be drier, being characterised by higher resistivities in the topsoil layers (Figure 7.8b) with Shale being the predominant lithology group. Pockets of darker blue areas could be an indication of subsurface water estimated at an approximate depth of 4.98m at the *E. camaldulensis* site and 7.91m at the *S. lancea* site.

Groundwater saturation in the Dankbaar sampling area in Welkom, indicated in the resitivity profile at an average depth of 7.91 m (Figure 7.8a) and the average groundwater table level reported in Table 7.8, confirms the presence of shallow groundwater sources. This implies that trees roots could access the "relatively" shallow groundwater and assist in containing contaminated groundwater seeping into surrounding lands. However, measurements of predawn leaf water potential undertaken during the drier winter months in 2004 and 2005, indicate an average value of -1.4 to -1.5MPa, therefore characterising these trees as being stressed. Also indicated are the high salinity levels in the area, illustrated by the high total dissolved solids, groundwater chloride and sulphate concentrations reported in Table 7.8 and shown in Figure 7.7 and is characterised by the fairly low resistivity values in Figure 7.8.a, even in the shallower soils. Therefore tree plantings could possibly assist in sequestering some of the contaminants present in the groundwater produced from mining activities and thereby could also reduce the movement of salts or pollutants to neighbouring streams and rivers (Funke, 1990; Hodgson *et al*., 2001; Rosner *et al*., 2001; Naicker *et al*., 2003).

In the Vaal River mining district, trees which are not experiencing winter-time plant water stress, and which are recommended for planting *E. camaldulenis* and *S. lancea*, are

illustrated in Figure 7.9. Site characteristics of unstressed areas which were found to be significantly different from the stressed areas are also shown ($p < 0.05$, Table 7.6). For the recommended *E. camaldulensis* sites, these include electrical conductivity and pH, and for *S. lancea*, the average % clay in the topsoil, electrical conductivity and pH. Groundwater table levels were not significantly different in this area, indicating that trees during winter would have access to water and would not be the limiting factor in the Vaal River mining district. The results indicate that unstressed trees would be affected by salinity levels reflected by the electrical conductivity of the groundwater and the pH of the groundwater.

The altitudinal gradient characteristic of the area ranges from 1280 to 1380 m. Geological formations stretching across the recommended planting areas are classified as Alluvium, Black Reef, Chert Rich dolomite, Dolomite Sand, Karoo and Ventersdorp (Anglo Ashanti, 2005). The major land-type characteristic in this area include Fa13, described as mesotrophic to eutrophic soils, with minimal development usually shallow on hard or weathering rock with or without intermittent diverse soils (ISCW, 1993).

Smaller areas in the region are represented by Bd13 and Bc23 land-types with red, yellow and greyish soils having a high base status (ISCW, 1993), characterising many of the unstressed sites mapped in Vaal River. The natural vegetation is categorised as the grassland biome within the Dry Highveld Grassland bioregion which generally experiences mean annual rainfall below 600mm (Mucina and Rutherford, 2006). This implies that the natural vegetation would be able to survive and grow under average rainfall conditions with shallower root systems compared to trees and forest plantations.

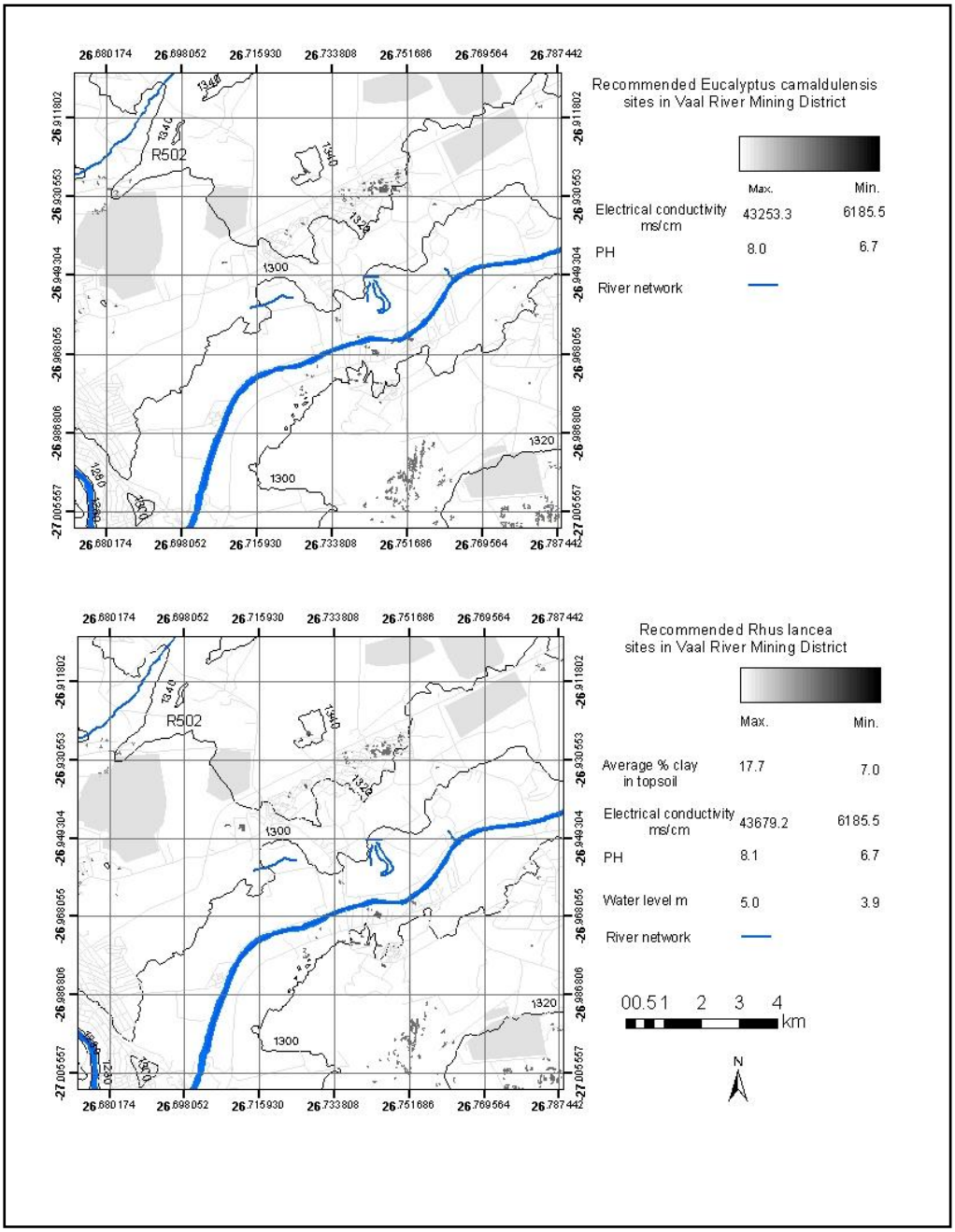


Figure 7.9 A shaded selection of unstressed areas in the Vaal River mining district recommended for planting <u>Eucalyptus camaldulensis</u> and <u>Searsia lancea</u> tree species. The graded scale represents the maximum (light grey) and minimum (black) values of site characteristic data representative of these unstressed areas.

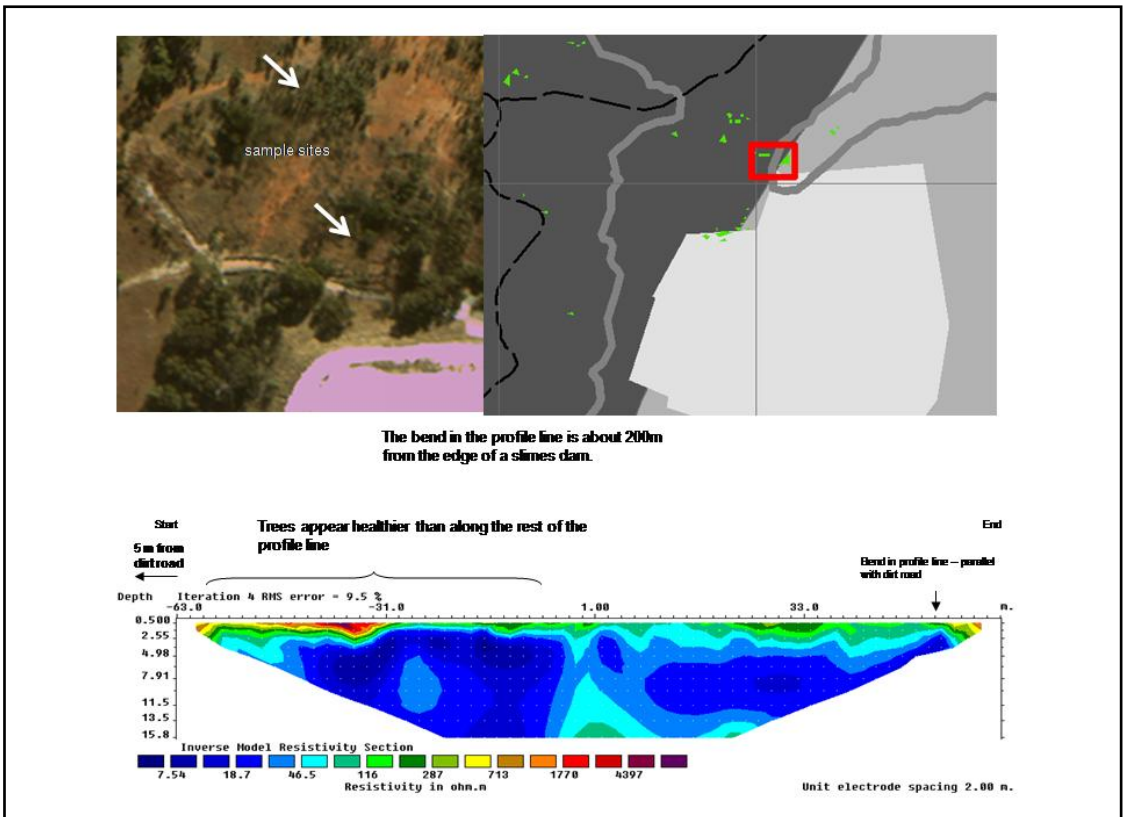


Figure 7.10 *Western Complex resistivity sampling site in the Vaal River mining district, (clockwise) arrows in the picture represent the location of trees at each sampling site; block demarcated in red represents the resistivity sampling area; unstressed areas mapped in green and the resistivity profile observed near the tailing storage facility.*

The Western Complex site is located approximately 200m from the edge of the Western Complex TSF (Figure 7.10). A dirt road separates the *E. camaldulensis* site from the TSF. This site is characterized by a cluster of young *E. camaldulensis* trees which appear unhealthy with poor growth characteristics. However, moving away from the TSF the trees appear healthier with green foliage and good growth characteristics. Within this site a group of trees were sampled within the apparent healthy vs. unhealthy clusters of trees. The healthy trees can potentially be because of an increase in the porosity of the soils. Higher porosity means it should be easier for the plants to get to subsurface water. The site is underlain by Andesite, which is an igneous rock. Depending on the phase of deposition, the lava can vary in composition and this affects weathering and eventually porosity.

A majority of the unstressed sites mapped for the Vaal River mining district extend across Bd13 and Bc23 land-types with red, yellow and greyish soils having a high base status (ISCW, 1993), low pH (minimum 6.75) and shallow groundwater table levels (an average 5.02 m) as shown in Table 7.8 and illustrated in Figure 7.10, from approximately 2.55m below the surface. Tree plantings in these areas highlighted in Figure 7.9 in the Vaal River mining district, could tap into the seepage water from the surrounding TSFs which are many in the area, and transpire greater quantities of water than the grasslands and wetlands presently in close proximity to the TSFs. Evaporation from groundwater sources, could result in reduced water table depths and slower lateral flows into the neighbouring lands and river systems such as the Vaal River, as it is known that the impact of the mines and the TSFs extends far beyond their localities as a result of dust pollution and the extent of groundwater plumes (Cogho *et al.*, 1990; Vivier *et al*., 2001).

In the West Wits mining district, the spatial distribution of unstressed areas recommended for planting *E. camaldulensis* and *E. sideroxylon* is shown in Figure 7.11. Quantitative site characteristics for the unstressed areas, which were found to be significantly different ($p < 0.05$; Table 7.7) from the stressed areas, are also shown. These included groundwater chloride concentration, electrical conductivity, pH, groundwater sulphate concentration, total dissolved solids and the groundwater table level.

The geology in these recommended areas has been classified as Rooihoogte quartzite shale chert breccia, Timeball Hill shale, Diabase intrusive, Timeball Hill ferruginous quartzite and Hekpoort andesite agglomerate (Anglo Ashanti, 2005). Two land-types found in this area are Fb15 and Fb5, described as eutrophic soils with minimal development, usually shallow on hard or weathering rock, with or without intermittent diverse soils with lime generally present in part or most of the landscape (ISCW, 1993).

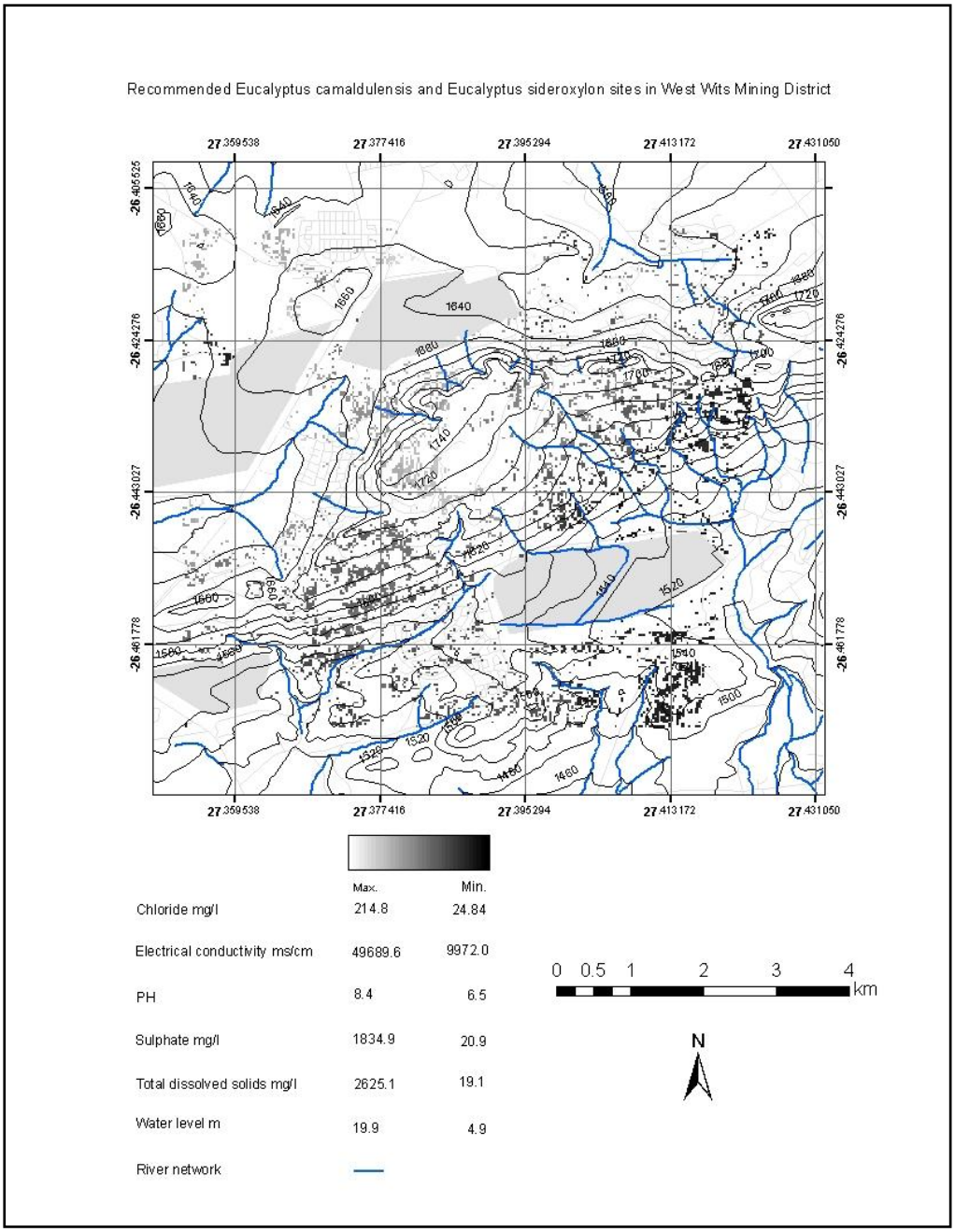


Figure 7.11 A shaded selection of unstressed areas in the West Wits mining district recommended for planting Eucalyptus camaldulensis and Eucalyptus siderxylon tree species. The graded scale represents the maximum (light grey) and minimum (black) values of site characteristic data representative of these unstressed areas.

Spatial patterns of unstressed trees mapped in the West Wit mining region extend across a topographical gradient from 1400 to 1740 m. The area exhibits a much denser river network with a higher mean annual rainfall of 651 mm compared to Welkom and Vaal River,

indicating higher water availability during the dry season. Two resistivity surveys undertaken on the Deelkraal farm and on the trial site just downslope from the Elandsridge TSF in the West Wits mining district are illustrated in Figures 7.12a and 7.12b respectively.

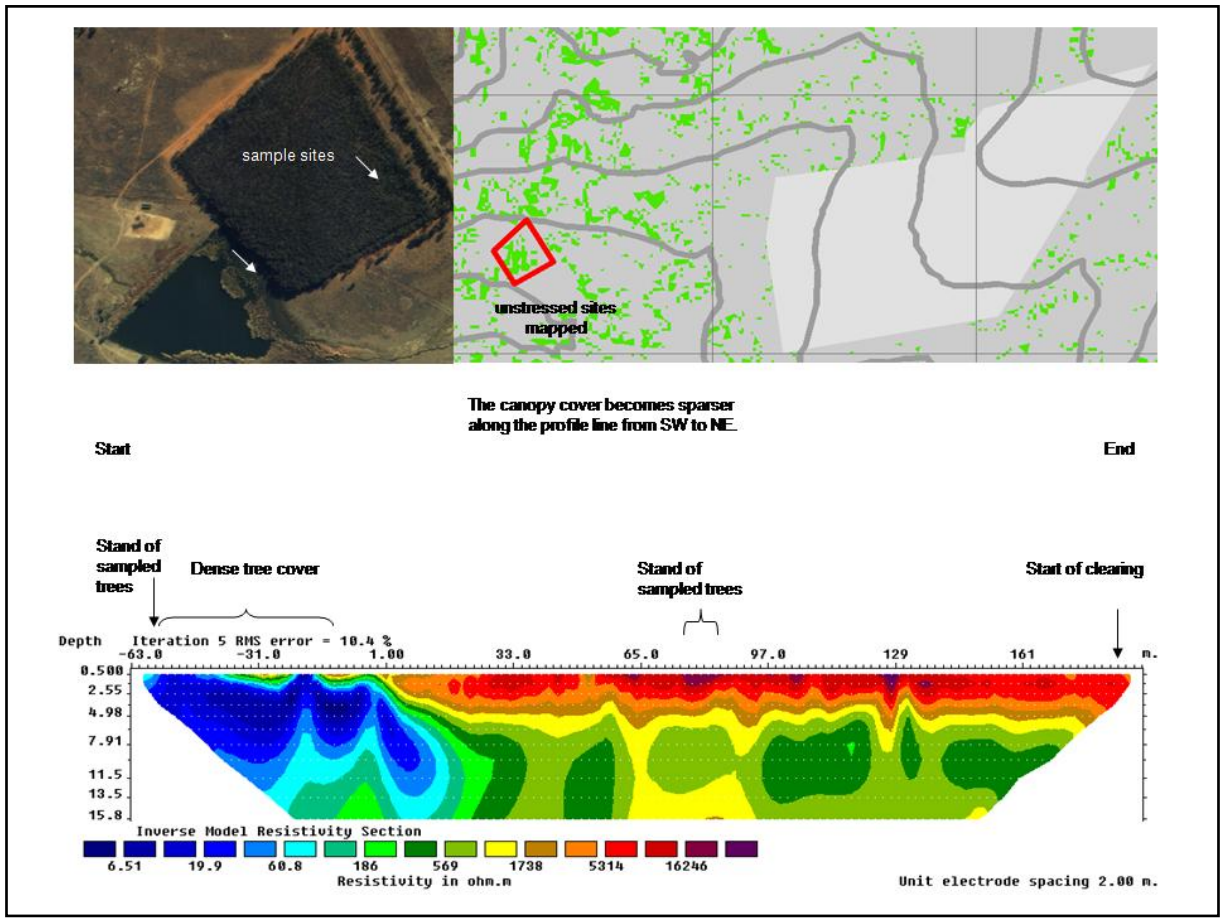


Figure 7.12a *Deelkraal farm resistivity sampling site in the West Wits mining district, (clockwise) arrows in the picture represent the location of trees at each sampling site; block demarcated in red represents the resistivity sampling area; unstressed areas mapped in green and the resistivity profile observed at the site.*

The Deelkraal Farm Site is a very interesting site, consisting of a stand or block of *E. sideroxylon* trees which extends to within approximately 10m of a little farm dam. The stand of trees is dense, green and visually healthy along the riparian edge and at least 20m moving upslope through the stand. However, very distinctly the trees begin to become less dense, the canopy is open, leaf area, tree height and diameter decreases, leaf colour changes from bright

dark green to yellow pale colour, and the trees are visually more stressed or unhealthy. The resistivity profile was located through the stand of trees shown in Figure 7.12a. Low resistivities from the start of the profile near the farm dam are indicative of wetter conditions shown in blue. Water in the area could also be contaminated by the nearby TSFs, which could result in saline conditions and hence low resistivities. However, as the upslope trees become sparse and visually unhealthy, with drier surface conditions, there is also a very distinct change in the resistivity profile. The drier conditions, possibly as a result of shallow bedrock, are reflected in the high resistivities shown in dark brown to orange on the inverse resistivity section. From the inverse model resistivity section it seems that there is a very significant lateral change in geology, possibly from clayey soils to shallow bedrock overlain by very dry sand. Therefore transformation within the stand from dense healthy trees to sparse unhealthy trees could be a result of a change in geology in this site, deeper weathering and more sediment deposition in the riparian zone, with the unstressed / healthy trees accessing seepage water from the dam and groundwater. Water seepage from the dam can also lower the resistivity significantly, especially if the water is saline. A good comparison between unstressed / visually healthy trees seen out in the field and those predicted using the predawn leaf water potential and GNDVI model for this area is shown in Figure 7.12a.

Figure 7.12b/...

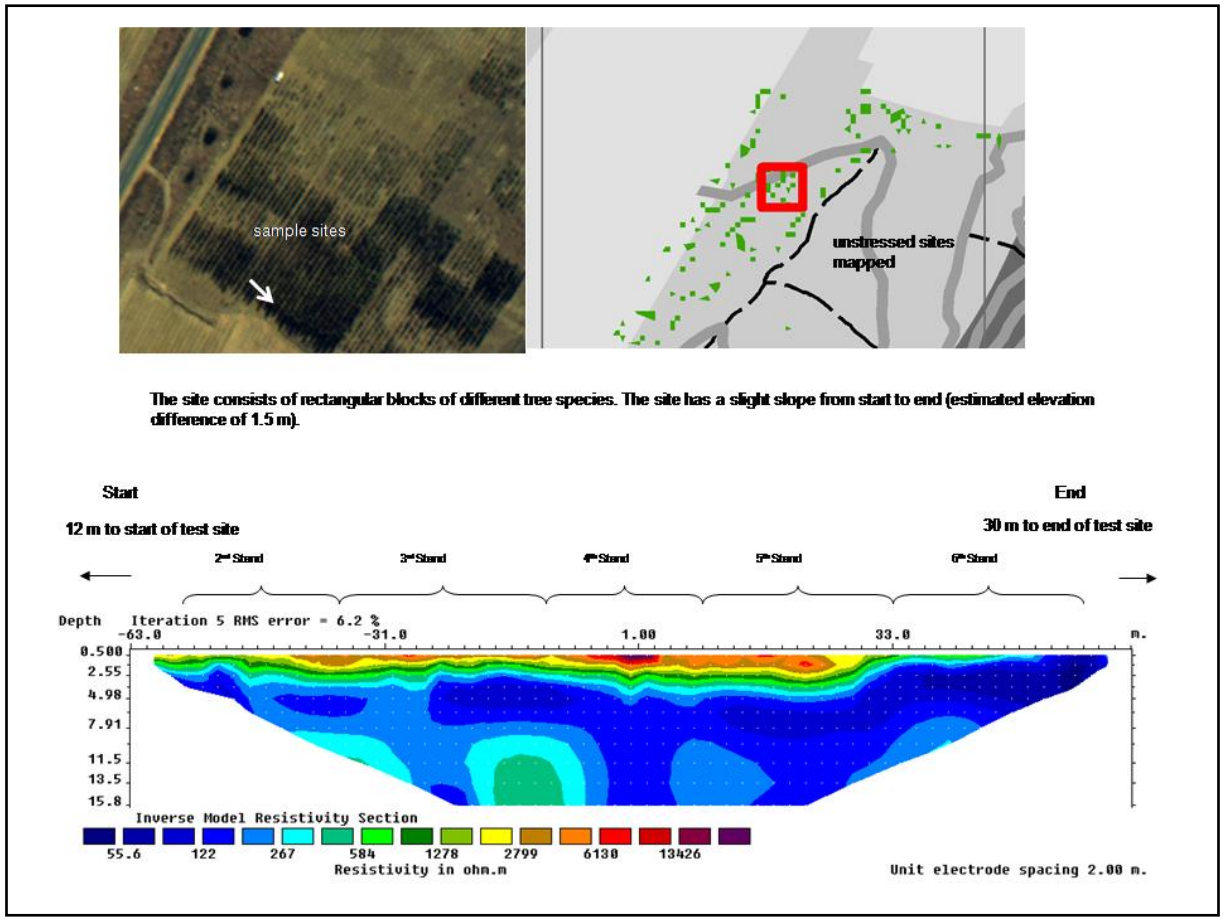


Figure 7.12b *Elandsridgeresistivity sampling site in the West Wits mining district, (clockwise) arrows in the picture represent the location of trees at each sampling site; block demarcated in red represents the resistivity sampling area; unstressed areas mapped in green and the resistivity profile observed downslope from the tailing storage facility.*

The trial site consists of blocks of exotic and indigenous tree species planted just downslope from the Elandsridge TSF in the West Wits mining district. A tarred road separates the trial from the TSF. At the bottom of the trial approximately 20m from the last block of trees is a wetland area. Sampling sites consisted of two blocks of *E. camaldulensis* trees of the same age, illustrated as the 2nd and 6th stand in Figure 7.12b. The resistivity profile is located within the middle of the blocks and runs from the 2nd to 6th block.

The predominant lithology group is shale. At the top of the slope near the 2nd stand, the medium to high resistivities are indicative of dry sand. This is underlain by weathered shale with a low resistivity. The highly weathered shale has a high clay content and this is reflected in the very low resistivity underlying the sand. The clay weathered shale is underlain by fractured shale which will eventually grade into unweathered shale. In the inverted section yellow/brown colours could be an indication of dry sand, blue highly weathered clay-rich shale, and green fractured shale. The influence of contaminants from the TSF at the top slope could affect salinity of the area, resulting in changes in salinity of the soil water at shallow depths. The changes in resistivity of the top sandy layer, from low at the start of the line to very high closer to the centre of the line reflect the influence of this change in salinity.

Salinity is commonly interpreted as the inverse of resistivity. The higher salinity is reflected as a lower resistivity zone at the top. The higher resistivity at depth (green area) along the start of the profile can potentially be an indication of lower water saturation due to the abstraction of water by the trees. The very low resistivity (strong blue band) throughout the profile is an indication of groundwater saturation of the clay. This intensifies at the end of the profile (6th stand) close to the vlei or wetland indicating higher salinity and subsurface saturated conditions. These results are supported by the significant differences in salinity conditions identified for stressed and unstressed sites in the area (Figure 7.11), which included groundwater chloride concentration, electrical conductivity, pH, groundwater sulphate concentration and total dissolved solids.

Larger areas of unstressed sites were identified and are recommended for future plantings of trees in the West Wits mining region (Figure 7.11) compared to smaller areas recommended for Welkom and Vaal River districts. The West Wits area exhibits a much denser river network, for trees to access water during the drier winter season. Furthermore, the changing geological formations and groundwater saturation illustrated in the resistivity surveys (Figure 7.12a and 7.12b) are indicators of areas in the West Wits mining district where trees could thrive, access contaminated water seeping from TSFs and reduce lateral flows into groundwater river systems. Also, the high salinity values are indicative of the contaminant

flows from the TSFs, where again trees could possibly sequester contaminants in the area and reduce lateral pollution into surrounding areas overtime.

7.5 CONCLUSIONS

In summary the process of identifying recommended sites were trees are not experiencing winter-time plant water stress for each species investigated per mining district was as follows:

- High resolution multispectral airborne images (75 cm) were used in an attempt to accurately classify tree species investigated in this study.
- Spatial patterns of stressed and unstressed areas were mapped using the vegetation spectral reflectance models derived in section 5.3.2.3 using satellite multispectral imagery.
- Classified vegetation maps were used to clip unstressed trees per tree species for each mining district.
- The kriging interpolation technique was used to create interpolated surfaces of site characteristic data obtained from AGES, APES and AGA.
- Random sample analyses between stressed and unstressed trees were extracted in order to determine whether site characteristics were significantly different (using t-tests)
- Interpolated site characteristic layers (Appendix 5) of unstressed areas, which displayed significant differences from stressed areas, were spatially linked to trees which were not experiencing winter-time plant water stress.
- The spatial patterns of unstressed trees have been illustrated in this chapter, as a specific aim of this study was to correlate the **spatial distribution of unstressed trees** to particular site characteristics that may be recognised and used to prioritise sites for the establishment of future block plantings. It is noted that areas not categorised as unstressed are considered stressed by the predawn leaf water potential and GNDVI model.

In the Welkom mining district, two dominant soil land-types are found in this area, Ae40 and Dc9 land-type. In the Dankbaar sampling area in Welkom, the very low resistivity is an indication of groundwater saturation from approximately 4.9 m below the surface, confirming the presence of shallow groundwater sources. This implies that trees roots could access the "relatively" shallow groundwater and assist in containing contaminated groundwater seeping into surrounding lands. Therefore tree plantings could possibly assist in sequestering some of the contaminants present in the groundwater produced from mining activities and thereby could also reduce the movement of salts or pollutants to neighbouring streams and rivers (Funke, 1990; Hodgson *et al*., 2001; Rosner *et al*., 2001; Naicker *et al*., 2003).

In the Vaal River mining district, groundwater table levels were not significantly different in this area, indicating that trees during winter would have access to water and would not be the limiting factor in the Vaal River mining district. However, unstressed trees could be affected by salinity levels such as the electrical conductivity of the groundwater and the pH of the groundwater. A majority of the unstressed sites mapped for the Vaal River mining district extend across Bd13 and Bc23 land-types with red, yellow and greyish soils having a high base status (ISCW, 1993), low pH (minimum 6.75) and shallow groundwater table levels (an average 5.02 m).

Larger areas of unstressed sites were identified and are recommended for future plantings of trees in the West Wits mining region compared to smaller areas recommended in the Welkom and Vaal River districts. The West Wits area indicates a much denser river network, with a higher mean annual rainfall of 651 mm compared to Welkom and Vaal River, indicating higher water availability during the drier season. Furthermore, the changing geological formations and groundwater saturation illustrated in the resistivity surveys are indicators of areas in the West Wits mining district where trees could thrive, access contaminated water seeping from TSFs and reduce lateral flows into groundwater river systems. Also, the high salinity values are indicative of the contaminant flows from the TSFs, where again trees could possibly sequester contaminants in the area and reduce lateral pollution into surrounding areas over time.

It is interesting to note that access to groundwater is not the limiting factor determining whether trees are stressed or not during the dry winter season, as this site characteristic was not significantly different between stressed and unstressed areas at all sites. This implies that unstressed sites which have been identified in each mining district do have access to groundwater during the drier winter season. As has been reported at the beginning of the thesis, this research project was heavily dependent on trees growing singly, in rows or in small groups, which experienced lower levels of competition from neighbouring plants. Therefore, these trees would have had a greater opportunity for extending root systems laterally, and the link between dry season tree water stress and groundwater accessibility could be have been influenced.

Earlier studies have reported on the surrounding lands and water systems of the Welkom, Vaal River and West Wits mining district to show increasing salinity levels over the years (Roos and Pieterse, 1995; Viver *et al*., 2001; Naicker *et al*., 2003; Winde *et al*., 2004a,b,c). An evaluation of the site characteristic data indicates that salinity levels possibly do affect whether trees are stressed or unstressed, as these characteristics such as groundwater chloride and sulphate concentrations, total dissolved solids and electrical conductivity displayed significant differences between stressed and unstressed areas in the three mining districts.

CHAPTER 8. GENERAL SYNTHESIS, CONCLUSIONS AND RECOMMENDATIONS

8.1 LITERATURE REVIEW CONCLUDING STATEMENTS

The review undertaken in this study clearly demonstrates that there has been extensive research on the detection and measurement of plant water stress using ground-based and remote sensing technologies. This review of commonly used ground based measurements of plant water stress and spectral reflectance indices was used as a stepping stone to further develop spectral plant water stress relationships for specific tree species in this research study. The review clearly highlights that ground-based techniques are more suited for localised measurements and for ground-truthing of remotely sensed data. The issue of scale is a major factor affecting the platform of remote sensing data to be used and the appropriate ground based measurements to be employed in the field for verifications studies. From this study, the measurement of predawn leaf water potential has been identified as a key methodology for linking remotely sensed assessments of plant water stress to actual plant water stress in the landscape. However, in large scale remote sensing applications which could stretch across several kilometres, practical approaches for ground truthing remote sensing imagery are advised, such as using predawn leaf water potential measurements to identify the extremes in plant water stress within a region.

Remote sensing research has identified several individual spectral bands and vegetation spectral reflectance indices which have been used to detect plant water stress. The collation of this information (section 3.2, Table 3.1) will be useful to researchers of several disciplines who are actively applying remote sensing technologies to vegetative research. Many of these earlier studies as shown in section 3.2, Table 3.1, have focused on broad spectral bandwidths, and it is recommended that plant stress researchers further investigate the potential of narrow hyperspectral bandwidths to detect and interpret patterns of plant stress. Furthermore, the importance of the red edge, defined as the region between 690 and 740 nm, has gained increasingly more attention over the years, and is seen as one of the most

important regions of the spectrum when investigating plant stress. It is also recommended that the results from hyperspectral studies should be incorporated in multispectral systems and technologies to allow for specialised high spectral resolution investigations to be undertaken with reduced data volumes in a cost-effective manner. Developers of remote sensing technologies should utilise the findings of these types of studies in order to optimise sensor systems. Optimal hyperspectral bands which best characterise different vegetation classes should be incorporated into multispectral systems through sensor modifications or spectral filters. Using this approach, researchers would no longer be restricted to existing specifications, but could tailor remote sensing model inputs to a particular application. The ultimate goal is to move from impractical, large data volumes and expensive sensor development towards practical low data volumes, high temporal resolution and cheaper sensor development. Most spectral indices have been derived for a single species with constant leaf size and shape, leaf surface and internal structure, implying that their usefulness varies with respect to species and site conditions. Therefore, the most commonly used indices reported in the literature must be evaluated against ground-truth data.

8.2 GENERAL SYNTHESIS ON VEGETATION SPECTRAL REFLECTANCE INDICES

Vegetation spectral reflectance indices, which were previously tested using hand-held spectral reflectance measurements (Chapter 4),were successfully applied to satellite medium and high resolution remote sensing data (Chapter 5) and the airborne multispectral and hyperspectral remote sensing data. The general trends identified in the use of vegetation spectral reflectance derived from different sources of remote sensing data to detect plant water stress included:

- Three spectral indices, *viz.* 695/690 (Carter, 1994), (850-710)/(850-680) (Datt, 1999) and (710/760) (Carter, 1994), derived from the red and near-infrared regions of the electromagnetic spectrum using leaf-level spectral reflectance data (Chapter 4), were identified as useful spectral indicators of plant water stress and could be linked to plant chlorophyll content.

- The popular water band index (900/970) (Penuelas *et al*., 1997), which was designed to capture changes in plant water content, when derived from leaf-level spectral reflectance data, was correlated to measurements of predawn leaf water potential. Such findings substantiate the importance of hyperspectral remote sensing research and the use of high spectral resolution data to identify subtle relationships between plant water content and narrow-band spectral reflectance data.
- Broadband vegetation indices, which capture changes in the visible region of the electromagnetic spectrum and which are sensitive to changes in plant pigment content, performed well when applied to the medium spectral resolution remote sensing data e.g. Proba Chris satellite data (Chapter 5). These indices included the normalised difference vegetation index (NDVI), the greenness normalised difference vegetation index (GNDVI) and the red edge normalised difference vegetation index (RENDVI).
- Narrow-band vegetation indices which are sensitive to changes in plant water content/plant water status and spectral changes in the red edge region of the spectrum, performed well when applied to high spectral resolution remote sensing data e.g. Hyperion satellite data (Chapter 5). These indices included red edge position (REP) and plant senescence reflectance indices (PSRI).
- The GNDVI, when derived using satellite remote sensing data, was considered to be a fairly robust index and was highly correlated to chlorophyll fluorescence and predawn leaf water potential.
- GNDVI has the potential to be used to map spatial patterns of winter-time plant stress for different genera/species and in different geographical locations when using satellite remote sensing data.
- Predawn leaf water potential measurements were found to be strongly correlated to spectral indices derived from high and medium spectral resolution satellite data.
- Two individual spectral wavebands acquired using airborne multispectral remote sensing data (Chapter 6), the green and blue band, which are sensitive to changes in plant pigment content in the visible region of the spectrum, was related to total carotenoid pigment content.

- Five vegetation spectral indices, four of which are sensitive to changes in plant pigment content ((850 – 710)/(850 – 680) (DATT, 1999), PSRI, GNDVI, NDVI), and normalised difference water index (NDWI) which captures changes in plant water content, performed well when applied to airborne hyperspectral remote sensing data (Chapter 6).
- The DATT (1999) spectral reflectance model (850 – 710)/(850 – 680), when derived from airborne remote data, was considered to be a fairly robust index, which was correlated to ground based measurements of chlorophyll fluorescence and predawn leaf water potential.
- Predawn leaf water potential measurements were found to be strongly correlated to spectral indices derived from the visible, near-infrared and short-wave infrared region of the airborne hyperspectral data.
- The highest adjusted R^2 value (90.5%) was obtained for the model derived between predawn leaf water potential (PLWP) and the water band index (WBI) when using hyperspectral satellite imagery. However, this model was derived only for the West Wits mining district and, as this study has clearly illustrated, that reflectance models are site- and species-specific, this model should not be applied across the Vaal River and Welkom mining districts. It is recommended future studies test this model on other species at other sites.

8.3 CONCLUDING REMARKS

Spectral reflectance analyses undertaken consistently identified specific spectral wavelengths which are useful as indicators of plant water stress, and could be further linked to other plant physiological conditions. Spectral bands extracted from the visible and near-infrared regions of the spectrum (550, 676, 680, 690, 695, 705, 710, 750, 760, 800, 900, 970 nm), including the red-edge region defined from 690 to 740 nm, used to derive the models for mapping spatial patterns of plant water stress in the Welkom, Vaal River and West Wits mining districts, were found to be important indicators of plant water stress. These results strongly support the research undertaken by several other researchers around the globe (Curran *et al*., 1990; Carter, 1993; Baret *et al*., 1994; Filella and Penuelas 1994; Gitelson and Merzlyak,

1996; Lichtenthaler *et al*., 1996; Blackburn, 1998b; Lelong *et al*., 1998; Blackburn, 1999; Gitelson *et al*., 2002; Clay *et al*. 2006; Fitzgerald *et al*. 2006; Blackburn 2007; Campbell *et al*. 2007).

The preliminary findings that plant stress does influence the wood anatomical characteristics, specifically radial vessel diameter, vessel frequency and wood density in *E. camaldulensis*, *E. sideroxylon* and *S. lancea* were shown for the three mining districts (Appendix 6). In general, trees experiencing higher plant water stress displayed smaller vessel diameters when compared to less stressed or healthy trees. These results are in accordance with studies which indicated that water stress in plants induces a decrease in xylem vessel diameters (Zimmerman and Milburn, 1982; Zhang *et al*., 1988; February, 1993; February, 1994; February *et al*., 1995; Lovisolo and Schubert, 1998; Naidoo *et al*., 2006). However, sites which were influenced by high levels of contaminated water also displayed smaller vessel diameters, indicating that the uptake of contaminants could affect the wood anatomy of plants. Trees considered to be experiencing higher plant water stress displayed higher vessel frequency.

8.4 RECOMMENDATIONS

The South African Government has ratified several international and national interventions and frameworks including the Copenhagen Accord (2009) to support sustainable use of our natural resources and protection of our country's environmental assets, including sustaining and protecting our water resources and biodiversity assets in South Africa. Considering these global and local pressures, efforts to reduce the movement of polluted water from near surface seepage and groundwater shallow aquifers into lands adjacent to the TSFs are paramount. Recommendations to use tree belts to absorb and transpire greater quantities of water than the grasslands and wetlands presently in close proximity to the TSFs could reduce water table depths and slow lateral contaminated flows into the surrounding lands.

The geophysical surveys undertaken in the three mining districts which provided detailed subsurface information on groundwater saturation and an indication of the salinity conditions

confirms the presence of "relatively" shallow and saline groundwater sources. This would imply that trees roots could access the "relatively" shallow groundwater even during the dry winter season and assist in containing contaminated groundwater seeping into surrounding lands.

Exploration of relationships between vegetation indices derived from leaf-level, satellite and airborne spectral reflectance data and ground-based measurements used as "surrogate" measures of plant water stress revealed that several prominent and recurring spectral reflectance indices could be applied to identify plant water stress within the Welkom, Vaal River and West Wits mining districts. The models recommended for mapping and detecting spatial patterns of plant water stress when using different sources of remote sensing data include:

- **Chlorophyll b DATT** spectral reflectance model (section 4.3.2.3) when derived from leaf-level spectral reflectance data, could be applied across all three mining districts.
- **Predawn leaf water potential GNDVI** spectral reflectance model (section 5.3.2.3) and **predawn leaf water potential water band** index spectral reflectance model (section 5.3.3.3) when utilising satellite multispectral and hyperspectral remote sensing data.
- **Carotenoid content green band** spectral reflectance model (section 6.3.1.3) can be used for airborne multispectral resolution data.
- **Predawn leaf water potential NDVI** spectral reflectance model (section 6.3.2.3) is best suited for airborne high spatial and hyperspectral resolution data.

It is evident from the proposed models that chlorophyll content, carotenoid content and predawn leaf water potential are important "surrogate" measures of plant water stress for the three species *E. camaldulensis*, *E. siderxylon* and *S. lancea* investigated in the Welkom, Vaal River and West Wits mining districts.

It is also recommended that future studies test the model derived between predawn leaf water potential and the water band index, which achieved the highest adjusted R^2 value (90.5%) when using hyperspectral satellite imagery obtained for the West Wits mining district.

Furthermore, a preliminary study also highlighted that plant stress does influence the wood anatomical characteristics (radial vessel diameter, vessel frequency and wood density) in *E. camaldulensis*, *E. sideroxylon* and *S. lancea* trees in the three mining districts (Appendix 6). Therefore, it is also recommended that a more rigorous approach, using simple wood coring technologies, could be developed to improve our understanding of long-term manifestations of water and contaminant stress on wood anatomy of plants without compromising on biomass production.

This study has clearly demonstrated the potential of using remote sensing technologies together with ground-based measurements to detect winter-time plant stress in *E. camaldulensis*, *E. sideroxylon* and *S. lancea* trees in the Welkom, Vaal River and West Wits mining districts. Such methodologies could be easily transferred to other industries such as agriculture in support of existing practices to spatially map and detect stress patterns in agricultural crops. Furthermore, remote sensing based surface energy balance models which are more readily used nowadays to simulate spatial patterns of evaporation, should be modified to include plant stress reflectance models, to allow users to evaluate the correlation between surface energy fluxes, evaporation and plant stress.

It is also recommended that the mining companies, such are AngloGold Ashanti together with government line departments such as Department of Agriculture, Forestry and Fisheries (DAFF) and Department Water and Environmental Affairs (DWEA), use information generated from such studies to support the development of catchment or site monitoring tools which can be used to assess the water use within a catchment on a regular time-step, and which can assist water and mine managers when making decisions regarding the water resources within catchments. More specifically, such operational tools could then be used to illustrate the “spatial” benefits of programmes such as the Mines Woodlands Project.

REFERENCES

ALDER, N.N., SPERRY, J. S. and POCKMAN, W.T., 1996, Root and stem xylem embolism, stomatal conductance, and leaf turgor in *Acer grandidentatum* populations along a soil moisture gradient. *Oecologia*, **105**, 293-301.

ALLEN, S.G. and NAKAYAMA, F.S., 1988, Relationship between crop water stress index and other physiological plant water status indicators in guayule. *Field Crops Research*, **18**, 287-296.

ANGELOPOULOS, K., DICHIO, B. and XILOYANNIS C., 1996,Inhibition of photosynthesis in Olive trees (*Olea Europaea* L.) during water stress and rewatering. *Journal of Experimental Botany*, **47**, 1093–1100.

ANGLOGOLD ASHANTI., 2004, Geological spatial maps for Vaal River and West Wits mining districts. Klerksdorp, North West Province, South Africa.

ARANDA, I., CASTRO, L., PARDOS, M., GIL, L. and PARDOS, J.A., 2005, Effects of the interaction between drought and shade on water relations, gas exchange and morphological traits in cork oak (*Querucus suber* L.) seedlings. *Forest Ecology and Management*, **210**, 117-129.

ARCGIS, 2009, version 9.3, ESRI GIS and Mapping Software.

ASNER, G.P., 1998, Biophysical and biochemical sources of variability in canopy reflectance. *Remote Sensing of Environment*, **64**, 234-253.

BANNARI, A., GUEDON, A.M., EL-HARTI, A., CHERKAOUI, F.Z. and EL-GHMARI, A., 2008, Characterization of slightly and moderately saline and sodic soils in irrigated agricultural and using simulated data of advanced land imaging (EO-1) sensor. *Communications in Soil Science and Plant Analysis*, **39**, 2795–2811.

BARET F. and JACQUEMOUD S., 1994, Model inversion to retrieve canopy characteristics from high spectral resolution data. In *Proceedings of the 6th International Symposium Physical Measurements and Signatures in Remote Sensing*, 17-21 January 1994, Val d'Isère (France).

BARET, F., VANDERBILT, V.C., STEVEN, M.D. and JACQUEMOUD, S., 1994, Use of spectral analogy to evaluate canopy reflectance sensitivity to leaf optical properties. *Remote Sensing of Environment*, **48**, 253-260.

BARRS, H.D. and WEATHERLY, P.E., 1962, A re-examination of the relative turgidity technique for estimating water deficits in leaves. *Australian Journal of Biological Sciences*, **15**, 413-428.

BATCHELARD, E.P., 1986, Effects of soil moisture stress on the growth of seedlings of three eucalypt species. III. Tissue-water relations. *Australian Forestry Research*, **16**, 155-163.

BECK, R., 2003, EO-1 User Guide v 2.3. USGS Earth Resources Observation Systems Data Center, 74p.

BELL, D.T., 2006, Australian trees for the rehabilitation of water logged and salinity damaged landscapes. *Australian Journal of Botany*, **47**, 697-716.

BEN-DOR, E., METTERNICHT, G., GOLDSHLEGER, N., MOR, E., MIRLAS, V. and BASSON, U., 2009, Chapter 3: Remove of remote sensing based methods to assess soil salinity. In: Remote sensing of soil salinization: Impact on land management. Edited by Graciela Metternicht and J. Alfred Zink. ISBN: 978-1-4200-6502-2, Published by: CRC Press, Pages: 377.

BEN-DOR, E., PATKIN, K., BANIN, A. and KARNIELI, A., 2002, Mapping of several soil properties using DAIS-7915 hyperspectral scanner data. A case study over soils in Israel. *International Journal of Remote Sensing*, **23**, 1043– 1062.

BEST, H.J., 1985, Water pollution aspects related to the mining industry. *Proceedings of the Mine Ventilation Society Symposium on Mine Water Systems 1985*.

BIAN, L., BUTLER, R., QUATTROCHI, DA. and ATKINSON, P.M., 1999, Comparing effects of aggregation methods on statistical and spatial properties of simulated spatial data. *Photogrammetry and Remote Sensing*, **65**, 73-84.

BLACKBURN, G.A., 1998a, Quantifying chlorophylls and carotenoids at leaf and canopy scales: an evaluation of some hyperspectral approaches. *Remote Sensing of Environment*, **66**, 273-285.

BLACKBURN, G.A., 1998b, Spectral indices for estimating photosynthetic pigment concentrations: a test using senescent tree leaves, *International Journal of Remote Sensing*, **19**, 657-675.

BLACKBURN, G.A., 1999, Relationship between spectral reflectance and pigment concentrations in stacks of deciduous broadleaves. *Remote Sensing of Environment,***70**, 224-237.

BLACKBURN, G.A., 2002, Remote sensing of forest pigments using airborne imaging spectrometer and LIDAR imagery. *Remote Sensing of Environment*, **82**, 311-321.

BLACKBURN, G.A., 2007, Hyperspectral remote sensing of plant pigments. *Journal of Experimental Botany*, **58**, 855-867.

BLIGHT, G.E., 1991, Erosion and anti-erosion measures for abandoned gold tailings dams. *Proceedings of the National Meeting of the American Society for Surface Mining and Reclamation, Durongo, Colorado, May 1991*: 323-330.

BLUM, A., SULLIVAN, C.Y., and EASTIN, J.D., 1973, On the pressure chamber technique for estimating leaf water potential in sorghum. *Agronomy*, **65**, 337-338

BOYER, J.S., 1968, Relationship of water potential to growth of leaves. *Plant Physiology*, **43**, 1056-1062.

BOYER, J.S., ANNOND, P.A and SHARP, RE., 1987, Light stress and leaf water relations. *Photoinhibition Topics in Photosynthesis*, **9**, 111-122.

BRIEMAN, L., and SPECTOR, P., 1992, Submodel selection and evaluation in regression: The X-random case. *International Statistical Review*, **60**, 291-319.

BURGESS, S.S.O., ADAMS, M.A., TURNER, N.C., WHITE, D.A. and ONG, C.K., 2001, Tree roots, conduits for deep recharge of soil water. *Oecologi*, **126**, 158-165.

CAMPBELL, G.S., 1990, Instrumentation of studying vegetation canopies for remote-sensing in optical and thermal infrared regions - water potential in soils and plants. *Remote Sensing Reviews*, **5**, 249-261.

CAMPBELL, P.K.E., MIDDLETON, E.M., McMURTREY, J.E., CORP, L.A., and CHAPPELLE, E.W., 2007, Assessment of vegetation stress using reflectance or fluorescence measurements. *Journal of Environmental Quality*, **36**, 832-845.

CANNY, M.J. and HUANG, C.X., 2006, Leaf water content and palisade cell size. *New Phytologist*, **170**, 75-85.

CARTER, G.A., 1993, Responses of leaf spectral reflectance to plant stress. *American Journal of Botany*, **80**, 239-243.

CARTER, G.A., 1994, Ratios of leaf reflectances in narrow wavebands as indicators of plant stress. *International Journal of Remote Sensing*, **15,** 697-703.

CASTRO-ESAU K.L., SANCHEZ-AZOFEIFA, G.A. and CAELLI, T., 2004, Discrimination of lianas and trees with leaf level hyperspectral data. *Remote Sensing of Environment*, **90,** 353-372.

CATSKY, J., 1969, Temperature effects in the measurement of water saturation deficit (relative water content) in tobacco and kale. *Biologia Plantarum*, **11**, 381-383.

CECCATO, P., FLASSE, S., TARANTOLA, S., JACQUEMOUD, S. and GREGOIRE, J-M., 2001, Detection of vegetation leaf water content using reflectance in the optical domain. *Remote Sensing of Environment*, **77**, 22-33.

CHAMBER OF MINES OF SOUTH AFRICA., 2004, Facts and figures. Produced by Communication Services of the Chamber of Mines of South Africa, Johannesburg.

CHAMPAGNE, C.M., STAENZ, K., BANNARI, A., McNAIRIN, H. and DEGUISE, J.C., 2003, Validation of a hyperspectral curve fitting model for the estimation of plant water content of agricultural canopies. *Remote Sensing of Environment*, **87**, 148-160.

CHAPPELLE, E.W., KIM, M.S., AND MCMURTREY, J.E., 1992, Ratio analysis of reflectance spectra RARS: an algorithm for the remote estimation of the concentrations of chlorophyll *a*, chlorophyll *b*, and carotenoids in soybean leaves. *Remote Sensing of Environment*, **39**, 239-247.

CHAVES, M.M., FLEXAS, J. and PINHEIRO, C., 2009, Photosynthesis under drought and salt stress: regulation mechanisms from whole plant to cell. *Annals of Botany*, **103**, 551–560.

CHEN, J., 1999, Spatial scaling of a remotely sensed surface parameter by contexture. *Remote Sensing of Environment*, **69**, 30–42.

CHEVREL, S., COURANT, C., COTTARD, F., COETZEE, H., BOURGIUGNON, A. and NTSUME, G., 2003, Very high resolution remote sensing coupled to GIS-based environmental assessment - East Rand goldfield, South Africa. French Council for Geosciences Report BRGM/RP-52724-FR.

CHOI, A.M., KUSTAS, B.W.P., ANDERSON, B.M.C., ALLEN, C.R.G., LI, D.F. and KJAERSGAARD, D.J.H., 2009, An inter-comparison of three remote sensing-based surface energy balance algorithms over a corn and soybean production region, Iowa, U.S. during SMACEX. *Agricultural and Forest Meteorology*. In press.

CHUN-JIANG, Z., JI-HUA, W., LIANG-YUN, L., WEN-JIANG, H. and QI-FA, Z., 2006, Relationship of 2100-2300nm spectral characteristics of wheat canopy to leaf area index and leaf N as affected by leaf water content. *Pedosphere*, **16**, 333-338.

CIFRE, J., BOTA, J., ESCALONA, J.M., MEDRANO, H. and FLEXAS, J., 2005, Physiological tools for irrigation scheduling in grapevine (*Vitis vinifera* L.) An open gate to improve water-use efficiency. *Agriculture, Ecosystems and Environment*, **106**, 159-170.

CLAY, D.E., CHANG, K.K.J., CLAY, S.A., and DALSTED, K., 2006, Characterizing water and nitrogen stress in corn using remote sensing. *Agronomy Journal*, **98**, 579-587.

CLEARY, B. and ZAERR, J. 1984, Guidelines for measuring plant moisture stress with a pressure chamber. PMS Instrument Company. Royal Oaks Drive, Corvallis, Oregon, USA.

COETZEE, H., WINDE F. and WADE, P., 2006, An assessment of sources, pathways, mechanisms and risks of current and potential future pollution of water and sediments in gold mining areas of the Wonderfontein spruit catchment, Gauteng, North West Province, South Africa. WRC Report No. 1214/1/06, ISBN 1-77005-419-7, Pretoria.

COGHO, V.E., VAN NIEKERK, L.J., PRETORIUS, H.P.J. and HODGSON, F.D.I., 1990, The development of techniques for the evaluation and effective management of surface and ground-water contamination in the Orange Free State Goldfields. Final Report to the WRC Steering Committee. COLLINS, W., CHANGE, S.H., RAINES, G., CANNEY, F. and ASHLEY, R., 1983, Airborne biogeophysical mapping of hidden mineral deposits. *Economic Geology*, **78**, 737-749.

CONGALTON, R.G. and MEAD, R.A., 1983, A quantitative method to test for consistency and correctness in photointerpretation. *Photogrammatric Engineering and Remote Sensing*, **49**, 69-74.

CONGALTON, R.G. and GREEN, K., 1993, A practical look at the sources of confusion in error matrix generation. *Photogrammetric Engineering and Remote Sensing*, **59**, 641-644.

CONGALTON, R.G., 1994, Accuracy assessment of remotely sensed data: future needs and directions. In: Proc. 12th Pecroa Symposium, American Society for Photogrammetry and Remote Sensing, Bethesda, MD (1994), 385-388.COOPS, N., DURY, S., SMITH, M.L., MARTIN, M. and OLLINGER, S., 2002, Comparison of green leaf eucalypt spectra using spectral decomposition. *Australian Journal of Botany*, **50**, 567-576.

COOPS, N., STONE, C., CULVENOR, D.S., CHISHOLM, L.A. and MERTON, R.N., 2003, Chlorophyll content in eucalypt vegetation at the leaf and canopy scales as derived from high resolution spectral data. *Tree Physiology*, **23**, 23-31.

COUNCIL FOR GEOSCIENCES., 1998, The mineral resources of South Africa. Handbook 16, Cape Town.

CSILLAG, F., PA´SZTOR, L. and BIEHL, L., 1993, Spectral band selection for the characterization of salinity status of soils. *Remote Sensing of Environment*, **43**, 231– 242.

CURRAN, P.J., DUNGAN, J.L. and GHOLZ, H.L., 1990, Exploring the relationship between reflectance red-edge and chlorophyll content in slash pine. *Tree Physiology*, **7**, 33-48.

CURRAN, P.J., DUNGAN, J.L., MACLER, B.A. and PLUMMER, S.E., 1992, The effect of a red leaf pigment on the relationship between red-edge and chlorophyll concentration. *Remote Sensing of Environment*, **35**, 69-75.

CURRAN, P.J., WINDHAM, W.R., & GHOLZ, H.L., 1995, Exploring the relationship between reflectance red edge and chlorophyll concentration in Slash Pine leaves. *Tree Physiology*, **15**, 203-206.

DATT, B., 1998, Remote sensing of chlorophyll a, chlorophyll b, chlorophyll a + b, and total carotenoid content in Eucalyptus leaves. *Remote sensing of Environment*, **66**, 111-121.

DATT, B., 1999, A new reflectance index for remote sensing of chlorophyll content in higher plants: tests using *Eucalyptus* leaves. *Journal of Plant Physiology*, **154**, 30-36.

DATTA, K. S. and SHARMA, K. D., 1990, Effect of chloride and sulphate types of salinity on characteristics of chlorophyll content photosynthesis and respiration of chickpea *Cicerarietinum* L. *Biologia Plantarum*, **32**, 391–395.

DE MENEZES, M., DE ASSIS, GOMES., MAGALHAES, A.M., LAGOA, A., LAZARO, C. AND EDUARDO, M., 2004, Interactions between leaf water potential, stomatal conductance and abscisic acid content of orange trees submitted to drought stress. *Brazilian Journal of Plant Physiology*, **16**, 155-161.

DE TAR, W.R., PENNER, J.V. and FUNK, H.A., 2006, Airborne remote sensing to detect plant water stress in full canopy cotton. *Transactions of the Society of Agricultural and Biological Engineers*, **49**, 655-665.

DEPARTMENT OF TOURISM, ECONOMIC and ENVIRONMENTAL AFFAIRS OF THE FREE STATE PROVINCE., 2002, The Waste Legkotla Conference, Bloemfontein.

DICHIO, B., XILOYANNIS, C., SOFO, A. and MONTANARO, G., 2006, Osmotic regulation in leaves and roots of olive trees during a water deficit and re-watering. *Tree Physiology*, **26**, 179-185.

DICKINSON, N.M., MACKAY J.M., GOODMAN, A. and PUTWAIN, P., 2000, Planting trees on contaminated soils: issues and guidelines. *Land Contamination and Reclamation*, **8**,87-101.

DIXON, H.H., 1914, Transpiration and the ascent of sap in plants. Macmillan, London. 75p.

DOWNES, G.M., WIMMER, R. AND EVANS, R. 2002, Understanding wood information: gains to commercial forestry through tree-ring research. *Dendrochronologia*, **20**, 37-51.

DUTKIEWICZ, A., LEWISA, M. and OSTENDORF, B., 2006, Mapping surface symptoms of dryland salinity with hyperspectral imagery. ISPRS Commission VII Mid-term Symposium Remote Sensing: From Pixels to Processes, Netherlands, 8-11 May 2006.

DYE, P.J., 1996, Response of Eucalyptus grandis trees to soil water deficits. *Tree Physiology*, 1**6**, 233-238.

DYE, P., 2004, Personal Communication. CSIR, Natural Resources and the Environment, Ecophysiology Research Group, Pietermaritzburg, South Africa.

DYE, P., WEIERSBYE, I.M., LABUSCHAGNE, P. and XABA, J., 2005, The pattern of water use and pollutant sequestration by *Searsia lancea* growing on acid mine drainage in the highveld region. Report by CSIR, Natural Resources and Environment and the University of the Witwatersrand to Anglogold Ashanti Ltd. (submitted).

DYE, P.J., 2002, 3-PG simulation of growth and water use of *Eucalyptus camaldulensis* in the Mahem Spruit catchment, Welkom. CSIR Report ENV-D-C 2002 016, Division of Water, Environment and Forestry, CSIR, Pretoria.

EDMANDS, J.D., BRABANDER, D.J. and COLEMAN, D.S. 2001, Uptake and mobility of uranium in black oaks: implications for biomonitoring depleted uranium-contaminated groundwater. *Chemosphere*, **44**, 789-795.

EITEL, J.U.H., GESSELER, P.E., SMITH, A.M.S. and ROBBERECHT, R., 2006, Suitability of existing and novel spectral indices to remote detect water stress in *Populus* spp. *Forest Ecology and Management*, **229**, 170-182.

ENVI 4.1. 2005. Spectral Analysis with ENVI. Global Services Research Systems Incorporated, 106p.

FARIFTEHA, J. and FARSHAD, T.A., 2006, Assessing salt-affected soils using remote sensing, solute modelling, and geophysics. *Geoderma*, **130**, 191–206.

FEBRUARY, E.C. 1993, Sensitivity of xylem vessel size and frequency to rainfall and temperature: implications for palaeontology. *Palaeontologia African*, **30**, 91-95.

FEBRUARY, E.C. 1994, Rainfall reconstruction using wood charcoal from two archeological sites in South Africa. *Quaternary Research*, **42**, 100-107.

FEBRUARY, E.C., STOCK, W.D., BOND, W.J. and LE ROUX, D.J. 1995, Relationships between water availability and selected vessel characteristics in *Eucalyptus grandis* and two hybrids. *IAWA*, **16**, 269-276.

FILELLA, I. and PENUELAS, J., 1994, The red edge position and shape as indicators of plant chlorophyll content, biomass and hydric status. *International Journal of Remote Sensing*, **15**, 1459-1470.

FITZGERALD, G.J., RODRIGUEZ, D., CHRISTENSEN, L.K., BELFORD, R., SADRAS, V.O. and CLARKE, T.R., 2006, Spectral and thermal sensing for nitrogen and water status in rainfed and irrigated wheat environments. *Precision Agriculture*, **7**, 233-248.

FOODY, G.M., 2004, Thematic map comparison: Evaluating the statistical difference in classification accuracy. *Photogrammetric Engineering and Remote Sensing*, **70**, 627-633.

FOODY, G.M. and MATHUR, A., 2006, The use of training sets containing mixed pixels for accurate hard image classification: Training on mixed spectral responses for classification by SVM. Remote Sensing of Environment, **103**, 179-189.

FOURTY, T. and BARET, F., 1997, Vegetation water and dry matter contents estimated from top of the atmosphere reflectance data: a simulation study. *Remote Sensing of Environment*, **61**, 34-45.

FUNKE, J.W. 1990, The water requirements and pollution potential of South African gold and uranium mines. Water Research Commission, Report No. KV 9/90, Pretoria, South Africa.

GAIA., 2003,*Proceedings of the Gaia global meeting, Penang, Malaysia, March 17-21, 2003.*

GAMON, J.A. and SURFUS, J.S., 1999, Assessing leaf pigment content and activity with a reflectometer. *New Phytologist*, **143**, 105-117.

GAO, B.C., 1995, Normalized difference water index for remote sensing of vegetation liquid water from space. *Proceedings of the International Society of Optical Engineering*, **2480**, 225-236.

GAUSMAN, H.W. and ALLEN, W.A., 1973, Optical parameters of leaves of 30 plant species. *Plant Physiology*, **52**, 57-62.

GAUSSMAN, H.W., 1977, Reflectance of leaf components. *Remote Sensing of Environment*, **6**, 1-9.

GENSTAT, 2008, version 11.1, VSN International Ltd.

GEORGE, R.J., NULSEN, R.A., FERDOWNSIAN, R. and RAPER, G.P., 1999, Interactions between trees and groundwaters in recharge and discharge areas – A survey of Western Australia sites. *Agricultural Water Management*, **39**, 91-113.

GIANNICO, C., 2004, Remote sensing of vegetation in the calabrian region. *Acta Astronautica*, **60**, 119-131.

GITELSON, A.A. and MERZLYAK, M.N., 1996, Signature analysis of leaf reflectance spectra: algorithm development for remote sensing of chlorophyll. *Journal of Plant Physiology*, **148**, 494-500.

GITELSON, A.A. and MERZLYAK, M.N., 1997, Remote estimation of chlorophyll content in higher plant leaves. *International Journal of Remote Sensing*, **18**, 2691-2697.

GITELSON, A.A., ZUR, Y., CHIVKUNOVA, O.B. and MERZLYAK, M.N., 2002, Assessing carotenoid content in plant leaves with reflectance spectroscopy. *Photochemistry and Photobiology*, **75**, 272-281.

GLENN, E.P., HUETE, A.R., NAGLER, P.L. and NELSON, S.G., 2008, Relationship between remotely sensed vegetation indices, canopy attributes and plant physiological processes: what vegetation indices can and cannot tell us about the landscape. *Sensors*, **8**, 2136-2160.

GOMES, M.M.A., LAGOA, M.M.A., MEDINA, C.L., MACHADO, E.C. and MACHADO, M.A., 2004, Interactions between leaf water potential, stomatal conductance and abscisic acid content of orange trees submitted to drought stress. *Brazilian Journal of Plant Physiology*, **16**, 155-161.

GONSAMO, A. and PELLIKKA, P., 2009, A new look at top-of-canopy gap fraction measurements from high-resolution airborne imagery. *EARSeL eProceedings*, **8**, 64-74.

GOOGLE EARTH, 2008, http://earth.google.com/ Accessed June 2008.

GOVENDER, M., DYE, P.J., WEIERSBYE, I.M., WITKOWSKI, E.T.F. and AHMED, F., 2009, Review of commonly used remote sensing and ground-based technologies to measure plant water stress. *Water SA*, **35**, 739-750.

GOVENDER, M., CHETTY, K., NAIKEN, V. and BULCOCK, H., 2008, A comparison of satellite hyperspectral and multispectral remote sensing imagery for improved classification and mapping of vegetation. *Water SA*, **34**, 147-154.

GOVINDJEE, DOWNTON W.J.S., FORK, D.C., and ARMOND, P.A., 1981, Chlorophyll a fluorescence transient as an indicator of water potential of leaves. *Plant Science Letter*, **20**, 191.

GREVEN, M.A., NEAL, A.S., STEVE GREEN, B.S., DICHIO, C.B.B. and CLOTHIER, B., 2009, The effects of drought on the water use, fruit development and oil yield from young olive trees. *Agricultural Water Management*, **96**, 1525-1531.

GUYOT, G. and BARET, F., 1988, Utilization of high spectral resolution to follow the state of vegetable cover. In *Proceedings 4th International Symposium Spectral Signatures of Objects in Remote Sensing*, 18-22 January, Aussois pp. 54-61.

HACKE, U. and SAUTER, J.J., 1996, Drought –induced xylem dysfunction in petioles, branches and roots of *Populus balsamifera* L. and *Alnus glutinosa* (L.) Gaertn. *Plant Physiology*, **111**, 413-417.

HARRIS, A., BRYANT, R.G. and BAIRD, A.J., 2006, Mapping the effects of water stress on *Sphagum*: Preliminary observations using airborne remote sensing. *Remote Sensing of Environment*, **100**, 363-378.

HAVAUX, M. and LANNOYE, R., 1983, Chlorophyll fluorescence induction: a sensitive indicator of water stress in maize plants. *Irrigation Science*, **4**, 147-151.

HE, Y. and MUI, A., 2010, Scaling up semi-arid grassland biochemical content from the leaf to the canopy level: challenges and opportunities. *Sensors*, 10, 11072-11087.

HICK, P. T. and RUSSELL, W. G. R., 1990, Some spectral considerations for remote sensing of soil salinity. *Australian Journal of Soil Research*, **28**, 417– 431.HODGSON, F.D.I., USHER,

B.H., SCOTT, R., ZEELIE, S., CRUYWAGEN, L.-M., and DE NECKER, E., 2001, Prediction techniques and preventative measures relating to the post operational impact of underground mines on the quality and quantity of groundwater resources. Water Research Commission, Report No. 699/1/01.

HONG, S.H., JAN M.H. HENDRICKX, J.M.H. and BORCHERS, B. 2009, Up-scaling of SEBAL derived evapotranspiration maps from Landsat (30 m) to MODIS (250 m) scale. *Journal of Hydrology*, **370**, 122–138.

HORLER, D.N.H., DOCKRAY, M. and BARBER, J., 1983, The red edge of plant reflectance. *International Journal of Remote Sensing*, **4**, 273-288.

HOWARI, F.M., GOODELL, P.C. and MIYAMOTO, S., 2002, Spectral properties of salt crusts formed on saline soils. *Journal of Environmental Quality*,**31**, 1453-1461.

HSIAO, T.C., 1973, Plant responses to water stress. *Annual Review Plant Physiology*, **24**, 519-570.

HSIAO, T.C., 1990, Measurements of plant water status. In *Irrigation of Agricultural Crops*, B.A. Stewart and D.R. Nielson (Eds.) *Agronomy Monograph*, **30**, 244-279.

HUNT, E.R. and ROCK, B.N., 1989, Detection of changes in leaf water content using near- and middle infrared reflectances. *Remote Sensing of Environment*, **30**, 43-54.

HUNT, G., SALISBURY, J. and LENHOFF, C., 1972, Visible and near infrared spectra of minerals and rocks: v. halides, phosphates, arsenates, venadates and borates. *Modern Geology*, **3**, 121–132.

INTRIGLIOLO, D.S. and CASTEL, J.R., 2006, Performance of various water stress indicators for prediction of fruit size response to deficit irrigation in plum. *Agricultural Water Management*, **83**, 173-180.

ISCW. 1993. Land type series. Department of Agricultural and Water Supply, Pretoria, Institute for Soil Climate and Water. *Memoirs on the Agricultural Natural Resources of South Africa*.

JACKSON, T.J., CHEN, D., COSH, M., LI, F., ANDERSON, M., WALTHALL, C., DORIASWAMY, P. and HUNT, E.R., 2004, Vegetation water content mapping using

Landsat data derived normalized difference water index for corn and soybeans. *Remote Sensing of Environment*, **92**, 475-482.

JACQUEMOUD, S., 1993, Inversion of the PROSPECT + SAIL canopy reflectance model from AVIRIS equivalent spectra: theoretical study. *Remote sensing of Environment*, **44**, 281-292.

JIANG, Z., HUETE, A.R., CHEN, J., CHEN, Y., LI, J., YAN, G. and ZANG, X., 2006, Analysis of NDVI and scaled difference vegetation index retrievals of vegetation fraction. *Remote sensing of Environment*, **101**, 366-378.

JOLY, R.J., 1985, Techniques for determining seedling water status and their effectiveness in assessing stress. In *Proceedings of Evaluating seedling quality: principles, procedures and predictive abilities of major tests*, October 16-18 1984. Forest Research Laboratory, Oregon State University, Corvallis.

JONES, H.G., 2004, Irrigation scheduling: advantages and pitfalls of plant-based methods. *Journal of Experimental Botany*, **55**, 2427-2436.

JUANG, K.W., LEE, D.Y. and ELLSWORTH, T.R., 2001, Using rank-order geostatistics for spatial interpolation of highly skewed data in a heavy-metal contaminated site. *Journal of Environmental Quality*, **30**, 894-903.

KRUCE, F., LEFKOFF, A., BOARDMAN, J., HEIDEBRECHT, K., SHAPIRO, A., BARLOON, P. and GOETZ, A., 1993, The spectral image processing system (SIPS) interactive visualization and analysis of imaging spectrometer data. *Remote Sensing of. Environment*, **44,** 145-163.

LAMONT, B.B. and WITKOWSKI, E.T.F., 1995, A test for lottery recruitment among four *Banksia* species based on their demography and biological attributes. *Oecologia***101**, 299-308.

LAMONT, B.B., REES, R.G., WITKOWSKI, E.T.F. and WHITTEN, V.A., 1994, Comparative size, fecundity and ecophysiology of roadside plants of *Banksia hookeriana*. *Journal of Applied Ecology*, **31**, 137-144.

LANDIS, J. and KOCH, G. 1977. The measurement of observer agreement for categorical data. *Biometrics*, **33**, 159-174.

LELONG, C.C.D., PINET, P.C. and POILVÉ, H., 1998, Hyperspectral imaging and stress mapping in agriculture: a case study on wheat in Beauce (France). *Remote Sensing of Environment*, **66**, 179-191.

LICHTENTHALER, H.K., 1987, Chlorophyll and carotenoids: pigments of photosynthetic biomembranes. *Methods in Enzymology*, **148**, 331-382.

LICHTENTHALER, H.K., ALEXANDER, A.C., MAREK, M.V., KALINA, J. and URBAN, O., 2007, Differences in pigment composition, photosynthetic rates and chlorophyll fluorescence images of sun and shade leaves of four tree species. *Plant Physiology and Biochemistry*, 1-12.

LICHTENTHALER, H.K., BUSCHMANN, C., RINDERLE, U. and SCHMUCH, G., 1996, Application of chlorophyll fluorescence in ecophysiology. *Radiation Environment Biophysics*, **25**, 297-308.

LILLESAND, T.M. and KIEFER, R.W., 1999, *Remote Sensing and Image Interpretation.* John Wiley and Sons, Inc. New Jersey.LINTON, M.J., SPERRY, J.S. AND WILLIAMS, D.G., 1998, Limits to water transport in *Juniperus osteosperma* and *Pinus edulis*: implications for drought tolerance and regulation of transpiration. *Functional Ecology*, **12**, 906-911.

LOVISOLO, C. and SCHUBERT, A. 1998, Effects of water stress on vessel size and xylem hydraulic conductivity in *Vitis vinifera L. Journal of Experimental Botany*, **29**, 693-700.

LU, C. and ZHANG, J., 1999, Effects of water stress on photosystem II photochemistry and its thermostability in wheat plants. *Journal of Experimental Botany*, **50**, 1199-1206.

LYNCH, S.D., and SCHULZE, R.E., 2006, Rainfall databases. In: Schulze, R.E. (Ed.). 2006. South African Atlas of Climatology and Agrohydrology. Water Research Commission, Pretoria, RSA, WRC Report 1489/1/06, Section 2.2.

MAIRE, le G., FRANÇOIS, C. and DUFRÊNE, E. 2004, Towards universal broad leaf chlorophyll indices using PROSPECT simulated database and hyperspectral reflectance measurements. *Remote Sensing of Environment*, **89**, 1 –28.

MANE, S.P., VASQUEZ-ROBINET, C., SIOSON, A.A., HEATH, L.S. and GRENE, R., 2011, Early PLDα-mediated events in response to progressive drought stress in *Arabidopsis*: a transcriptome analysis. *Journal of Experimental Botany*, **58**, 241-252.

MARIGNANI, M., DEL VICO, E. and MACCHERINI, S., 2007, Spatial scale and sampling size affect the concordance between remotely sensed information and plant community discrimination in restoration monitoring. *Biodiversity Conservation*, **16**, 3851–3861.

MEAGHER, R.B., 2000, Phytoremdiation of toxic elemental and organic pollutants. *Current opinion in Plant Biology*, **3**,153-162.

MERZLYAK, M.N., SOLOVCHENKO, A.E., and GITELSON, A.A., 2003a, Reflectance spectral features and non destructive estimation of chlorophyll, carotenoid and anthocyanin content in apple fruit. *Postharvest Biology and Technology*, **27**, 197-211.

MERZYLAK, M.N., GITELSON, A.A., CHIVKUNOVA, A.E., SOLOVCHENKO, E., and POGOSYAN, S.I., 2003b, Application of reflectance spectroscopy for analysis of higher plant pigments. *Russian Journal of Plant Physiology*, **50**, 704-710.

METCALFE, J.C., DAVIES, W.J. and PEREIRA, J.S., 1990, Leaf growth of Eucalyptus globulus seedlings under soil water deficit. *Tree Physiology*, **6**, 221-227.

METTERNICHT, G. I., 1998, Fuzzy classification of JERS-1 SAR data: An evaluation of its performance for soil salinity mapping. *Ecological Modelling*, **111,** 61–74.

METTERNICHT, G. I. and ZINCKB, J.A., 2003, Remote sensing of soil salinity: potentials and constraints. *Remote Sensing of Environment*, **85**, 1 –20.

MILLER, B.D. and HANSEN, G.K., 1975, Exclusion errors in pressure chamber estimates of leaf water potential. *Annals of Botany*, **39**, 915-920.

MILTON, N.M. and MOUAT, D.A., 1989, Remote sensing of vegetation responses to natural and cultural environmental conditions. *Photogrammetric Engineering and Remote Sensing*, **55**, 1167-1173.

MIZELLE, A.R., SCORGIE, H. and ANNEGARN, H., 1996, Size distribution, dispersion and deposition of airborne dust in the mining environment. *Proceedings of the 27th Annual Conference of the National Association of Clean Air*.

MOHAMMED, G.H., SAMPSON, P.H., COLOMBO, S.J., NOLAND, T.L. and MILLER, J.R., 1997, Bioindicators of forest sustainability: development of a forest condition rating system for Ontario. Forest Research Information Paper No. 137, Ontario Forest Research Institute, 22p.

MOUGENOT, B., POUGET, M. and EPEMA, G., 1993, Remote sensing of salt affected soils. *Remote Sensing Reviews*, **7**, 241–259.

MUCINA, L., and RUTHERFORD, M.C., 2006, The vegetation of South Africa, Lesotho and Swaziland. South African National Biodiversity Institute, Pretoria. 807p.

MULDERS, M., 1987, Remote sensing development in soil science. Amsterdam, The Netherlands: Elsevier, 379 p.

MüLLER, N.J.C., 1874, Investigations about the diffusion of the atmospheric gases and the gas removal under different lighting terms. *Annals for Scientific Botany*, **9**, 36-49.

MURTHA, P.A., 1982, Detection and analysis of vegetation stress. In *Remote sensing for resource management*, C.J. Johannsen and J.L. Sanders (Eds.) Soil Conservation Society of America. Ankeny, Iowa, pp 141-158.

MUSICK, H. B. and PELLETIER, R.E., 1986, Response of some Thematic Mapper band ratios to variation in soil water content. *Photogrammetry Engineering Remote Sensing***, 52**, 1661–1668.

MUSICK, H. B. and. PELLETIER, R.E., 1988, Response to soil moisture of spectral indexes derived from bidirectional reflectance in Thematic Mapper wavebands. *Remote Sensing of Environment*, **25**,167-184.

MUTANGA, O. and SKIDMORE, A.K., 2007, Red edge shift and biochemical content in grass canopies. *Journal of Photogrammetry and Remote Sensing*, **62**, 34-42.

NAICKER, K., CUKROWSKA, E. and MCCARTHY, T.S., 2003, Acid mine drainage arising from gold mining activity in Johannesburg, South Africa and environs. *Journal of Environmental Pollution*, **122**, 29-40.

NAIDOO, S., ZBONAK, A. and AHMED, F. 2006, The effect of moisture availability on wood density and vessel characteristics of *Eucalyptus grandis* in the warm temperate region of South Africa. Paper presented in IUFRO symposium Wood structure and properties, September 2006, Sielnica, Slovakia.

NAUMANN, J.C., ANDERSON, J.E. and YOUNG, D.R., 2008, Linking physiological responses, chlorophyll fluorescence and hyperspectral imagery to detect salinity stress using the physiological reflectance index in the coastal shrub Myrica cerifera. *Remote sensing of Environment*, **112**, 3865-3875.

NETONDO, G.W., ONYANGO J.C., and BECK, E, 2004, Sorghum and Salinity II: Gas exchange and chlorophyll fluorescence of sorghum under salt stress. *Crop Science*, **44,** 806-811.

NETTO, A.T., CAMPOSTRINI, E., DE OLIVEIRA, J.G. and BRESSAN-SMITH, R.E., 2005, Photosynthetic pigments, nitrogen, chlorophyll *a* fluorescence and SPAD-502 readings in coffee leaves. *Scientia Horticulturae*, **104**, 199-209.

NORTES, P.A., PASTOR-PÉREZ, A., EGEA, G., CONEJERO, W. and DOMINGO, R., 2005, Comparison of changes in stem diameter and water potential values for detecting water stress in young almond trees. *Agricultural Water Management*, **77**, 296-307.

ÖGREN, E., 1990, Evaluation of chlorophyll fluorescence as a probe for drought stress in willow leaves. *Plant Physiology*,**93**, 1280-1285.

ÖQUIST, G. and WASS, R., 1988, A portable, microprocessor operated instrument for measuring chlorophyll fluorescence kinetics in stress physiology. *Physiologia Plantarum*, **73**, 211-217.

ÖQUIST, G., 1987, Environmental stress and photosynthesis. In *Progress in Photosynthesis Research*, J. Biggins (Ed.) (Dordrecht: Martinus Nijhoff Publishers), **4**, 1-10.

OKEREKE, C.S., ESU, E.O. and EDET, A.E., 1998, Determination of potential groundwater sites using geological and geophysical techniques in the Cross River State, southeastern Nigeria. *Journal of African Earth Sciences*, **27**, 149-163.

OUNIS, A., EVAIN, S., FLEXAS, J., TOSTI, J. and MOYA, I., 2001, Adaptation of a PAM-fluorometer for remote sensing of chlorophyll fluorescence. *Photosynthesis Research*, **68**, 113-120.

PADILLA, K.L. and ANDERSON, K.A. 2002, Trace element concentration in tree-rings: biomonitoring centuries of environmental change. *Chemosphere*, **49**, 575-585.

PANDEY, U. K. and SAXENA, H. K., 1987, Effects of soil salinity on chlorophyll, photosynthesis, respiration and ionic composition at various growth stages in paddy. *Indian Journal of Agricultural Chemistry*, **20**, 149–156.

PELLEGRINO, A., GOZÉ, E., LEBON, E. and WERY, J., 2006, A model based diagnostic tool to evaluate the water stress experienced by grapevine in field sites. *European Journal of Agronomy*, **25**, 49-59.

PENUELAS, J., FILELLA, I., BIEL, C., SERRANO, L., and SAVE, R., 1995, The reflectance at the 950-970 region as an indicator of plant water status. *International Journal of Remote Sensing*, **14**, 1887-1905.

PENUELAS, J., ISLA, R., FILELLA, I. and ARAUS, J. L., 1997b, Visible and near-infrared reflectance assessment of salinity effects on barley. *Crop Science*, **37**, 198–202.

PENUELAS, J., PINOL, J., OGAYA, R. And FILELLA, I. 1997. Estimation of plant water concentration by the reflectance water index WI (R900/R970). *International Journal of Remote Sensing*, **18**, 2869-2875.

PEPPER, R.G., and CRAIG, G.F., 1986, Resistance of selected *Eucalyptus* species to soil salinity in Western Australia. *Journal of Applied Ecology*, ***23***, 977-987.

PETERSON, J.A., GRONINGER, J.W., SEILER, J.R. and MOU, P., 2001, Utility and limitations of chlorophyll fluorescence for the determination of growth limitations in trees. Unpublished paper.

PINKARD, E.A., PATEL, V. and MOHAMMED, C., 2006, Chlorophyll and nitrogen determination for plantation-grown *Eucalyptus nitens* and *Eucalyptus globulus* using a non-destructive meter. *Forest Ecology and Management*, **223**, 211-217.

PIRZAD, A., SHAKIBA, M.R., AB-SALMASI, S.Z, MOHAMMADI, S.A.,DARVISHZADEH, R. and SAMADI, A., 2011, Effect of water stress on leaf relative water content, chlorophyll, proline and soluble carbohydrates in *matricaria chamomilla* L. *Journal of Medicinal Plants*, **5**, 2483-2488.

PLAUT, Z., GRIEVE, C. M. and MAAS, E. V., 1990, Salinity effects on CO2 assimilation and diffusive conductance of cowpea leaves. *Physiologia Plantarum*, **79**, 31–38.

POSS, J.A., RUSSELL, W.B. and GRIEVE, C.M., 2006, Estimating yields of salt- and water-stressed forages with remote sensing in the visible and near infrared. *Journal of Environmental Quality*, **35**, 1060 -1071.

POYNTON, R.J., 1979, Tree plantings in Southern Africa, Volume 2: Eucalypts. 882p.

PU, R., GE, S., KELLY, N.M. and GONG, P., 2003, Spectral absorption features as indicators of water status in coast live oak (*Quercus agrifolia*) leaves. *International Journal of Remote Sensing*, **24**, 1799-1810.

PULLES, W., 1992, Water pollution: it's management and control in the South African gold-mining industry. *Journal of Mining and Ventilation Society of South Africa*, Feb. 1992.

QUINN, G.P. and KEOUGH, M.J., 2002, Experimental design and data analysis for biologist. Cambridge University Press, United Kingdom, 537p.

RESEARCH SYSTEMS INC., 2005, RSI Training Series: Spectral Analysis with ENVI. 4990 Pearl East Circle, Boulder, CO 80301, 106p.

RITCHIE, G.A. and HINCKLEY, T.M., 1975, The pressure chamber as an instrument for ecological research. *Advances in Ecological Research*, **9**, 165-255.

ROCK, B.N., HOSHIZAKI, T. and MILLER, J.R., 1988, Comparison of in situ and airborne spectral measurements of the blue shift associated with forest decline. *Remote Sensing of Environment*, **24**, 109-127.

ROLANDO, C.A. and LITTLE, K.M., 2003, Using chlorophyll fluorescence to determine stress in *Eucalyptus grandis* seedlings. *Southern African Forestry Journal*, **197**, 5-12.

ROSNER, T., BOER, R., REYNEKE, R., AUCAMP, P., and VERMAAK, J., 2001, A preliminary assessment of pollution contained in the unsaturated and saturated zone beneath reclaimed gold-mine residue deposits. Water Research Commission, Report No. 797/1/01.

SALEM, H.S., 2000, Modelling of lithology and hydraulic conductivity of shallow sediments from resistivity measurements using Schlemberger vertical electric soundings. *Energy Sources*, **23**, 599-618.

SALISBURY, F.B. and ROSS, C.W., 1992, *Plant Physiology* (California: Wadsworth Publishing Company), Fourth Edition, 682p.

SCHAPER, H. and CHACKO, E.K., 1991, Relation between extractable chlorophyll and portable chlorophyll meter readings in leaves of eight tropical and subtropical fruit tree species. *Journal of Plant Physiology*, **138**, 674-677.

SCHEPERS, J.S., BLACKMER, T.M., WILHELM, W.W. and RESENDE, M., 1996, Transmittance and reflectance measurements of corn leaves from plants with different nitrogen and water supply. *Journal of Plant Physiology*, **148**, 523–529.

SCHOLANDER P.F., HAMMEL H.T., BRADSTREET E.A. and HEMMINGSEN, E.A., 1965, Sap pressure in vascular plants. *Science*, **148,** 339–346.

SCHULZE, R.E., MAHARAJ, M., LYNCH, S.D. and MELVIL-THOMPSON, B., 1997, South Africa Atlas of Agrohydrology and Climatology. Water Research Commission Report TT82/96. Pretoria.

SEPULCRE-CANTÓ, G., ZARCO-TEJADA, P.J., JIMÉNEZ-MUNOZ, J.C., SOBRINO, J.A., DE MIGUEL, E., and VILLALOBOS, F.J., 2006, Detection of water stress in an olive orchard with thermal remote sensing imagery. *Agricultural and Forest Meteorology*, **136**, 31-44.

SHEN, Y., ZHENG, R.S. and YAN, C.Y., 2005, Estimation models for vegetation water content at both leaf and canopy levels. *Institute of Electrical and Electronics Engineers*, **2**, 1387-1389.

SIKUKU P. A., NETONDO G. W., ONYANGO J. C. and MUSYIMI D. M.,2010, Chlorophyll fluorescence, protein and chlorophyll content of three Nerica rainfed rice varieties under varying irrigation regimes. *Journal of Agricultural and Biological Science*, **5**, 19-25.

SILVA, E.C., NOGUEIRA, R.J.M.C., VALE, F.H.A., DE ARAUJO, F.D. and PIMENTA, M.A., 2009, Stomatal changes induced by intermittent drought in four umbu tree genotypes. *Brazilian Journal of Plant Physiology*, **21**, 33-42.

SIMS, D.A. and GAMON, J.A., 2002, Relationships between leaf pigment content and spectral reflectance across a wide range of species, leaf structures and development stages. *Remote Sensing of Environment*, **81**, 337-354.

SMITH, R. and PRICHARD, T., 2003, Using a pressure chamber in wine grapes: UC Cooperative Extension http://www.cesonoma.ucdavis.edu/vitic/pdf/wine_grape_pressure_chamber.pdf . (Accessed 2 October 2006)

SOUTH AFRICAN WEATHER SERVICE., 2006, Climate statistics for the period 1961 to 1990. Climate of South Africa, WB42.

SPERRY, J.S. and SALIENDRA, N.Z., 1994, Intra- and inter-plant variation in xylem cavitation in *Betula occidentalis*. *Plant, Cell and Environment*, **17**, 1233-1241.

STARK, R., 2001, Remote sensing techniques for monitoring vegetation condition. Department of Geological and Environmental Sciences, Ben-Gurion University of the Negev.

STIMSON, H.C., BRESHEARS, D.D., USTIN, S.L. and KEFAUVER, C., 2005, Spectral sensing of foliar water conditions in two co-occurring conifer species: *Pinus edulis* and *Juniperus monosperma*. *Remote Sensing of Environment*, **96**, 108-118.

STONE, C., CHISHOLM, L. and COOPS, N., 2001, Spectral reflectance characteristics of eucalypt foliage damaged by insects. *Australian Journal of Botany*, **49**, 687-698.

STRACHAN, I.B., PATTEY , E. and BOISVERT, J.B., 1999, Impact of nitrogen and environmental conditions on corn as detected by hyperspectral reflectance. *Remote sensing of Environment*, **80**, 213-214.

STRAKER, C.J., WEIERSBYE, I.M. and WITKOWSKI, E.T.F. 2007, Arbuscular mycorrhiza status of gold and uranium tailings and surrounding soils of South Africa's deep level gold mines: I. Root colonization and spore levels. *South African Journal of Botany*, **73**, 218-225.

STRASSER, R.J. and TSIMILLI-MICHAEL, M., 2001, Stress in plants, from daily rhythm to global changes detected and quantified by the JIP-Test. *Chimie Nouvelle (SRC)*, **75**, 3321-3326.

STRASSER, R.J., STRIVASTAVA, A. and TSIMILLI-MICHAEL, M., 2001, Analysis of the fluorescent transient. In *Chlorophyll fluorescence: A signature of photosynthesis*, G.C. Papageorgiou and W.J.S. Govindjee (Eds.) (Dordrecht: Kluwer Academic Publishers).

STYLINSKI, C.D., GAMON, J.A. and OECHEL, W.C., 2002, Seasonal patterns of reflectance indices, carotenoid pigments and photosynthetic evergreen chaparral species. *Oecologia*, **131**, 366-374.

TABBAGH, A., DABAS, M., HESSE, A. and PANISSOD, C., 2000, Soil resistivity: a non-invasive tool to map soil structure horizonation. *Geoderma*, **97**, 393-404.

THOMAS, D.S and EAMUS, D., 1999, The influence of predawn leaf water potential on stomatal responses to atmospheric water content at constant Ci and on stem hydraulic conductance and foliar ABA concentrations. *Journal of Experimental Botany*, **50**, 243-251.

THOMAS, D.S., MONTAGU, K.D. and CONROY, J.P. 2004, Changes in wood density of *Eucalyptus camaldulensis* due to temperature – the physiological link between water viscosity and wood anatomy. *Forest Ecology and Management*, **193**, 157-165.

THOMLINSON, J.R., BOLSTAD, P.V. and COHEN, W.B. 1999. Coordinating methodologies for scaling landcover classifications from site-specific to global: steps toward validating global map products. *Remote Sensing of Environment*, **70**, 16-28.

TUCKER, C.J., 1979, Red and photographic infrared linear combinations for monitoring vegetation. *Remote Sensing of the Environment*, **8**, 127-150.

TUCKER, C.J., 1980, Remote sensing of leaf water content in the near infrared. *Remote Sensing of Environment*, **10**, 23-32.

TURHAN, H. and GENC, L., 2008, Assessment of the effect of salinity on the early growth stage of the common sunflower *(Sanay cultivar)* using spectral discrimination techniques. *Journal of Biotechnology*, **7**, 750-756.

TURNER, N.C., 1981, Techniques and experimental approaches for the measurement of plant water status. *Plant and Soil*, **58**, 339-366.

TURNER, N.C., 1988, Measurement of plant water status by the pressure chamber technique. *Irrigation Science*, **9**, 289-308.

TYREE, M.T. and DAINTY, J., 1973, The water relations of hemlock (*Tsuga canadiensis*). II. The kinetics of water exchange between symplast and apoplast. *Canadian Journal of Botany*, **51**, 1481-

TYREE, M., ENGELBRECHT, B., VARGAS, G. and KURSAR, T., 2003, Desiccation tolerance of five tropical seedlings in Panama, relationship to a field assessment of drought performance. *Plant Physiology*, **132**, 1439-1447.

UNITED STATES ENVIRONMENTAL PROTECTION AGENCY., 1997, The feasibility of lining tailings ponds. United States of America, Solid Waste Unit, 9p.

VAN AS, D., LEUSCHNER, A.H., BAIN, C.A.R. and GRUNDLING, A., 1992, Public exposure to radioactivity from mine dumps through atmospheric and aquatic pathways. *Proceedings of Disposal of Mining Wastes*, AEC.AEK, Johannesburg, November 1992.

VAN DER MESCHT, A., DE RONDE, K., VAN DER MERWE, T., LAURIE, R., BESTER, C. and WENZEL, C., 1997, Evaluation of chlorophyll fluorescence as a measure of drought tolerance in *Eucalyptus grandis*. In *4th IUFRO Conference on silviculture and improvement of Eucalypts*, Embrapa, Salvador, Brazil, 117-124.

VAN RENSBURG, H.J. 2001. Modelling of contaminant migration in the Mahemspruit area west of Welkom. *Report to Anglogold AQS/AGL/2001/002.AquiSim Consulting (Pty) Ltd.* 69p.

VAN RENSBURG, L., KRUGER, G.H.J., EGGENBERG, P. and STRASSER, R.J., 1996, Can screening criteria for drought resistance in *Nicotiana tabacum L.* be derived from the polyphasic rise of the chlorophyll a fluorescent transient (OJIP). *South African Journal Botany*, **62**, 337-341.

VEGTER, J.R., 1995, An explanation of a set of national groundwater maps. WRC Report TT74/95, Water Research Commission, Pretoria, RSA.

VENTER, F. and VENTER J., 1996, Making the most of indigenous trees. 1st edition, Pretoria: Briza Publications.

VERMA, K., SAXENA, A., BARTHWAL, A. and DESHMUKH, S., 1994, Remote sensing technique for mapping salt affected soils. *International Journal of Remote Sensing*, **15**, 1901–1914.

VIVIER, J.J.P., MYBURGH, J.A., PRETORIUS, S.J., JANSE VAN RENSBURG, H.J. AND DE JAGER, F., 2001, Geohydrological assessment to determine the status and impact of contamination from the tailings dams on the groundwater in the Bokkamp Dam aquifer catchment. *Report to Anglogold GC/R/01/10/10, Southern African Geoconsultants Geocon and AquiSim Consulting (Pty) Ltd.*75p.

WAGNER, F., HÉRAULT, B., STAHL, C., BONAL, D. and ROSSI, V., 2011, Modelling water availability for trees in tropical forests. *Agricultural and Forest Meteorology*, In Press.

WANG, D., WILSON, C. and SHANNON, M.C., 2002, Interpretation of salinity and irrigation effects on soybean canopy reflectance in the visible and near-infrared spectrum domain. *International Journal of Remote Sensing*, **23**, 811-824.

WARING, R.H. and CLEARY, B.D., 1967, Plant moisture stress: evaluation by pressure bomb. *Science*, **155**, 1248-1254.

WATMOUGH, S.A. 1999, Monitoring historical changes in soil and atmospheric trace metal levels by dendrochemical analysis. *Environmental Pollution*, **106**, 391-403.

WEATHERLEY, P.E., 1950, Studies in the water relations of the cotton plant. I. The field measurement of water deficits in leaves. *New Phytologist*, **49**, 81-97.

WEIERSBYE, I.M., 2002, The Containment of Pollution from Tailings Dams: The Sustainable Vegetation of Slimes Dam Project and the Mine Woodlands Project. Invited Review and Discussion Document for a nationwide initiative in partnership with Government and Mining. Directorate of Community Forestry, Department of Water Affairs and Forestry,

Pretoria and Directorate of Mine Rehabilitation, Department of Minerals and Energy, Pretoria, WITS_GOVT_20/07/02V2, 71p.

WEIERSBYE, I.M., 2004; 2005; 2006; 2008, Personal communication. Restoration and Conservation Biology Research Group, School of Animal Plant and Environmental Sciences, University of the Witwatersrand, Johannesburg, South Africa.

WEIERSBYE, I.M., WITKOWSKI, E.T.F. and REICHARDT, M. 2006, Floristic composition of gold and uranium tailings dams, and adjacent polluted areas, on South Africa's deep level mines. *Bothalia*, **36**, 101-127.

WEIERSBYE, I.M., WITKOWSKI, E.T.F., DYE, P.J., VIVIER, J.J.K., VAN RENSBURG, H.J., HERBERT, M., AMIS, J., PARSONS, J., REICHARDT, M., FOURIE, L., HOLMWOOD, R and VAN WYK, A., 2002, The containment of pollution from tailings dams: the sustainable vegetation of slimes dams project and the mine woodlands project. Invited report to the Directorate of Community Forestry, Department of Water Affairs and Forestry, and the Directorate of Mine Rehabilitation, Department of Minerals and Energy, WITS GOVT 20/07/02V2: 1-72.

WHITE, D.A., TURNER, N.C. and GALBRAITH, J.H., 2000, Leaf water relations and stomatal behaviour of four allopatric Eucalyptus species in Mediterranean south-western Australia. *Tree Physiology*, **20**, 1157-1165.

WHITEHEAD, A, D., and BEADLE, C.L., 2004, Physiological regulation of productivity and water use in Eucalyptus: a review. *Forest Ecology and Management*, **193,** 113-140.

WIEGAND, C. L., RHOADES, J. D., ESCOBAR, D. E. and EVERITT, J. H., 1994, Photographic and video graphic observations for determining and mapping the response of cotton to soil salinity. *Remote Sensing of Environment*, **49**, 212– 223.

WINDE, F., 2009, Uranium pollution of water resources in mined-out and active goldfields of South Africa - a case study in the Wonderfontein spruit catchment on extent and sources of u-contamination and associated health risks. International Mine and Water Conference, Pretoria, South Africa, ISBN Number: 978-0-9802623-5-3.

WINDE, F., WADE, P. and VAN DER WALT, I.J., 2004a, Gold tailings as a source of waterborne uranium contamination of streams-Koekemoer Spruit (Klerksdorp gold fields, South Africa). Part I. Uranium migration along the aqueous pathway. *Water SA*, **30**, 219-225.

WINDE, F., WADE, P. and VAN DER WALT, I.J., 2004b, Gold tailings as a source of waterborne uranium contamination of streams-Koekemoer Spruit (Klerksdorp gold fields, South Africa). Part II. Dynamics of groundwater-stream interactions. *Water SA*, **30**, 227-232.

WINDE, F., WADE, P. and VAN DER WALT, I.J., 2004c, Gold tailings as a source of waterborne uranium contamination of streams-Koekemoer Spruit (Klerksdorp gold fields, South Africa). Part III. Fluctuations of stream chemistry and their impacts on uranium mobility. *Water SA*, **30**, 233-239.

WITKOWSKI, E.T.F. and WEIERSBYE, I.M. 1998a, Establishment of plants on gold slimes dam-winter survey. *Plant Ecology and Conservation Series*, No. 4, Report to the Anglo-American Corporation, 40p.

WITKOWSKI, E.T.F. and WEIERSBYE, I.M., 1998b, Establishment of plants on gold slimes dams: characterization of the slimes and adjacent soils. *Plant Ecology and Conservation Series*, **6**, AngloGold Ltd, 111p.

WITKOWSKI, E.T.F., LAMONT, B.B., WALTON, C. and RADFORD, S., 1992, Leaf demography, sclerophyll and ecophysiology of two Banksias with contrasting leaf life spans. *Australian Journal of Botany*,**40**, 849-62.

YAMASAKI, S. and DILLENBURG, L.R., 1999, Measurements of leaf relative water content in *Araucaria angustifolia*. *Revista Brasileira de Fisiologia Vegetal*, **11**, 69-75.

YOUNG, P. and WALLIS, S., 1985, Recursive estimation: A unified approach to the identification estimation, and forecasting of hydrological systems. *Applied Mathematics and Computation*, **17**, 299-334.

YU, K.F., KAMBER, B.A., LAWRENCE, M.G., GREIG, A. and ZHAO, J.X. 2007, High precision analysis on annual variations of heavy metals, lead isotopes and rare earth elements in mangrove tree rings by inductively coupled plasma mass spectrometry. *Nuclear instruments and methods in physics research Section B: Beam interaction with materials and atoms*, **225**, 399-408.

ZAGOLSKI, F., PINEL, V., ROMIER, J., ALCAYDE, D., GASTELLU-ETCHEGORRY, J.P, GIORDANO, G., MARTY, G., MOUGIN, E. and JOFFRE, R., 1996, Forest canopy chemistry with high spectral resolution remote sensing. *International Journal of Remote Sensing*, **17**, 1107-1128.

ZARCO-TEJADA, P.J., MILLER, J.R., MOHAMMED, G.H. and NOLAND, T.L., 2000, Chlorophyll fluorescence effects on vegetation apparent reflectance. I. Leaf-level measurements and model simulation. *Remote Sensing of Environment*, **74**, 582-595.

ZARCO-TEJADA, P.J., RUEDA, C.A. and USTIN, S.L., 2003, Water content estimation in vegetation with MODIS reflectance data and model inversion methods. *Remote Sensing of Environment*, **85**, 109-124.

ZHANG, M., USTIN, S., REJMANKOVA, E. and SANDERSON, E., 1997, Monitoring Pacific coast salt marshes using remote sensing. *Ecological Applications*, **7**, 1039– 1053.

ZHANG, X., DENG, L. and BAAS, P. 1988, The ecological wood anatomy of the Lilacs (Syringa oblate var.giraldii) on Mount Taibei in North-western China. *IAWA Bulletin*, **9**, 24-30.

ZIMMERMANN, M.H. 1983, Xylem structure and the ascent of sap. Springer series in wood science 1. Springer, Berlin.

ZIMMERMANN, M.H. and MILBURN, J.A. 1982, Transport and storage of water. In: Pirson, A. and Zimmermann, M.H. eds. Encyclopedia of plant physiology, Vol 12B, New York, Springer Verlag.

ZWART, S.J. and BASTIAANSSEN, W.G.M., 2007, SEBAL for detecting spatial variation of water productivity and scope for improvement in eight irrigated wheat systems. *Agricultural Water Management*, **89**, 287-296.

APPENDIX 1: REVIEW PAPER

Review

Review of commonly used remote sensing and ground-based technologies to measure plant water stress

M Govender[1,2*], PJ Dye[1], IM Weiersbye[1], ETF Witkowski[1] and F Ahmed[3]

[1]School of Animal, Plant and Environmental Sciences, University of the Witwatersrand, Johannesburg, PO Wits 2050, South Africa
[2]CSIR Natural Resources and the Environment, [c/o] School of Environmental Sciences, University of KwaZulu-Natal, Private Bag X01, Scottsville, 3209, South Africa
[3]Remote sensing GIS and spatial modelling, School of Environmental Sciences, University of KwaZulu-Natal, Durban 4041, South Africa

Abstract

This review provides an overview of the use of remote sensing data, the development of spectral reflectance indices for detecting plant water stress, and the usefulness of field measurements for ground-truthing purposes. Reliable measurements of plant water stress over large areas are often required for management applications in the fields of agriculture, forestry, conservation and land rehabilitation. The use of remote sensing technologies and spectral reflectance data for determining spatial patterns of plant water stress is widely described in the scientific literature. Airborne, space-borne and hand-held remote sensing technologies are commonly used to investigate the spectral responses of vegetation to plant stress. Earlier studies utilised multispectral sensors which commonly collect four to seven spectral bands in the visible and near-infrared region of the electromagnetic spectrum. Advances in sensor and image processor technology over the past 3 decades now allow for the simultaneous collection of several hundred narrow spectral bands resulting in more detailed hyperspectral data. The availability of hyperspectral data has led to the identification of several spectral indices that have been shown to be useful in identifying plant stress. Such studies have revealed strong linear relationships between plant pigment concentration and the visible (VIS) and near-infrared (NIR) reflectance, while plant water content has been linked to specific bands in the short-wave infrared (SWIR) region of the spectrum. Ground-truthing is essential to identifying useful reflectance information for detecting plant water stress, and four commonly used ground-based methods *viz.* predawn leaf water potential, leaf chlorophyll fluorescence, leaf pigment concentrations and leaf water content are reviewed for their, usefulness and practical application.

Keywords: leaf chlorophyll fluorescence, leaf-water content, plant pigment concentrations, plant water stress, predawn leaf water potential, remote sensing

Introduction

All living organisms including plants need an adequate supply of water to ensure both their growth and survival. Water in plants is required to permit vital processes such as photosynthesis, respiration and nutrient uptake. Plants absorb water from the soil through their roots, which is then transported to their stems, leaves and flowers for the maintenance of the different vital processes. When water supply is insufficient, plants may suffer water stress which could then compromise their growth production, reproduction and survival.

Water stress in plants is a complex physiological response to the limited availability of water to a plant. When plants suffer from water stress, a series of harmful plant-water interactions occur, which may disrupt a plant's physiology. These include a decrease in cell water potential, cell turgor and relative water content (Hsiao, 1973).

The available water to plants is usually expressed in terms of water potential. Water potential is commonly assessed by measuring predawn leaf water potential; a direct measure of plant water stress. Measurements at predawn directly evaluate the water status of the plant, because during night-time hours under zero transpiration, plant water potential equilibrates to the available soil water (Cleary and Zsarr, 1984). Cleary and Zsarr (1984) suggested that a predawn leaf water potential of less than -0.8 MPa is an indication of stressed vegetation. Indirect measurements may also be used to detect plant water stress. The more commonly used techniques include measurements of relative leaf water content, plant chlorophyll pigment content and chlorophyll fluorescence. Other, less frequently applied measurements used in verifying remote sensing studies include variations in trunk or stem diameters or even xylem vessel characteristics.

Although characterising cavitations in xylem vessels is potentially a useful technique for understanding the response to water stress in a plant, this method is time-consuming, costly and not suitable for use over large spatial scales. It has been shown in many plant species that roots are more vulnerable to cavitation than stems, and thus root cavitation is more suited to characterise plant water stress between species (Sperry and Saliendra, 1994; Alder et al., 1996; Hacke and Sauter, 1996; Linton et al., 1998).

Reliable detection and prediction of plant water stress is desirable for numerous agricultural, forestry, conservation and land rehabilitation applications. Various remote and ground-based technologies are available for the measurement of plant water stress.

* To whom all correspondence should be addressed.
☎ +2733 2605276; fax: +2733 260 5266;
e-mail: MGovender@ssir.co.za
Received 1 August 2008; accepted in revised form 14 September 2009.

Available on website http://www.wrc.org.za
ISSN 0378-4738 (Print) = Water SA Vol. 35 No. 5 October 2009
ISSN 1816-7950 (On-line) = Water SA Vol. 35 No. 5 October 2009

Remote sensing technologies which utilise spectral reflectance data have increasingly been used for determining spatial patterns of plant water stress (Yamasaki and Dillenburg, 1999; Ceccato et al., 2001; Sims and Gamon, 2002; Pu et al., 2003; Jackson et al., 2004; Stimson et al., 2005; Chun-Jiang et al., 2006; Clay et al., 2006; De Tar et al., 2006; Eitel et al., 2006; Fitzgerald et al., 2006; Harris et al., 2006; Sepulcre-Canto et al., 2006; Campbell et al., 2007; Hope et al., 2009). Important advantages of remote sensing technologies include cost-effectiveness, efficiency in displaying spatial patterns at a variety of scales, and versatility in revealing a variety of structural and physiological characteristics of water-stressed plants. Despite numerous successful case studies, the selection of suitable remote sensing methodologies and reflectance algorithms remains difficult, due to the influence of vegetation diversity and site conditions on vegetation spectral reflectance.

This paper reviews the detection of plant water stress using remote sensing technologies and ground-based techniques commonly used to identify water stress in plants and which are suitable for ground-truthing remotely-sensed imagery. Within the scope of this review, no distinction is made between the technologies used for acquiring the remote sensing data, but rather the focus is on highlighting vegetative spectral sensitivities which have been used to detect plant water stress. The ground-based techniques reviewed are based on measurements of predawn leaf water potential (Dixon, 1914), leaf chlorophyll fluorescence (Muller, 1874), leaf water content (Weatherley, 1950) and leaf pigment concentrations (Lichtenthaler, 1987).

Detection of plant water stress using remote sensing

The application of remote sensing technologies for plant and environmental studies became widespread during the 1980s. These studies made use of low spatial and spectral resolution (60 m to 80 m and 4 spectral bands) multispectral data. Multispectral remote sensing data commonly consist of 4 to 7 broad spectral bands in the visible (VIS) and near infrared (NIR) regions of the electromagnetic spectrum. These datasets were acquired using airborne, satellite and ground-based spectrometers. Early airborne systems consisted of a multispectral camera mounted on board a light aircraft. Spectrometers at this time were bulky, heavy instruments which were not easily transportable in the field; therefore most measurements were taken in laboratories.

Remote sensing technologies have advanced significantly over the past 10 to 15 years. With the development of hyperspectral remote sensing technologies, researchers have benefited from significant improvements in the spectral and spatial properties of the data, allowing for more detailed plant and environmental studies. These technologies acquire many hundreds of spectral bands across the spectrum from 400 nm to 2 500 nm, using satellite, airborne or hand-held devices. The Casi or Hymap airborne imagers are examples of commonly used hyperspectral imagers which acquire high spectral and spatial resolution images. A distinct advantage of most airborne imagers is their capability to acquire at least 200 or more spectral bands at less than 5 m spatial resolution. Advances in spectrometry have also resulted in state-of-the-art portable field instruments which allow for the collection of hand-held hyperspectral signatures. The Hyperion sensor is currently the only hyperspectral satellite system available for research.

In recent years, there has been an expanding body of literature concerning the relationship between the spectral

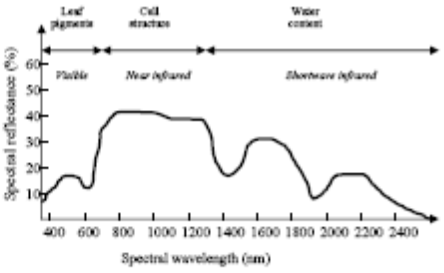


Figure 1
Typical reflectance sensitivities as controlled by leaf pigments, cell structure and water content (adapted from Gaussman, 1977)

reflectance properties of vegetation and the structural characteristics of vegetation and pigment concentration in leaves. The spectral characteristics of vegetation are governed primarily by scattering and absorption characteristics of the leaf internal structure and biochemical constituents, such as pigments, water, nitrogen, cellulose and lignin (Asner, 1998; Coops et al., 2002). Pigments are the main determinants controlling the spectral responses of leaves in the visible wavelengths (Gaussman, 1977). Chlorophyll pigment content, in particular, is directly associated with photosynthetic capacity and productivity (Gaussman, 1977; Curran et al., 1992). Reduced concentrations of chlorophyll are indicative of plant stress (Curran et al., 1992). On the other hand, cellular structure and water content of leaves are the main determinants in the near- and mid-infrared wavelengths as shown in Fig. 1.

A summary of important findings since the early 1980s which highlights specific regions of the electromagnetic spectrum and their relation to vegetation spectral reflectance properties is presented in Table 1. Many of the earlier studies focused on broad spectral bands such as the VIS and NIR regions (350 nm to 1 300 nm), which could be used in vegetation studies. More recent work has highlighted the importance of more specific narrow-band regions such as the red edge (maximum slope of vegetation reflectance from 690 nm to 740 nm) for predicting plant stress (Clay et al., 2006; Fitzgerald et al., 2006; Blackburn, 2007; Campbell et al., 2007). The extent of the literature is indicative of the importance of relationships between plant stress and both plant chlorophyll and water content. Plant chlorophyll and water content have thus been used as 'surrogates' of plant stress, under the assumption that decreases in chlorophyll and water content are indicative of plant stress. Numerous individual spectral bands and vegetation spectral reflectance indices have been identified for use in predicting plant chlorophyll content and water content.

Spectral indicators of plant chlorophyll content

In stressed vegetation, leaf chlorophyll content decreases, thereby changing the proportion of light-absorbing pigments, leading to a reduction in the overall absorption of light (Murtha, 1982; Zarco-Tejada et al., 2000). These changes affect the spectral reflectance signatures of plants through a reduction in green reflection and an increase in red and blue reflections, resulting in changes in the normal spectral reflectance patterns of plants (Murtha, 1982; Zarco-Tejada et al., 2000). Thus,

Available on website http://www.wrc.org.za
ISSN 0378-4738 (Print) = Water SA Vol. 35 No. 5 October 2009
ISSN 1816-7950 (On-line) = Water SA Vol. 35 No. 5 October 2009

Table 1
Some milestones in the historical development of understanding of vegetation spectral reflectance characteristics in specific regions of the electromagnetic spectrum

Region of the spectrum	Vegetation spectral reflectance characteristics	Author(s)
VIS, NIR and MIR	Pigments, cellular structure and water content of leaves	Gausman (1977)
1 550 to 1 750 nm	Correlation of MIR reflectance to leaf water contents	Tucker (1980)
SWIR (1 400 to 2 500 nm)	Reflectance is influenced by liquid water in plant tissue	Tucker (1980) Ceccato et al. (2001)
VIS	Changes in red, green and blue reflectance due to chloroplast deterioration	Murtha (1982)
Red Edge	Movement of red edge towards shorter wavelengths during senescence or stress induced chlorosis	Collins et al. (1983) Rock et al. (1988); Milton and Mouat (1989)
Red Edge	Red edge defined from 690 to 740 nm is also sensitive to chlorophyll content	Horler et al. (1983) Curran et al. (1990) Blackburn (1999)
Red Wavelengths	Displacement in the slope of the red wavelengths towards longer wavelengths as chlorophyll content increases	Horler et al. (1983)
Thematic Band 5 to 7 (1 550 to 1 750 nm and 2 080 to 2 350 nm)	Ratio of Band 5 to 7 highly correlated with water content of soils and vegetation	Musick and Pelletier (1986; 1988)
VIS and NIR	Estimated chlorophyll *a*, *b* and total carotenoid content using equations and specific extinction coefficients	Lichtenthaler (1987)
Red Edge	Increase in the relative proportion of chlorophyll *a* will result in movement of red edge towards longer wavelengths, independent of total chlorophyll content and vice versa	Guyot and Baret (1988)
NIR (700 to 1300 nm) and MIR (1 300 to 2 500 nm)	Detection of plant water stress in oak, sweetgum and conifers	Hunt and Rock (1989)
820 and 1 600 nm	Significant relationship between the equivalent water thickness and a moisture stress index between reflectance value measured at 1 600 nm and reflectance value measured at 820 nm	Hunt and Rock (1989)
550 and 700 nm	Maximum sensitivity to a wide range of chlorophyll contents	Curran et al. (1990) Gitelson and Merzlyak (1996) Lichtenthaler et al. (1996) Datt (1999)
Red Edge	Chlorophyll content of branches of slash pine (*Pinus elliottii engelm*) predicted using red edge	Curran et al. (1990)
VIS (491 to 575 nm); Red (647 to 760 nm)	Increased reflectance in response to plant stress regardless of the stress agent	Carter (1993)
NIR plateau	Weak water absorption features at 1 000 and 1 200 nm Deepening of the 2 water-absorption features as leaf area index increased	Gao (1995) Asner (1998)
860 nm and 1240 nm	Normalised difference water index as an estimate of vegetation water content	Gao (1995)
550, 700 and longer than 750 nm	Specific wavelengths sensitive to pigment variations and chlorophyll assessment at leaf level for maple and chestnut leaves	Gitelson and Merzlyak (1996)
Reflectance at 550 and 700 nm, and 500 and 670 nm	Highly correlated in yellow-green to dark green leaves	Gitelson and Merzlyak (1996)
Maximum reflectance at 750 nm, lowest reflectance between 400 to 500 nm.	Highly correlated in chestnut leaves	Gitelson and Merzlyak (1996)
670 to 680 nm	Reflectance at 670 to 680 nm was insensitive to chlorophyll *a* above 70 mg·m^{-2} in tobacco leaves (*Nicotiana tabacum L.*) due to saturation of the relationship between light absorption and pigment concentration.	Lichtenthaler et al. (1996)
VIS, NIR	Reflectance at wavelengths with high absorption coefficients should be more sensitive to low concentrations of chlorophyll *a*, while spectral regions with low absorption should be more sensitive to higher chlorophyll *a* concentrations	Lichtenthaler et al. (1996) Blackburn (1999)
550, 700 and 750 nm	The reflectance indices (R_{700}/ R_{550} and R_{750}/ R_{550}) were identified as having strong linear relationships with total chlorophyll concentration at the leaf scale in horse chestnut (*Aesculus hippocastanum L.*) and Norway maple (*Acer platanoides L.*) leaves	Lichtenthaler et al. (1996) Gitelson and Merzlyak (1996) Gitelson et al. (2002) Blackburn (1999)
SWIR (1530 and 1720 nm)	Reflectance is influenced by liquid water in plant tissue and can be used as an estimate for vegetation water content	Foutry and Baret (1997)

Available on website http://www.wrc.org.za
ISSN 0378-4738 (Print) = Water SA Vol. 35 No. 5 October 2009
ISSN 1816-7950 (On-line) = Water SA Vol. 35 No. 5 October 2009

VIS, NIR, SWIR	Variability in tissue optical properties is wavelength dependent Green foliage lowest variation in VIS, highest NIR Standing litter minimum variation in VIS and NIR, highest in SWIR Woody stems lowest variation in SWIR, highest in NIR	Asner (1998)
1 700 nm, 2 000 nm, 2 200 nm	Features associated with lignin and other organic compounds	Asner (1998)
650, 635, and 470 nm	Concentrations of chlorophyll *a*, chlorophyll *b*, and carotenoids were best correlated with reflectance indices (R_{650}, R_{635} and R_{470}), respectively in the leaves of 4 deciduous tree species at different stages of senescence	Blackburn (1998a)
676 and 810 nm	Chlorophyll *a* and chlorophyll *b* concentrations were strongly correlated with reflectance index (R_{676}) in the visible wavelengths and reflectance index (R_{810}) in the near-infrared on bracken (*Pteridium aquilinum*) canopies. Possible correlation to canopy structural development which has a direct influence on near-infrared reflectance.	Blackburn (1998b)
740 to 820 nm; 680 and 760 nm	Higher reflectance values between 740 to 820 nm; and more pronounced maximum slope between 680 and 760 nm (red edge) is related to vegetation with healthier green leaf development, i.e. higher biomass and leaf area index	Lelong et al. (1998) Jacquemoud (1993) Baret and Jacquemoud (1994) Baret et al. (1994) Filella and Penuelas (1994)
Red and NIR	Relation between water deficiency (stress) to spectral features in the 740 to 820 nm and red edge range in wheat	Lelong et al. (1998)
Red Edge	The first derivative of pseudoabsorbance, δ(Log 1/Reflectance), was highly correlated with canopy pigment concentration per unit area in the red edge region. Canopy and leaf scale concentrations per unit mass of chlorophyll *a*, chlorophyll *b*, and carotenoids were strongly related to δ(Log 1/Reflectance) and the second derivative of pseudoabsorbance (δδ(Log 1/Reflectance), but different wavelengths were optimal at each scale.	Blackburn (1999)
VIS	Moderately correlated to chlorophyll concentration	Blackburn (1999)
VIS (Green) and NIR	Ratio indices highly correlated to chlorophyll concentration	Blackburn (1999)
Red Edge	Wavelength position of red edge related to chlorophyll concentration, and characteristics of the amplitude of the 1st and 2nd derivatives of reflectance and pseudo absorbance were more strongly correlated with chlorophyll	Blackburn (1999)
Red, NIR (850 nm, 710 nm, 680 nm)	Vegetation indices used to predict chlorophyll content of eucalypt vegetation at the leaf and crown scale	Datt (1999)
850, 710 and 680 nm	850, 710 and 680 nm wavelengths produced the highest correlations with leaf chlorophyll content	Datt (1999)
Red Edge	With decreasing chlorophyll content, senescence or stressed induced chlorosis the red edge moves to shorter wavelengths, and is due to a reduction in the depth and breadth of the chlorophyll absorption feature	Stone et al. (2001) Rock et al. (1988) Datt (1999)
VIS, NIR	Relationships between spectral reflectance properties of *Eucalyptus* vegetation and a range of physiological and morphological parameters. Results indicate a shift of red edge towards shorter wavelengths with decreasing chlorophyll content.	Stone et al. (2001)
900 and 970 nm	Water index is derived from the ratio between reflectance measured at 900 nm and 970 nm and used as a measure of plant water content	Champagne et al. (2003)
NIR, Red Edge	Canopy level spectral and thermal estimation of water status and nitrogen content using spectral and thermal indices	Fitzgerald et al. (2006)
NIR and VIS	Degree of water stress strongly correlated to spectral bands from VIS and NIR regions viz. 686, 811, 860, 850 bands using hyperspectral and multispectral data	De Tar et al. (2006)
Thermal bands	Detection of water stress using thermal remote sensing imagery	Sepulcre-Canto et al. (2006)
NIR and SWIR	Indices formulated from the weaker NIR liquid water absorption bands (980 and 1200) are linear in response to moisture fluctuations, and are strongly correlated to hydrological measures. Could be used to estimates near-surface and surface wetness at the landscape scale.	Harris et al. (2006)
Red Edge	Detection of plant water stress using wavelengths associated with red edge	Clay et al. (2006) Blackburn (2007) Campbell et al. (2007)

VIS = Visible; NIR = Near Infrared; MIR = Middle Infrared; SWIR = Shortwave Infrared

detecting changes from the normal (unstressed) spectral reflectance patterns is the key to interpreting plant stress.

Specific reflectance wavelengths in the red and near infrared region of the spectrum, which are sensitive to plant chlorophyll pigment variation, have been identified. Reflectance from 550 nm and 700 nm shows maximum sensitivity to a wide range of chlorophyll contents (Curran et al., 1990; Carter, 1993; Gitelson and Merzlyak, 1996; Lichtenthaler et al., 1996, Datt, 1999). However, there is little agreement on the optimum wavelengths to be used in the remote assessment of plant chlorophyll content.

Available on website http://www.wrc.org.za
ISSN 0378-4738 (Print) = Water SA Vol. 35 No. 5 October 2009
ISSN 1816-7950 (On-line) = Water SA Vol. 35 No. 5 October 2009

Indices have been derived using a combination of specific reflectance wavelengths for the remote assessment of chlorophyll content (Curran et al., 1990; Jacquemoud, 1993; Baret and Jacquemoud, 1994; Baret et al., 1994; Filella and Penuelas, 1994; Gitelson and Merzylak, 1996; Lichtenthaler et al., 1996; Blackburn, 1998a; Blackburn, 1998b; Lelong et al., (1998); Blackburn, 1999; Datt, 1999; Stone et al., 2001; Coops et al., 2003). These indices have been typically derived through correlations between leaf reflectance and leaf chlorophyll content, and are often developed for a single species with constant leaf size and shape, leaf surface and internal structure (Datt, 1999). However, the relationship between chlorophyll content and leaf or canopy reflectance is not necessarily generic and caution needs to be taken when applying these indices over different vegetation types or biomes for the prediction of plant water stress (Coops et al., 2003).

In the remote assessment of plant water stress, total chlorophyll and chlorophyll *a* content have been identified as key spectral indicators. Chlorophyll *a* absorbs strongly in the red wavelengths because of electron transitions of the chlorophyll molecules. As the chlorophyll concentration increases, there is an apparent displacement in the slope of the spectral curve in the red wavelengths towards longer wavelengths (Horler et al., 1983). However, in a stressed plant there is a shift towards shorter wavelengths, often reported as the 'blue shift' (Carter, 1993).

The interdependence of chlorophyll *a* and total chlorophyll provide an appropriate measure of changes in spectral reflectance due to plant water stress. If the relative proportion of chlorophyll *a* were to increase there would be a movement of the red edge to longer wavelengths, independent of total chlorophyll content. Likewise, a decrease in the relative proportion of chlorophyll *a* would result in a movement of the red edge to shorter wavelengths, also independent of total chlorophyll content. However, the effect of a changing $^{\text{chlorophyll a}}/_{\text{chlorophyll b}}$ ratio on the red edge is likely to be minor and has proved difficult to observe compared to the effect of the total chlorophyll content (Guyot and Baret, 1988). Therefore, red reflectance is considered a reliable metric for total chlorophyll content and changes in leaf pigments (Horler et al., 1983).

When chlorophyll content is used as a measure of plant water stress, the placement and shape of the spectral red edge are important indicators of plant water stress (Horler et al., 1983, Curran et al., 1990, Blackburn, 1999; Blackburn, 2007). This relationship is used to explain the movement of the red edge to shorter wavelengths during different expressions of plant water stress, such as senescence or stress-induced chlorosis (Collins et al., 1983; Rock et al., 1988; Milton and Mount, 1989; Clay et al., 2006; Campbell et al., 2007).

Spectral indicators of plant water content

Plant water content at the leaf and canopy scales is often estimated using specific spectral reflectance bands and spectral reflectance indices from near infrared, middle infrared (MIR) and short-wave infrared (SWIR) regions of the electromagnetic spectrum (Tucker, 1980; Hunt and Rock, 1989; Gao, 1995; Zarco-Tejada et al., 2003; Jackson et al., 2004; Shen et al., 2005; Chun-Jiang et al., 2006).

NIR and MIR spectral bands are highly correlated to water content of vegetation and soils (Tucker, 1980; Hunt and Rock, 1989; Musick and Pelletier, 1986; 1988). Spectral bands from these regions have been used to delineate stressed trees from non-stressed trees (Tucker, 1980; Hunt and Rock, 1989; Musick and Pelletier, 1986; 1988). In these regions of the electromagnetic spectrum, leaf water content has been remotely assessed using bands 1 550 nm to 1 750 nm (Tucker, 1980), as well as the ratio of spectral bands 1 550 nm to 1 750 nm and 2 080 to 2 350 nm (Musick and Pelletier, 1986; 1988). However, in laboratory experiments a good relationship was identified between water content, leaf area, and the spectral index derived using 820 nm and 1 600 nm spectral reflectance bands (Hunt and Rock, 1989). In these experiments MIR reflectance increased with decreasing leaf water content in California oak, blue spruce, soybean and sweetgum (Hunt and Rock, 1989).

In the SWIR region (1 400 nm to 2 500 nm), field measurements have shown significant changes to this region of the spectrum resulting from changes in the water content of plants (Tucker, 1980; Ceccato et al., 2001). Several relationships have been identified between specific spectral bands in the SWIR region and different ground-based measurements of plant water stress such as relative water content, leaf water potential, stomatal conductance, and cell wall elasticity (Foutry and Baret, 1997; Pu et al., 2003). In particular, Foutry and Baret (1997) reported that the spectral wavelengths at 1 530 nm and 1 720 nm are most appropriate for assessing plant water content in both woody and herbaceous plant species.

Several spectral indices have been derived to detect changes in plant water content for the remote assessment of plant water stress. The sensitivity of such spectral indices to changes in plant water content is influenced by the internal leaf structure. Therefore, some spectral indices may not be suitable for the detection of low or moderate levels of plant water stress (Eitel et al., 2006). Two spectral indices that have been successfully used are the normalised difference water index (Gao, 1995) and water band index (Penuelas et al., 1995).

The normalised difference water index (Gao, 1995) is commonly used and accepted as an accurate estimate of plant water content. This index consists of the ratio of the difference between reflectance measured at 860 nm and 1 240 nm, and the sum of reflectance measured at 860 nm and 1 240 nm respectively (Gao, 1995). At these narrowband wavelengths, vegetation canopies have similar radiation-scattering properties, but slightly different liquid water absorption properties. Therefore, this index has been successfully applied to remotely detect plant water content for various tree species (Gao, 1995; Jackson et al., 2004; Stimson et al., 2005; Eitel et al., 2006).

The water band index is derived from the ratio of reflectance measured at 900 nm and 970 nm (Penuelas et al., 1995). This spectral index has been correlated with ground-based measurements of plant water content at both the leaf and canopy scales. It is, however, more sensitive to leaf water content than the water content of the whole plant. This is advantageous in agricultural applications, where leaf water content changes more noticeably in response to drought conditions than the water content of the entire plant foliage (Champagne et al., 2003).

Factors affecting spectral reflectance from leaf to canopy scales

The levels of spectral reflectance from a plant leaf or canopy are determined by a variety of factors. The factors that play a role in the spectral reflectance from a plant leaf or canopy include: species, site, age or maturity of plants or foliage, nutrient status, and leaf orientation, effects of variable irradiance, variable background, and the geometrical arrangement of the object/scene, sensor, and surface, orientation of the ground

Available on website http://www.wrc.org.za
ISSN 0378-4738 (Print) = Water SA Vol. 35 No. 5 October 2009
ISSN 1816-7950 (On-line) = Water SA Vol. 35 No. 5 October 2009

surface in relation to the location of the sun and remote sensing device and meteorological conditions (Asner, 1998; Coops et al., 2003). Their individual or combined effects are relevant for measurements with ground-based field spectrometers, airborne and satellite remote sensing technologies.

Remote sensors differ extensively in their ability to discriminate targets. Spatial resolution varies from less than a metre to several kilometres, with some models requiring input parameters from various data sources with different spatial resolutions (Chen, 1999). Furthermore, vegetation cover can be spatially highly heterogeneous, and variability within a pixel is likely to introduce uncertainties when processing and applying remote sensing imagery at different spatial resolutions (Jiang et al., 2006).

Spectral data collected at the leaf scale usually contain the least amount of variability and are most easily correlated to ground-truthing experiments at the same spatial scale. Ground-truthing in conjunction with remote sensing surveys is often undertaken at the leaf scale, due to the complexity of ground-truthing at larger spatial scales, and the difficulty in accounting for the significant variability in canopy reflectance. Therefore, spectral features and relationships which have been identified at the leaf scale in such studies have often also been applied generically at canopy and landscape scales (Mohammed et al., 1997; Datt, 1999; Zarco-Tejada et al., 2000; Coops et al., 2003).

Despite the difficulty in reproducing canopy reflectance, attempts have been made by stacking leaves on top of each other for below-canopy spectral measurements (Blackburn, 1999; Datt, 1999; Coops et al., 2003). The disadvantage of the leaf-stacking method is that it is unable to represent the absolute radiation interactions which occur at the canopy scale. It also fails to replicate, for example, canopy architecture, leaf angle distribution, the reflectance of trunks and branches, and the contribution of the wider canopy outside of the instrument field of view. Thus, its use is limited. It does, however, assist in controlling the impact of variables such as background reflectance, irradiation levels and sun-target-sensor geometry which do affect spectral reflectance measurements of the canopy scale.

The removal of atmospheric and background interferences is necessary when processing remote sensing data. Various types of calibration models can be applied depending upon the quantity and quality of calibration data recorded during the remote sensing acquisition surveys. Alternatively, the removal of atmospheric and background interferences could be omitted when vegetation spectral reflectance indices, which account for differences in atmospheric and background effects, were applied in sparsely vegetated environments (Giannico, 2004). Furthermore, the magnitude of atmospheric and background interferences is greater as spatial resolution decreases from ground to stand and canopy levels; and spectral resolution increases from multispectral to hyperspectral data.

Detection of plant water stress using ground-based measurements

Simple and quick ground-truthing methods which utilise portable instruments are needed for the measurement of plant water stress. Commonly used techniques address aspects of the plant water status and plant pigment concentration.

Predawn leaf water potential

Predawn leaf water potential measurements, often undertaken with a pressure chamber, are useful for determining plant water stress. At predawn, xylem water potential has equilibrated with soil water potential after a night of negligible transpiration. At this time, plant water potential is usually at its minimum for the day (Cleary and Zaerr, 1984).

The pressure chamber is most commonly used for estimating leaf water potential, having the advantage of simplicity, reliability, instantaneous measurements, low capital cost and portability (Scholander et al., 1965; Boyer, 1968; Ritchie and Hinckley, 1975). The equipment design has not changed significantly over the past 4 decades since Scholander et al. (1965) used this technique to measure the water relations of trees and shrubs. Manual operation is still required, therefore this technique is considered slow and time-consuming for any commercial or operational applications (Jones, 2004).

Measurement of predawn leaf water potential has gained wide acceptance among researchers. It is commonly used as a plant water stress indicator (Aranda et al., 2005; Nortes et al., 2005; Intrigliolo and Castel, 2006; Pellegrino et al., 2006) and has also been used to describe the water status of different species within a habitat (Scholander et al., 1965; Lamont and Witkowski, 1995). Predawn leaf water potentials have been shown to differ among species in the same habitat (Witkowski et al., 1992; Lamont and Witkowski, 1995), within a species across different habitats, and with leaf age (Witkowski et al., 1992) and within a species across different plant sizes (Lamont et al., 1994). Typical plant water potential measurements of unstressed plants range from -0.15 MPa for plants under saturated soil conditions and low atmospheric demand (Cleary and Zaerr, 1984) to -2.0 MPa for 'tank' plants such as cactus, which can store water (Scholander et al., 1965). Conversely, stressed plants such as creosote bush and juniper growing in more arid regions could achieve plant water potentials of -8.0 MPa (Scholander et al., 1965), while for desert plants it can be much higher. Predawn leaf water potential measurements have also been successfully used in agricultural applications to evaluate plant water stress. Such applications have included estimates of transpiration of soil water and assessments of crop water stress resulting from irrigation scheduling of grapevine field sites and fruit orchards (Intrigliolo and Castel, 2006; Pellegrino et al., 2006). Predawn leaf water potentials have also been coupled with stem water potential measurements and fluctuations in trunk diameters to quantify water stress of young almond trees for irrigation management (Nortes et al., 2005).

Despite the wide application of predawn pressure chamber measurements, numerous sources of error and measurement problems have been identified (Ritchie and Hinckley, 1975). These need to be minimised in order to ensure accurate readings, and can be grouped into 4 categories, viz. speed of measurement in the field; appropriate selection and processing of samples; reduction in pressurisation problems with the chamber; and correct identification of the end point.

In the field, speed of measurement is of major importance. Moisture loss between time of sampling and measurement must be minimised (Ritchie and Hinckley, 1975; Turner, 1988; Campbell, 1990; Hsiao, 1990; Smith and Prichard, 2003). Measurements should take place directly after excision of the plant sample. If this is not possible, samples should be enclosed in plastic bags immediately after cutting and stored in a cool dark place until required. However, if time-delays occur between predawn sampling and actual measurements, this could result in inaccurate measurements (Clear and Zaerr, 1984; Turner, 1988).

Great care should be taken in selecting and processing samples. It is important to standardise the sampling process

Available on website http://www.wrc.org.za
ISSN 0378-4738 (Print) = Water SA Vol. 35 No. 5 October 2009
ISSN 1816-7950 (On-line) = Water SA Vol. 35 No. 5 October 2009

with respect to leaf age and development stages when making a comparison between plant species (Witkowski et al., 1992). Damaged samples (crushed leaf petiole or torn leaf blades) and re-cutting of sample stems (Scholander et al., 1965), lead to a break in the tension in the xylem water, and should thus be avoided (Clear and Zaerr, 1984; Turner, 1988). Furthermore, the portion of the leaf or stem external to the seal in the pressure chamber unit must be minimised to reduce exclusion errors (Miller and Hansen, 1975; Hsiao, 1990).

Several technical guidelines must be adhered to in order to reduce pressurisation problems within the chamber. Failure to achieve pressure equilibrium should be addressed by ensuring that the seal used in the pressure chamber is made of rubber that is sufficiently elastic to fill the indentations of irregularly shaped petioles, but not so soft that it disintegrates under pressure. For very irregular petioles, a quick-setting silicon compound can be used. However, this slows down the number of leaves that can be measured (Turner, 1988). High-pressure grease or a silicon adhesive compound should be used on the stopper to prevent or reduce leakage and to prevent leaf damage. Studies on the optimal rates of pressurisation of the chamber and the effects of rapid pressure and heat build-up within the chamber have shown that fast rates of pressurisation can lead to both underestimates or overestimates of water potential depending on the gradients of water potential in the sample (Waring and Cleary, 1967; Blum et al., 1973; Tyree and Dainty, 1973; Turner, 1981). Therefore, Turner (1981) suggested an average pressurisation rate of 0.025 MPa·s^{-1}. Furthermore, caution must be taken in the use of the compressed gas within the pressure chamber. Pressure-release valves protect the pressure gauges and also help prevent over-pressurisation of the chamber (Turner, 1988). A binocular microscope or safety glasses should be used to protect the operator's eyes if any material is forced out through the seal during pressurisation (Turner, 1988).

Correct identification of the endpoint, when the xylem sap just returns to the cut surface of the xylem, is critical for accurate estimation of the water potential (Ritchie and Hinckley, 1975; Turner, 1988; Campbell, 1990; Hsiao, 1990; Smith and Prichard, 2003). Use of a binocular microscope or magnifying glass may be necessary to minimise poor endpoint recognition.

Field equipment required for leaf water potential measurements is relatively easy to set up within a specific location, but can be cumbersome when there are many sample sites which are not in close proximity to each other. When accounting for the time required for setting up of the instrument, gathering of samples and the actual measurement at predawn, only a limited number of measurements is possible within this timeframe. Therefore, from a practical view point this method would be more appropriate for localised measurements, as compared to large-scale measurements.

Leaf chlorophyll fluorescence

Over the past decade, chlorophyll fluorescence kinetics has been used more extensively to provide considerable information on the organisation and function of the photosynthetic apparatus (Govindjee et al., 1981). Information is gathered more readily and repeatedly outside the laboratory using portable optical systems and compact chlorophyll fluorescence meters.

The functioning of the photosynthetic apparatus is dependent on the process of photosynthesis, whereby light energy is absorbed and converted into organic compounds. Several environmental factors, including water, light and nutrients, affect this process and may lead to plant stress. Therefore, the photosynthetic apparatus has been recognised as being a good indicator of stress and stress adaptation of a plant and is associated with the measurement of chlorophyll fluorescence (Salisbury and Ross, 1992; Strasser and Tsmilli-Michael, 2001; Strasser et al., 2001). Also, because changes in chlorophyll fluorescence may occur before any physical signs of tissue or chlorophyll deterioration are manifested in the plant, stress can be detected before the onset of physical damage (Lichtenthaler et al., 2007).

Chlorophyll fluorescence measurements can be described using the typical phases of a temporary fluorescence signal or transient. During a typical fluorescence transient, the fluorescence rises rapidly from a ground state, O (or F_o) initial or minimal fluorescence, when all electron acceptors are fully oxidised, or open, to a maximum level, P (or F_m), when all electron acceptors are highly reduced, or closed and are unable to accept and transfer electrons (Rolando and Little, 2003). Various parameters representing subsequent phases in a typical fluorescence transient can yield information on how stress affects the functioning of the photosynthetic system (Strasser et al., 2001; Rolando and Little, 2003). Photochemical efficiency is a common parameter used to assess the effect of environmental stresses on the photosynthetic mechanism (Strasser and Tsmilli-Michael, 2001). The photochemical efficiency of Photosystem II (PSII) is estimated by F_v/F_m, which is the ratio of variable fluorescence (F_v) to maximum fluorescence (F_m). Most healthy plants exhibit F_v/F_m values of around 0.8 (Peterson et al., 2001).

In most studies on the applications of chlorophyll fluorescence, the F_v/F_m ratio is used as an indicator of water stress (Govindjee et al., 1981; Havaux and Lannoye, 1983; Ögren, 1990; Van Rensburg et al., 1996; Van der Mescht et al., 1997; Lu and Zhang, 1999; Peterson et al., 2001; Rolando and Little, 2003; Cifre et al., 2005). In these studies, it has been well documented that at the chloroplast level, the function of the thylakoid membrane is sensitive to environmental stress (Öquist, 1987). Studies which have focused on deep-rooted exotic tree species have suggested that a decrease in F_v/F_m is due to drought-induced injury to the thylakoid structures affecting photosynthetic electron transport (Van Rensburg et al., 1996; Van der Mescht et al., 1997; Lu and Zhang, 1999). These results indicated that F_v/F_m of drought-stressed trees was lower than the control trees, especially in the more drought-intolerant trees. Van Rensburg et al. (1996) found that the decrease in F_v/F_m was due largely to an increase in F_o, an indication of permanent damage to the PSII. PSII appears to be particularly sensitive to a number of stress factors including freezing temperatures and drought (Öquist and Wass, 1988). Rolando and Little (2003) also showed a decrease in F_v/F_m of water-stressed *Eucalyptus grandis* seedlings, resulting from a rise in F_o and a decrease in F_m. Since this ratio is a reflection of the maximum yield of primary photochemistry, F_v/F_m is also used as an indicator of tree or seedling vigour.

Water stress leads to several other changes in the photosynthetic apparatus of plants. Low water potential has been observed to cause a decrease in the quantum yield of O_2 evolution in chloroplasts and leaves from sunflower plants; a decrease in the ability of the coupling factor isolated from spinach leaves to bind fluorescent nucleotides; and a decrease in the ratio of the maximum to the minimum fluorescence in the red algae *Porphyrs sanjuanesis* (Govindjee et al., 1981). Data presented on the relationship between maximum to minimum fluorescence ratios and the water potential of leaves of

Nerium oleander, *Atriplex triangularis* and *Tolmiea menziesii*, suggest that water stress blocks electron flow to the reaction centre chlorophyll *a* of PSII (Govindjee et al. (1981). It was clear from these results that the ratio of maximum to minimum fluorescence decreases from a high value of 4.0 in well-watered *Nerium oleander* plants (water potential -0.8 MPa) to a low value of 1.1 in a severely stressed plant (water potential -3.9 MPa). In all cases examined, the ratio decreased as the water potential decreased. Because of these results, Govindjee et al. (1981) concluded that water stress inhibited electron flow of PSII in the 3 species examined, and that this ratio serves as a qualitative indicator of leaf water potential.

The use of chlorophyll fluorescence ratios as an index of plant water stress has gained increasing acceptance in recent years, and is commonly measured using hand-held relatively low-cost portable instruments which are simple, rapid and non-destructive (Peterson et al., 2001; Strasser et al., 2001; Strasser and Tsmilli-Michael, 2001; Rolando and Little, 2003; Cifre et al., 2005; Lichtenthaler et al., 2007). With the development of an internal saturating light source in portable field fluorescence meters, chlorophyll fluorescence measurements can now be undertaken at any time of the day, from shaded or sunlit samples.

Chlorophyll fluorescence measurements can be used in conjunction with other techniques as a relatively quick initial screening method for assessing plant stress within a localised area. There have also been significant advances in the application of chlorophyll fluorescence at larger spatial scales over the past decade, allowing for spatial detection of chlorophyll fluorescence parameters using laser-based fluorometers (Ounis et al., 2001; Cifre et al., 2005). Such technological improvements in chlorophyll fluorescence measurements would complement the ground-truthing of remote sensing imagery. However, further investigations are needed to establish its applicability for different crops under different conditions (Cifre et al., 2005). A disadvantage is that these instruments have not yet been designed for commercial or operational use.

Chlorophyll and carotenoid pigment concentration

Plant pigment concentrations vary with species, ecotype and phenology, and are also affected by season and various kinds of natural and anthropogenic stresses (Gitelson and Merzylak, 1997). Healthy plants, those capable of maximum growth, are generally expected to have higher chlorophyll pigment concentrations than unhealthy plants. Reduced chlorophyll concentrations are often associated with stressed plants, with variations in total chlorophyll to carotenoid ratios used as stress indicators (Netto et al., 2005; Lichtenthaler et al., 2007). Carotenoids play an important role in protecting the photosynthetic apparatus, and regulate the flow of energy into and out of the photosynthetic system (Sims and Gamon, 2002; Netto et al., 2005). Two commonly used approaches have been adopted to quantify chlorophyll and carotenoid pigment concentrations in plants, *viz.* conventional chemical methods and field chlorophyll meters. Conventional chemical methods of pigment quantification require destructive sampling and time-consuming laboratory analyses, whereas chlorophyll meters are simple, portable field instruments which permit rapid non-destructive measurements.

Conventional analytical chemistry methods used for estimating chlorophyll and carotenoid pigment concentrations are seen to be most accurate, provided that correct sampling and laboratory procedures are followed. These methods make use of spectrophotometry to estimate pigment concentrations in plant extractions from the linear absorption characteristics of these pigments in polar extractants at specific wavelengths. Concentrations are calculated taking cognisance of the extractant and the specific extinction coefficients as described in Lichtenthaler (1987). Two precautions are recommended when sampling and during laboratory analysis: rapid and efficient collection of samples which must be immediately frozen using liquid nitrogen to prevent pigment deterioration, and minimal loss of pigment during laboratory extraction and dilution procedures in order to reduce the variability of the results. If the research is taking place in remote areas, liquid nitrogen can be substituted with sufficient dry ice or ice packs (Curran et al., 1990; Datt, 1998; Pinkard et al., 2006).

Chlorophyll meters are portable field instruments that allow for non-destructive repetitive sampling; they have successfully been used to estimate the chlorophyll content of many plant species (Schaper and Chacko, 1991; Netto et al., 2005; Pinkard et al., 2006). A chlorophyll index derived from two peak reflectance wavelengths, 650 nm and 940 nm, is used to estimate the observed chlorophyll content in a sample. However, several factors such as different plant species, leaf weight, leaf age and growing conditions may affect the relationship between the chlorophyll index and actual chlorophyll concentration. Therefore, calibration curves are required for many species, site and experimental conditions (Pinkard et al., 2006).

Leaf-water content

Relative leaf water content is an indirect and gross estimate of the changes in the water content in leaves (Canny and Huang, 2006). Most water in leaves resides in mesophyll cells. Volumetric changes in these cells occur as the balance shifts between the rate of evaporation from leaves and the rate of water supply to the leaves. Volumetric changes in the leaves of plants affect many internal plant conditions such as tension in the cell walls, exchange of water and carbon dioxide across cell membranes, osmotic pressure of vacuole contents, cell and tissue turgor, cell-to-cell contact and transport of water.

Measurements of the relative water content of leaf tissue are commonly used to assess the water status of plants (Barrs and Weatherley, 1962; Catsky, 1969; Turner, 1981; Joly, 1985; Yamasaki and Dillenburg, 1999; Shen et al., 2005; Canny and Huang, 2006). Relative leaf water content is expressed as the ratio of three weight determinations *viz.* fresh weight; dry weight and turgid weight of the leaf sample. It is calculated as the ratio of fresh weight minus dry weight to turgid weight minus dry weight.

It is important that sampling procedures are meticulous to prevent evaporative losses of water from the leaf samples (Barrs and Weatherley, 1962; Catsky, 1969; Turner, 1981; Joly, 1985; Yamasaki and Dillenburg, 1999; Shen et al., 2005; Canny and Huang, 2006). Samples must be stored immediately in plastic bags and kept in a cool, dark place to reduce moisture loss prior to fresh weight measurements. Furthermore, the validity of relative water content measurements depends on the precision of the three weight determinations; a reliable estimate of turgid weight being the most critical (Joly, 1985).

A typical water absorption curve for a leaf shows a high initial rate of absorption, followed by a prolonged period of slow absorption (Yamasaki and Dillenburg, 1999). The amount of water initially absorbed has been commonly interpreted as being the amount of water needed to compensate for the water deficit of the plant tissue. Further water absorption is driven

Available on website http://www.wrc.org.za
ISSN 0378-4738 (Print) = Water SA Vol. 35 No. 5 October 2009
ISSN 1816-7950 (On-line) = Water SA Vol. 35 No. 5 October 2009

by cell expansion, so that mass changes occurring during this phase are not used in the estimation of the relative water content of the sample. Therefore, an accurate measurement of turgid weight should be determined at the end of the first initial phase of water absorption (Yamasaki and Dillenburg, 1999).

Water absorption periods usually recommended for conifers range from 12 to 48 hours, which is much longer than the 4 hour period usually required for most broad leaved plants (Yamasaki and Dillenburg, 1999). To reduce water absorption periods, smaller leaf disks which absorb water more quickly are commonly used instead of larger whole leaves (Barrs and Weatherley, 1962). This method may however, also allow more water infiltration through intercellular spaces, thereby resulting in a greater water absorption per unit of leaf mass, when compared to absorption in whole leave (Barrs and Weatherley, 1962; Joly, 1985).

Measuring the relative leaf water content of plants is a simple yet time-consuming process. Comparative measurements between stressed and unstressed plants should be undertaken during the morning when differences in water potentials between plants are greatest (Cleary and Zaerr, 1984). Due to these time constraints this method is most appropriate for localised ground-truthing measurements.

Comparison of ground-based measurement techniques for measuring plant water stress

It has been suggested in this review that all 4 ground-based measurements, *viz.* predawn leaf water potentials, chlorophyll fluorescence, chlorophyll and carotenoid pigment concentrations and leaf water content can be used successfully to measure or assess plant water stress. However, these 4 methods are not suitable for large spatial scale sampling, and would be most useful for localised studies or for localised ground-truthing of remote sensing applications. Sampling protocols for ground-truthing applications are dependent upon the spatial scales at which the remote sensing studies are being undertaken, viz. leaf, canopy, stand or landscape scale and, hence sample sizes will differ accordingly. A summary of some of the advantages and disadvantages of each ground-based method is listed in Table 2.

These 4 ground-based measurements vary in their practical use as well as in the physiological processes measured. Differences in these methods as well as the processes measured may be affected by different sources of variability, which in turn may affect the strength of the relationship to spectral indices (Stimson et al., 2005). As a result, strong relationships may exist between certain ground measurements and spectral indices, while others may be poorer for a specific plant species. For example the water band index derived by Gao (1995) focused on water content of vegetation and therefore could be more strongly correlated to leaf water content measurements than plant pigment concentrations and vice versa.

Different ground-based measurements of plant water stress may be preferred depending upon the research conditions under which a particular method is being applied. For airborne and satellite remote sensing vegetation studies, ground-truthing techniques which are cost effective, efficient and reliable and can be applied over localised ground-truthing regions within a reasonable time-frame of acquiring the remote sensing images would be preferred. Under such research conditions measurements of chlorophyll fluorescence or leaf water content would be more suited. On the other hand, measurements of predawn leaf water potential or chlorophyll pigment concentrations could be used for smaller-scale intensive sampling. However, should costs be constraining factor predawn leaf water

Table 2
Advantages and disadvantages of 4 ground-based methods for measuring plant water stress

Ground-based method for measuring plant water stress	Advantages	Disadvantages
Predawn leaf water potential	Simple, reliable, instantaneous measurement, low capital cost, portable, direct indication of plant water stress. All parts of plant at predawn should be at same water potential.	Slow and time-consuming for landscape-scale measurements; not suitable for use over large spatial scales; can be cumbersome when sampling sites are not in close proximity to each other; destructive sampling. Pre-dawn sampling is inconvenient.
Leaf chlorophyll fluorescence	Hand-held portable, lightweight field instruments, simple, rapid non-destructive sampling, relatively low capital cost, internal saturating light source present in latest models, measurements can be taken at any time of the day, technology advances for remote sensing applications using laser-based fluorometers.	Not designed for use over large spatial scales.
Chlorophyll and carotenoid pigment concentrations	a. Conventional analytical chemistry methods Foundations in well-researched methodologies of spectrophotometry. b. Chlorophyll meter Simple, portable, non-destructive sampling, allows for repeated measurements on the same sample over time, instantaneous measurement	Problem in keeping leaves fresh to avoid chlorophyll degradation. Destructive sampling, time consuming. Calibration required to obtain actual chlorophyll concentrations for different species and environments.
Leaf water content	Simple, no capital costs, low precision analytical measurements	Validity dependent on precision of weight determinations, time-consuming, destructive sampling

Available on website http://www.wrc.org.za
ISSN 0378-4738 (Print) = Water SA Vol. 35 No. 5 October 2009
ISSN 1816-7950 (On-line) = Water SA Vol. 35 No. 5 October 2009

potential measurements would be preferred over laboratory analyses of plant chlorophyll pigment concentrations.

In summary it is recommended that a more complete but practical approach to assessing plant water stress is adopted. At least one ground-based technique such as plant pigment concentrations, chlorophyll fluorescence or relative leaf water content should be used for localised ground-truthing measurements to identify gradients in plant water stress, followed by intensive predawn leaf water potential measurements along these gradients to identify the extremes in plant water stress.

Concluding remarks

This review demonstrates that there has been extensive research on the detection and measurement of plant water stress using ground-based and remote sensing technologies. Ground-based techniques are more suited for localised measurements and for ground-truthing of remotely sensed data. Remote sensing research has identified several individual spectral bands and vegetation spectral reflectance indices which have been used to detect plant water stress. Many of the earlier studies have focused on broad spectral bandwidths and it is recommended that plant stress researchers utilise the spectral findings to further investigate the potential of narrow hyperspectral bandwidths to detect and interpret patterns of plant stress. Furthermore, the importance of the red edge defined as the region between 690 and 740 nm has gained increasingly more attention over the years, and is seen as one of the most important regions of the spectrum when investigating plant stress. It is also recommended that the results from hyperspectral studies should be incorporated in multispectral technologies through modified imaging systems or spectral filters to allow for specialised high spectral resolution investigations to be undertaken with reduced data volumes in a cost-effective manner. Most spectral indices have been derived for a single species with constant leaf size and shape, leaf surface and internal structure, implying that their usefulness varies with respect to species and site conditions. Therefore, the most commonly used indices reported in the literature must be evaluated against ground-truthing data. Ground-truthing of remote sensing data is not an easy task especially when considering different temporal and spatial scales. Depending upon the scale at which an investigation is being undertaken, it is recommended that a practical approach to assessing plant water stress is adopted through the use of at least one ground-based measurement, viz. plant pigment concentrations, chlorophyll fluorescence or relative leaf water content to identify gradients in plant stress, and to then undertake predawn leaf water potential measurements along this gradient, specifically to identify the extremes in plant water stress.

Acknowledgements

Acknowledgement for funding for this work is made to the Mine Woodlands Project (School of Animal, Plant and Environmental Sciences, University of the Witwatersrand, Johannesburg, South Africa), the South African Department of Trade and Industry (THRIP funding), AngloGold Ashanti Ltd. and the CSIR.

References

ALDER NN, SPERRY JS and POCKMAN WT (1996) Root and stem xylem embolism, stomatal conductance, and leaf turgor in *Acer grandidentatum* populations along a soil moisture gradient. *Oecol.* 105 293-301.

ARANDA I, CASTRO L, PARDOS M, GIL L and PARDOS JA (2005) Effects of the interaction between drought and shade on water relations, gas exchange and morphological traits in cork oak (*Quercus suber* L.) seedlings. *For. Ecol. Manage.* 210 117-129.

ASNER GP (1998) Biophysical and biochemical sources of variability in canopy reflectance. *Remote Sens. Environ.* 64 234-253.

BARET F and JACQUEMOUD S (1994) Model inversion to retrieve canopy characteristics from high spectral resolution data. *Proc. 6th Int. Symp. Physical Measurements and Signatures in Remote Sensing.* 17-21 January 1994, Val d'Isère, France.

BARET F, VANDERBILT VC, STEVEN MD and JACQUEMOUD S (1994) Use of spectral analogy to evaluate canopy reflectance sensitivity to leaf optical properties. *Remote Sens. Environ.* 48 253-260.

BARRS HD and WEATHERLY PE (1962) A re-examination of the relative turgidity technique for estimating water deficits in leaves. *Aus. J. Biol. Sci.* 15 413-428.

BLACKBURN GA (1998a) Quantifying chlorophylls and carotenoids at leaf and canopy scales: an evaluation of some hyperspectral approaches. *Remote Sens. Environ.* 66 273-285.

BLACKBURN GA (1998b) Spectral indices for estimating photosynthetic pigment concentrations: a test using senescent tree leaves. *Int. J. Remote Sens.* 19 657-675.

BLACKBURN GA (1999) Relationship between spectral reflectance and pigment concentrations in stacks of deciduous broadleaves. *Remote Sens. Environ.* 70 224-237.

BLACKBURN GA (2007) Hyperspectral remote sensing of plant pigments. *J. Exp. Bot.* 58 855-867.

BLUM A, SULLIVAN CY and EASTIN JD (1973) On the pressure chamber technique for estimating leaf water potential in sorghum. *Agron.* 65 337-338

BOYER JS (1968) Relationship of water potential to growth of leaves. *Plant Phys.* 43 1056-1062.

CAMPBELL GS (1990) Instrumentation of studying vegetation canopies for remote-sensing in optical and thermal infrared regions - water potential in soils and plants. *Remote Sens. Rev.* 5 249-261.

CAMPBELL PKE, MIDDLETON EM, McMURTREY JE, CORP LA and CHAPPELLE EW (2007) Assessment of vegetation stress using reflectance or fluorescence measurements. *J. Environ. Qual.* 36 832-845.

CANNY MJ and HUANG CX (2006) Leaf water content and palisade cell size. *New Phytol.* 170 75-85.

CARTER GA (1993) Responses of leaf spectral reflectance to plant stress. *Am. J. Bot.* 80 239-243.

CATSKY J (1969) Temperature effects in the measurement of water saturation deficit (relative water content) in tobacco and kale. *Biol. Plantarum* 11 381-383.

CECCATO P, FLASSE S, TARANTOLA S, JACQUEMOUD S and GREGOIRE J-M (2001) Detection vegetation leaf water content using reflectance in the optical domain. *Remote Sens. Environ.* 77 22-33.

CHAMPAGNE CM, STAENZ K, BANNARI A, McNAIRIN H and DEGUISE JC (2003) Validation of a hyperspectral curve fitting model for the estimation of plant water content of agricultural canopies. *Remote Sens. Environ.* 87 148-160.

CHEN J (1999) Spatial scaling of a remotely sensed surface parameter by contexture. *Remote Sens. Environ.* 69 30-42.

CHUN-JIANG Z, JI-HUA W, LIANG-YUN L, WEN-JIANG H and QI-FA Z (2006) Relationship of 2 100-2 300nm spectral characteristics of wheat canopy to leaf area index and leaf N as affected by leaf water content. *Pedosphere* 16 333-338.

CIFRE J, BOTA J, ESCALONA JM, MEDRANO H and FLEXAS J (2005) Physiological tools for irrigation scheduling in grapevine (*Vitis vinifera* L.) An open gate to improve water-use efficiency. *Agric. Ecosys. Environ.* 106 159-170.

CLAY DE, CHANG KKJ, CLAY SA, and DALSTED K (2006) Characterizing water and nitrogen stress in corn using remote sensing. *Agron. J.* 98 579-587.

CLEARY B and ZAERR J (1984) Guidelines for Measuring Plant Moisture Stress with a Pressure Chamber. PMS Instrument

Available on website http://www.wrc.org.za
ISSN 0378-4738 (Print) = Water SA Vol. 35 No. 5 October 2009
ISSN 1816-7950 (On-line) = Water SA Vol. 35 No. 5 October 2009

Company. Royal Oaks Drive, Corvallis, Oregon, USA.
COLLINS W, CHANGE SH, RAINES G, CANNEY F and ASHLEY R (1983) Airborne biogeophysical mapping of hidden mineral deposits. *Econ. Geol.* 78 737-749.
COOPS N, DURY S, SMITH ML, MARTIN M and OLLINGER S (2002) Comparison of green leaf eucalypt spectra using spectral decomposition. *Aust. J. Bot.* 50 567-576.
COOPS N, STONE C, CULVENOR DS, CHISHOLM LA and MERTON RN (2003) Chlorophyll content in eucalypt vegetation at the leaf and canopy scales as derived from high resolution spectral data. *Tree Physiol.* 23 23-31.
CURRAN PJ, DUNGAN JL and GHOLZ HL (1990) Exploring the relationship between reflectance red edge and chlorophyll content in slash pine. *Tree Physiol.* 7 33-48.
CURRAN PJ, DUNGAN JL, MACLER BA and PLUMMER SE (1992) The effect of a red leaf pigment on the relationship between red-edge and chlorophyll concentration. *Remote Sens. Environ.* 35 69-75.
DATT B (1998) Remote sensing of chlorophyll a, chlorophyll b, chlorophyll a + b, and total carotenoid content in Eucalyptus leaves. *Remote Sens. Environ.* 66 111-121.
DATT B (1999) A new reflectance index for remote sensing of chlorophyll content in higher plants: tests using *Eucalyptus* leaves. *J. Plant Physiol.* 154 30-36.
DE TAR WR, PENNER JV and FUNK HA (2006) Airborne remote sensing to detect plant water stress in full canopy cotton. *Trans. Soc. Agric. Bio. Eng.* 49 655-665.
DIXON HH (1914) *Transpiration and the Ascent of Sap in Plants.* Macmillan, London. 75p.
EITEL JUH, GESSELER PE, SMITH AMS and ROBBERECHT R (2006) Suitability of existing and novel spectral indices to remote detect water stress in *Populus* spp. *For. Ecol. Manage.* 229 170-182.
FILELLA I and PENUELAS J (1994) The red edge position and shape as indicators of plant chlorophyll content, biomass and hydric status. *Int. J. Remote Sens.* 15 1459-1470.
FITZGERALD GJ, RODRIGUEZ D, CHRISTENSEN LK, BELFORD R, SADRAS VO and CLARKE TR (2006) Spectral and thermal sensing for nitrogen and water status in rainfed and irrigated wheat environments. *Precis. Agric.* 7 233-248.
FOUTRY T and BARET F (1997) Vegetation water and dry matter contents estimated from top of the atmosphere reflectance data: a simulation study. *Remote Sens. Environ.* 61 34-45.
GAO BC (1995) Normalized difference water index for remote sensing of vegetation liquid water from space. *Proc. Int. Soc. Optical Eng.* 2480 225-236.
GAUSSMAN HW (1977) Reflectance of leaf components. *Remote Sens. Environ.* 6 1-9.
GIANNICO C (2004) Remote sensing of vegetation in the calabrian region. *Acta Astronaut.* 60 119-131.
GITELSON AA and MERZLYAK MN (1996) Signature analysis of leaf reflectance spectra: algorithm development for remote sensing of chlorophyll. *J. Plant Physiol.* 148 494-500.
GITELSON AA and MERZLYAK MN (1997) Remote estimation of chlorophyll content in higher plant leaves. *Int. J. Remote Sens.* 18 2691-2697.
GITELSON AA, ZUR Y, CHIVKUNOVA OB and MERZLYAK MN (2002) Assessing carotenoid content in plant leaves with reflectance spectroscopy. *Photochem. and Photobiol.* 75 272-281.
GOVINDJEE DOWNTON WJS, FORK DC and ARMOND PA (1981) Chlorophyll a fluorescence transient as an indicator of water potential of leaves. *Plant Sci. Letter* 20 191.
GUYOT G and BARET F (1988) Utilization of high spectral resolution to follow the state of vegetable cover. *Proc. 4th Int. Symp. Spectral Signatures of Objects in Remote Sens.* 18-22 January, Aussois, France. pp. 54-61.
HACKE U and SAUTER JJ (1996) Drought-induced xylem dysfunction in petioles, branches and roots of *Populus balsamifera* L. and *Alnus glutinosa* (L.) Gaertn. *Plant Physiol.* 111 413-417.
HARRIS A, BRYANT RG and BAIRD AJ (2006) Mapping the effects of water stress on *Sphagnum*: Preliminary observations using airborne remote sensing. *Remote Sens. Environ.* 100 363-378.
HAVAUX M and LANNOYE R (1983) Chlorophyll fluorescence induction: a sensitive indicator of water stress in maize plants. *Irrig. Sci.* 4 147-151.
HOPE A, BURVALL A, GERMISHUYSE T and NEWBY T (2009) River flow responses to changes in vegetation cover in a South Africa fynbos catchment. *Water SA* 35 55-60.
HORLER DNH, DOCKRAY M and BARBER J (1983) The red edge of plant reflectance. *Int. J. Remote Sens.* 4 273-288.
HSIAO TC (1973) Plant responses to water stress. *Ann. Rev. Plant Physiol.* 24 519-570.
HSIAO TC (1990) Plant-atmosphere interactions, evapo-transpiration, and irrigation scheduling. *Acta Hort.* 278 55-66.
HUNT ER and ROCK BN (1989) Detection of changes in leaf water content using near- and middle infrared reflectances. *Remote Sens. Environ.* 30 43-54.
INTRIGLIOLO DS and CASTEL JR 2006 Performance of various water stress indicators for prediction of fruit size response to deficit irrigation in plum. *Agric. Water Manage.* 83 173-180.
JACKSON TJ, CHEN D, COSH M, LI F, ANDERSON M, WALTHALL C, DORIASWAMY P and HUNT ER (2004) Vegetation water content mapping using Landsat data derived normalized difference water index for corn and soybeans. *Remote Sens. Environ.* 92 475-482.
JACQUEMOUD S (1993) Inversion of the PROSPECT + SAIL canopy reflectance model from AVIRIS equivalent spectra: theoretical study. *Remote Sens. Environ.* 44 281-292.
JIANG Z, HUETE AR, CHEN J, CHEN Y, LI J, YAN G and ZANG X (2006) Analysis of NDVI and scaled difference vegetation index retrievals of vegetation fraction. *Remote Sens. Environ.* 101 366-378.
JOLY RJ (1985) Techniques for determining seedling water status and their effectiveness in assessing stress. *Proc. Evaluating Seedling Quality: Principles, Procedures and Predictive Abilities of Major Tests.* 16-18 October 1984, Forest Research Laboratory, Oregon State University, Corvallis, US.
JONES HG (2004) Irrigation scheduling: advantages and pitfalls of plant-based methods. *J. Exp. Bot.* 55 2427-2436.
LAMONT BB, REES RG, WITKOWSKI ETF and WHITTEN VA (1994) Comparative size, fecundity and ecophysiology of roadside plants of *Banksia hookeriana*. *J. App. Ecol.* 31 137-144.
LAMONT BB and WITKOWSKI ETF (1995) A test for lottery recruitment among four *Banksia* species based on their demography and biological attributes. *Oecol.* 101 299-308.
LELONG CCD, PINET PC and POILVÉ H (1998) Hyperspectral imaging and stress mapping in agriculture: a case study on wheat in Beauce (France). *Remote Sens. Environ.* 66 179-191.
LICHTENTHALER HK (1987) Chlorophyll and carotenoids: Pigments of photosynthetic biomembranes. *Methods Enzym.* 148 331-382.
LICHTENTHALER HK, ALEXANDER AC, MAREK MV, KALINA J and URBAN O (2007) Differences in pigment composition, photosynthetic rates and chlorophyll fluorescence images of sun and shade leaves of four tree species. *Plant Physiol. Biochem.* 1-12.
LICHTENTHALER HK, BUSCHMANN C, RINDERLE U and SCHMUCH G (1996) Application of chlorophyll fluorescence in ecophysiology. *Radiat. Environ. Biophys.* 25 297-308.
LINTON MJ, SPERRY JS AND WILLIAMS DG (1998) Limits to water transport in *Juniperus osteosperma* and *Pinus edulis*: implications for drought tolerance and regulation of transpiration. *Funct. Ecol.* 12 906-911.
LU C and ZHANG J (1999) Effects of water stress on photosystem II photochemistry and its thermostability in wheat plants. *J. Exp. Bot.* 50 1199-1206.
MILLER BD and HANSEN GK (1975) Exclusion errors in pressure chamber estimates of leaf water potential. *Ann. Bot.* 39 915-920.
MILTON NM and MOUAT DA (1989) Remote sensing of vegetation responses to natural and cultural environmental conditions. *Photogramm. Eng. Remote Sens.* 55 1167-1173.
MOHAMMED GH, SAMPSON PH, COLOMBO SJ, NOLAND TL and MILLER JR., (1997) Bioindicators of Forest Sustainability: Development of a Forest Condition Rating System for Ontario. Forest Research Information Paper No. 137, Ontario Forest Research Institute, Ontario, Canada. 22 pp.

Available on website http://www.wrc.org.za
ISSN 0378-4738 (Print) = Water SA Vol. 35 No. 5 October 2009
ISSN 1816-7950 (On-line) = Water SA Vol. 35 No. 5 October 2009

MULLER NJC (1874) Investigations about the diffusion of the atmospheric gases and the gas removal under different lighting terms. *Ann. Sci. Bot.* 9 36-49.
MURTHA PA (1982) Detection and analysis of vegetation stress. In: CJ Johannsen and JL Sanders (eds.) *Remote Sensing for Resource Management*. Soil Conservation Society of America. Ankeny, Iowa, USA. pp 141-158.
MUSICK HB and PELLETIER RE (1986) Response of some Thematic Mapper band ratios to variation in soil water content. *Photogramm. Eng. Remote Sens.* 52 1661–1668.
MUSICK HB and PELLETIER RE (1988) Response to soil moisture of spectral indexes derived from bidirectional reflectance in Thematic Mapper wavebands. *Remote Sens. Environ.* 25 167-184.
NETTO AT, CAMPOSTRINI E, DE OLIVEIRA JG and BRESSAN-SMITH RE (2005) Photosynthetic pigments, nitrogen, chlorophyll *a* fluorescence and SPAD-502 readings in coffee leaves. *Sci. Hortic.* 104 199-209.
NORTES PA, PASTOR-PÉREZ A, EGEA G, CONEJERO W and DOMINGO R (2005) Comparison of changes in stem diameter and water potential values for detecting water stress in young almond trees. *Agric. Water Manage.* 77 296-307.
ÖGREN E (1990) Evaluation of chlorophyll fluorescence as a probe for drought stress in willow leaves. *Plant Physiol.* 93 1280-1285.
ÖQUIST G and WASS R (1988) A portable, microprocessor operated instrument for measuring chlorophyll fluorescence kinetics in stress physiology. *Physiol. Plantarum* 73 211-217.
ÖQUIST G (1987) Environmental stress and photosynthesis. In: J Biggins (ed.) *Progress in Photosynthesis Research*. Martinus Nijhoff Publishers, Dordrecht, The Netherlands. Vol. IV 1-10.
OUNIS A, EVAINS, FLEXAS J, TOSTI J and MOYA I (2001) Adaptation of a PAM-fluorometer for remote sensing of chlorophyll fluorescence. *Photosyn. Res.*68 113-120.
PELLEGRINO A, GOZÉ E, LEBON E and WERY J (2006) A model based diagnostic tool to evaluate the water stress experienced by grapevine in field sites. *Eur. J. Agron.* 25 49-59.
PENUELAS J, FILELLA I, BIEL C, SERRANO L and SAVE R (1995) The reflectance at the 950-970 region as an indicator of plant water status. *Int. J. Remote Sens.* 14 1887-1905.
PETERSON JA, GRONINGER JW, SEILER JR and MOU P (2001) Utility and limitations of chlorophyll fluorescence for the determination of growth limitations in trees. *Proc. 10th Bienn. Southern Silvicult. Res. Conf.* LA, USA?. USDA Technical Report. SRS-30. 480-484.
PINKARD EA, PATEL V and MOHAMMED C (2006) Chlorophyll and nitrogen determination for plantation-grown *Eucalyptus nitens* and *Eucalyptus globulus* using a non-destructive meter. *For. Ecol. Manage.* 223 211-217.
PU R, GE S, KELLY NM and GONG P (2003) Spectral absorption features as indicators of water status in coast live oak (*Quercus agrifolia*) leaves. *Int. J. Remote Sens.* 24 1799-1810.
RITCHIE GA and HINCKLEY TM (1975) The pressure chamber as an instrument for ecological research. *Adv. Ecol. Res.*9 165-255.
ROCK BN, HOSHIZAKI T and MILLER JR (1988) Comparison of in situ and airborne spectral measurements of the blue shift associated with forest decline. *Remote Sens. Environ.* 24 109-127.
ROLANDO CA and LITTLE KM (2003) Using chlorophyll fluorescence to determine stress in *Eucalyptus grandis* seedlings. *S. Afr. For. J.* 197 5-12.
SALISBURY FB and ROSS CW (1992) *Plant Physiology* (4th edn.). Wadsworth Publishing Company, California, USA. 682 pp.
SCHAPER H and CHACKO EK (1991) Relation between extractable chlorophyll and portable chlorophyll meter readings in leaves of eight tropical and subtropical fruit tree species. *J. Plant Physiol.* 138 674-677.
SCHOLANDER PF, HAMMEL HT, BRADSTREET EA and HEMMINGSEN EA (1965) Sap pressure in vascular plants. *Sci.* 148 339-346.
SEPULCRE-CANTÓ G, ZARCO-TEJADA PJ, JIMÉNEZ-MUNOZ JC, SOBRINO JA, DE MIGUEL E and VILLALOBOS FJ (2006) Detection of water stress in an olive orchard with thermal remote sensing imagery. *Agric. For. Meteorol.* 136 31-44.
SHEN Y, ZHENG RS and YAN CY (2005) Estimation models for vegetation water content at both leaf and canopy levels. *Inst. Elec. Electron. Eng.* 2 1387-1389.
SIMS DA and GAMON JA (2002) Relationships between leaf pigment content and spectral reflectance across a wide range of species, leaf structures and development stages. *Remote Sens. Environ.* 81 337-354.
SMITH R and PRICHARD T (2003) Using a pressure chamber in winegrapes: UC Cooperative Extension. www.cesonoma.ucdavis.edu/viti/pdf/wine_grape_pressure_chamber.pdf (Accessed 2 October 2006).
SPERRY JS and SALIENDRA NZ (1994) Intra- and inter-plant variation in xylem cavitation in *Betula occidentalis*. *Plant, Cell Environ.* 17 1233-1241.
STIMSON HC, BRESHEARS DD, USTIN SL and KEFAUVER C (2005) Spectral sensing of foliar water conditions in two co-occurring conifer species: *Pinus edulis* and *Juniperus monosperma*. *Remote Sens. Environ.* 96 108-118.
STONE C, CHISHOLM L and COOPS N (2001) Spectral reflectance characteristics of eucalypt foliage damaged by insects. *Aust. J. Bot.* 49 687-698.
STRASSER RJ and TSIMILLI-MICHAEL M (2001) Stress in plants, from daily rhythm to global changes detected and quantified by the JIP-Test. *J. Chim. Nouv.* 75 3321-3326.
STRASSER RJ, SRIVASTAVA A and TSIMILLI-MICHAEL M (2001) Analysis of the fluorescent transient. In: GC Papageorgiou and WIS Govindjee (eds.) *Chlorophyll Fluorescence: A Signature of Photosynthesis*. Kluwer Academic Publishers, Dordrecht, The Netherlands.
TUCKER CJ (1980) Remote sensing of leaf water content in the near infrared. *Remote Sens. Environ.* 10 23-32.
TURNER NC (1981) Techniques and experimental approaches for the measurement of plant water status. *Plant and Soil* 58 339-366.
TURNER NC (1988) Measurement of plant water status by the pressure chamber technique. *Irrig. Sci.* 9 289-308.
TYREE MT and DAINTY J 1973 The water relations of hemlock (*Tsuga canadensis*). II. The kinetics of water exchange between symplast and apoplast. *Can. J. Bot.* 51 1481-1489.
VAN DER MESCHT A, DE RONDE K, VAN DER MERWE T, LAURIE R, BESTER C and WENZEL C (1997) Evaluation of chlorophyll fluorescence as a measure of drought tolerance in *Eucalyptus grandis*. *Proc. 4th IUFRO Conf. on Silviculture and Improvement of Eucalypts*. August 1997, Embrapa, Salvador, Brazil. 117-124.
VAN RENSBURG L, KRUGER GHJ, EGGENBERG P and STRASSER RJ (1996) Can screening criteria for drought resistance in *Nicotiana tabacum L.* be derived from the polyphasic rise of the chlorophyll *a* fluorescent transient (OJIP). *S. Afr. J. Bot.* 62 337-341.
WARING RH and CLEARY BD (1967) Plant moisture stress: evaluation by pressure bomb. *Sci.* 155 1248-1254.
WEATHERLEY PE (1950) Studies in the water relations of the cotton plant. I. The field measurement of water deficits in leaves. *New Phytol.* 49 81-97.
WITKOWSKI ETF, LAMONT BB, WALTON C and RADFORD S (1992) Leaf demography, sclerophylly and ecophysiology of two banksias with contrasting leaf life spans. *Aust. J. Bot.* 40 849-62.
YAMASAKI S and DILLENBURG LR (1999) Measurements of leaf relative water content in *Araucaria Angustifolia*. *Rev. Bras. Fisiol. Veg.* 11 69-75.
ZARCO-TEJADA PJ, MILLER JR, MOHAMMED GH and NOLAND TL (2000) Chlorophyll fluorescence effects on vegetation apparent reflectance. I. Leaf-level measurements and model simulation. *Remote Sens. Environ.* 74 582-595.
ZARCO-TEJADA PJ, RUEDA CA and USTIN SL (2003) Water content estimation in vegetation with MODIS reflectance data and model inversion methods. *Remote Sens. Environ.* 85 109-124.

Available on website http://www.wrc.org.za
ISSN 0378-4738 (Print) = Water SA Vol. 35 No. 5 October 2009
ISSN 1816-7950 (On-line) = Water SA Vol. 35 No. 5 October 2009

APPENDIX 2: PROTOCOLS FOR GROUND-BASED MEASUREMENTS OF PLANT WATER STRESS

A. Predawn leaf water potential measurements

1. Setup up a pressure chamber system with a compressed air cylinder.
2. Ensure enough light is available (torches, lamps, spot lights) for predawn measurements. Have field notes and pen ready to take readings.
3. Use labelled plastic bags to collect leaf samples from individual sample trees. Immediately seal with a loose top knot to prevent moisture loss from leaves.
4. The rate regulator should be set to exhaust during setup. This regulator closes clockwise and opens anti-clockwise.
5. Use a sharp razor blade to cut a leaf with a long stalk. Only cut once, or use another leaf stalk.
6. Take out chamber and secure leaf stalk through rubber bung with prestik. Place in chamber. Replace the chamber and ensure it is properly fastened. During measurement, if a noise is created from air escaping, this indicates that there is a leak in the seal between the leaf stalk and the prestik around the rubber bung. If this is the case, the procedure should be re-started from the beginning and a new sampled must prepared.
7. The first gauge should read approximately 17 MPa from the cylinder.
8. The second gauge should read approximately 2 to 3 MPa, which allows air into the hose and chamber.
9. Use a magnifying glass to carefully watch the tip of the stalk. As soon as the first droplet of water appears at the tip of the stalk, a reading must be taken. Record all readings in a field book or in field notes.

B. Analytical measurement of leaf chlorophyll pigment content

Collection of leaf samples:

1. In preparation for the field sampling, ensure that a cooler box with sufficient ice packs and ice is on-hand to keep leaf samples frozen.
2. Label zip-lock plastic bags using a permanent marker and labels.
3. Collect leaf samples from each sample tree (at least 25 to 30 leaves) to ensure enough leaf material for 5 replicate analyses.
4. Immediately remove air from bag and seal properly.
5. Place labelled sample bag into cooler box to ensure that sample is frozen quickly to prevent chlorophyll degradation.
6. To prevent mixing of sample bags, staple samples bags from the same site and same tree species immediately together.
7. On return to the laboratory ensure that all sample bags are transferred from cooler box into a deep-freezer and are kept frozen until laboratory analysis.

Laboratory analysis:

1. In the laboratory ensure minimal unnatural light and draw blinds if necessary.
2. Using a sharp pair of scissors, cut 2 to 3 leaves into fine pieces.
3. Clean, dry and label 25 centrifuge test tubes representing 5 samples of 5 replications each. Place test tube into a test tube rack.
4. Measure 0.1g of the finely cut leaf sample into labelled test tube using a fine weighing balance.
5. Add 5ml of 100% methanol to each sample using a bottle dispenser.
6. Dissolve leaf sample in methanol using an ultra turax for 1minute.
7. Add another 5ml of 100% methanol to each sample using a bottle dispenser, increasing the total volume to 10ml.
8. Centrifuge the test tubes at a speed 6 for 8 minute.
9. Using a finette pipette dispense 2ml of supernatant from each centrifuged test tube into cuvette. Dilute with 2ml of methanol.
10. Read the samples through a spectrophotometer calibrated at 665.2 nm, 652.4 nm and 470 nm.
11. Relative pigment contents can be estimated using the equations developed by Lichtenthaler (1987):

$$Chlorophyll\,a = 16.72(A665.2) - 9.16(A652.4)$$

$$Chlorophyll\,b = 34.09(A652.4) - 15.28(A665.2)$$

$$Chlorophyll\,a+b = 1.44(A665.2) + 24.93(A652.4)$$

$$Carotenoid\,x+c = \frac{(000 * A470 - 1.63[Chlorophyll\,a] + 104.96[Chlorophyll\,b]}{221}$$

C. Leaf chlorophyll fluorescence measurements using fluorescence meter

1. Connect the PAR clip with the external illuminator which has a long silver cable. Ensure that the illuminator is pointing downward, and that the illuminator and PAR clip align in order to tighten the screws. To the PAR clip, connect the lamp jack. Connect the PAR clip cable to the fluorescence meter accessory jack.
2. Connect the long silver cable to the front panel of the fluorescence meter. Line up the plug-ins so that they do not cross over (2 at the top: left a detector connector, right a actinic connector) and (bottom right saturation connector and left small trigger connector).
3. Power the fluorescence meter on only when all components are connected properly.
4. Use the selection wheel on front panel to navigate between the available measurement options.
5. Set the system test mode to the yield option. Use the test setup key to setup the parameters for measurements and the default yield mode parameter dataset to begin measurements.
6. Set the run data screen model to auto-log and ensure that the number of samples and the file number is 1 when starting measurements.
7. When the connection and setup is complete begin the sample readings. Try to select samples leaves from different areas of the tree, with at least 5 replicates per sample tree.
8. Always press the ‘measure’ tab using the option on the front panel rather than the trigger switch on the PAR clip, as the trigger switch is quite sensitive and sometimes does not work.
9. Only up to 25 readings can be stored on the fluorescence meter before the internal program begins to overwrite readings starting from the beginning (i.e. first reading). Therefore a maximum of 5 trees should be sampled (5 trees at 5 replicates each) before downloading the readings onto a floppy disk and thereafter to a laptop. Do not download trace data.
10. In order to export data to floppy disc all files must be ‘tagged’ using the tag option and then export to floppy disc.

11. To ensure that there is sufficient power for field measurements, the fluorescence meter and laptop batteries must be charged each evening. The fluorescence meter charger plugs into bottom of the meter and should charge all through the night.

D. Field based measurements of relative leaf water content

1. Collect leaf samples per sample tree and immediately store in plastic bags tied up lightly to prevent moisture loss.
2. To obtain a representative sample, collect leaves from midway and upper regions of the tree.
3. Set up a field scale and labelled specimen containers.
4. Calibrate the scale using an empty specimen container.
5. Prepare 5 replicates for each sample tree.
6. Gather a stack of leaves from each sample tree. Trim of the tips and stalks using a sharp scissors. Cut through the stack of leaves, approximately 2 equal horizontal halves. Overlay 2 halves and cut approximately 1x1cm leaf discs into specimen containers.
7. Adjust each filled specimen container to 3g. Therefore the fresh weight (FW) of every sample should be 3g.
8. Top up each specimen container with water and seal tightly.
9. Allow the leaf discs/pieces to be immersed in water overnight.
10. Drain the water from each specimen container carefully to avoid any loss of leaf material.
11. Blot excess water from specimen container by hold a piece of paper towel over the top of the container and shaking a few times. Once again ensure that no leaf material is lost.
12. Setup scale and appropriately labelled small brown paper bags.
13. Calibrate the field scale using an empty small brown paper bag.
14. Empty leaf discs from specimen container into small brown paper bag. Use a tweezer if necessary to remove leaf discs from specimen container and place in brown paper bag. Ensure that no leaf material is lost.
15. Weigh bag with leaf discs to obtain turgid weight (TW). Record results in field notes for each sample site, sample tree and replicate readings.
16. Carefully fold the opening of the bag a few times to ensure that no leaf material can be lost.
17. Peg or clip all replicate bags from the same sample tree together using paper clips.
18. Store in box.
19. On return from field trip, immediately place all sample bags into a dryer/oven at 60 degrees Celsius for 24 hours.

20. Setup field scale.
21. Reweigh each sample bag for the dry weight (DW), and record results in the field notes.
22. Calculate the relative leaf water content of the leaves (RWC) using the formulae: RWC = (FW-DW)/(TW-DW).

APPENDIX 3: RESULTS OF THE COMPLETE REGRESSION ANALYSIS

Chapter 4 (Section 4.3.2.3) Selection of the best model

Regression analysis
Response variate: Chlb
Fitted terms: Constant + Datt + Species + Datt.Species
Summary of analysis

Source	d.f.	s.s.	m.s.	v.r.	F pr.
Regression	5	37.99	7.5985	34.34	<.001
Residual	69	15.27	0.2213		
Total	74	53.26	0.7197		

Percentage variance accounted for 69.3
Standard error of observations is estimated to be 0.470.
Estimates of parameters

Parameter	estimate	s.e.	t(69)	t pr.
Constant	-1.449	0.461	-3.14	0.002
Datt	4.600	0.693	6.64	<.001
Species E_sider	2.82	1.54	1.83	0.071
Species Searsia lancea	-1.90	1.16	-1.63	0.107
Datt.Species E_sider	-4.31	2.25	-1.92	0.059
Datt.Species Searsia lancea	3.80	1.62	2.35	0.022

Parameters for factors are differences compared with the reference level:

Factor	Reference level
Species	E_camal

Chapter 5 (Section 5.3.3.3) Selection of the best model when using the Hyperion data

Regression analysis
Response variate: PLWP_2005
Fitted terms: Constant, WBI
Summary of analysis

Source	d.f.	s.s.	m.s.	v.r.	F pr.
Regression	1	57.875	57.8745	182.07	<.001
Residual	18	5.722	0.3179		
Total	19	63.596	3.3472		

Percentage variance accounted for 90.5
Standard error of observations is estimated to be 0.564.
Estimates of parameters

Parameter	estimate	s.e.	t(18)	t pr.
Constant	20.97	1.68	12.51	<.001
WBI	-22.77	1.69	-13.49	<.001

Chapter 5 (Section 5.3.3.3) Selection of the best model when using the Proba Chris data

Regression analysis
Response variate: PLWP
Fitted terms: Constant + GNDVI + Species + GNDVI.Species + District + GNDVI.District
Summary of analysis

Source	d.f.	s.s.	m.s.	v.r.	F pr.
Regression	9	70.74	7.8596	46.73	<.001
Residual	65	10.93	0.1682		
Total	74	81.67	1.1036		

Percentage variance accounted for 84.8
Standard error of observations is estimated to be 0.410.
Estimates of parameters

Parameter	estimate	s.e.	t(65)	t pr.
Constant	-4.169	0.627	-6.65	<.001
GNDVI	28.22	5.69	4.96	<.001
Species E_sider	5.025	0.560	8.97	<.001
Species R_lancea	2.798	0.621	4.50	<.001
GNDVI.Species E_sider	-60.29	4.43	-13.60	<.001
GNDVI.Species R_lancea	-23.54	5.34	-4.41	<.001
District Welkom	0.690	0.384	1.79	0.077
District West Wits	3.239	0.697	4.65	<.001
GNDVI.District Welkom	-13.58	3.87	-3.51	<.001
GNDVI.District West Wits	-25.39	6.11	-4.16	<.001

Parameters for factors are differences compared with the reference level:

Factor	Reference level
Species	E_camal
District	Vaal River

Chapter 6 (Section 6.3.1.3) Selection of the best model when using the multispectral airborne imagery

Regression analysis
Response variate: Cxc_J2005
Fitted terms: Constant + GREEN + District + Species + GREEN.Species + GREEN.District
Summary of analysis

Source	d.f.	s.s.	m.s.	v.r.	F pr.
Regression	9	6.909	0.76763	9.26	<.001
Residual	65	5.391	0.08294		
Total	74	12.300	0.16621		

Percentage variance accounted for 50.1
Standard error of observations is estimated to be 0.288.
Estimates of parameters

Parameter	estimate	s.e.	t(65)	t pr.
Constant	2.262	0.474	4.78	<.001
GREEN	-0.01164	0.00637	-1.83	0.072
District Welkom	-0.227	0.557	-0.41	0.684
District WestWits	1.699	0.747	2.28	0.026
Species E_sider	-4.70	1.60	-2.94	0.005
Species Searsia lancea	0.083	0.435	0.19	0.850
GREEN.Species E_sider	0.0672	0.0246	2.73	0.008
GREEN.Species Searsia lancea	-0.00315	0.00648	-0.49	0.628
GREEN.District Welkom	0.00792	0.00858	0.92	0.359
GREEN.District West Wits	-0.0156	0.0100	-1.55	0.126

Parameters for factors are differences compared with the reference level:

Factor	Reference level
District	Vaal River
Species	E_camal

Chapter 6 (Section 6.3.2.3) Selection of the best model when using the hyperspectral airborne imagery

Regression analysis

Response variate: PLWP

Fitted terms: Constant + NDWI + District + Species + NDWI.Species

Summary of analysis

Source	d.f.	s.s.	m.s.	v.r.	F pr.
Regression	7	64.52	9.2177	34.96	<.001
Residual	65	17.14	0.2637		
Total	72	81.66	1.1342		

Percentage variance accounted for 76.8

Standard error of observations is estimated to be 0.513.

Estimates of parameters

Parameter	estimate	s.e.	t(65)	t pr.
Constant	2.43	1.60	1.52	0.134
NDWI	-3.15	1.42	-2.22	0.030
District Welkom	-4.34	1.67	-2.59	0.012
District West Wits	-3.10	1.65	-1.88	0.065
Species E_sider	-1.882	0.215	-8.75	<.001
Species Searsia lancea	0.740	0.237	3.12	0.003
NDWI.Species E_sider	27.60	2.68	10.31	<.001
NDWI.Species Searsia lancea	-0.641	0.261	-2.46	0.017

Parameters for factors are differences compared with the reference level:

Factor	Reference level
District	Vaal River
Species	E_camal

APPENDIX 4: OBSERVATION POINTS USED TO CREATE INTERPOLATED HYDROCHEMISTRY SURFACES

Mining District	Name of observation point	Latitude (dd)	Longitude (dd)
Welkom	bh73	-27.94712571	26.57987594
Welkom	bh74	-27.94502646	26.57511145
Welkom	bh75	-27.94113123	26.57861099
Welkom	bh78	-27.96454273	26.56343765
Welkom	bh92	-27.98600952	26.52464388
Welkom	bh93	-27.98652955	26.52633130
Welkom	bh94	-27.98327699	26.54610434
Welkom	bh95	-27.95507676	26.50929215
Welkom	bh109	-27.97736463	26.54228126
Welkom	bh110	-27.97254722	26.54587331
Welkom	bh119	-27.96134985	26.56637073
Welkom	bh126	-27.95689550	26.52966739
Welkom	bh127	-27.93926994	26.51326971
Welkom	bh128	-27.94730044	26.50533190
Welkom	bh201	-27.98262052	26.53124218
Welkom	bh56	-28.00774701	26.52368667
Welkom	bh58	-27.98101911	26.56553719
Welkom	bh81	-28.00696112	26.52309097
Welkom	bh82	-28.00697127	26.52243724
Welkom	bh83	-28.00671447	26.52285968
Welkom	bh84	-28.00547934	26.52234234
Welkom	bh204	-27.99014180	26.56116833
Welkom	bh51	-27.94947389	26.48361745
Vaal River	Vr37	-26.92287821	26.67782905
Vaal River	Vr03	-26.92562565	26.68558976
Vaal River	Vr02	-26.91989294	26.78292698
Vaal River	Gn01	-26.95059599	26.77488036
Vaal River	Gn02	-26.95642114	26.77078500
Vaal River	Gn03	-26.94942064	26.78056866
Vaal River	K02	-26.98022332	26.73580516
Vaal River	Vrm06	-26.99057443	26.77224713
Vaal River	Vrm07	-26.98675748	26.77544161
Vaal River	Vr27	-26.96361443	26.71177468

Mining District	Name of observation point	Latitude (dd)	Longitude (dd)
Vaal River	NT-BH1	-26.93124939	26.69361699
Vaal River	NT-BH3	-26.93325145	26.70134441
Vaal River	NT-BH2	-26.93118708	26.69364344
Vaal River	NT-BH4	-26.93610977	26.69728388
Vaal River	WP-BH3	-26.95521700	26.68548500
Vaal River	WP-BH6	-26.96417800	26.70493900
Vaal River	WP-BH4	-26.94230200	26.70465300
Vaal River	WP-BH5	-26.95043800	26.69450400
Vaal River	WP-BH2	-26.95523400	26.68557100
West Wits	MBH2	-26.42609800	27.35851100
West Wits	MBH3	-26.42368000	27.36531000
West Wits	MBH4	-26.42217300	27.37186100
West Wits	MBH5	-26.41581600	27.38312700
West Wits	MBH6	-26.41332100	27.40116000
West Wits	MBH7	-26.41975600	27.40464100
West Wits	MBH8	-26.41108900	27.40535200
West Wits	MBH9	-26.41060400	27.42302100
West Wits	MBH10	-26.43405700	27.43711100
West Wits	MBH11	-26.45659300	27.42258700
West Wits	MBH12	-26.45795800	27.41582400
West Wits	MBH13	-26.44828800	27.40448000
West Wits	MBH14	-26.46574400	27.36629600
West Wits	MBH15	-26.47091000	27.36722000
West Wits	MBH16	-26.47185300	27.36266400
West Wits	MBH17	-26.47029500	27.35321700
West Wits	MBH18	-26.44041500	27.36143300
West Wits	MBH23	-26.44630351	27.40695213
West Wits	MBH24	-26.44826800	27.40819900
West Wits	MBH25	-26.44800200	27.40664400
West Wits	MBH26	-26.44760200	27.40760500
West Wits	MBH27	-26.41624200	27.39261000
West Wits	MBH28	-26.41992500	27.39560000

Observation points used to create interpolated groundwater table level surfaces

Mining District	Name of observation point	Latitude (dd)	Longitude (dd)
Welkom	bh73	-27.94712571	26.57987594
Welkom	bh74	-27.94502646	26.57511145
Welkom	bh75	-27.94113123	26.57861099
Welkom	bh78	-27.96454273	26.56343765
Welkom	bh94	-27.98327699	26.54610434
Welkom	bh119	-27.96134985	26.56637073
Welkom	bh126	-27.95689550	26.52966739
Welkom	bh51	-27.94947389	26.48361745
Vaal River	VR27	-26.96361443	26.71177468
Vaal River	VR29	-26.95612853	26.71343638
Vaal River	VR28	-26.95024517	26.71508254
Vaal River	VR31	-26.92474137	26.70086930
Vaal River	VR32	-26.92158728	26.70744020
Vaal River	VRM27	-26.95304423	26.68548188
Vaal River	VRM26	-26.95306085	26.68556814
Vaal River	VRM25	-26.94826584	26.69450149
Vaal River	VRM24	-26.93610977	26.69728388
Vaal River	VRM23	-26.93124939	26.69361699
Vaal River	VRM21	-26.93118708	26.69364344
Vaal River	VRM20	-26.93325145	26.70134441
Vaal River	VRM19	-26.94013022	26.70465018
Vaal River	VRM13	-26.96294360	26.70111173
Vaal River	VRM12	-26.95984606	26.68301626
West Wits	MB38	-26.43406100	27.34206576
West Wits	MB36	-26.43990507	27.35589822
West Wits	MB31	-26.42429357	27.37204080
West Wits	MB18	-26.43827353	27.36143224
West Wits	MB08	-26.40894501	27.40535864
West Wits	MB06	-26.41118354	27.40116140
West Wits	MB05	-26.41367920	27.38313138
West Wits	MB04	-26.42003194	27.37186118
West Wits	MB03	-26.42154029	27.36531547

APPENDIX 5: INTERPOLATED SURFACES USED TO CHARACTERISE UNDSTRESSED SITES IN EACH MINING DISTRICT

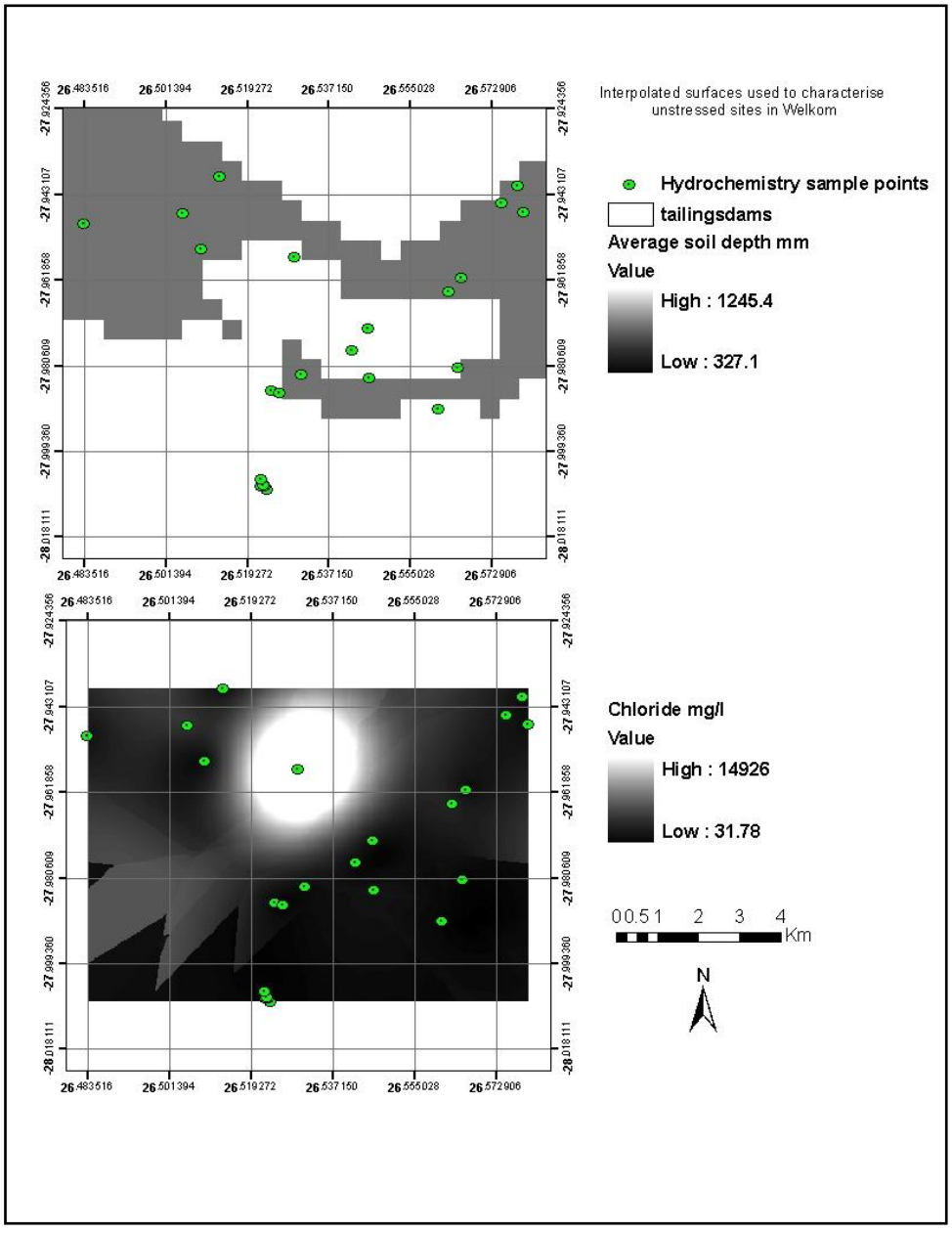


Figure A1 *Interpolated surfaces of average soil depth and chloride concentrations in the Welkom mining district.*

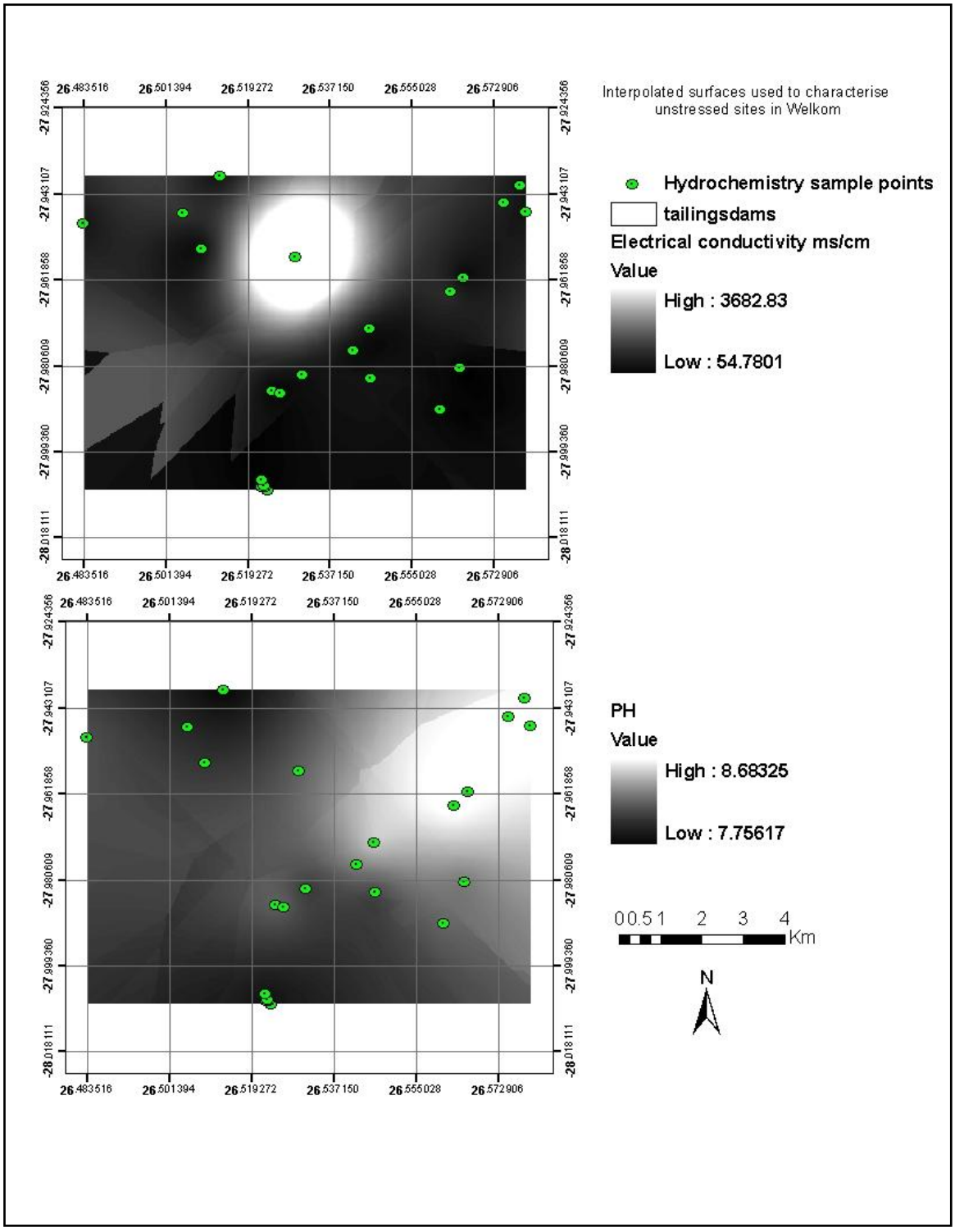


Figure A2 Interpolated surfaces of electrical conductivity and pH in the Welkom mining district.

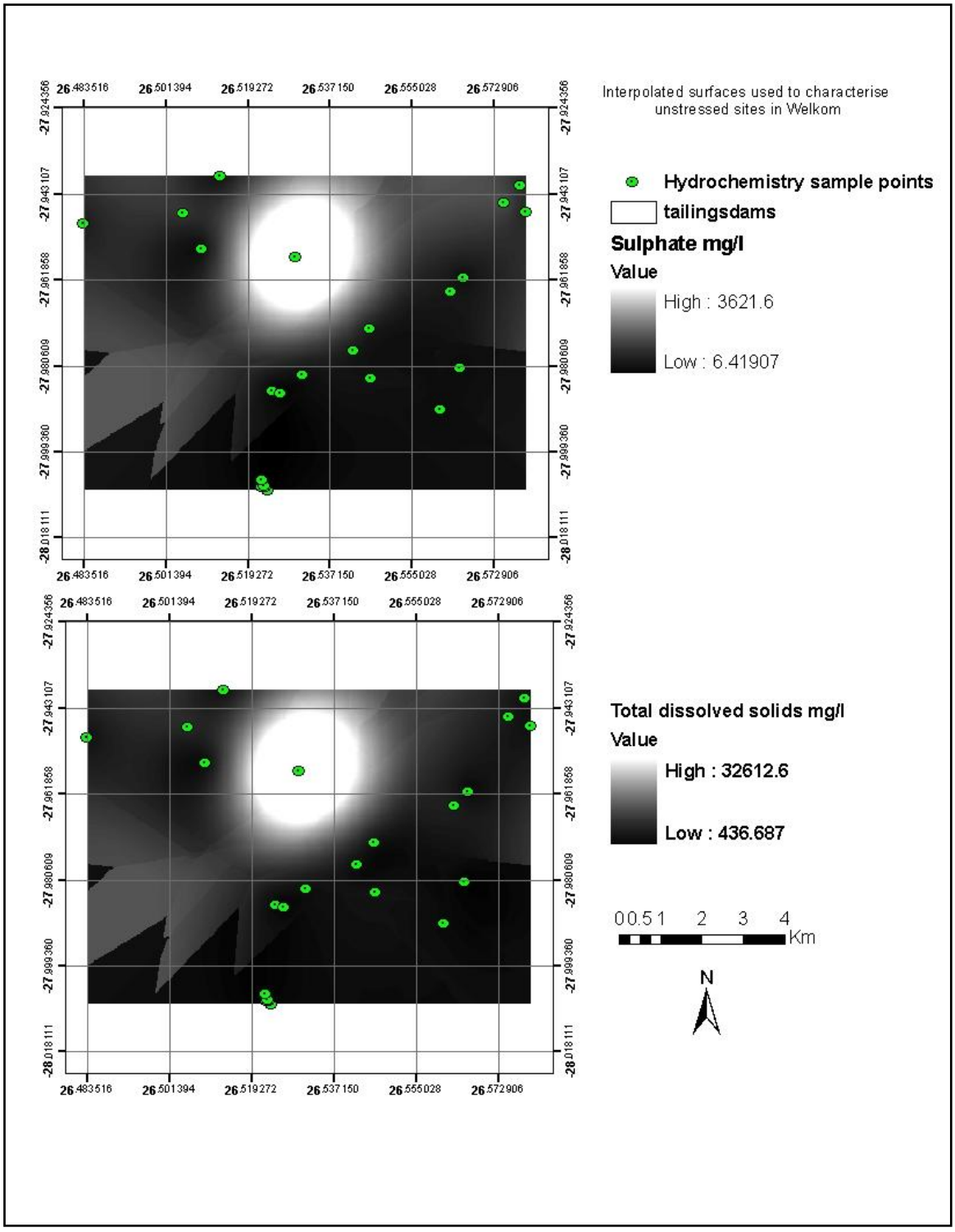


Figure A3 *Interpolated surfaces of sulphate concentrations and total dissolved solids in the Welkom mining district.*

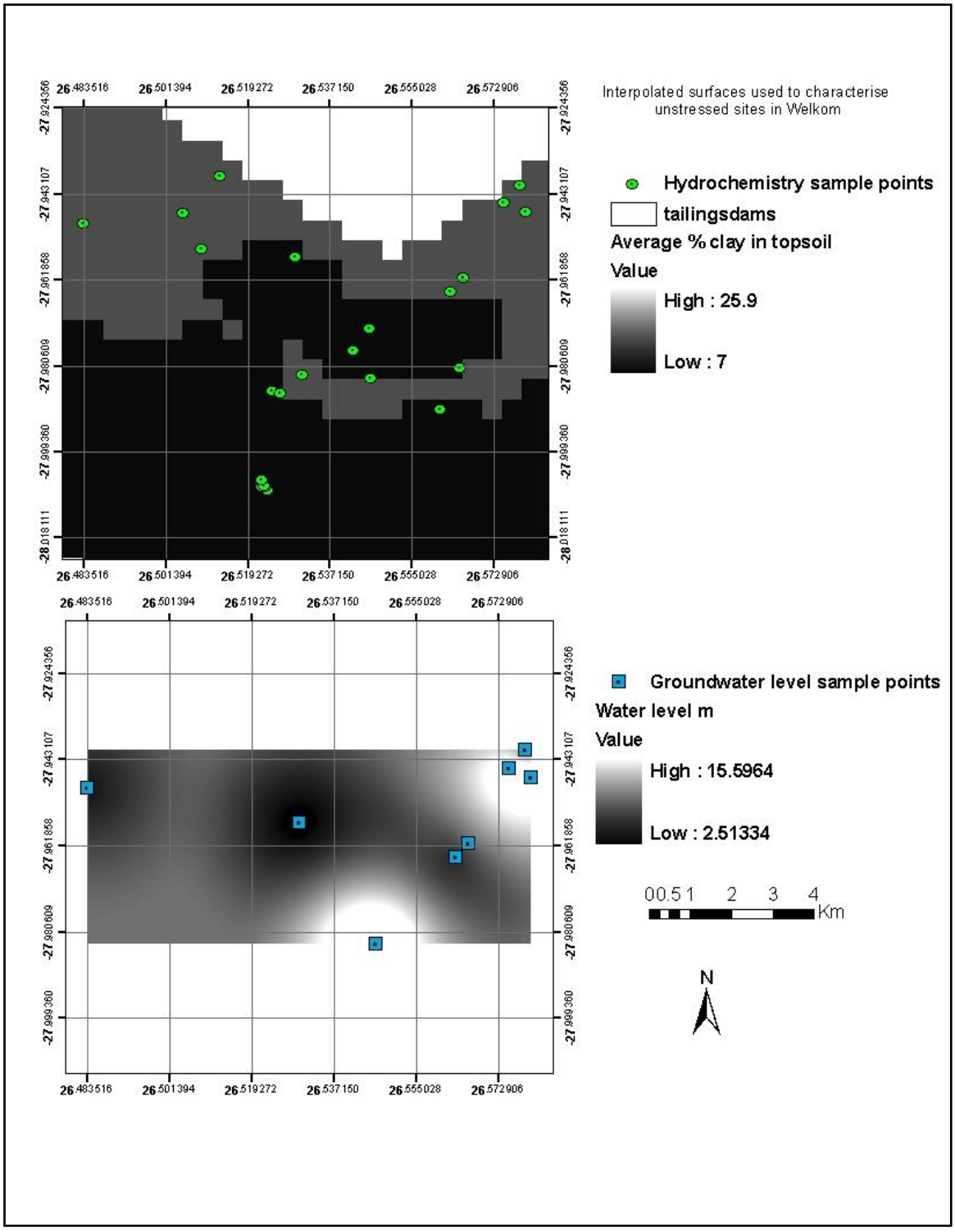


Figure A4 *Interpolated surfaces of topsoil clay (%) and groundwater table level in the Welkom mining district.*

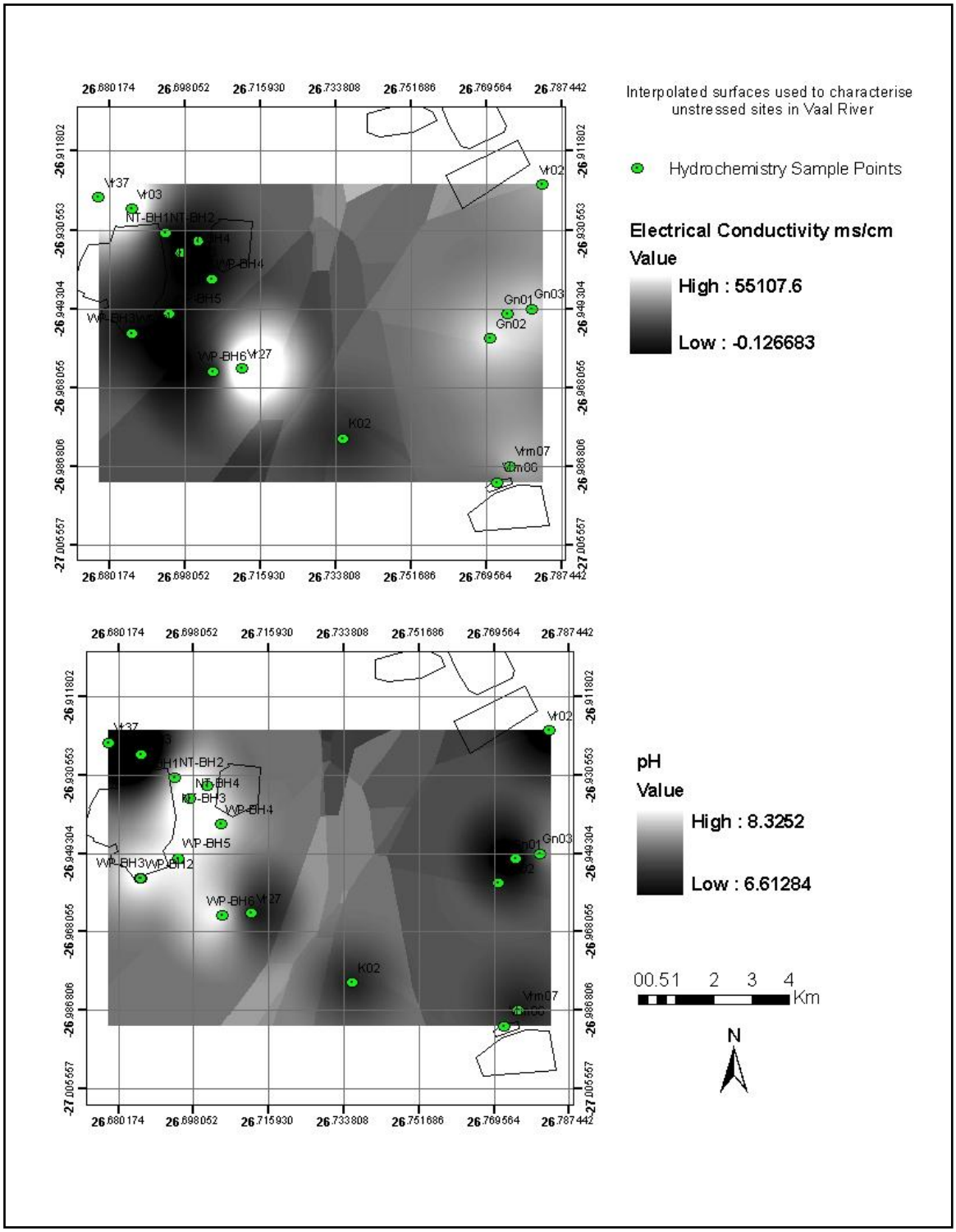


Figure A5 Interpolated surfaces of electrical conductivity and pH in the Vaal River mining district.

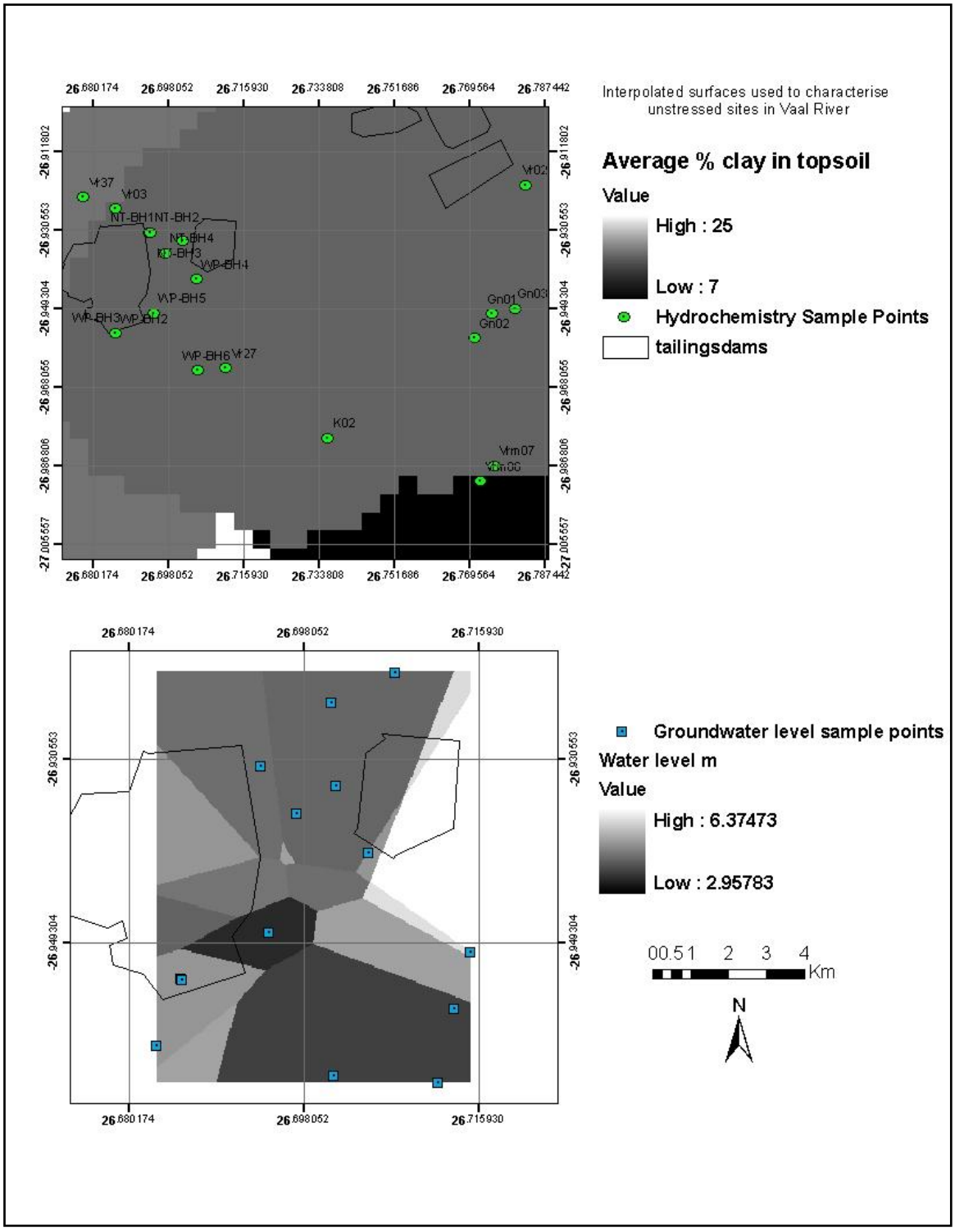


Figure A6 *Interpolated surfaces of topsoil clay (%) and groundwater table level in the Vaal River mining district.*

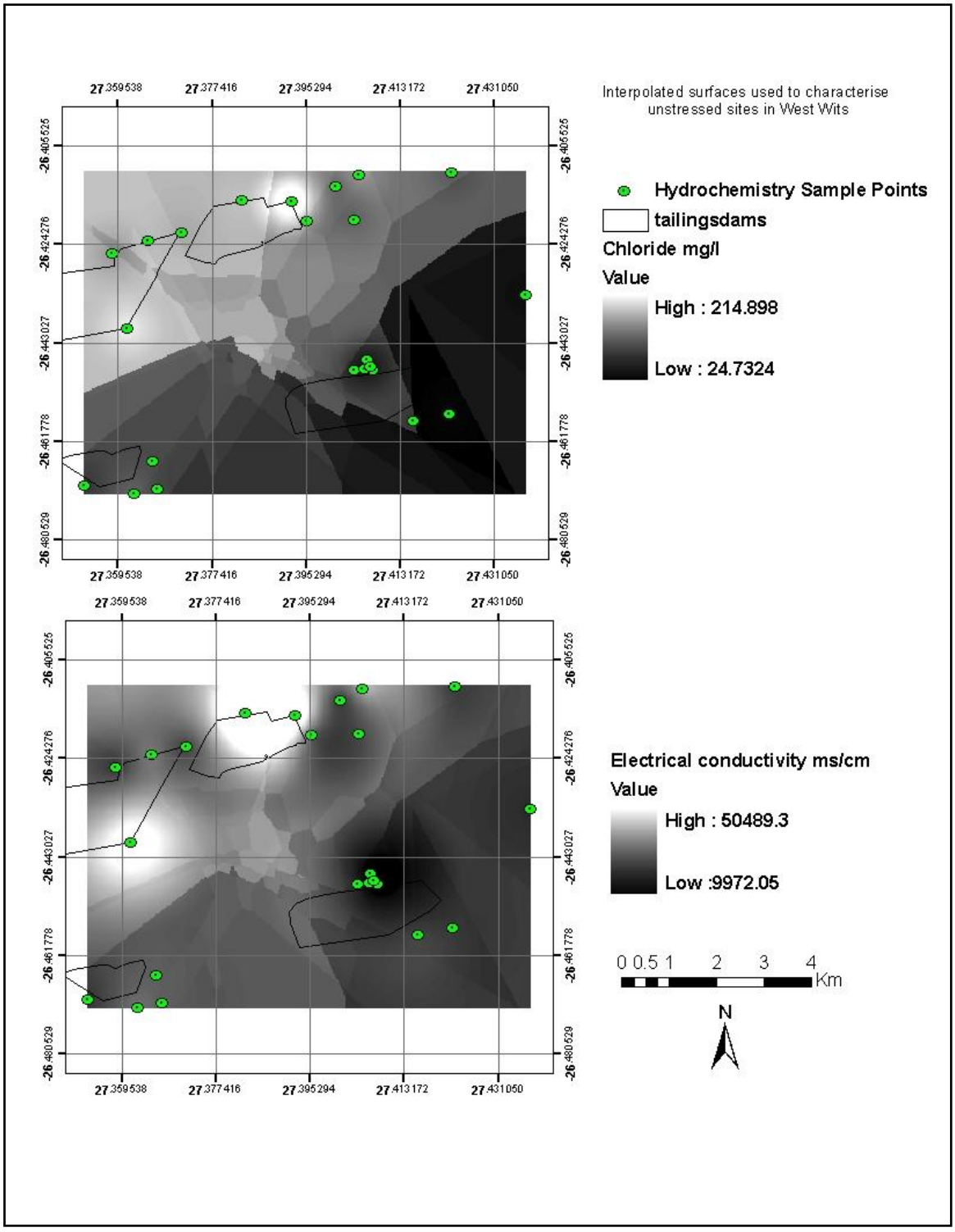


Figure A7 *Interpolated surfaces of chloride concentrations and electrical conductivity in the West Wits mining district.*

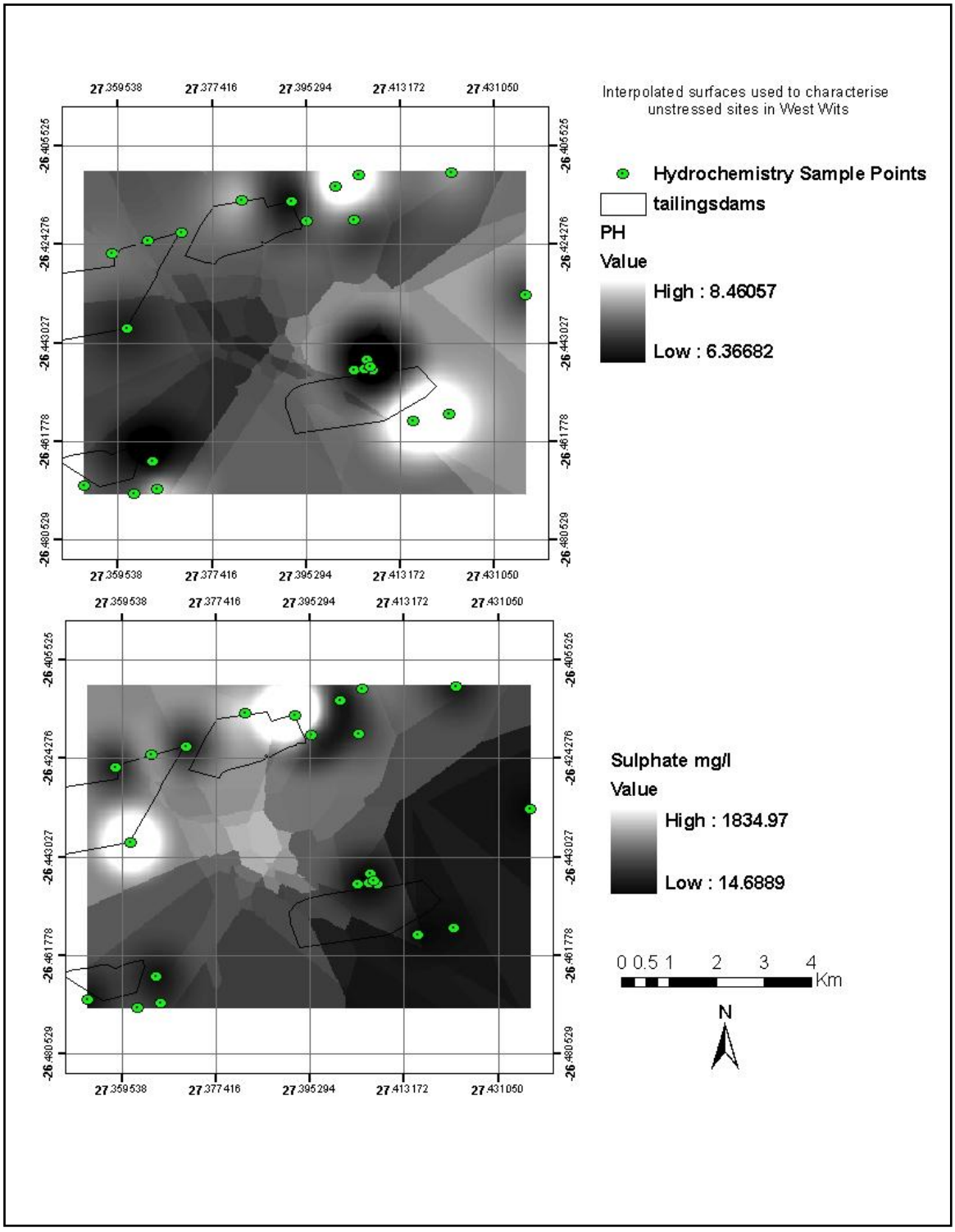


Figure A8 Interpolated surfaces of pH and sulphate concentrations in the West Wits mining district.

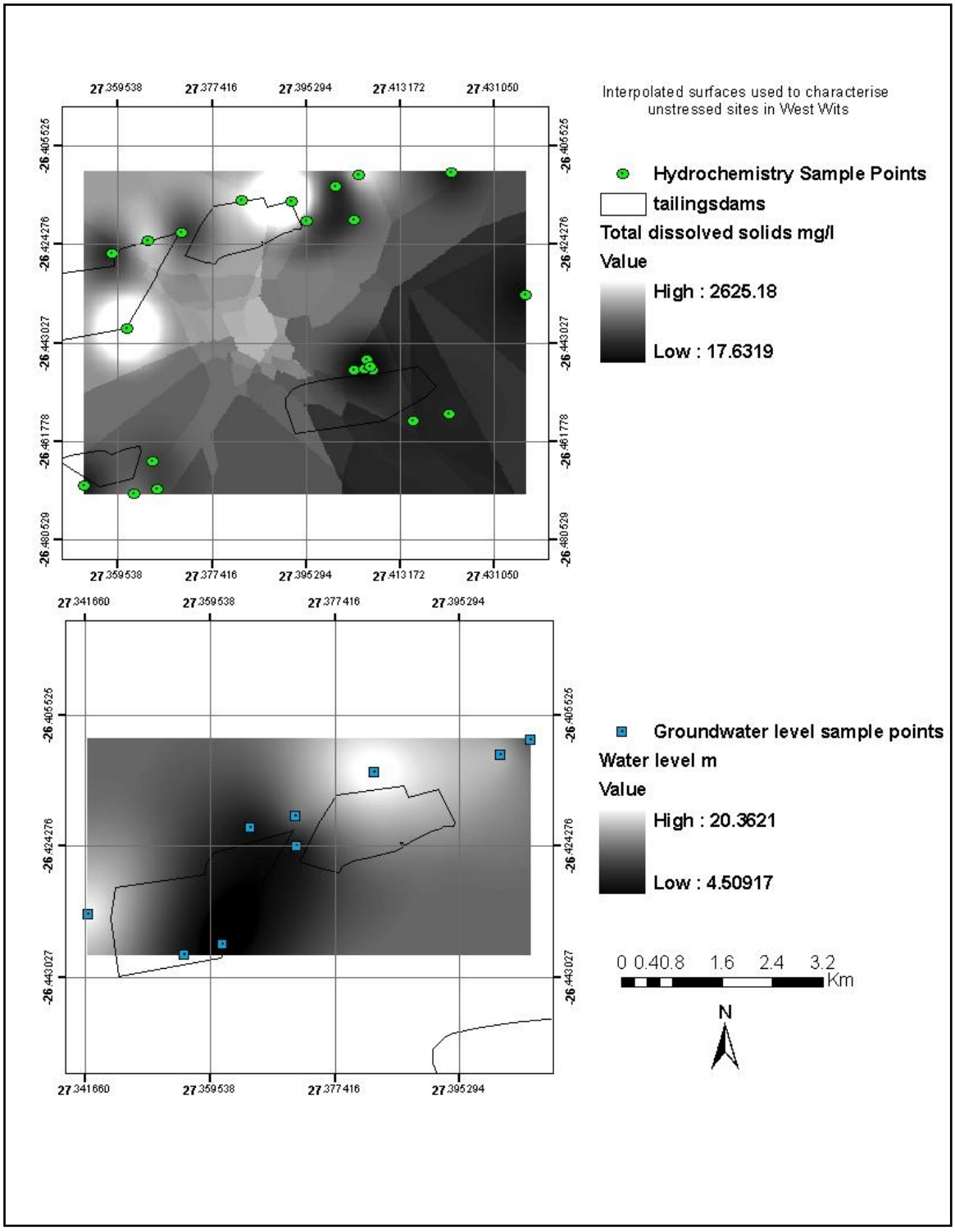


Figure A9 *Interpolated surfaces of total dissolved solids and groundwater table level in the West Wits mining district.*

APPENDIX 6: DIFFERENCES IN XYLEM VESSEL CHARACTERISTICS AND WOOD DENSITY RESULTING FROM PLANT STRESS

ABSTRACT

The aim of this preliminary study was to evaluate whether differences in wood anatomy characteristics, such as xylem vessel diameter, vessel frequency and wood density, could be used as non-destructive measures for identifying trees experiencing plant stress.

Seventy two wood core samples were extracted and analysed from two forestry species, *Eucalyptus camaldulensis* and *E. sideroxylon*, and the indigenous *Searsia lancea* in Welkom, Vaal River and West Wits mining districts. A predawn leaf water potential of -0.8 MPa was used as a benchmark to separate stressed from unstressed trees. Relative differences in radial vessel diameter, vessel frequency and wood density were examined.

Comparisons of the radial vessel diameter and vessel frequency measurements revealed significant differences in three of the five comparative sampling sites ($p < 0.05$). Density analyses were significantly different for all five comparative sampling sites ($p < 0.01$).In general, trees experiencing higher plant water stress displayed smaller vessel diameters, compared to less stressed or healthy trees. Sites which were influenced by high levels of contaminated water also displayed smaller vessel diameters, indicating that uptake of contaminants could affect the wood anatomy of plants. Trees considered to be experiencing higher plant water stress displayed higher vessel frequency.

The primary conclusion was that plant stress does influence the wood anatomical characteristics (radial vessel diameter, vessel frequency and wood density) in *E. camaldulensis*, *E. sideroxylon* and *S. lancea* in the three mining districts.

Keywords: plant stress, radial vessel diameter, vessel frequency, wood density

INTRODUCTION

Variations in the wood anatomical characteristics and the structure of trees result from a complex web of plant physiological interactions and environmental forcing functions (Downes *et al*., 2002). Several studies have revealed relationships between wood anatomical characteristics and environmental forcing factors such as temperature and rainfall (Lovisolo and Schubert, 1998; Zimmermann, 1983; February *et al*., 1995; Thomas *et al*., 2004; Naidoo *et al*., 2006). It is therefore useful to know how trees respond to the various individual contributing factors that result from varying environmental conditions, including water stress and environmental pollution.

Studies have indicated that plant stress resulting from varying levels of environmental contamination and water availability may manifest in plants as differences in xylem vessel size, vessel frequency and wood density characteristics (Lovisolo and Schubert, 1998; Zimmermann, 1983; Zhang *et al*., 1988; February, 1993; 1994; February *et al*., 1995; Thomas *et al*., 2004; Naidoo *et al*., 2006). In the gold and uranium mining regions of South Africa, environmental hazards resulting from the storage of high pulverised rock waste in tailings storage facilities contribute towards contamination and pollution of the environment (Van As, 1992; Straker *et al*., 2007).

The degradation of the environment and surrounding lands spreads far beyond these waste deposits and tailing storage facilities, with erosion and acid mine drainage from tailing storage facilities having severe impacts on nutrient cycling in polluted soils (Witkowski and Weiersbye, 1998b; Weiersbye *et al*., 2006). Research has shown that xylem vessel diameters increase, while vessel frequencies decrease with increases in available water (Zhang *et al*., 1988, February, 1993; 1994; February *et al*., 1995; Naidoo *et al*., 2006). Furthermore, it has also been shown through tree ring analysis that transition metals and metalloids are taken up and manifested in the anatomy of trees (Watmough, 1999; Edmands *et al*., 2001; Padilla and Anderson, 2002; Yu *et al*., 2007).

This study presented a unique opportunity to examine the xylem anatomical responses in plants attributed to water or contaminant stress in mining environments. Relative differences in xylem vessel diameter, vessel frequency and wood density attributed to plant stress were identified in wood cores extracted from *Eucalyptus camaldulensis, Eucalyptus sideroxylon* and *Searsia lancea* in Welkom, Vaal River and West Wits gold mining districts. This preliminary research study may usefully contribute towards a more rigorous approach to developing quantitative wood anatomy as a non-destructive tool for identifying trees which are experiencing plant stress.

MATERIALS AND METHODS

This study was conducted during winter in July 2004. Seventy two wood core samples were extracted from two forestry species, *Eucalyptus camaldulensis* and *Eucalyptus sideroxylon*, and the indigenous *Searsia lancea* in Welkom, Vaal River and West Wits mining districts. Trees sampled were selected from comparative sampling sites reported on in Chapters 4 to 6. Table B.1 provides a descriptive summary of the sampling sites including the mining district and species sampled, their geographical location, local soils and geology and a classification of stressed and unstressed sites.

Table B.1 Description of the comparative wood core sampling sites classified according to predawn leaf water potential.

Mining District	Tree Species	Site Code	Geographic Coordinates (dd)	Site Description	Soil Description	Geology	Site classification according to predawn leaf water potential (MPa)
VR	SL	RLVR1	-26.92301; 26.69820	Sampled on a slightly raised topography near a mine dump; lower contaminant levels and total dissolved solids.	Glenrosa and/or Mispah forms (other soils may occur), mesotrophic, lime rare or absent in the entire landscape, average soil depth 421.7 mm.	Dolomite/ Quartzite	stressed (-1.07)
VR	SL	RLVR2	-26.93418; 26.69592	Approximately 1 km southwards from RLVR1, between two tailing storage facilities, higher total dissolved solids, higher water availability due to seepage from the two tailing storage facilities	Glenrosa and/or Mispah forms (other soils may occur), mesotrophic, lime rare or absent in the entire landscape, average soil depth 421.7 mm.	Dolomite	stressed (-1.18)
VR	EC	ECVR1	-26.99288; 26.78289	Sampled near a tailing storage facility deep groundwater table ~ 20m.	Plinthic catena: dystrophic and/or mesotrophic; red soils not widespread, upland duplex and margalitic soils rare, average soil depth 918.1 mm.	Dolomite	stressed (-0.93)
VR	EC	ECVR2	-26.99332; 26.78250	high water availability, located within a water channel which flows parallel to the tailing storage facility.	Glenrosa and/or Mispah forms (other soils may occur),eutrophic, lime rare or absent in the entire landscape, average soil depth 421.7 mm.	Dolomite	unstressed (-0.57)
VR	EC	ECVR3	-26.92922; 26.68182	Approximately 200 m from the edge of the Western Complex tailing storage facility, a cluster of young *E. camaldulensis* trees which appeared to be visually unhealthy showing signs of reduced biomass, reduced tree height and yellow to brown leaf colour.	Plinthic catena: eutrophic; red soils not widespread, upland duplex and margalitic soils rare, average soil depth 387 mm.	Andesite	stressed (-0.96)
VR	EC	ECVR4	-26.92970; 26.62100	Close to tailing storage facility20 m northwards from site ECVR3 , clump of green healthy trees.	Plinthic catena: eutrophic; red soils not widespread, upland duplex and margalitic soils rare, average soil depth 387 mm.	Andesite	unstressed (-0.68)

Mining District	Tree Species	Site Code	Geographic Coordinates (dd)	Site Description	Soil Description	Geology	Site classification according to predawn leaf water potential (MPa)
WW	ES	ESWW1	-26.43899; 27.33024	Extreme opposite direction of ESWW2 within the stand, Thinner trees, less dense and visually unhealthy, lower water availability.	Glenrosa and/or Mispah forms (other soils may occur), non calcarious, lime rare or absent in upland soils but generally present in low-lying soils, average soil depth 503 mm.	Shale	stressed -1.78
WW	ES	ESWW2	-26.43969; 27.32871	Stand of dense, green and visually healthy trees along the riparian edge, approximately 10m from farm dam, high water availability, shallow groundwater table < ~ 5m.	Glenrosa and/or Mispah forms (other soils may occur), non calcarious, lime rare or absent in upland soils but generally present in low- lying soils, average soil depth 503 mm.	Shale	stressed -0.95
W	SL	RLW1	-27.96695; 26.55075	Approximately 100 m from the edge of the Dankbaar Pan, located on cattle farmland, trees high water availability, very flat area, groundwater reported to have high electrical conductivity levels influenced by drainage pathways from the pan.	Prismacutanic and/or pedocutanic diagnostic horizons dominant. Non calcarious. In addition, one or more of: vertic, melanic, red structure diagnostic horizon, average soil depth 748.3 mm	Shale	stressed -1.31
W	SL	RLW2	-28.03361; 26.51199	Approximately 20 km away from the pan on an agricultural farm.	Red-yellow apedal, freely drained soils; red, eutrophic, high base status, >300 mm deep (no dunes), average soil depth 1245.4 mm.	Shale	stressed -1.37

W = Welkom; VR = Vaal River, WW = West Wits; EC = E. camaldulensis; ES = E. sideroxylon; RL = S. lancea

In the field, five replicate trees were sampled at breast height on comparative sites in each of the three mining districts. Wood cores were extracted, sealed in plastic zip-lock bags, and then analysed for xylem vessel diameter, vessel frequency and wood density. Some of the very dry cores broke into fragments and were consequently excluded from the analysis. During this survey, predawn leaf water potential measurements were used to classify stressed and unstressed sites, were a value of -0.8 MPa was used as a benchmark to separate stressed from unstressed trees (Cleary and Zaerr, 1984). The comparative sampling sites were also provided with a unique code to facilitate comparative analyses.

At the CSIR Forestry and Forests Products laboratory, radial strips of uniform thickness were cut from the wood cores using a twin-blade saw and stored at a constant temperature of 24ºC and 65% relative humidity. Strips were scanned at 0.5 mm intervals in a radial-longitudinal face from pith-to-bark using a gamma-ray densitometer, which was custom made in South Africa (1997), to determine the density profile. Pith-to-bark radial strips used for density measurements were then cut in transverse sections (25 µm) using a Leica base sledge microtome (Germany). Sections were mounted in ethanol on a glass slide and examined using a Leica fluorescent microscope (Germany). Measurements of radial vessel diameter (in mm) and vessel frequency were determined from pith-to-bark under 50x magnification with exposed window of 2 mm in radial direction and 0.5 mm in tangential direction (1 mm square) using image analysis software (Leica Qwin, Germany).

Statistical analyses of the radial vessel diameter, vessel frequency and wood density of the comparative sampling sites were undertaken using STATISTICA version 5.5 (1999). Means and standard deviations of the sites were derived, and significant differences between sites were determined using the t-test.

RESULTS

Comparisons between radial vessel diameter, vessel frequency and density measurements were undertaken to detect any significant differences between the five comparative sampling sites. The means and standard deviations for each sampling site and statistical tests for

significant differences are shown in Table B.2. The mean radial vessel diameter measurements ranged from 49.31 µm for the *E. camaldulensis* site sampled close to the Western Complex TSF in Vaal River (ECVR3) to 88.80µm for the *E. camaldulensis* site sampled near Mispah TSF in Vaal River (ECVR1). The mean vessel frequency measurements ranged from 10.78 for ECVR1 to 19.51 for *S. lancea* sampled on farmland in Welkom (RLW2). The lowest density measurements were obtained for *E. camaldulensis* trees sampled in a water channel near the Mispah TSF in Vaal River (ECVR2), while the highest density measurements were obtained for *E. sideroxylon* trees sampled in West Wits (ESWW1).

Significant differences between the means of each comparative sampling site were assessed using a t-test (Table B.2). Comparison of the radial vessel diameter measurements revealed significant differences between three of the five comparative sampling sites. The results indicated that there were no significant differences in radial vessel diameter for the sites RLVR1 and RLVR2 ($t = 0.28$, 74df, $P = 0.777$) and ECVR1 and ECVR2 ($t = -1.47$, 63df, $P = 0.146$). Vessel frequency measurements revealed that there were also no significant differences between sites RLVR1 and RLVR2 ($t = -0.38$, 74df, P 0.708) and ECVR3 and ECVR4 ($t = -1.36$, 74df, $P = 0.178$). However, the results of the density analyses were significantly different for all five comparative sampling sites.

Table B.2 Means and standard deviations of xylem vessel and density characteristics measured from the five comparative sampling sites.

Variable	Summary Statistics	Site RLVR1	Site RLVR2	t-test	Site ECVR1	Site ECVR2	t-test	Site ECVR3	Site ECVR4	t-test	Site ESWW1	Site ESWW2	t-test	Site RLW1	Site RLW2	t-test
Radial vessel diameter (µm)	*Mean*	62.28	62.77	*t = 0.28 74df P = 0.777*	88.80	84.39	*t = -1.47 63df P = 0.146*	49.31	66.24	*t = -10.35 53df P < 0.001*	59.95	66.50	*t = -2.65 74df P = 0.010*	53.53	60.41	*t = 3.82 47df P < 0.001*
	Standard Deviation	7.76	6.99		15.53	9.99		4.34	9.09		12.31	8.98		10.39	3.92	
Vessel frequency (mm^{-2})	*Mean*	17.89	17.53	*t = -0.38 74df P = 0.708*	10.78	12.15	*t = 2.38 59df P = 0.020*	13.08	14.32	*t = -1.36 74df P = 0.178*	15.31	13.14	*t = 2.32 58df P = 0.024*	15.53	19.51	*t = 2.88 43df P = 0.006*
	Standard Deviation	4.24	4.08		3.05	1.77		4.33	3.54		4.98	2.84		8.18	2.45	
Density ($g.cm^{-3}$)	*Mean*	0.8454	0.8690	*t = 7.47 92df P < 0.001*	0.7233	0.6675	*t = -10.58 73df P < 0.001*	0.7621	0.7803	*t = -3.12 80df P = 0.002*	0.8729	0.8032	*t = 12.94 83df P < 0.001*	0.8342	0.8179	*t = -2.91 75df P = 0.005*
	Standard Deviation	0.0133	0.0170		0.0311=	0.0182		0.0222	0.0330		0.0215	0.0299		0.0329	0.0198	

EC = E. camaldulensis; ES = E. sideroxylon; RL =S. lancea; W = Welkom; VR = Vaal River, WW = West Wits

Pith to bark measurements were then compared for each comparative sampling site in order to investigate the trends across the width of the core samples. Figure B.1 illustrates the radial vessel diameter, vessel frequency and wood density measured from pith to bark for selected comparative sampling sites. In general minor differences were visible between samples for the first 7 mm measured from pith to bark, as shown in Figure B.1a, b, d and e. However, consistently larger differences were apparent between *E. camaldulensis* trees (ECVR3 and ECVR4) sampled near the Western Complex tailing storage facility in Vaal River mining district (Figure B.1c). Figure B.1c illustrates larger mean radial vessel diameter measurements from pith to bark at the ECVR4 site compared to ECVR3 site. Differences in radial vessel diameter measurements were also visible between comparative sampling sites ESWW1 and ESWW2 in West Wits, and RLW1 and RLW2 in Welkom. Radial vessel diameters measured between 9 and 38 mm were generally larger at ESWW2 and RLW2 site compared to ESWW1 and RLW1 site respectively.

Figure B.2 illustrates differences in mean vessel frequency measured from pith to bark at the five comparative sampling sites. Differences in mean vessel frequency, measured from pith to bark, were highly variable across the wood core samples (Figure B.2 a to d). Vessel frequencies ranged between 5 and 40 mm^{-2}. Mean vessel frequencies were generally higher, between 11 and 38 mm from pith to bark, at the RLW2 site when compared to RLW1 (Figure B.2e).

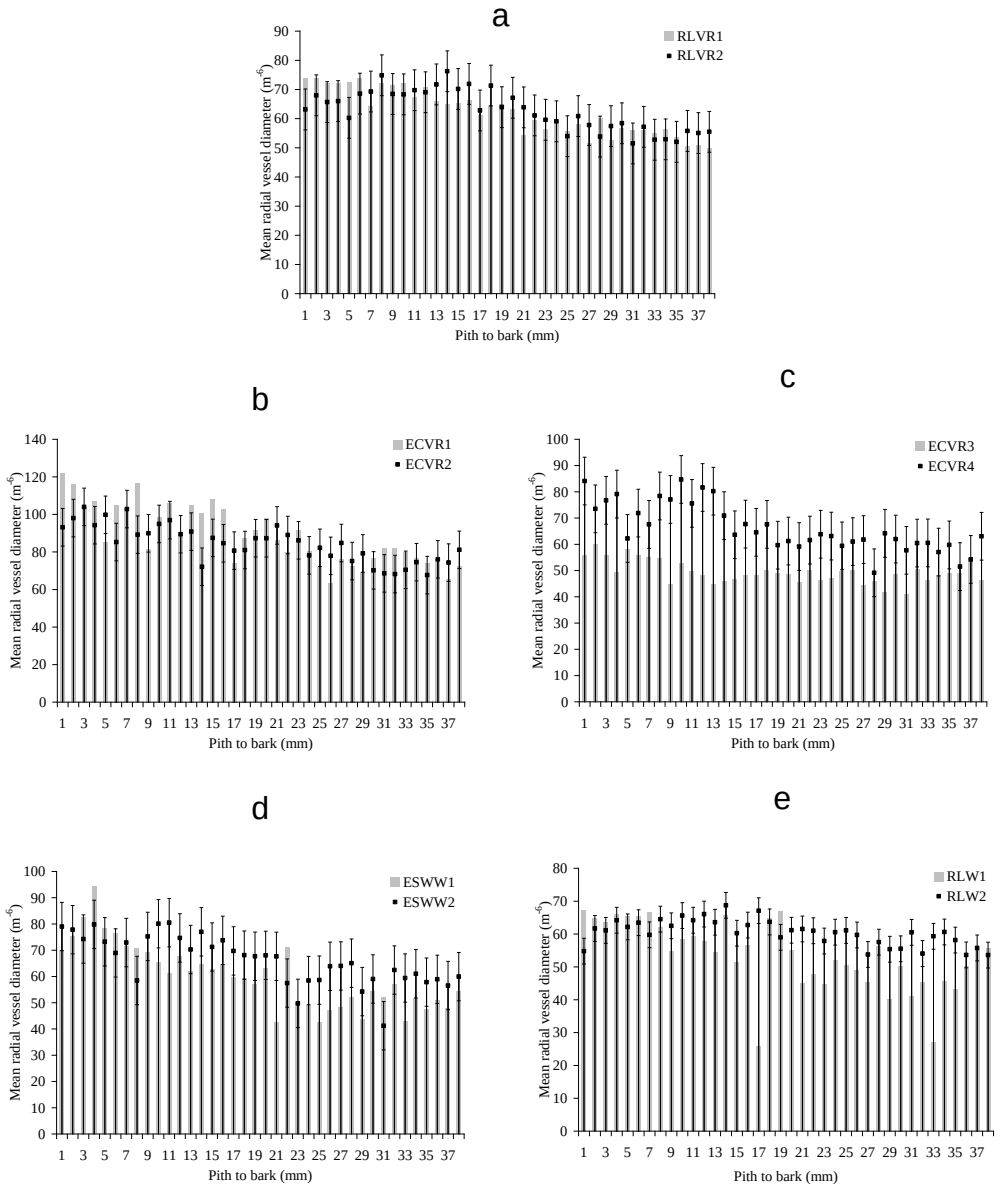


Figure B.1 Radial vessel diameter measured from pith to bark for a) S. lancea at site RLVR1 and RLVR2, b) E. camaldulensis at site ECVR1 and ECVR2 and c) site ECVR3 and ECVR4 in Vaal River, d) E. sideroxylon at site ESWW1 and ESWW2sampled in West Wits and, e) S. lancea at site RLW1 and RLW2sampled in Welkom.

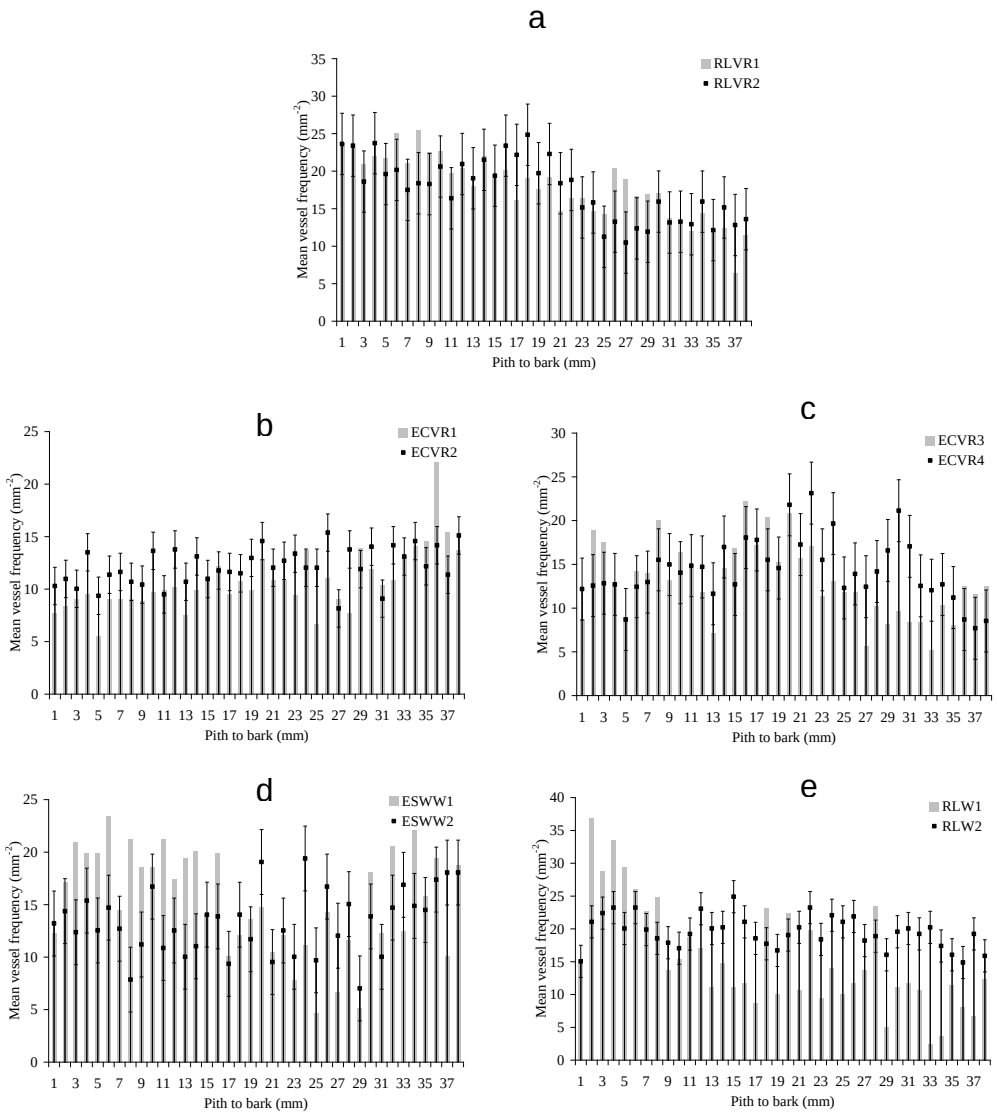


Figure B.2 Mean vessel frequency measured from pith to bark for a) S. lancea at site RLVR1 and RLVR2, b) E. camaldulensis at site ECVR1 and ECVR2 and c) site ECVR3 and ECVR4 in Vaal River, d) E. sideroxylon at site ESWW1 and ESWW2sampled in West Wits and, e) S. lancea at site RLW1 and RLW2sampled in Welkom.

Figure B.3 illustrates differences in density measured from pith to bark at the five comparative sampling sites. Density measurements ranged from 0.6 to 0.95g.cm^{-3}. Incremental measurements were generally higher at the RLVR2 site compared to RLVR1 site (Figure B.3a). Minor differences were apparent at the four remaining comparative sampling sites, as shown in Figure B.3 b to e. In general, density measurements were less variable across the sites when compared to mean radial vessel diameter and vessel frequency measurements.

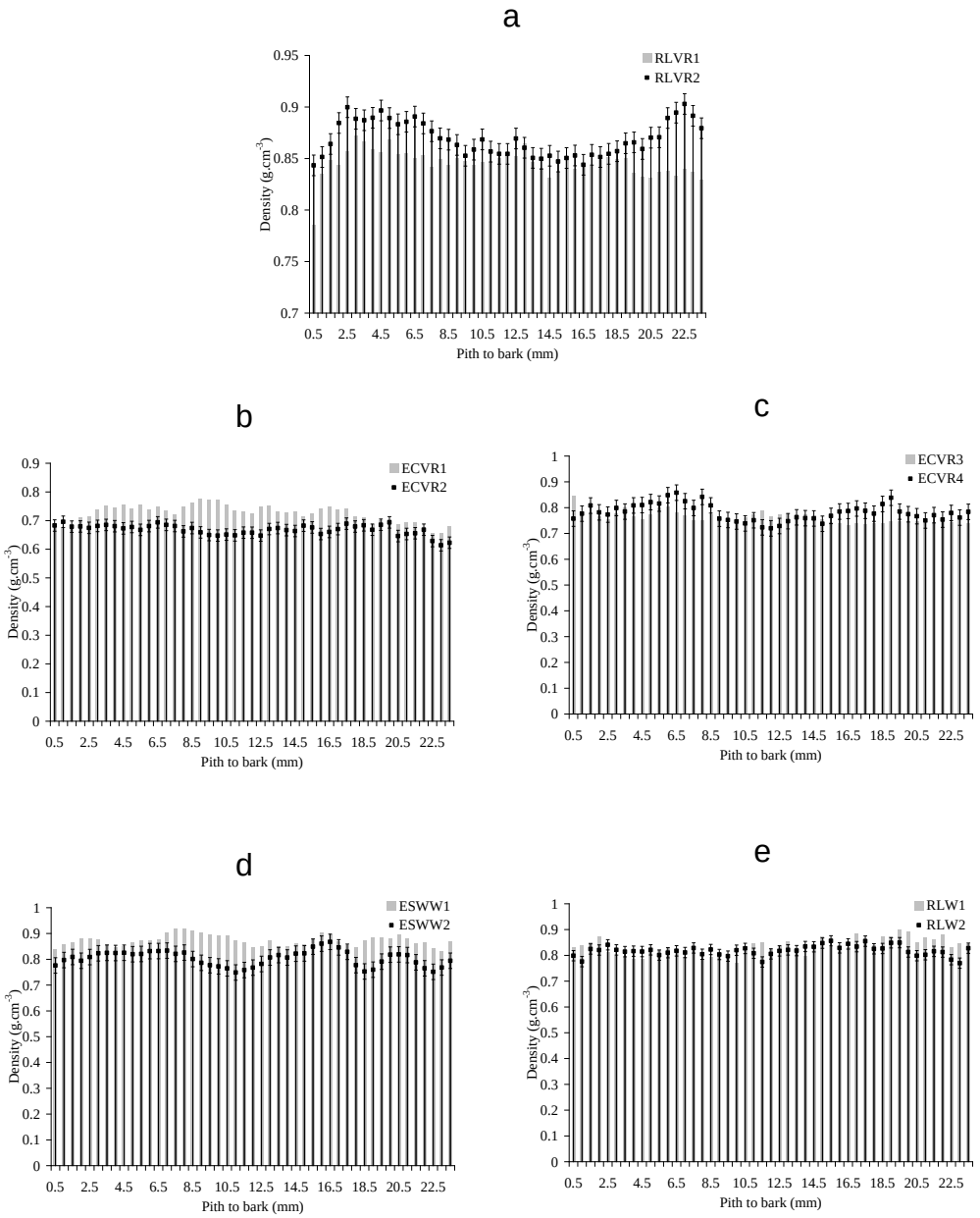


Figure B.3 Density measured from pith to bark for a) S. lancea at site RLVR1 and RLVR2, b) E. camaldulensis at site ECVR1 and ECVR2 and c) site ECVR3 and ECVR4 in Vaal River, d) E. sideroxylon at site ESWW1 and ESWW2 sampled in West Wits and, e) S. lancea at site RLW1 and RLW2 sampled in Welkom.

DISCUSSION

Statistical comparative analyses were undertaken for xylem vessel size, frequency and wood density measurements for the five comparative sampling sites. Comparison of the radial vessel diameter and vessel frequency measurements revealed significant differences in three

of the five comparative sampling sites ($p < 0.05$). However, the results of the density analyses were significantly different for all five comparative sampling sites ($p < 0.01$).

Site RLVR1 is characterised by *S. lancea* trees that were sampled on slightly raised topography near a TSF, an area considered to have lower contaminant levels and total dissolved solids compared to *S. lancea* trees sampled at Site RLVR2, approximately 1 km southwards between two TSFs. Site RLVR2 has higher total dissolved solids and higher water availability due to seepage from the two tailing storage facilities (Weiersbye, 2005). Wood density measurements were found to be statistically different at the two sites ($p < 0.001$); while radial vessel diameter ($p = 0.777$) and vessel frequency ($p = 0.708$) measurements were not significantly different.

At sites ECVR1 and ECVR2, *E. camaldulensis* trees were sampled near a TSF located in the Vaal River mining district. Trees sampled at Site ECVR2 were located within a water channel which flows parallel to the tailing storage facility. Vessel frequency measurements were significantly different ($p = 0.020$) between the two sites, with lower frequency measurements obtained at ECVR1 compared to ECVR2 site. Wood density measurements were also significantly different ($p < 0.001$), with lower values obtained at the ECVR2 site, where trees were sampled in a water channel. Radial vessel diameter measurements were not significantly different at the two sites ($p = 0.146$). Differences in vessel frequency and wood density could imply differences in wood anatomy characteristics resulting from contaminant up-take from the water channel.

At sites ECVR3 and ECVR4, *E. camaldulensis* trees were also sampled approximately 200 m from the edge of the Western Complex TSF located in Vaal River. Site ECVR3 was characterised by a cluster of young *E. camaldulensis* trees which appeared to be visually unhealthy, showing signs of reduced biomass, reduced tree height and yellow to brown leaf colour. Approximately 20 m northwards lay Site ECVR4 consisting of a clump of healthier, young green *E. camaldulensis* trees. In general, the mean radial vessel diameter, vessel frequency and wood density measurements were higher at ECVR4 site compared to ECVR3 site. However, significant differences were determined between radial vessel diameter ($p < 0.001$) and wood density ($p = 0.002$) measurements. Differences between vessel frequency

measurements were smaller and were not significant ($p = 0.178$; mean difference = 1.24 mm^{-2}).

Sites ESWW1 and ESWW2 consisted of a stand of *E. sideroxylon* trees, which were situated approximately 10 m from a small dam on the Deelkraal Farm in the West Wits mining district. The stand of trees could be characterised as being dense, green and visually healthy along the riparian edge, but at least 20 m ahead, the trees began to thin, became less dense and were visually more stressed or unhealthy. The ESWW2 site was located along the riparian edge and the ESWW1 site at least 20 m ahead within the stand. Radial vessel diameter measurements were generally larger in trees sampled along the riparian edge (Site ESWW2) compared to trees sampled away from the farm dam (Site ESWW1) ($p = 0.010$). Vessel frequency ($p = 0.024$) and wood density ($p < 0.001$) measurements were significantly higher in the more stressed trees sampled within the stand (Site ESWW1) compared to the trees sampled along the riparian edge (Site ESWW2).

Site RLW1 was characterised by *S. lancea* trees located approximately 100 m from the edge of Dankbaar Pan, which is located on cattle and agricultural farmland within the Welkom mining district. This area is very flat and the groundwater is reported to have high electrical conductivity levels influenced by drainage pathways from the pan itself (I. Weiersbye, 2004 pers comm.). The comparative Site RLW2 was selected approximately 20 km away from the pan on an agricultural farm. A trend of larger radial vessel diameters and vessel frequencies was observed in trees sampled on the agricultural farmland (Site RLW2) compared to trees sampled near the pan (Site RLW1). In contrast, the mean wood density measured in trees near the pan (Site RLW1) was greater compared to trees sampled on the agricultural farmland (Site RLW2). Radial vessel diameter ($p = < 0.001$) and vessel frequency ($p = 0.006$) and wood density ($p = 0.005$) measurements were significantly different at the two sites.

In general, trees experiencing higher plant water stress displayed smaller vessel diameters (Site ECVR3, Site ESWW1), compared to less stressed or healthy trees (Site ECVR4, Site ESWW2). These results are in accordance with studies which indicated that water stress in plants induces a decrease in xylem vessel diameters (Zimmerman and Milburn, 1982; Zhang

et al., 1988; February, 1993; 1994; February *et al*., 1995; Lovisolo and Schubert, 1998; Naidoo *et al*., 2006). However, sites which were influenced by high levels of contaminated water (ECVR2, RLW1) also displayed smaller vessel diameters, indicating that the uptake of contaminants could affect the wood anatomy of plants. Trees considered to be experiencing higher plant water stress displayed higher vessel frequency (Site ESWW1, Site RLW2).

Incremental pith to bark measurements of radial vessel diameter, vessel frequency and wood density for each comparative sampling site clearly illustrated differences in the wood anatomy of each comparative sampling site. Consistently larger radial vessel diameter values were obtained for each segment measured from pith to bark at Site ECVR4 when compared to ECVR3; in contrast to larger wood density values obtained at Site ESWW1 when compared to ESWW2. Greater variability in vessel frequency measurements were observed, while less variability in the wood density measurements from pith to bark between sites were found.

CONCLUSION

It can be concluded from this preliminary study that plant stress does influence the wood anatomical characteristics (radial vessel diameter, vessel frequency and wood density) in *E. camaldulensis*, *E. sideroxylon* and *S. lancea* in the three mining districts. However, more detailed plant physiological studies are required to improve our understanding of long-term manifestations of water stress on wood anatomy of plants. This preliminary study highlighted the potential for using simple techniques to obtain wood cores to investigate wood anatomy of trees. A more rigorous approach should be adopted for developing a tool for identifying trees which are experiencing plant stress without compromising on biomass of the trees.